

# The Amyloid Precursor Protein and Cell Viability in Diseases of the Ageing Brain

Ph.D. Thesis

Mallory Gough BSc (Hons)

Lancaster University

August 2013

I, Mallory Gough confirm that the work presented in this thesis is my own and has not been submitted in substantially the same form for the award of a higher degree elsewhere. Where information has been derived from other sources, I confirm this has been indicated in the thesis.

Signed

Submitted in part fulfilment of the requirements for the degree of Doctor of Philosophy

UNIVERSITY LIBRARY

1

15 JAN 2015

LANCASTER

ProQuest Number: 11003800

All rights reserved

INFORMATION TO ALL USERS

The quality of this reproduction is dependent upon the quality of the copy submitted.

In the unlikely event that the author did not send a complete manuscript and there are missing pages, these will be noted. Also, if material had to be removed, a note will indicate the deletion.



ProQuest 11003800

Published by ProQuest LLC (2018). Copyright of the Dissertation is held by the Author.

All rights reserved.

This work is protected against unauthorized copying under Title 17, United States Code  
Microform Edition © ProQuest LLC.

ProQuest LLC.  
789 East Eisenhower Parkway  
P.O. Box 1346  
Ann Arbor, MI 48106 – 1346

# **The Amyloid Precursor Protein and Cell Viability in Diseases of the Ageing Brain**

Ph.D. Thesis

Mallory Gough BSc (Hons)

Lancaster University, August 2013

## **Abstract**

The amyloid precursor protein (APP) has been extensively studied in relation to Alzheimer's disease, but the physiological function of the protein has yet to be determined. One possible role for APP may be to protect cells against the detrimental effects of excess copper. In the current study I have investigated which regions of the APP molecule participate in this putative function. I have used both Du145 and SH-SY5Y mammalian cell systems to explore this question, relating the generated results to both cancer and Alzheimer's Disease. Initial studies using western blotting showed that a range of prostate cancer cell lines express APP, and that increased APP expression levels may represent a more advanced stage of cancer progression. Exogenous copper altered the expression levels of APP in Du145 cells, immediately indicating the intricate relationship between APP and copper. Subsequently, using MTS assays, I found that APP can indeed enhance cell viability in the face of copper, in both of the cell systems stated above. This role is isoform dependent, being specific to the APP<sub>695</sub> isoform, which is predominantly found in the brain. N-terminal copper binding and copper binding within the A $\beta$  region of the APP holoprotein appeared to be a prerequisite for this action. The intracellular domain was also required in order to enhance cell viability, and the importance of this region was assigned to specific tyrosine residues within the domain. APP over-expression in Du145 cells also appeared to induce a partial epithelial to mesenchymal transition of the cells. Along with suggesting a possible physiological function for APP, these data suggest that prostate cancer epithelial cells metastasising to the brain might utilise APP to protect them against the increased copper levels found in this organ.

## Table of Contents

The Amyloid Precursor Protein and Cell Viability in Diseases of the Ageing Brain .....	1
Abstract.....	2
Table of Contents.....	3
List of figures.....	9
List of Tables .....	12
Acknowledgements.....	13
1. Literature Review .....	14
1.1. Introduction .....	15
1.2. Alzheimer's Disease .....	15
1.2.1. Incidence and aetiology .....	15
1.2.2. Pathology.....	17
1.2.3. Diagnosis and treatment.....	19
1.3. Prostate Cancer.....	20
1.3.1. Incidence and aetiology .....	21
1.3.2. Pathology .....	22
1.3.3. Diagnosis and treatment.....	23
1.4. The amyloid precursor protein (APP).....	24
1.4.1. APP structure .....	25
1.4.1. APP proteolysis.....	26
1.4.2. Amyloidogenic processing.....	26
1.4.3. Non-amyloidogenic processing .....	28
1.5. Lipid rafts and APP proteolysis.....	32
1.6. The physiological role of APP and its metabolites.....	32
1.6.1. Functions of the APP holoprotein .....	33
1.6.2. Functions of the APP cytosolic domain.....	35
1.6.3. Functions of sAPP $\alpha$ .....	39
1.6.4. Functions of sAPP $\beta$ .....	41
1.6.5. Functions of the soluble AICD .....	42
1.6.6. Functions of $\beta$ -amyloid peptides.....	43
1.7. APP and metals - copper .....	43
1.7.1. Copper binding to the APP ectodomain.....	44
1.7.2. Copper-mediated APP expression.....	45
1.7.3. Copper-mediated APP proteolysis .....	46

1.7.4.	APP and copper homeostasis.....	47
1.7.5.	APP and the reduction of divalent copper.....	49
1.7.6.	Copper in A $\beta$ aggregation .....	51
1.8.	APP and metals – iron .....	52
1.8.1.	Iron in the expression and proteolysis of APP .....	52
1.8.2.	APP and the metabolism of iron .....	53
1.8.3.	Iron and the A $\beta$ peptide.....	53
1.9.	The roles of APP and copper in Alzheimer’s disease .....	53
1.9.1.	Mechanisms of A $\beta$ -mediated neurotoxicity.....	54
1.9.2.	Copper and Alzheimer's disease pathogenesis.....	55
1.10.	The roles of APP and copper in cancer .....	56
1.10.1.	APP and cancer .....	56
1.10.2.	APP and prostate cancer .....	60
1.10.3.	Copper and cancer pathogenesis.....	61
1.11.	Aims of the current project.....	65
2.	Materials and Methods.....	68
2.1.	Materials .....	69
2.2.	Molecular biology .....	70
2.2.1.	Preparation of agar plates .....	70
2.2.2.	Bacterial transformation .....	70
2.2.3.	Bacterial suspension cultures.....	70
2.2.4.	DNA purification.....	70
2.2.5.	Spectrophotometric quantification of DNA .....	71
2.2.6.	Agarose gel electrophoresis .....	71
2.2.7.	Site-directed mutagenesis polymerase chain reaction (PCR).....	72
2.2.8.	Restriction enzyme digests / DNA linearization.....	73
2.2.9.	Ethanol precipitation of plasmid DNA.....	73
2.3.	Mammalian cell culture .....	74
2.3.1.	Growth incubations.....	74
2.3.2.	Freezing down cell stocks.....	74
2.3.3.	Cell counting.....	74
2.3.4.	Transient transfection using lipofectamine .....	75
2.3.5.	Stable transfection using lipofectamine .....	75
2.3.6.	Stable transfection of Du145 cells using nucleofection.....	76

2.3.7.	Stable transfection using electroporation .....	76
2.3.8.	Small interfering RNA (siRNA) transfection of Du145 cells .....	77
2.4.	Protein analysis .....	79
2.4.1.	Preparation of concentrated conditioned medium samples and cell lysates .....	79
2.4.2.	Bicinchoninic acid (BCA) protein assay .....	80
2.4.3.	Sodium dodecylsulphate - polyacrylamide gel electrophoresis (SDS-PAGE) .....	82
2.4.4.	Immunoblotting .....	83
2.4.5.	Immunoblotting Stripping and re-probing Western Blots .....	84
2.4.6.	Amido black staining .....	84
2.5.	Lipid raft isolation .....	85
2.6.	Cell viability and morphology analysis .....	85
2.6.1.	Methanethiosulfonate (MTS) cell viability assay .....	85
2.6.2.	Cell morphology documentation using optical microscopy .....	86
2.7.	Immobilized metal chelate affinity chromatography (IMAC) .....	86
2.8.	Statistical analysis .....	87
3.	Characterisation of constitutive wild-type APP expression and proteolysis in cell lines.....	88
3.1.	Introduction .....	89
3.2.	APP expression and proteolysis .....	89
3.3.	The effect of dihydrotestosterone on APP expression and proteolysis in LNCaP cells .....	95
3.4.	$\alpha$ -secretase expression .....	98
3.4.1.	ADAM10 expression .....	98
3.4.2.	ADAM17 expression .....	99
3.4.3.	The effect of dihydrotestosterone on ADAM10 and ADAM17 expression in LNCaP cells .....	100
3.5.	Summary .....	102
4.	The effects of copper on endogenous APP expression and proteolysis in prostate cancer epithelial cells .....	103
4.1.	Introduction .....	104
4.2.	The effect of copper on LNCaP cell viability .....	104
4.3.	The effect of copper on the expression and shedding of endogenous APP in LNCaP cells.....	106
4.4.	The effect of copper on PC-3 cell viability .....	110
4.5.	The effect of copper on the expression and shedding of endogenous APP in PC-3 cells.....	111

4.6.	The effect of copper on Du145 cell viability .....	113
4.7.	The effect of copper on the expression and shedding of endogenous APP in Du145 cells.....	114
4.8.	Summary .....	117
5.	The effect of full-length APP construct expression on Du145 cell viability in the presence of copper.....	119
5.1.	Introduction .....	120
5.2.	Endogenous APP transcript analysis in Du145 cells.....	120
5.3.	Over-expression of APP isoform constructs in Du145 cells .....	123
5.4.	The effect of APP isoform over-expression on Du145 cell viability in the presence of copper.....	125
5.5.	The effect of ablating endogenous APP expression on Du145 cell viability in the presence of copper .....	128
5.6.	Summary .....	130
6.	The APP cytosolic domain is a prerequisite for enhanced Du145 cell viability in the presence of copper .....	132
6.1.	Introduction .....	133
6.2.	The expression and proteolysis of APP cytosolic domain mutant constructs in Du145 cells.....	133
6.3.	The effects of APP cytosolic domain mutations on the viability of Du145 cells in the presence of copper .....	137
6.4.	APP regulates the raft association of caveolin-1 .....	137
6.5.	Potential intracellular signalling pathways influenced by APP over-expression .....	142
6.6.	Summary .....	145
7.	The APP ectodomain and enhanced Du145 cell viability in the presence of copper .....	147
7.1.	Introduction .....	148
7.2.	The expression and proteolysis of the APP copper binding domain construct in Du145 cells.....	149
7.3.	The effect of E1 copper binding domain mutations on the viability of Du145 cells in the presence of copper .....	152
7.4.	The role of the soluble APP ectodomain in promoting Du145 cell viability in the presence of copper; stable over- expression of sAPP $\alpha$ .....	154
7.5.	The role of the soluble APP ectodomain in promoting Du145 cell viability in the presence of copper; inhibition of endogenous ectodomain generation.....	158
7.6.	The role of the soluble APP ectodomain in promoting Du145 cell viability in the presence of copper; the effect of recombinant sAPP $\beta$ .....	163
7.7.	Summary .....	165

8. APP-induced morphological changes in Du145 cells .....	167
8.1. Introduction .....	168
8.2. The effect of APP <sub>695</sub> over-expression on Du145 cell morphology .....	168
8.3. APP <sub>695</sub> -induced morphological changes in Du145 cells are not associated with neuroendocrine differentiation .....	168
8.4. APP <sub>695</sub> -induced morphological changes in Du145 cells are associated with epithelial-to-mesenchymal transition .....	172
8.5. APP-induced epithelial-to-mesenchymal transition in Du145 cells is isoform specific .....	174
8.6. The APP <sub>695</sub> cytosolic domain is involved in epithelial-to-mesenchymal transition in Du145 cells .....	177
8.7. The E1 copper binding domain is a prerequisite for APP <sub>695</sub> -induced epithelial-to-mesenchymal transition in Du145 cells .....	178
8.8. Attempted artificial induction of epithelial-to mesenchymal transition by enhancing endogenous APP expression .....	180
8.9. Summary .....	183
9. The role of copper binding in APP proteolysis and the viability of SH-SY5Y cells.....	184
9.1. Introduction .....	185
9.2. The expression and proteolysis of APP <sub>695</sub> copper binding mutants in SH-SY5Y cells	185
9.3. The effects of APP <sub>695</sub> copper binding mutants on the viability of SH-SY5Y cells in the presence of copper .....	189
9.4. The expression and proteolysis of APP <sub>770</sub> copper binding mutants in SH-SY5Y cells	190
9.5. The effects of APP <sub>770</sub> copper binding mutants on the viability of SH-SY5Y cells in the presence of copper .....	194
9.6. APP binds copper despite mutation of the E1 or A $\beta$ copper binding domains .....	195
9.7. Summary .....	196
10. Discussion.....	199
10.1. Introduction .....	200
10.2. Characterisation of constitutive wild-type APP expression and proteolysis in cell lines .....	200
10.3. The effects of copper on endogenous APP expression and proteolysis in prostate cancer epithelial cells.....	202
10.4. The effect of full-length APP construct expression on Du145 cell viability in the presence of copper .....	203
10.5. The APP cytosolic domain is a prerequisite for enhanced Du145 cell viability in the presence of copper .....	204
10.6. The APP ectodomain and enhanced Du145 cell viability in the presence of copper	207

10.7. APP-induced morphological changes in Du145 cells .....	210
10.8. The role of copper binding in APP proteolysis and the viability of SH-SY5Y cells.....	212
10.8. Future directions .....	215
10.9. Summary .....	216
References .....	218

## List of figures

Figure 1.1. The pathological hallmarks of Alzheimer's disease.....	18
Figure 1.2. UK prostate cancer statistics from 2008-2010.....	21
Figure 1.3. Schematic of APP functional domains and copper binding sites.....	26
Figure 1.4. Proteolysis of the amyloid precursor protein via the amyloidogenic and non-amyloidogenic processing pathways.....	27
Figure 1.5. Schematic of the $\gamma$ -secretase mediated cleavage of APP.....	29
Figure 1.6. Protein binding interactions of the amyloid precursor protein intracellular domain.....	36
Figure 3.1. APP expression levels in cell lysates.....	91
Figure 3.2. sAPP $\alpha$ shedding into conditioned culture medium.....	92
Figure 3.3. sAPP $\beta$ in conditioned cell culture medium.....	94
Figure 3.4. The effect of DHT on APP expression in LNCaP cells.....	95
Figure 3.5. The effect of DHT on sAPP $\alpha$ shedding from LNCaP cells.....	96
Figure 3.6. The effect of DHT on sAPP $\beta$ release from LNCaP cells.....	97
Figure 3.7. ADAM10 expression in cell lysates.....	99
Figure 3.8. ADAM17 expression in cell lysates.....	100
Figure 3.9. The effect of DHT on ADAM10 expression in LNCaP cells.....	101
Figure 3.10. The effect of DHT on ADAM17 expression in LNCaP cells.....	101
Figure 4.1. The effect of copper on LNCaP cell viability.....	105
Figure 4.2. The effect of copper on APP expression in LNCaP cells.....	107
Figure 4.3. The effect of copper on soluble APP production from LNCaP cells.....	109
Figure 4.4. The effect of copper on PC-3 cell viability.....	110
Figure 4.5. The effect of copper on APP expression in PC-3 cells.....	112
Figure 4.6. The effect of copper on soluble APP production from PC-3 cells.....	112
Figure 4.7. The effect of copper on Du145 cell viability.....	113
Figure 4.8. The effect of copper on APP expression in Du145 cells.....	115
Figure 4.9. The effect of copper on soluble APP production from Du145 cells.....	116
Figure 5.1. Endogenous APP transcript expression in Du145 cells.....	122
Figure 5.2. Schematic showing the APP isoform constructs used in the current study.....	123
Figure 5.3. APP isoform over-expression in Du145 cells.....	124
Figure 5.4. Soluble APP produced by Du145 cells over-expressing APP isoform constructs.....	125
Figure 5.5. The effects of APP isoform construct over-expression on Du145 cell viability in the	

presence of copper.....	127
Figure 5.6. APP expression and proteolysis in siRNA transfected Du145 cells.....	129
Figure 5.7. Viability of siRNA transfected Du145 cells.....	130
Figure 6.1. Schematic representing APP intracellular domain mutant constructs.....	134
Figure 6.2. APP intracellular domain mutant over-expression in Du145 cells.....	135
Figure 6.3. Soluble APP generation by Du145 cells over-expressing APP intracellular domain mutants.....	136
Figure 6.4. The effects of APP intracellular domain mutant over-expression on Du145 cell viability in the presence of copper.....	138
Figure 6.5. Analysis of protein distribution in sucrose gradients prepared from Du145 cells transfected with either vector alone, wild-type APP <sub>695</sub> or APP <sub>695</sub> ΔICD.....	139
Figure 6.6. Analysis of APP distribution in sucrose gradients prepared from Du145 cells transfected with either vector alone, wild-type APP <sub>695</sub> or APP <sub>695</sub> ΔICD.....	140
Figure 6.7. Analysis of caveolin-1 distribution in sucrose gradients prepared from Du145 cells transfected with either vector alone, wild-type APP <sub>695</sub> or APP <sub>695</sub> ΔICD.....	141
Figure 6.8. ERK1 expression in Du145 cells over-expressing APP intracellular domain mutants.....	143
Figure 6.9. ERK1 expression in Du145 cells over-expressing APP isoforms.....	144
Figure 7.1. Schematic representing the APP N-terminal copper binding domain deficient construct.....	149
Figure 7.2. APP N-terminal copper binding domain mutant over-expression in Du145 cells.....	150
Figure 7.3. Soluble APP generation by Du145 cells over-expressing the APP <sub>695</sub> ΔCuBD construct.....	151
Figure 7.4. The effect of APP <sub>695</sub> ΔCuBD mutant over-expression on Du145 cell viability in the presence of copper.....	153
Figure 7.5. Detection of the soluble APP <sub>770</sub> construct using the anti-FLAG antibody.....	155
Figure 7.6. Detection of the soluble APP <sub>770</sub> construct using the antibody 22C11.....	156
Figure 7.7. Lack of soluble APP <sub>770</sub> degradation by Du145 cell lysates.....	157
Figure 7.8. Inhibition of APP α-secretase activity by G1254023X in wild-type APP <sub>695</sub> -transfected Du145 cells.....	159
Figure 7.9. The effect of APP α-secretase inhibition on the viability of APP <sub>695</sub> -transfected Du145 cells in the presence of copper.....	160
Figure 7.10. Inhibition of APP β-secretase activity by β-secretase inhibitor IV in Du145 cells.....	162

Figure 7.11. The effect of APP $\beta$ -secretase inhibition on the viability of APP <sub>695</sub> -transfected Du145 cells in the presence of copper.....	163
Figure 7.12. Detection of soluble APP derivatives in conditioned medium from mock- and APP <sub>695</sub> $\beta$ -transfected HEK cells.....	164
Figure 7.13. The effect of recombinant sAPP $\beta$ on the viability of Du145 cells in the presence of copper.....	165
Figure 8.1. APP <sub>695</sub> - induced morphological changes in Du145 cells.....	169
Figure 8.2. Decreased NSE expression and secretion in APP <sub>695</sub> -transfected Du145 cells.....	171
Figure 8.3. APP <sub>695</sub> -transfection is associated with epithelial-to-mesenchymal transition in Du145 cells.....	173
Figure. 8.4. The effect of APP isoforms on EMT in Du145 cells.....	175
Figure. 8.5. The effect of APP C-terminal constructs on EMT in Du145 cells.....	176
Figure. 8.6. The effect of APP E1 domain copper binding ablation on EMT in Du145 cells...	179
Figure 8.7. The effect of NGF- $\beta$ on APP expression and proteolysis in Du145 cells.....	181
Figure 8.8. The effect of HGF on APP expression in Du145 cells.....	182
Figure 9.1. Schematic representing APP <sub>695</sub> copper binding mutant constructs.....	186
Figure 9.2. APP <sub>695</sub> copper binding domain mutant over-expression in SH-SY5Y cells.....	187
Figure 9.3. Soluble APP generation by SH-SY5Y cells over-expressing the APP <sub>695</sub> copper binding constructs.....	188
Figure 9.4. The effect of APP <sub>695</sub> copper binding mutant over-expression on SH-SY5Y cell viability in the presence of copper.....	187
Figure 9.5. Schematic representing APP <sub>770</sub> copper binding mutant constructs.....	191
Figure 9.6. APP <sub>770</sub> copper binding domain mutant over-expression in SH-SY5Y cells.....	192
Figure 9.7. Soluble APP generation by SH-SY5Y cells over-expressing the APP <sub>770</sub> copper binding constructs.....	193
Figure 9.8. The effect of APP <sub>770</sub> copper binding mutant over-expression on SH-SY5Y cell viability in the presence of copper.....	195
Figure 9.9. Binding of APP constructs to metal affinity spin columns.....	197
Figure 10.1. NED in Du145 cells.....	211

## List of Tables

Table 1.1. The physiological processes associated with APP adaptor proteins.....	38
Table 1.2. Tissue copper levels in cancer.....	62
Table 1.3. Serum copper levels in cancer.....	63
Table 2.1. The composition of resolving gels used in SDS-PAGE.....	81
Table 2.2. The composition of stacking gel used in SDS-PAGE.....	81
Table 2.3. Primary antibody dilutions.....	83
Table 5.1. RT-PCR primers employed in the current study.....	121

## Acknowledgements

I would like to thank my supervisor Dr. Ed Parkin for his help and support throughout my PhD, particularly for his time spent reading and correcting this thesis. I would also like to thank our previous lab group members, Edd and Cath, for teaching me the ropes in the lab and for always being there when I needed help, entertainment or something to bang my head against! I would also like to thank my fellow PhD students, who provided support, distraction, transport, food and friendships which I couldn't have done without. Finally, I would like to thank the Biotechnology and Biological Sciences Research Council for funding my PhD research and providing me with the opportunity to attend some fantastic conferences.

# 1. Literature Review

---

## 1.1. Introduction

The amyloid precursor protein (APP) is a ubiquitously expressed protein of unknown physiological function. The protein is singularly most noted for its role in the pathogenesis of the neurodegenerative condition Alzheimer's disease (AD) (1) and, more recently, in the development of various cancers, notably prostate cancer (2). In the case of the latter disease, although it is rare, cancerous cells can metastasize to the brain (3). In the current study, the role of APP in promoting cell viability in the brain in both of these diseases of ageing is examined.

## 1.2. Alzheimer's Disease

Alzheimer's disease (AD) is the most common form of dementia, the latter of which is defined by cognitive impairment which interferes with daily life (4). AD was first described by the German psychiatrist and neurophysiologist Alois Alzheimer, in 1906. The disease is most commonly diagnosed in people over 65 years of age, although the less-prevalent early-onset AD can occur much earlier in life (5).

### 1.2.1. Incidence and aetiology

Ferri *et al.* (6) estimated that 24.3 million people have dementia worldwide and that there are 4.6 million new cases every year. In the UK alone, the cost of dementia is thought to be £23 billion per year (7). AD is believed to account for 50-60% of dementia cases (5), with approximately 500,000 people suffering from the disease in the UK (8). Population based studies in Europe have suggested that the prevalence of AD in people above the age of 65 is 4.4% (4).

Initially, the symptoms of AD may be mistaken as natural signs of aging. However, after time, the severity of the condition becomes apparent. Mild cognitive impairment (MCI) is the term which describes these initial symptoms (5). Progression from MCI to AD takes place at a rate of approximately 10-15% per year. The foremost symptom of AD is a progressive loss of episodic memory (4). This may then be accompanied by language and visuospatial deficits and the impairment of executive functions. As the disease progresses further, behavioural disturbances are often developed, and towards the end of the disease process, patients lose the ability to stand, reverting to a vegetative state. The average duration of AD between diagnosis and death is 8-12 years. Astonishingly, the time lapse between the pathophysiological beginnings of AD and onset of symptoms is approximately 20-30 years (9).

The predominant risk factor for developing AD is age. Of those individuals aged 60-65, 0.08% develop the disease each year, whereas the incidence rate for those over the age of 85 is 6.48% per year (10). This association of AD with age may be due to a lifetime exposure to different risk factors; possibly a combination of genetic susceptibility, biological factors and environmental exposures.

The familial form of AD (FAD) is thought to account for less than 3% of all AD cases and is inherited in an autosomal dominant fashion (11). FAD is also known as early-onset AD, as the onset is likely to be before the age of 65. Mutations in the amyloid precursor protein (APP) (chromosome 21), presenilin 1 (chromosome 14) and the presenilin 2 (chromosome 1) genes, have been implicated in FAD (5).

The apolipoprotein E4 (ApoE4) allele has been implicated as a risk factor for late-onset AD (LOAD), with each inherited copy of the allele lowering the age of disease onset by almost 10 years (12). Possessing one ApoE4 allele increases the risk of developing LOAD approximately three-fold, and homozygosity for the allele increases the risk of developing AD

by up to fifteen times (13). Other genetic links have been implicated as risk factors for LOAD, such as those genes encoding various amyloid degrading enzymes (14), but none of these factors are as closely linked to the risk of developing the disease as the ApoE4 allele.

In addition to genetic factors, there are also many other risk factors for AD. Elevated blood pressure in middle age, diabetes, prediabetes, hyperinsulinemia, cerebrovascular disease, severe atherosclerosis, cardiovascular disease and cigarette smoking have all been linked to an elevated risk of AD (4). Conversely, anti-hypertensive calcium channel blocking drugs, light to moderate alcohol consumption, low serum cholesterol, cholesterol lowering drugs and a diet of more fish, vegetables and low saturated fat may decrease the risk of developing the disease (4). There is also evidence that an intellectually active lifestyle may protect against AD through increasing neural and cognitive reserve which affords the brain more chance of coping with the pathological effects of the condition.

### **1.2.2. Pathology**

The brain of an AD patient exhibits global atrophy i.e. a reduction in overall size, but particularly in the hippocampus and temporal lobes (4). The two main pathological hallmarks of AD are extracellular amyloid plaques and intracellular neurofibrillary tangles (NFTs) (*Fig.1.1*). The main constituent of amyloid plaques is the 1-43 amino acid, amyloid beta ( $A\beta$ )-peptides. The most prevalent forms of  $A\beta$  in the brain are  $A\beta_{1-40}$  and  $A\beta_{1-42}$  with the  $A\beta_{1-42}$ -peptide thought to be the primary neurotoxic species in AD (15). Indeed some FAD associated PS1 and PS2 mutations exert their effects by increasing the  $A\beta_{1-42}:A\beta_{1-40}$  production ratio (16). The core of amyloid plaques consists of  $A\beta$  fibrils about 7-10 nm in length alongside non-fibrillar forms of  $A\beta$ , often in association with metals such as zinc, copper and iron (17, 18). This core is surrounded by dystrophic dendrites and axons, activated microglia, and reactive astrocytes. The entire plaque complex is usually spherical,



**Figure 1.1. The pathological hallmarks of Alzheimer's disease.** The image shows A $\beta$  plaques and NFTs in the cerebral cortex. Taken from Blennow *et al.* (5).

with a diameter of approximately 200  $\mu\text{m}$  which can initiate inflammation of the surrounding area (19).

NFTs are comprised of a hyperphosphorylated form of the microtubule associated protein tau (*Fig.1.1*), which forms paired helically twisted protein filaments (PHFs) confined to the cell cytoplasm (20). Phosphorylation of tau inversely correlates with its attachment to microtubules, so when it becomes hyperphosphorylated, it dissociates from the microtubules completely and instead forms NFTs. The presence of hyperphosphorylated tau in the neurons decreases the efficiency of axonal transport, which results in synaptic defects and memory impairments (21). However, NFTs are believed to have a lesser involvement in AD than A $\beta$  pathology (22).

### 1.2.3. Diagnosis and treatment

Initial AD diagnosis relies on the exclusion of other possible causative conditions. As such, the patient's medical history is first consulted and routine blood tests are performed in order to ensure that there are no other underlying problems (4). Physical and neurological examinations are performed to ensure that the patient is not suffering from an alternative form of dementia. Following this, neuroimaging techniques such as positron emission tomography (PET), computerised tomography (CT) or magnetic resonance imaging (MRI) are often used to analyse the brain and identify any gross morphological changes. The psychiatric and cognitive performance of the patient are then evaluated using the criteria of the National Institute of Neurological and Communicative Diseases and Stroke and the Alzheimer's Disease and Related Disorders Association (NINCDS-ADRDA), to aid diagnosis (5). Currently the most definite method of diagnosis is post-mortem neuropathology, but even this does not give a definitive diagnosis, because as many as 20-40% of non-AD sufferers have enough plaques and NFT's to satisfy the AD diagnostic criteria. Researchers are hopeful that, in the future, A $\beta$ , total tau and phosphorylated tau levels in the CSF and perhaps even plasma might be used as reliable biomarkers for AD (reviewed in (23)).

Currently, acetylcholinesterase (AChE) inhibitors are the most widely used treatment for AD. These inhibitors inhibit the degradation of the cholinergic neurotransmitter, acetylcholine (ACh), but tend to treat the symptoms rather than deal with the underlying cause of the disease (4). However, they can be beneficial in improving the cognitive, behavioural and functional deficits associated with AD for a limited period of time. Four AChE inhibitors thus far are licensed as a treatment for AD; donepezil, rivastigmine, galantamine, and in some countries tacrine.

Memantine, another therapeutic used in the treatment of AD, targets *N*-methyl-D-aspartate (NMDA) receptors (24). These receptors are activated by amino acids such as glutamate, and kill the cell through excess calcium influx; a process known as excitotoxicity. Memantine is a non-competitive NMDA receptor antagonist and promotes cell survival.

The majority of future AD therapeutic possibilities rely on either the inhibition of A $\beta$ -peptide formation or the post-formation dissolution of A $\beta$ -oligomers and/or aggregates. Thus, these methods include anti-fibrillation agents,  $\beta$ - and  $\gamma$ -secretase inhibitors,  $\gamma$ -secretase modulators,  $\alpha$ -secretase stimulators, APP targeting antibodies, metal attenuating compounds, gene therapy,  $\beta$ -sheet breaker peptides and A $\beta$  aggregation targeting antibodies (5, 24-27). However, as A $\beta$  targeting therapeutics have thus far lacked success, a huge amount of research is still being carried out in regards to tau and NFT's in AD, so therapeutics targeting tau kinases and phosphatases and the clearance of hyperphosphorylated tau are promising future therapeutic strategies for AD (28).

Therapeutics that target the symptoms of AD have also been suggested, such as behaviour modifying drugs, anti-inflammatory drugs, antioxidants, astrocyte-modulating agents, caspase inhibitors and neurotrophins (5, 24, 29, 30).

### **1.3. Prostate Cancer**

Prostate cancer (PCa) develops in the prostate, a gland in the male reproductive system responsible for the production of seminal fluid. This cancer can metastasize primarily to the surrounding bones and lymph nodes, but in rare cases it also metastasises to distant organs such as the brain.

### 1.3.1. Incidence and aetiology

Prostate cancer (PCa) accounts for one quarter of all male cancer cases in the UK, and is therefore the most common cancer in men (31) (Cancer research UK, 2010).

Approximately 36,000 men are diagnosed with the disease each year in the UK, and in 2008 913,000 men worldwide were diagnosed with PCa.

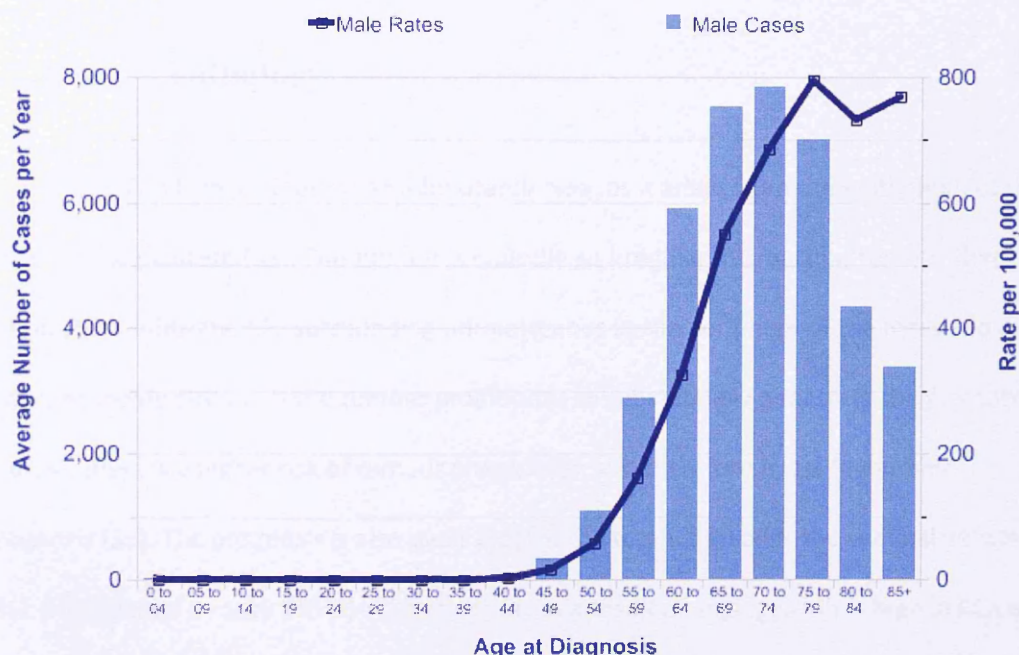


Figure 1.2. UK prostate cancer statistics from 2008-2010. Average number of new cases per year and age specific incidence rates is shown. Taken from Cancer research UK (31).

The strongest, yet unavoidable, risk factor for PCa is also age, with the risk increasing at 50 and remaining elevated until the age of 85 years and beyond (Fig. 1.2) (32). However, there is also a genetic element to the disease (33). If a male has a first degree relative who developed PCa before the age of 50, his chances of developing a carcinoma himself are increased two-three fold. In addition, PCa is strongly associated with ethnicity, with black men from North America developing PCa on average ten years earlier than white men (34).

Diet may also play a role in the development of PCa. The strongest link to diet is that of animal fat consumption leading to an increased risk of developing the disease, possibly related to fat content affecting the handling of testosterone within the body (34). Vegetarian men are thought to have up to a 50% lower risk of developing PCa compared to meat eaters. There are also some possible protective factors in the diet, such as vitamin E, vitamin A, vitamin C, lycopenes, selenium and isoflavonoids (34). This suggests that a varied, healthy diet is likely to decrease the probability of developing PCa.

### **1.3.2. Pathology**

The PCa tumour is often an adenocarcinoma, as it arises from the epithelium of the glands in the prostate (33). The tumour is typically an irregular microacinar tumour that continues to infiltrate into surrounding normal glands at the periphery of the mass and into the surrounding stroma. If the tumour proliferates to substantially penetrate the prostate capsule, there is a higher risk of tumour progression and therefore a less favourable prognosis (35). The prognosis is also more bleak if the tumour invades the seminal vesicles (36). Microvessel density (MVD) of the tumour, as a result of angiogenesis is high in PCa as in other forms of cancer, and once a tumour reaches the size at which it requires its own blood supply a worse prognosis is likely (37).

Prostatic carcinomas, in their early stages, seem to be dependent on androgen levels for their growth (38). Androgen receptors (ARs) bind sex steroids in the prostate and stimulate transcription of specific genes (39). The gene encoding the AR consists of CAG repeats, and an association has been identified between lower numbers of these repeats and more aggressive forms of PCa.

Prostatic carcinomas release various marker substances whilst proliferating, two of the most relevant being prostate specific acid phosphatase and prostate specific antigen

(PSA) (40). PSA is the most clinically relevant of the two and levels in the serum often negatively correlate with prognosis (41). PSA levels also have a huge role in the diagnosis of PCa (42). Other biological markers have also been associated with the development of prostatic carcinomas, such as a reduction in E-cadherin levels (43). E-cadherin is an epithelial adhesion molecule and levels can reduce by up to 50% in cases of PCa. This, in theory, would allow cells to proliferate and metastasise more effectively. Enhanced activity of the insulin-like growth factor signalling system has also been demonstrated to benefit the growth of prostatic carcinomas (40). Mutations in the tumour suppressor, p53, gene are associated with the onset of PCa, along with many other cancers, and p53 reactivity can be a marker of a particularly aggressive form of PCa (44).

### **1.3.3. Diagnosis and treatment**

There are four key methods by which PCa is diagnosed (33). Digital rectal examination is the primary method. The prostate is conveniently located alongside the rectum, and the presence of an adenocarcinoma causes a stromal reaction, resulting in a hard tumour nodule in the posterior lobe of the prostate, obliterating the usually palpable median groove which can be felt during a digital examination. Following this primary diagnostic procedure, a transrectal ultrasonography and needle biopsy may follow. The most radical advance in PCa detection so far is the measurement of PSA levels. PSA is a glycoprotein produced by the prostate epithelium which is involved in the liquefaction of semen. Elevated PSA levels are often associated with PCa, but as PSA levels increase with age and fluctuate with inflammation, they are not directly indicative of PCa.

PCa patients are assessed and put into a risk category based on tumour stage (TNM category), Gleason score and PSA level, which aids the choice of treatment (34). The adenocarcinoma of approximately 70% of men diagnosed with PCa is confined to the

prostate gland with no negative impact on health (33). This begs the question of whether treatment is worthwhile. If the tumour is identified as low-risk, there seems to be no benefit in radical treatment strategies, as many men can die with PCa rather than from it. However, those localised tumours with a higher Gleason score or PSA value would be treated with prostatectomy or radiotherapy to prevent future metastasis.

Locally advanced PCa patients, where the tumour has metastasised within the pelvis are usually treated with radiotherapy combined with androgen ablation therapy (33). This is effective for those early stage tumours which still rely on androgens to proliferate. It can be carried out by removing the supply of androgens or by blocking AR's, or by a combination of the two. In the case of metastatic PCa, androgen ablation is also routine, but only effective if the tumour cells are still dependent on androgens for survival. As the disease progresses, it has the potential to become hormone refractory, possibly due to mutations in ARs. At this stage chemotherapy might be the only option, but with limited success.

Those individuals who may have an extremely high risk of developing PCa due to a family history of the disease may benefit from taking 5-alpha dihydrotestosterone (DHT) reductase inhibitors, as the prostate is dependent on DHT to function (33).

#### **1.4. The amyloid precursor protein (APP)**

The pathology and progression of both Alzheimer's disease and prostate cancer are linked to the metabolism of the amyloid precursor protein (APP). The specific links between the diseases and APP will be discussed in later sections in this review, whilst the below sections will deal with the general cell biology of the protein.

### 1.4.1. APP structure

APP is a type 1 integral membrane protein consisting of a small cytoplasmic domain, a single helical membrane spanning region, and a large ectodomain (45). Mammalian APP exists in three main isoforms containing 695, 751 and 770 amino acids, with APP<sub>695</sub> being the predominant isoform in neurons (45). These isoforms are generated by alternative splicing of exons 7, 8 and 15 in the *APP* gene (46). The main difference between the isoforms is that APP<sub>695</sub> does not possess the Kunitz protease inhibitor (KPI) domain found in APP<sub>751</sub> and APP<sub>770</sub>, whilst APP<sub>770</sub> contains an additional OX-2 domain (47). The APP ectodomain can be divided into 2 distinct domains; the E1 and E2 domains (Reviewed in (48)), which contain distinct functional regions (*Fig. 1.3*). The E1 domain contains the growth factor like domain (or heparin binding domain; HDB) and the copper binding domain, which are linked to the E2 domain via an acidic region. The E2 domain consists of a RERMS sequence and the central APP domain (containing a heparan sulphate proteoglycan-binding site), which in conjunction with the A $\beta$ -peptide region and a juxtamembrane linker comprises the 'carbohydrate domain' of the protein (reviewed in (49)). In the larger APP isoforms, the KPI and OX-2 domains are inserted prior to the E2 domain of the protein. The intracellular domain of APP consists of 47 amino acid residues and contains the YENPTY motif which may be involved in mediating the endocytosis of the protein, interactions with binding partners and initiation of downstream signalling cascades through the phosphorylation of its tyrosine residues (48, 50).

APP is post-translationally modified in various ways, including N-glycosylation, O-glycosylation, sialylation, chondroitin sulphate glycosaminoglycan modification, sumoylation and phosphorylation, and each isoform may contain different levels of each modification, making size differences possible due to factors other than amino acid content alone (45).

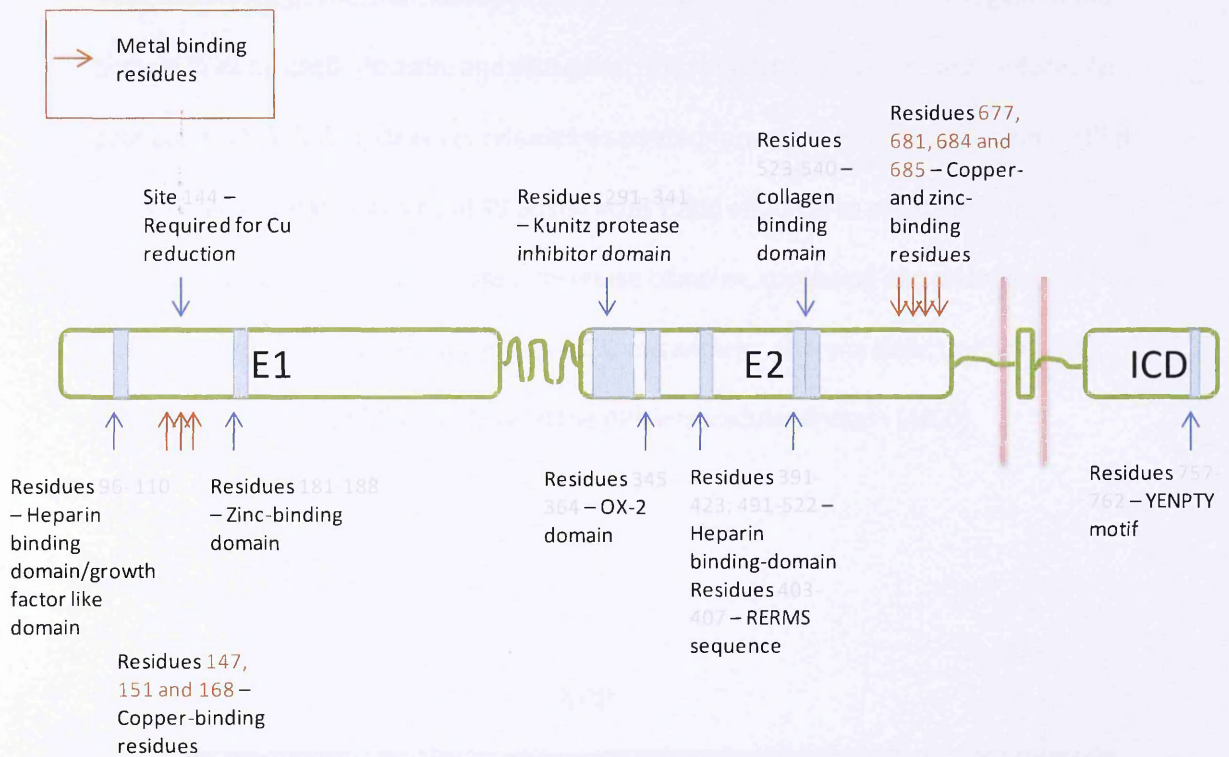


**Figure 1.3. Schematic of APP functional domains and copper binding sites.** Amino acid numbering is based on the 770 amino acid isoform (Uniprot KB website, (48)).

#### 1.4.1. APP proteolysis

APP proteolysis can follow one of two pathways (*Fig. 1.4*). The pathway that ultimately leads to the toxic entities involved in AD pathogenesis, the amyloid beta ( $A\beta$ )-peptides, is entitled the amyloidogenic pathway, and the alternative pathway, the non-amyloidogenic pathway (45).

#### 1.4.2. Amyloidogenic processing

The amyloidogenic pathway involves the cleavage of APP by the  $\beta$ -secretase, beta-site APP cleaving enzyme 1 (BACE1) (51). This cleavage is believed to take place primarily through co-localisation of APP and BACE1 in the endosomal compartments, whereas relocation of APP to the cell surface promotes the non-amyloidogenic cleavage of APP

(reviewed in (52)). The internalization of APP is dependent on the YENPTY region of the protein in its cytosolic domain, and disruption of this internalization process reduces A $\beta$  production (53). BACE1 cleavage releases a secreted form of the APP ectodomain (sAPP $\beta$ ), leaving a C-terminal fragment of 99 amino acids (C99) attached to the membrane (45). Subsequent cleavage of C99 by the  $\gamma$ -secretase complex, consisting of presenilin (PS) 1 or 2, nicastrin (Nct), presenilin enhancer 2 (Pen2), and anterior pharynx defective 1 (Aph-1), results in liberation of A $\beta$ -peptides and the APP intracellular domain (AICD).

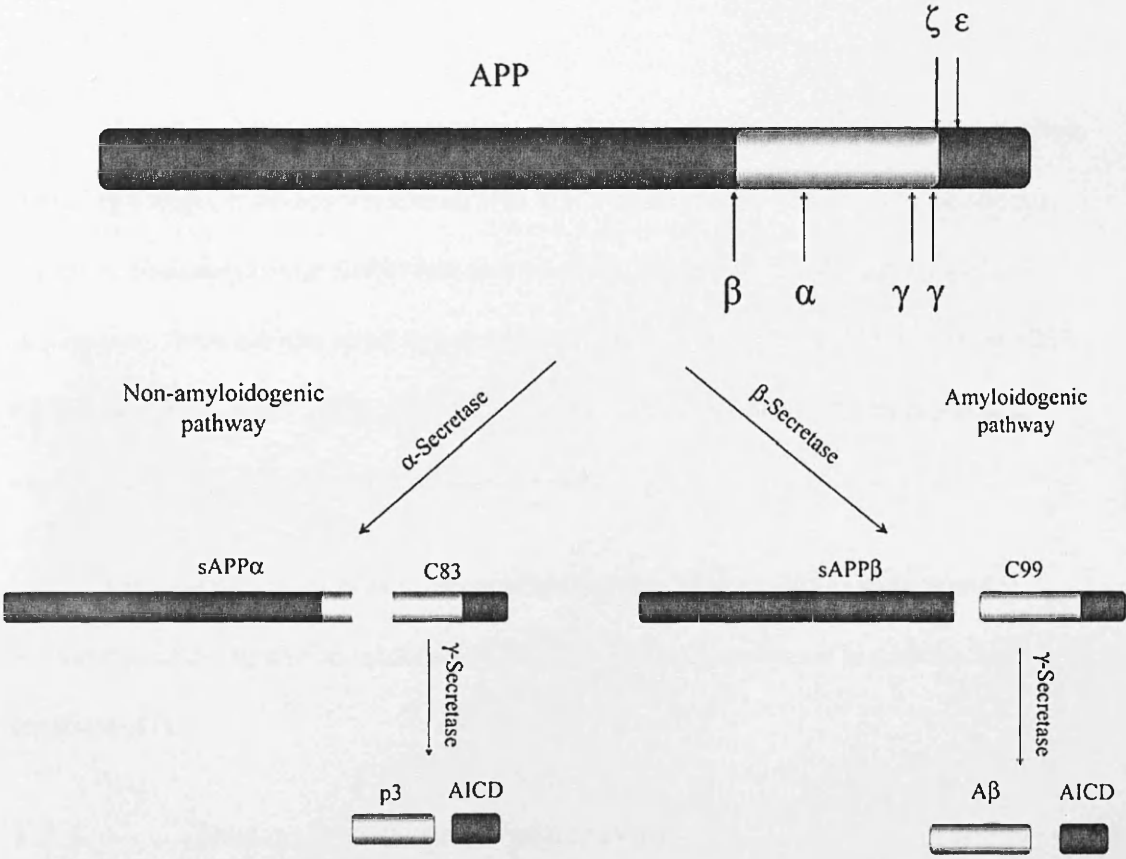


Figure 1.4. Proteolysis of the amyloid precursor protein via the amyloidogenic and non-amyloidogenic processing pathways. (Jacobsen *et al.* 2009 (45)).

BACE1 is an aspartic protease which exhibits optimal activity at an acidic pH akin to that in the endosomal system and the Golgi apparatus (54). The active site of BACE1 resides within the lumen of the aforementioned vesicles, and the enzyme can only cleave membrane-bound substrates (Reviewed in (55)). When the enzyme is knocked out *in vivo*, A $\beta$  is no longer generated and amyloid pathology disappears, suggesting that BACE1 is the primary  $\beta$ -secretase involved in amyloid pathology (Reviewed in (56)).

The  $\gamma$ -secretase complex is composed of PS, Nct, Pen2 and Aph-1, with the presenilins acting as the catalytic site of the complex. In addition, the complex has a number of potential regulatory proteins (including TMP21 and gSAP) which may influence cleavage of the APP molecule (57).

The  $\gamma$ -secretase complex can selectively and sequentially cleave at  $\epsilon$ -,  $\delta$ - and  $\gamma$ - sites, liberating a range of A $\beta$ -peptide species (*Fig. 1.5*). Approximately 90% of these A $\beta$  species are the comparatively inert A $\beta$ 40 type, and less than 10% comprises of the toxic A $\beta$ 42 species (58). There are also small amounts of some alternately sized peptides, such as A $\beta$ 37, A $\beta$ 38, A $\beta$ 43, A $\beta$ 46, A $\beta$ 47, A $\beta$ 48, A $\beta$ 49 which exist *in vivo*, some of which may represent intermediate stages of cleavage pathways (58-60).

The  $\gamma$ -secretase complex localises at membranes both at the cell surface and in endosomes, allowing it to co-localise with both the  $\alpha$ - and  $\beta$ -secretases in addition to its APP substrate (61).

### **1.4.3. Non-amyloidogenic processing**

When APP is processed via the non-amyloidogenic pathway, the protein is cleaved by an  $\alpha$ -secretase activity within the A $\beta$  domain, thereby precluding the formation of intact A $\beta$ -peptides. This releases sAPP $\alpha$  into the extracellular environment, and leaves a C-terminal fragment of 83 amino acids (C83) anchored in the plasma membrane (45). Subsequent

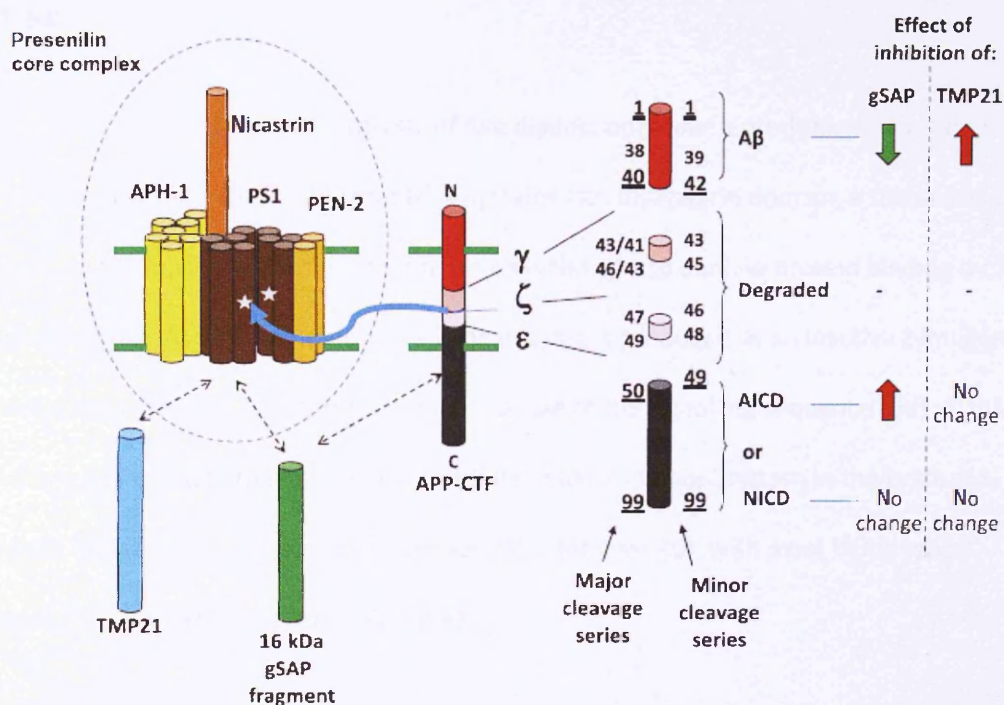


Figure 1.5. Schematic of the  $\gamma$ -secretase mediated cleavage of APP. (St. George-Hyslop *et al.* (57))

$\gamma$ -secretase cleavage of C83 liberates the non-toxic p3 fragment and the AICD into the cell cytoplasm. The  $\alpha$ -secretase activity takes place in the cell surface plasma membrane when the  $\alpha$ -secretase co-localises with APP (62).

The  $\alpha$ -secretase activity involved in the non-amyloidogenic proteolysis of APP is constituted by one or more members of the a disintegrin and metalloproteinase (ADAM) family of zinc metalloproteinases. ADAMs, like APP, are type 1 membrane proteins and, in their mature state, are between 70 and 90 kDa in size (63). The ADAMs have a common modular ectodomain structure consisting of a cysteine-rich domain which can interact with cell surface proteoglycans, a disintegrin domain which can bind to cell adhesion integrin molecules, a zinc-binding metalloproteinase domain, a large prodomain that keeps the metalloproteinase site of the newly synthesised protein inactive via a cysteine switch, and an N-terminal signal sequence. Activation of the ADAMs, which involves the removal of the

ADAM prodomain by proprotein convertase activity, takes place in the trans-golgi network (63, 64) .

The ADAM 10 protein consists of five distinct domains; a prodomain, a catalytic domain containing a zinc-binding motif, a cysteine rich disintegrin domain, a transmembrane region, and a short cytoplasmic domain, which is thought to contain protein binding motifs and nuclear localisation sequences (65). The enzyme is produced as an inactive zymogen, which enters the secretory pathway after cleavage of the signalling sequence (66). ADAM10 is widely expressed in the human body with a broad expression pattern in the brain (65, 67), and the enzyme has a large number of substrates (at least 40), with most being type 1 transmembrane proteins such as APP (68).

The original evidence pointing towards ADAM10 being an APP  $\alpha$ -secretase was provided by Lammich *et al.* (69) who over-expressed ADAM10 in HEK cells and saw a 4-fold increase in sAPP $\alpha$  secretion compared to untransfected cells. Furthermore, ADAM10 is co-expressed with APP and BACE1 in human cortical neurons (70), suggesting that the enzyme might well be responsible for physiologically-relevant processing of APP in the brain. Mice over-expressing human APP<sub>[V717I]</sub> crossed with ADAM10 over-expressing mice demonstrate reduced AD pathology and alleviated symptoms (71). They produce less A $\beta$ -peptide and have a reduced plaque deposition and increased sAPP $\alpha$  production, along with an elevated learning and memory potential. In contrast, mice expressing an ADAM10 dominant-negative mutant (E384A in the zinc-binding motif) crossed with the APP<sub>[V717I]</sub> transgenic line, exhibited increased A $\beta$  production, elevated plaque deposition and vascular pathology along with defects in long term potentiation and cognition. Finally, when ADAM10 expression is knocked out or down in primary neuronal cultures, the  $\alpha$ -secretase processing of APP is reduced, suggesting that ADAM10 is indeed the primary  $\alpha$ -secretase in the brain (Reviewed in (72)).

ADAM17 is also known as tumour necrosis factor- $\alpha$  converting enzyme (TACE) and CD156q and has a structure that is extremely similar to ADAM10, with the same domains and a similarly wide substrate specificity (73). Using TACE knockout mice, Buxbaum *et al.* (74) found that ADAM17 was a primary  $\alpha$ -secretase in the phorbol ester-regulated cleavage of APP, but not in constitutive sAPP $\alpha$  release. The potential role of ADAM17 in regulated sAPP $\alpha$  secretion is further supported by the proof that ADAM17 cleaves a synthetic APP peptide at the appropriate site, however the cleavage of full-length membrane bound APP by ADAM17, and the kinetics of the cleavage are unconfirmed. Therefore it is possible that ADAM17 is acting indirectly, encouraging  $\alpha$ -secretase proteolytic activity resulting in APP cleavage (75). ADAM17 is primarily localised to endothelial cells and astrocytes in the human central nervous system (76) and expression studies in prenatal, postnatal and mature mice showed only a partial overlap of APP and ADAM17 expression (70), suggesting that it may only have a small role in  $\alpha$ -secretase activity. In CHO cells, the use of TAPI, an ADAM17 inhibitor, showed that phorbol ester-regulated sAPP $\alpha$  secretion was inhibited at the cell surface, and partially inhibited intracellularly, suggesting ADAM17 exhibits a dual localisation (77).

A range of ADAMs (ADAMs 8, 9, 10, 12,15, 17, 19, 20, 21, 28, 30, and 33) have been found to possess an active protease domain and are involved in ectodomain shedding (63). Of these, both ADAM9 and ADAM15 have been suggested as potential sheddases of ADAM10 itself (78). Three other ADAM proteins that are capable of exhibiting  $\alpha$ -secretase cleavage of APP *in vitro* are ADAM19, ADAM33 and ADAM8 (79-81). However, even though there are a large number of ADAMs implicated in the  $\alpha$ -shedding of APP, it is ADAM10 that is thought to be most physiologically relevant in the pathogenesis of AD.

## 1.5. Lipid rafts and APP proteolysis

Lipid rafts are membrane microdomains rich in cholesterol and sphingolipids, which can cluster proteins involved in specific cellular processes (82). It has been suggested that the amyloidogenic processing of APP preferentially takes place in these structures. An association of both APP and BACE1 with lipid rafts has been demonstrated (83, 84). Also, cross-linking APP and BACE1 at the cell surface co-localises these proteins to lipid rafts with a concomitant elevation in A $\beta$  production (85). This effect was no longer apparent when lipid rafts were disrupted by cholesterol depletion. The subsequent processing of APP in lipid rafts by  $\gamma$ -secretase has also been suggested, based on the fact that inhibition of  $\gamma$ -secretase activity can increase the abundance of APP C-terminal fragments in the raft fraction (86). In contrast, the non-amyloidogenic processing of APP is thought to occur within the non-raft region of the membrane (Reviewed in (87)).

As previously discussed, one of the most important genetic risk factors for AD is the possession of the apolipoprotein E (ApoE)  $\epsilon$ 4 allele (88). ApoE has a number of identified functions including roles in cholesterol transport and metabolism, and receptor mediated uptake of lipoproteins (Reviewed in (89)). ApoE has also been shown to interact with A $\beta$  and to co-localise with A $\beta$  in lipid rafts in the AD brain (90, 91).

## 1.6. The physiological role of APP and its metabolites

A definite physiological function for APP remains to be determined, but the protein might be involved in many aspects of general cell maintenance and growth, especially in neurons (45). Equally, the physiological role of APP may be mediated by either the full-length holoprotein or by means of the proteolytic fragments generated via the amyloidogenic or non-amyloidogenic pathways. Some potential functions of the protein are discussed below.

### 1.6.1. Functions of the APP holoprotein

A triple knockout in mice of APP and the APP-like proteins (APLP), APLP1 and APLP2 resulted in 100% mortality, suggesting that APP-like proteins are essential for survival and/or embryogenesis (92). Knocking out the APP gene in mice also results in reduced body and brain size, impaired long term potentiation, reduced grip strength, increased corpus callosum degeneration and an increase in seizure frequency (93).

It has been proposed that APP is a contributor to the maturation and differentiation of neurons as it is up-regulated during these processes (Reviewed in (94)). The same authors also demonstrated enhanced anterograde transport of APP to synapses where levels of APP secretion correlated with synaptogenesis. APP knockdown in zebra fish causes defective axonal outgrowth, suggesting that the protein also has a key role in this process (95). Furthermore, the retina of APP knockout mice exhibit reduced neuronal development and inner retinal circuitry but without any deleterious effects on visual function (96). This again suggests a role for APP in the establishment of neuronal networks.

A role in neuroprotection has been suggested as another putative physiological function of APP, as a number of experiments involving the reduction of APP levels have resulted in reduced cell survival and elevated apoptosis. However, this effect was not consistent across studies utilizing different models (Reviewed in (97)). The role of APP in neuroprotection will be discussed in more detail in subsequent sections in the current report relating to individual APP metabolites.

Using quantitative immunofluorescence, Szpankowski *et al.* (98) demonstrated that in murine hippocampal cells, the level of APP correlated with levels of the kinesin-1 light chain and the heavy chain of cytoplasmic dynein within axonal vesicles. Furthermore, genetic

reduction of APP reduces the association of these motor proteins with vesicles carrying APP cargoes, suggesting that the protein may regulate its own vesicular axonal transport.

APP has also been associated with the generation and modulation of synapses. APP over-expression experiments *in vivo* suggest that the protein can increase activity of L-type calcium channels which, concomitantly, increases medium after hyperpolarisation (mAHP) and lowers excitability of the APP-expressing neurons (Reviewed in (99)). This function of APP in the maintenance of neuronal calcium homeostasis indicates that the protein plays an influential role in synaptic transmission. A role for APP has also been suggested in the regulation of dendritic spine structure and functions, the loss of which are common in learning and memory deficits (Reviewed in (99)). Both long term potentiation (LTP) and long term depression (LTD), which underlie the processes of learning and memory and require synaptic plasticity, have also been shown to be affected by APP over-expression and deficiency (Reviewed in (99)). Knockdown of APP, APLP1 and APLP2 in a cell-culture system identified a significant down-regulation of methionine adenosyltransferase II alpha (MAT2A) following a comprehensive proteomic study (100). As MAT2A is involved in the process of neurotransmitter methylation this study further implicates APP in the regulation of synaptic function.

APP may also play a role in cell adhesion, as it is able to bind to collagen I, laminin and glycosaminoglycans (101) and has been found in adhesion patches associated with integrins (102). An RHDS sequence located within the A $\beta$  domain has been directly associated with this cell adhesion property (103).

An initial association of APP with the innate immune system has been suggested by Puig *et al.* (104) who used gut ileum tissue from wild-type and APP knockout mice to show that the protein regulated immune cell phenotype, their secretions and general intestinal function.

APP has also been implicated in the binding and homeostasis of copper. This concept will be discussed in detail in later sections within the current review.

### **1.6.2. Functions of the APP cytosolic domain**

A wealth of data has been generated implicating APP as a cell surface receptor, able to initiate downstream signalling cascades via the YENPTY motif in the cytosolic domain of the protein (45). Whether such cascades are initiated via the full-length holoprotein containing the cytosolic domain, or via the truncated C-terminal fragments (predominantly C83 and C99), remains to be fully elucidated.

Firstly, it has been suggested that APP may act as a G-protein coupled receptor. Okamoto *et al.* (105) used a phospholipid vesicle system to demonstrate that N-terminal APP ligand binding (in this case, mimicked using the 22C11 anti-APP N-terminal antibody) stimulated activation of the  $G_0$  complex; a process dependent on residues His657-Lys676 in the cytosolic domain of APP<sub>695</sub>. This suggests that it is this C-terminal region of APP which associates with the  $G_0$  complex. However, this proposal is controversial, as similar *in vivo* experiments actually resulted in decreased  $G_0$  activation (106). Nonetheless, in both cases, an interaction between the cytosolic domain of APP and the  $G_0$  complex was demonstrated, suggesting that the role of APP as a G-protein coupled receptor should be investigated further.

The  $G_0$  complex is coupled with signalling cascades involved in the regulation of calcium channels and apoptosis, and therefore, may be a driver of these activities. Indeed, evidence supports a role for APP-G-protein signalling in apoptosis, as substitutions of APP's Val642 for Ile, Phe or Gly results in G-protein dependent apoptosis and ligand independent activation of  $G_0$  (Reviewed in (107)).

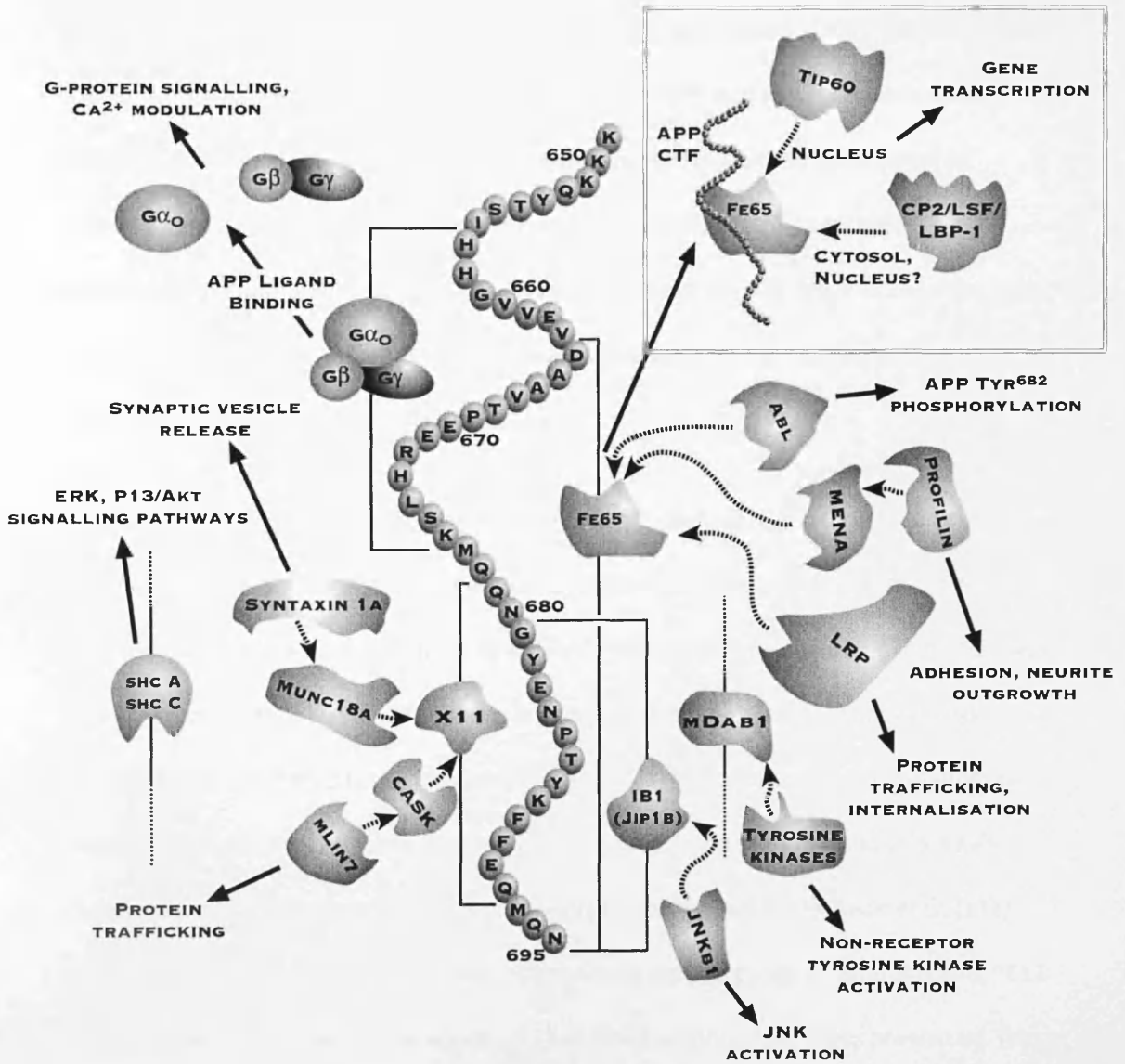


Figure 1.6. Protein binding interactions of the amyloid precursor protein intracellular domain. Proteins which interact with specific regions of the intracellular domain are shown, and their subsequent interacting partners and the potential physiological consequences of these interactions are also described. The green square isolates the interactions dependent on the release of the APP C-terminal fragment from the membrane into the cytosol (Adapted from Turner *et al.* 2003 (107)).

APP, or its C-terminal fragments can interact with various adaptor proteins (*Fig. 1.6*) including X11, Fe65, Dab1, c-Abl, Shc, JIP-1, Numb and Grb2, some of which may influence the secretase-mediated proteolysis of APP itself or be involved in other processes such as neuronal cell migration, axonal elongation and dendritic arborisation (108). The Shc and Grb2 proteins are SH2 and PTB interacting adaptors, so APP may initiate downstream signalling cascades through these adaptors, likely through influencing the MAPK/ERK pathway but also possibly through ras, PI3K and JNK signalling pathways (109). The aforementioned adaptor proteins are involved in the induction of a range of cellular events which are detailed in *Table 1.1*. This could indirectly involve APP in regulation of all of these cellular events, through initiation of signalling.

Experiments performed using *Drosophila* sLNV neurons showed that the over-expression of human APP stimulated axonal extension and arborisation, the effect of which was traced to the YENPTY motif in the cytosolic domain of the protein (110). This effect was only apparent when the cytosolic domain was membrane bound and not once the soluble AICD had been generated (111). Phosphorylation of APP at Thr668 (APP<sub>695</sub> numbering) can stimulate the localisation of APP into neuritic-like processes in neuronal and COS-1 cell systems, and the consequential stimulation of process extension (112). Ando *et al.* (113) demonstrated that phosphorylated APP localises to the growth cones of differentiating PC12 cells and that differentiation was impaired when APP phosphorylation was prevented. These data indicate a role for phosphorylated APP in neuronal outgrowth during differentiation.

<b>Adaptor protein</b>	<b>Involved in</b>	<b>Reference</b>
X11/Mint	Regulation of neuronal signalling, trafficking and plasticity, and modulation of APP processing	Rogelj <i>et al.</i> 2006 (114)
Fe65	Synaptic plasticity	Schettini <i>et al.</i> 2010 (50)
Dab1	Endocytosis, cellular growth, proliferation, homeostasis	Pilecka <i>et al.</i> 2007 (115)
c-Abl tyrosine kinase	Regulation of the actin cytoskeleton, regulation of the cell cycle, regulation of the apoptotic/cell cycle response to stress, development of the central nervous system	Schlatterer <i>et al.</i> 2011 (116)
Shc	Early cardiovascular development, neuronal differentiation, lifespan determination	Wills and Jones 2012 (117)
JIP-1	Regulating JNK signalling, axonal transport	Koushika S.P. 2008 (118)
Numb	Cell fate determination, cell division, endocytosis, cell adhesion, cell migration and ubiquitination of substrates	Gulino <i>et al.</i> 2010 (119)
Grb2	Cell cycle progression, actin-based cell motility, epithelial morphogenesis, angiogenesis and vasculogenesis	Giubellino <i>et al.</i> 2008 (120)

**Table 1.1. The physiological processes associated with APP adaptor proteins.**

### 1.6.3. Functions of sAPP $\alpha$

Most of the detrimental effects seen in APP knockouts can be reversed by application of sAPP $\alpha$ , suggesting that this fragment carries out the majority of the functional activities associated with APP (121).

sAPP $\alpha$  is thought to promote neurite outgrowth, synaptogenesis and cell adhesion and may also be involved in learning and memory (122). The fragment is also involved in cell growth, proliferation and migration, and is involved in the migration of neuronal precursors to the cortical plate and in the regulation of stem cell differentiation (58).

Decreasing APP expression in fibroblasts resulted in a reduced growth rate that could be corrected by the addition of recombinant sAPP $\alpha$  (123). This growth promoting activity was thought to be mediated by a pentapeptide sequence (RERMS) located between residues 403 and 407, inclusive, of APP (124). Caille *et al.* (125) demonstrated, *in vivo*, that an sAPP $\alpha$  fusion protein enhanced the proliferation of EGF-responsive progenitors in the subventricular zone of the adult brain, and that the inhibition of endogenous  $\alpha$ -secretase activity had the opposite effect. The authors proposed that these effects were mediated by sAPP $\alpha$ -enhanced epidermal growth factor (EGF) activity. sAPP $\alpha$  also regulates basal cell proliferation in the skin epidermis and the differentiation and proliferation of thyroid follicle epithelial cells (111).

It is thought that the activation of MAPK/ERK signalling by sAPP $\alpha$  might form the molecular basis by which the fragment enhances cell proliferation (126). Demars *et al.* (127) identified a growth factor-like activity of sAPP $\alpha$  in neural progenitor cells, mesenchymal stem cells and human decidua parietalis placenta stem cells, which acts independently of EGF and basic fibroblast growth factor but in conjunction with ERK/MAPK signalling pathway. This sAPP induced proliferation may be mediated by its ability to bind to a proteinaceous

endothelial cell surface receptor within membrane raft microdomains to induce an intracellular signalling cascade (128). Another factor involved in the role of sAPP $\alpha$  as a growth promoter is likely to be its possession of various growth factor like- and heparin binding- domains.

sAPP $\alpha$  has been shown to have a neuroprotective function by Corrigan *et al.* (129). The authors demonstrated that, compared to wild-type mice, APP knockout mice exhibited greater hippocampal damage and lesion volume when subjected to moderate, controlled cortical impact injury. The knockout mice also subsequently demonstrated increased impairment of motor and cognitive function and all of these detrimental effects could be alleviated by the introduction of exogenous sAPP $\alpha$ . A neuroprotective role for sAPP $\alpha$  is further suggested by the fact that the injection of this fragment into rat brains following traumatic injury enhances motor and cognitive function (97).

sAPP $\alpha$  may also be involved in the maintenance of synapses. Using an APP knockout mouse model, Tyan *et al.* 2012 demonstrated that, when APP was depleted, spine density was decreased and that this effect could be partially restored by exogenous sAPP $\alpha$  (130). The authors also observed a reduction in apical dendritic length and arborisation in the hippocampus of aged mice upon APP knockout, with an accompanied reduction in LTP.

At the molecular level, sAPP $\alpha$  has also been shown to inhibit the stress-activated JNK signalling pathway, preventing the death of PC12 cells (131), and to protect neurons against the effects of oxygen-glucose deprivation (132). The mechanism of this action is believed to be linked to the ability of sAPP $\alpha$  to inhibit calcium currents and increase potassium currents in order to stabilize the membrane potential of neurons. sAPP $\alpha$  is also associated with a range of cell survival signalling pathways including the PI3K/Akt, NF- $\kappa$ B, ERK and p38 mitogen-activated protein kinase/MEF2 pathways (97). In addition, the enhancement of a

range of gene products associated with neuroprotection has been linked to increased sAPP $\alpha$  levels including MnSOD, peroxiredoxin-2, catalase, insulin-like growth factor 2 and insulin-like growth factor-binding protein 2 (97).

sAPP $\alpha$  may even have the ability to protect cells against starvation-induced cell death by disrupting the dimerization of the APP holoprotein itself (133). It has been suggested that trans dimerization of full-length APP via the E1 domain may take place across the synaptic cleft and be involved in signal mediation, and that sAPP $\alpha$  might act as a competitive inhibitor of these processes (134).

#### **1.6.4. Functions of sAPP $\beta$**

sAPP $\alpha$  only contains 17 more amino acids than the alternative secreted ectodomain, sAPP $\beta$ , and most of the regions attributed to its functions are present on both fragments. However, sAPP $\alpha$  is decidedly more functionally active than sAPP $\beta$ , perhaps due to the heparin binding domain located at the C-terminal of sAPP $\alpha$  but not sAPP $\beta$  (107). Nevertheless, sAPP $\beta$  has been specifically implicated in a small number of physiological events.

A knock-in of a recombinant sAPP $\beta$  protein in mouse models does not rescue the lethality and neuromuscular junction defects of a double APP/APLP2 knockout, suggesting that the soluble APP $\beta$  derivative of APP does not possess a comparable protective effect to its  $\alpha$ -derivative counterpart (135). However, in the same models, sAPP $\beta$  up regulated transthyretin and Klotho gene expression. Transthyretin is a carrier of the thyroid hormone thyroxine and is therefore involved in regulation of metabolism (136), whereas Klotho is a membrane bound enzyme which has been shown to extend ageing, perhaps through resistance to oxidative stress (137), relating sAPP $\beta$  production to metabolism and ageing.

sAPP $\beta$  seems to be involved in axonal pruning and induction of neuronal death through the activation of death receptor 6 and caspase activity (138). The fragment has also been shown to decrease cell growth in neuronal B103 cells (139). Furthermore, Freude *et al.* (140) identified sAPP $\beta$  as a driver of human embryonic stem cell differentiation towards a neural cell fate.

### 1.6.5. Functions of the soluble AICD

The combined cleavage of APP by  $\alpha$ - or  $\beta$ -secretases and the  $\gamma$ -secretase complex is thought to represent an 'outside-in' signalling pathway referred to as regulated intramembrane proteolysis (RIP), resulting in the intracellular generation of the soluble AICD fragment (141).

Although different lengths of AICD can be generated depending on the site of  $\gamma$ -secretase cleavage, all of the generated fragments possess the YENPTY motif, enabling binding to adaptor proteins such as Fe65 and the subsequent enhancement of fragment stability (142). Through recruitment of the histone deacetylase TIP60 and, potentially, CP2/LSF/LBP-1, and subsequent nuclear translocation, this complex can activate genes such as p53, GSK3 $\beta$ , neprilysin, EGFR, KAI, LRP and APP itself (121, 142-144). Thus, AICD generation seems to be linked to various cellular processes including the regulation of the cell cycle, metabolism, neuronal cell development, protein degradation, cell proliferation and lipid homeostasis (121, 142-144). Genes involved in calcium regulation and cytoskeletal dynamics such as transgelin,  $\alpha$ 2actin, and tropomyosin can also be activated by this mechanism (142, 143).

The AICD may exhibit a cytotoxic behaviour either directly or through the subsequent generation of smaller cytotoxic proteolytic fragments (reviewed in Zheng and Koo (142)).

## 1.6.6. Functions of $\beta$ -amyloid peptides

Whilst, at high concentrations  $A\beta$  is toxic to cells, at the lower concentrations found in normal brain tissue the peptides may actually have beneficial effects (145, 146).  $A\beta$  appears to provide protection to neurons at picomolar concentrations, potentially through multiple mechanisms involving insulin like growth factor-1, PI3K/Akt, ERK1, ERK2 and/or protein kinase C signal transduction pathways and transcriptional regulation by cAMP response element-binding (CREB) protein (reviewed in (146)). Furthermore, the inhibition of  $A\beta$  generation has been shown to impair growth in a range of cell lines and this detrimental effect can be reversed, at least in neuronal cells, through the addition of exogenous  $A\beta$  (147). Furthermore, Whitson *et al.* (148) showed that a peptide consisting specifically of residues 1-28 of  $A\beta$  enhanced the survival of hippocampal pyramidal neurons *in vitro*. Surprisingly  $A\beta$  has even been linked specifically to the protection of cells *in vitro* against oxidative damage induced by copper and iron, but not hydrogen peroxide ( $H_2O_2$ ) (149).

$A\beta$ -peptides may also play a role in synaptic plasticity as picomolar levels are capable of enhancing LTP in mouse hippocampus (whereas nanomolar concentrations impair LTP) (150). These proteolytic fragments may also influence the transport and/or metabolism of lipids through their ability to interact competitively with lipid binding sites on ApoE (151). In fact,  $A\beta$  has been shown to inhibit cholesterol from binding to low density lipoprotein (LDL), which prevents cholesterol transport into cells and therefore reduces intracellular cholesterol levels (152).

## 1.7. APP and metals - copper

Copper is an essential component of many enzymes and proteins and vital for energy metabolism (153). The metal is widely distributed around the body, with the highest concentrations found in the kidney and liver, closely followed by the brain, suggesting that

copper is of great importance in this latter organ (153). However, when present in excess, the metal is cytotoxic, making copper homeostatic mechanisms of paramount importance for healthy cells, especially for those cells located in organs containing high levels of copper. Over the last decade it has become increasingly apparent that APP is closely linked to the metabolism of copper and may have a physiological role in the homeostasis of the metal and/or the protection of cells against copper-mediated toxicity (154-156). The links between APP and copper are discussed below.

### **1.7.1. Copper binding to the APP ectodomain**

Residues 124-189 of the APP E1 domain have been identified as a copper binding domain (E1 CuBD), the structure of which has been determined using nuclear magnetic resonance spectroscopy. It consists of an  $\alpha$ -helix and a triple stranded  $\beta$ -sheet, imparting a fairly rigid structure to the domain (154). The structure of the E1 CuBD is classified as a Type 2 non-blue Cu(II) centre, utilising a number of nitrogen and oxygen atoms in ion binding. Residues His147, His151 and Tyr168 have been implicated in Cu(II) binding with a  $K_d$  of 10 nM whilst Met170 is thought to be involved in the reduction of Cu(II) to Cu(I) *in vitro* (157, 158). The E1 CuBD has a surface location, and its structure demonstrates a putative ability to transfer copper ions, suggesting a possible role in transfer of copper ions to and from other proteins (154).

Dahms *et al.* (159) also identified a copper binding domain in the E2 region of APP (E2 CuBD) in which four histidine residues (His313, His382, His432 and His436) appear to coordinate Cu(II) competitively with Zn(II) at physiological concentrations. Binding of copper within this E2 domain of APP causes a large structural conformational change, suggesting that copper binding to the membrane bound holoprotein may impact on its interaction with other proteins, both intra- and extra-cellularly.

### 1.7.2. Copper-mediated APP expression

When Lin *et al.* (160) treated PC12 cells with 50 and 100  $\mu$ M copper, they noticed an increase in APP transcription levels, which decreased when the copper concentration was raised further to 200  $\mu$ M. Treatment of these cells with the antioxidant and metal chelator, curcumin, resulted in almost a complete prevention of the copper induced increase in APP transcription. The transcriptional effects of copper on APP were also reduced using alternative antioxidants suggesting that it was the oxidative activity of copper which induced APP transcription.

Cater *et al.* (161) found that, in copper deficient cells, APP mRNA levels were reduced whereas the APP protein level was maintained, suggesting that copper deficiency may increase the rate of APP translation. Similarly, Armendariz *et al.* (162) used cells that contained abnormally high levels of copper to demonstrate that steady-state APP gene expression was up-regulated by the metal. This effect was also seen when control cells were treated with copper, suggesting that both endogenous and exogenous copper can regulate APP expression. Bellingham *et al.* (163) found that cells depleted of copper, as a consequence of increased copper efflux, exhibited a decline in APP mRNA levels with a concomitant decline in APP protein levels. The authors also identified the site of a copper responsive regulatory element within the *APP* gene promoter region between nucleotides -490 and +104.

These *in vitro* data have been supported by *in vivo* work performed by Mao *et al.* (164) in Sprague-Dawley rats. These results also implicated copper in up regulation of APP expression and potentially  $\beta$ -processing of the protein. The rats were supplied with copper enriched drinking water for three months, and the treated rats suffered cognitive impairment in comparison to controls. This cognitive decline was accompanied by increased

APP and BACE-1 mRNA and protein levels, which returned to normal upon cessation of treatment.

### 1.7.3. Copper-mediated APP proteolysis

Copper binding to the APP ectodomain may also be involved in the regulation of its proteolysis. Spoerri *et al.* (165) demonstrated that mutation of histidine residues 147, 149 and 151 to asparagine within the APP E1 CuBD decreased production of sAPP $\alpha$ , sAPP $\beta$  and A $\beta$ . These mutants demonstrated a decreased maturation of the holoprotein, perhaps due to impaired ER-to-Golgi trafficking, suggesting that copper binding at the E1 CuBD may be involved in these processes.

The addition of extracellular copper (2-5  $\mu$ M) to SH-SY5Y cells can attenuate A $\beta$  production (166) as the metal appears to disperse APP and  $\gamma$ -secretases from lipid rafts and promote localisation of the former to the cell surface through inhibition of flotillin-2-mediated endocytosis. This promotes  $\alpha$ -secretase as opposed to  $\beta$ -secretase cleavage of the protein. It appears that the reverse may be true in the AD-afflicted brain where free copper levels are reduced, promoting A $\beta$  production and concomitant A $\beta$  and copper co-localisation in lipid rafts (167). Borchardt *et al.* (168) also demonstrated that copper attenuated A $\beta$  production in a Chinese-hamster ovary (CHO) cell model, where copper supplementation resulted in decreased A $\beta$  production and a consequential increase in the production of sAPP $\alpha$  and p3 through the alternative processing pathway. Conversely, Baumkotter *et al.* (134) suggested that copper might be involved in the dimerization of APP leading to an increased generation of A $\beta$ -peptides.

The APP secretase, BACE-1, has been shown to interact directly with copper via its cytoplasmic domain and, indirectly, through interaction with the copper chaperone for

superoxide dismutase-1 (169). However, whether such interactions result in altered APP proteolysis remains to be determined.

Cater *et al.* (161) also showed that human fibroblast cells genetically prone to copper accumulation preferentially produced sAPP $\alpha$ , whereas those prone to copper deficiency primarily processed APP via the amyloidogenic pathway. Copper deficient SH-SY5Y neuroblastoma cells also produced elevated levels of A $\beta$ , but did not exhibit alterations in APP expression levels or in production of the alternate proteolytic fragments, suggesting that the observed effect may have been due to the inhibition of A $\beta$  degradation.

An *in vivo* model using transgenic APP23 mice which have elevated APP expression levels, demonstrated that increased availability of copper decreased the CNS A $\beta$  levels and plaque burden (170). Transgenic toxic-milk (Tx<sup>l</sup>) and CRND8 mice provide further evidence that elevated copper levels may attenuate A $\beta$  production (171). The Tx<sup>l</sup> mice express a mutant ATPase7b which favours cellular copper accumulation and CRND8 mice are an AD model with a heavy A $\beta$  plaque burden. Studies using these transgenic mice demonstrated that elevated intracellular copper levels resulted in a decreased plaque burden and plasma A $\beta$  levels with a concomitant increase in survival. However APP holoprotein, sAPP $\alpha$  and A $\beta$  levels in total brain were not significantly different between control and transgenic mice. So although the reduction in plaque burden and plasma A $\beta$  levels could be due to a reduced production of A $\beta$ , it could also be explained by increased clearance of peripheral A $\beta$  pools.

#### **1.7.4. APP and copper homeostasis**

APP may be involved in copper efflux and homeostasis, as over-expression of the protein in mice resulted in reduced brain copper levels and reduced superoxide dismutase 1 activity, which could be corrected by supplementing drinking water with copper (170). Consistent with this effect, increased brain copper concentrations have been observed in

APP knockout mice (156). Post-mortem AD brain tissue also showed reduced copper levels in comparison to controls, possibly due to enhanced APP levels in the disease-afflicted brain (171).

When a peptide replicating residues 18-350 of the APP extracellular domain was over-expressed in yeast cells, intracellular copper concentrations were reduced by approximately 40%, suggesting that it is this E1 CuBD in the extracellular domain of APP specifically that is involved in copper efflux (156). When a similar peptide containing histidine to asparagine mutations at positions 147, 149 and 151 (within the E1 CuBD) was employed, intracellular copper levels were enhanced, implicating these copper binding residues specifically in the ability of APP to enhance cellular copper efflux.

Cerpa *et al.* (172) demonstrated that, when a synthetic peptide consisting of the APP E1 CuBD (residues 135-156), was co-injected with copper into the brains of mice, the peptide prevented the normal neurotoxic effects of the metal and prevented the associated behavioural changes. This suggests that the APP E1 CuBD has a role in protection against neurotoxic copper concentrations. In seeming contradiction of this theory, neurons derived from APP knockout mice are less sensitive to copper toxicity than wild-type neuronal cultures, suggesting that APP may actually promote the toxic effects of copper in a tissue/cell dependent manner (173); a function which has been attributed to the reduction of Cu(II) to Cu(I) by the cysteine residue of the CuBD (174).

Indeed, over-expression of APP does appear to enhance the reduction of extracellular Cu(II) to Cu(I) in HEK293 cells (175). Both APP over-expression and provision of APP135-155 peptides comprising the E1 CuBD of the protein by Suazo *et al.* (175) assisted with Cu uptake into HEK293 cells, pinpointing this region as crucial for this function. However, those cells over-expressing APP were significantly more viable upon exposure to

exogenous copper, suggesting that the reduction and uptake of copper has a protective function, perhaps by creating a 'copper sink' so that ROS production cannot take place.

In Tg2576 mice, which over-express the Swedish mutant form of APP and therefore accumulate A $\beta$  plaques exponentially over their lifespan, brain copper levels are reduced by ~16% by 16 months (176). This effect was coupled with reduced zinc, elevated manganese and unchanged iron levels using age- and sex-matched controls. Follow-up experiments using TgC100.wt mice, which over-express the C-terminal 100 amino acid residues of APP, including the A $\beta$  region, demonstrated trends of reduced copper and iron levels, increased manganese and cobalt levels, but unchanged zinc levels. This suggests that copper and other metal binding sites within the A $\beta$  region of APP, or interactions with intracellular adaptor proteins by the APP C-terminus have an important role in homeostatic metal regulation by the protein.

### **1.7.5. APP and the reduction of divalent copper**

The APP E1 CuBD binds to Cu(II) and reduces it to Cu(I) *in vitro* (177). This is likely to result in increased neurotoxicity in the brain, such as that seen in AD, due to generation of ROS and induction of oxidative damage; an effect that has been observed by White *et al.* (173) in primary neuronal cultures. In fact, Cu(I) has been shown to directly cause the lipoprotein peroxidation and free radical production that initiate neuronal damage *in vitro* (178). The sulphur atom of the Met170 residue in the APP E1 CuBD moves closer to bound Cu(II) and away from Cu(I), suggesting that this residue has a paramount role in reduction of copper (158). Multhaup *et al.* (179) implicate the generation of a disulphide bridge between cysteines 144 and 158 of APP in the reduction of copper ions. In confirmation of this supposition, mutation of Cys144 to alanine abolishes the reducing capacity demonstrated by wild-type APP (174).

However, in seeming contradiction to the work described in the previous paragraph, Cerpa *et al.* (172) demonstrated that the intra-hippocampal injection of a peptide comprising the APP E1 CuBD into rats, protected against Cu(II) induced neurotoxicity. This effect was reversed upon mutation of the Cys144 residue, but not the His147/149 residues, suggesting that APP E1 CuBD-induced reduction of Cu(II) facilitates neuroprotection in rats, when presented with exogenous copper. This effect confirms the idea previously presented by Suazo *et al.* (175) that APP may bind, reduce and transport copper into cells in order to create a sink of toxic copper which can no longer induce ROS production and oxidative damage.

The A $\beta$ -peptide itself also has metal reducing potential, with the ability to rapidly reduce Cu(II) and Fe(III) to Cu(I) and Fe(II), respectively (180). A $\beta$ /Cu complexes can generate H<sub>2</sub>O<sub>2</sub> from oxygen, which contributes to cellular toxicity (181, 182). Zinc binding to A $\beta$ , displacing Cu(II), reduces the oxidative damage caused by this peptide, suggesting a specific role for copper as the metal that drives this process. This peroxidase activity of A $\beta$  is driven by electrons donated by both the reduced Cu ion and by the Tyr10 residue of the A $\beta$ -peptide (182). Interestingly, this tyrosine residue is not present in rodent APP and these animals do not, inherently, develop AD.

The sulphur atom of Met35 is thought to be critical in the A $\beta$ -induced production of H<sub>2</sub>O<sub>2</sub>, as transgenic mice expressing human APP lacking Met631 (equivalent to the Met35 of the A $\beta$ -peptide) do not suffer the same brain oxidative damage as their wild-type APP expressing counterparts (183). However, whether or not this Met35 residue of the A $\beta$ -peptide is responsible specifically for copper induced A $\beta$  oxidation is still unclear. In fact, Ciccotosto *et al.* (184) demonstrate that mutation of this residue to valine does not decrease the Cu(II) induced production of H<sub>2</sub>O<sub>2</sub> in primary mouse neuronal cortical cells. The residues

His6, His13 and His14 are also potential candidates for the redox activity which is initiated upon binding of the A $\beta$ -peptide to copper ions (185).

In seeming contradiction to the fact that A $\beta$  enhances copper-induced oxidative damage through the reduction of metal ions, A $\beta$  present in the CSF and blood plasma has been shown to act as an antioxidant (186). When A $\beta$ 1-40 is present at 0.1-1 nM in these biological fluids, it can inhibit oxidation of CSF lipoproteins and plasma low density lipoprotein. The A $\beta$ 1-42 peptide also demonstrated an antioxidant capacity, albeit at a lower efficacy than A $\beta$ 1-40. These data suggest that, under certain conditions, A $\beta$  may chelate metal ions preventing their reduction and the associated production of toxic oxidative species. In support of this theory, Feaga *et al.* (187) confirmed that monomeric A $\beta$ -peptide bound more tightly to Cu(I) than Cu(II), suggesting that it possesses the ability to sequester this reactive ion.

#### **1.7.6. Copper in A $\beta$ aggregation**

In addition to the copper binding domains within the ectodomain of APP, the A $\beta$ -peptide itself can bind copper, with the histidine residues at positions 6, 13 and 14 thought to be involved in metal co-ordination (188).

The normal extracellular copper concentration in the brain is 0.2–1.7  $\mu$ M, whereas the concentration of copper in amyloid plaques is  $\sim$ 400  $\mu$ M (189), suggesting that the metal is involved in plaque formation (190). Indeed, in some *in vitro* experiments the interaction of copper with A $\beta$  induces its aggregation, and *in vivo* copper causes A $\beta$  deposition into amyloid plaques (191). Furthermore, it has been demonstrated that the treatment of APP Tg2576 mice with a copper/zinc chelator greatly impairs plaque formation and that mutation of the A $\beta$  His13 residue reduces the propensity of the peptide to aggregate (192, 193). Once

formed, A $\beta$  complexes containing copper are also significantly more resistant to disaggregation than metal-free peptides (194).

Furthermore, it is possible that regional copper/metal availability may be a determining factor in terms of which parts of the brain are most affected by amyloid plaque deposition. For example, both the cerebellar cortex and locus ceruleus contain relatively high copper concentrations (153) and also exhibit high levels of amyloid plaque deposition and cell loss in AD (195, 196).

It should also be noted that studies do exist suggesting that copper may actually discourage the aggregation of A $\beta$  (197). The apparent contradictions between these studies and those described earlier in this section might be explained by the propensity of A $\beta$  to bind copper depending on its aggregation state, with aggregated A $\beta$ (1-42) having a much stronger copper binding strength than its monomeric counterpart (198).

## **1.8. APP and metals – iron**

In addition to its relationship with copper (discussed above), APP is also believed to have an intimate relationship with another metal, iron. Some of the links between iron and APP are discussed below.

### **1.8.1. Iron in the expression and proteolysis of APP**

Iron appears to be involved in both the expression and proteolysis of APP. The 5'UTR region of the APP transcript contains an iron-responsive element (199). Additionally, APP translation is influenced by the same constellation of RNA-binding proteins (including the iron-regulatory proteins 1 and 2) which control ferritin translation, providing further evidence that iron and iron-related proteins are involved in the regulation of APP translation.

Moreover, Bodovitz *et al.* (200) demonstrated that in HEK293 cells, production of the neuroprotective sAPP $\alpha$  increases with iron availability, and decreases following iron chelation.

### **1.8.2. APP and the metabolism of iron**

In HEK293T cells, and in cortical tissue, APP demonstrates ferroxidase activity and is involved in iron export (201). Ablation of APP in these models promotes iron retention. In a mouse model, APP ablation not only increased intra-neuronal iron levels, but also resulted in elevated levels of oxidative stress, dependent on the ferroxidase activity of APP. This suggests that APP mediated iron-export may reduce oxidative stress in the AD brain.

### **1.8.3. Iron and the A $\beta$ peptide**

Ha *et al.* (202) demonstrated, using a solid template created by immobilizing A $\beta$  oligomers onto an N-hydroxysuccinimide ester-activated solid surface, that the metal iron can also induce the aggregation of A $\beta$ . Indeed, iron has been shown to co-localise with A $\beta$  to form the amyloid plaque core in the AD brain (203).

Additionally, Tabner *et al.* (204) demonstrated that *in vitro* the interaction between A $\beta$  and iron can result in the production of hydroxyl radicals. This suggests that the presence of iron in the human AD brain may result in oxidative damage, and contribute to A $\beta$  induced neurotoxicity.

## **1.9. The roles of APP and copper in Alzheimer's disease**

The amyloid cascade hypothesis states that an imbalance between the generation of A $\beta$  from APP, and its clearance, is responsible for AD pathogenesis (205). More recently, the specific toxic entity in AD has been identified as oligomeric A $\beta$ , rather than the amyloid plaques, which are instead thought of as a sink or a 'tombstone' for A $\beta$  (206). These soluble

oligomers are spherical in shape, 2 – 6 nm in diameter and range from dimers to 24-mers (207, 208). Cortical levels of A $\beta$ , including A $\beta$  oligomers, correlate with memory impairment.

### **1.9.1. Mechanisms of A $\beta$ -mediated neurotoxicity**

The precise mechanism of A $\beta$ -mediated cytotoxicity remains to be fully established, but there are several hypotheses in this respect. Extracellular A $\beta$  oligomers may bind to nerve growth factor receptors on the surface of neurons, triggering cellular apoptosis (208). They have also been implicated in pore formation in the plasma membrane of cells, which could lead to abnormal ion flow and potential cell death (209). A $\beta$  oligomers are also known to bind to the cellular prion protein causing synaptic dysfunction (210), or NMDA receptors causing oxidative stress and consequential synapse loss (209). The oligomers also bind insulin and Frizzled receptors (208). Binding to the insulin receptor impairs kinase activity, resulting in insulin receptor loss from the cell surface. Binding of the oligomers to the Frizzled receptor can stimulate tau phosphorylation, resulting in the formation of the other pathological hallmark of AD, NFTs. All of these effects ultimately lead to cell death.

Intracellular A $\beta$  oligomers also have the potential to stimulate cell death. Although A $\beta$  oligomers are not often intracellularly located, they can be imported into the cell by receptor-mediated endocytosis (211) and the peptides are generated in the first instance by BACE1-mediated cleavage in endosomes (212). One theory as to how intracellular A $\beta$  oligomers might exert their cytotoxicity is through their ability to inhibit proteasomal activity, resulting in the accumulation of unwanted proteins and, ultimately, cell death (213). Also, in mitochondria, A $\beta$ -peptides can interfere with electron transport chain activity, resulting in potential neuronal death and synaptic dysfunction (214).

A $\beta$ -peptides can generate reactive oxygen species (ROS) which can have devastating effects on cellular homeostasis through DNA damage and through lipid and protein

peroxidation, whilst simultaneously providing the opportunity for NFT development (214, 215). Furthermore, inflammation caused by the association of astrocytes and microglia with the A $\beta$  in amyloid plaques can have dual implications (30, 214). The inflammatory cells can fuel further A $\beta$  deposition and simultaneously trigger ROS stimulated neuronal damage.

### **1.9.2. Copper and Alzheimer's disease pathogenesis**

The link between aberrant copper homeostasis and AD has been known for some time, and meta-analysis of data confirms that serum copper levels in AD patients are, on average, higher than healthy control subjects (216, 217). Copper accumulates in amyloid plaques with high levels of  $\beta$ -sheet conformation A $\beta$  (218) and the surrounding brain tissue in AD patients appears to be depleted of copper in comparison to controls (219).

There has even been speculation that the so called AD epidemic in developed countries is due to leached copper from water pipes increasing dietary copper content and driving the onset of the disease (220). The authors of the study linked copper with Alzheimer's disease through various mechanisms. First, ApoE4, which imparts an elevated risk for AD does not bind copper, whereas the E2 and E3 isoforms do. This may suggest that the inability of the former isoform to bind and relocate copper might be linked to disease pathogenesis. Second, elevated copper ingestion in murine AD models increased brain AD-like pathology and caused a reduction in cognition. Third, APP, A $\beta$ ,  $\beta$ -secretase and Tau can all bind copper and are heavily involved with the onset of AD. Finally, the authors noted that free copper levels in the blood are inversely associated with cognition in both AD and non-AD patients.

As discussed in section 1.7.6. (above), copper has also been shown to influence the kinetics of A $\beta$  aggregation, the type of aggregation intermediate formed, and the precipitation of A $\beta$  aggregations (221). Furthermore, the binding of A $\beta$  to copper can

produce reactive oxygen species and damage plasma membranes, thereby contributing to the neurotoxicity caused by the peptides (188).

Due to the clear involvement of copper in AD pathogenesis, various copper chelating compounds have been considered for therapeutic use. The copper chelators trientine, penicillamine, bathophenanthroline and bathocuproine were shown to deplete copper and solubilise A $\beta$  in AD brain tissue (222). The metal chelator, clioquinol, was subjected to a phase II clinical trial using patients suffering from moderately severe AD, where reduced cognitive deterioration and plasma A $\beta$ 42 levels were observed following treatment (223). Another copper chelator, D-penicillamine, has been shown to reduce oxidative stress in AD patients but without positive effects on cognitive ability (224). Preliminary tests using the metal chelators cyclen and cyclam have shown that in neuronal cells these compounds can reduce the toxicity of metal-A $\beta$ 40 complexes, likely through solubilisation of aggregates, conversion of the  $\beta$ -sheet morphology of aggregates and through inhibition of H<sub>2</sub>O<sub>2</sub> production (225). Finally, curcumin and synthetic curcumin analogues have also demonstrated therapeutic potential in terms of their ability to reduce A $\beta$  aggregation *in vitro* (226).

## **1.10. The roles of APP and copper in cancer**

Although APP is known primarily for its role in AD, the protein has more recently been implicated in the pathogenesis of various cancers, as has the metal, copper. Whether a link between APP and copper exists in relation to cancer is more speculative.

### **1.10.1. APP and cancer**

APP has been recognised as a contributory factor in disease progression in a range of cancers including melanoma, oral squamous cell carcinoma, pancreatic cancer, colon

carcinoma, murine embryonal carcinoma, neuroblastoma and PCa (227-233). In oral squamous cell carcinoma tissues, APP mRNA expression has been found to be doubled in the majority of malignant samples, compared to non-cancerous matched tissues (228). Those patients with increased APP mRNA levels exhibited a lower survival rate, possibly due to the increased rate of tumour growth driven by APP expression. Similarly, APP mRNA expression has been found to be elevated by 50-fold in papillary thyroid carcinoma cells in comparison to the adjacent thyroid tissue (234). Again, higher APP levels were associated with enhanced malignant potential. A possible explanation for the increased APP expression exhibited by these malignancies could involve the role of the p53 tumour suppressor gene in the suppression of APP expression (235). If the p53 tumour suppressor gene exhibits any abnormalities, as may be the case in malignancies, it may also lose its ability to suppress APP expression, resulting in the observed elevations in APP expression. This may also explain why aberrant APP expression is not observed in all malignancies. Botelho *et al.* (227), demonstrated that, when APP expression was suppressed in a metastatic melanoma cell line, proliferation was impaired and the cells became terminally differentiated and more susceptible to chemotherapeutic intervention.

It is possible that the enhanced proliferation of cancerous cells caused by APP might be related to the ability of the protein to bind heparin (236), collagen (237) or integrins (238), all of which are components of the extracellular matrix. Adhesion has previously been shown to enhance the proliferation of keratinocytes and de-adhesion to promote differentiation (239). It has been demonstrated that APP is over-expressed and can enhance extramedullary infiltration of leukaemia cells, which decreases survival rate (240). This effect has been attributed to a role for APP in migration of these cells, likely due to its ability to adhere to the extracellular matrix. The KPI domain (residues 289-345) of APP may also contribute to proliferative activity, as neural stem cells over-expressing sAPP<sub>770</sub>, as opposed to sAPP<sub>695</sub>, showed increased proliferation (241).

It would seem that the soluble APP ectodomain, sAPP $\alpha$ , is sufficient to enhance the proliferation of many cancerous cell lines. In SW837 human colon carcinoma cells, down-regulation of APP expression resulted in a reduced proliferation that could be reversed if conditioned media containing sAPP $\alpha$  was added to the cells (230). If the conditioned media was pre-treated with an anti-APP N-terminal antibody (22C11) the reduced proliferation could no-longer be negated. The fact that the antibody 22C11 binds amino acids 66-82 at the N-terminal of APP, suggests that the extreme N-terminal of APP may directly participate in enhancing cell proliferation (230). This effect was also observed by Ohsawa *et al.* (242) in rat neural stem cells, where sAPP<sub>695</sub> stimulated proliferation through the promotion of DNA synthesis. Hansel *et al.* (243) demonstrated that, in a pancreatic cancer cell line, binding of the 22C11 antibody to sAPP could reduce proliferation, and the addition of purified sAPP could enhance proliferation of these cells (243). Notably a structural analysis of APP amino acids 28-123 has shown that this region of the protein has strong structural homology to the cysteine-rich growth factors, confirming the theory that this region of the protein may be specifically causative of cellular proliferation (244).

In fact, some lines of evidence suggest that the inhibition of sAPP $\alpha$  generation might be a suitable therapeutic intervention point for the treatment of cancer. Evidence exists to suggest that ADAM10 (the secretase responsible for sAPP $\alpha$  generation) is upregulated in melanoma metastasis (245). Furthermore, the inhibition of sAPP $\alpha$  production in psoriatic keratinocytes, using hydroxamic-acid-based zinc metalloproteinase inhibitors, has been shown to dramatically reduce cell proliferation; an effect of which could be rescued by the addition of exogenous sAPP (246).

There is also evidence to suggest that sAPP may act as a ligand to activate signalling pathways in a *trans* fashion, thereby enhancing the proliferation of cancer cells. Using the thyroid and thyroid carcinoma cell lines, RFTL- 5 and FTC-133, respectively, Krause *et al.*

(247) found that insulin and bovine thyrotropin (TSH) increased both the expression of APP and the secretion of sAPP. They also found that protein kinase C (PKC) activation increased sAPP release and postulated that sAPP activated a signalling pathway upon binding a receptor on the surface of distal cells. Evidence that sAPP binds directly to the cell surface has been generated using FRTL-5 and PC-12 cells by Hoffmann *et al.* (248). This was achieved using a recombinant form of APP (sAPPrec), which enabled visualization of its localization on the cell surface. The molecule to which sAPPrec bound to at the cell surface was sensitive to aldehyde fixation, suggesting a proteinaceous nature like many receptors in cell signalling pathways. These sAPPrec binding proteins were localised in lipid rafts on the cell surface, which is typical of glycosylphosphatidylinositol (GPI)-anchored proteins, suggesting that the receptor may be a GPI-anchored protein.

The APP ectodomain may also facilitate cancer development through the inhibition of apoptosis. Wehner *et al.* (249) demonstrated that UV-B induced apoptosis in human keratinocytes was increased by the addition of an anti-sAPP $\alpha$  antibody. The authors also showed that staurosporine-induced apoptosis could also be attenuated by the addition of recombinant sAPP $\alpha$ . This suggests that sAPP $\alpha$  may act by both inducing proliferation and inhibiting apoptosis to promote cancer cell growth.

Release of the AICD into the cytoplasm has also been associated with increased cell proliferation due to the altered gene expression induced by this proteolytic fragment of APP (247). The mRNA expression of various AICD-binding proteins (Fe65, ShcA and JIP1) has been shown to increase in thyroid carcinoma cells compared to normal thyroid cells. Furthermore, it has been suggested that these proteins aid enhanced sAPP secretion, possibly contributing to signalling via the molecule. However, in SH-SY5Y cells, over-expression of the AICD actually resulted in reduced proliferation and induced apoptosis (250). This effect may be due to the interaction of AICD with binding partners such as CUX1 and SPT5 to reduce

proliferation. The stimulation of apoptosis by the AICD in SH-SY5Y cells has been related to a direct interaction between p53 and AICD, promoting the apoptotic function of the former protein (251). Apoptosis has also been associated with caspase-mediated cleavage at amino acid 664 in the AICD and release of apoptosis inducing APP fragments into the cytoplasm (252). These contradictory data suggest that the interaction partners and consequential gene activation and phenotypic effects induced by AICD may be dependent on location and cell type, but could play a role in cancerous cell proliferation.

Finally, it is possible that A $\beta$  may inhibit cell proliferation, such that enhanced generation of sAPP $\alpha$  via the non-amyloidogenic pathway with reciprocally reduced A $\beta$  production would negate this inhibitory effect in cancer cells. Zhao *et al.* (253) used human glioblastoma, breast cancer and mouse melanoma cell lines to investigate the effects of A $\beta$  on cell proliferation. Conditioned media from cells over-expressing APP and containing increased levels of A $\beta$  caused decreased proliferation compared to untransfected cell lines. Furthermore, it was established that the inhibition of proliferation was initiated by A $\beta$  only, and not sAPP $\alpha$  or sAPP $\beta$ . However, the opposite seems to be true in human embryonic stem cells in which soluble and fibrillar (but not oligomeric) A $\beta$  have been shown to induce cell proliferation, whilst the inhibition of  $\beta$ -secretase suppressed proliferation (254). The A $\beta$ 1-42-peptide also induces the proliferation of glial cells (255) and A $\beta$ , at nanomolar concentrations, stimulates the growth of PC12 cells (256) suggesting a cell type-dependent role of A $\beta$  in relation to the stimulation or inhibition of proliferation.

### **1.10.2. APP and prostate cancer**

Takayama *et al.* (2) used chromatin immunoprecipitation (ChIP) and genome tiling array analysis to identify APP as a primary androgen target gene in the hormone-sensitive PCa cell line, LNCaP. The authors also showed that the *APP* gene contained androgen

receptor binding sites (ARBS) in its transcriptional regulation region. Androgens were found to enhance both APP mRNA and protein expression in LNCaP cells, and sAPP was found to enhance cell proliferation. Furthermore, the implantation of wild-type and APP-depleted LNCaP cells into nude mice resulted in significantly reduced tumour formation in the mice implanted with the latter. The authors also demonstrated that APP immunoreactivity in a cancerous prostate correlated with a poor prognosis.

Further evidence relating APP to PCa comes from the fact that chemical castration in men with PCa increases plasma A $\beta$  levels, associating testosterone inversely with A $\beta$  (257). Cell culture systems and rodent models have also been used to investigate the relationship between androgens and A $\beta$ , and the conclusions drawn appear to imply that androgens negatively regulate A $\beta$  levels (reviewed in Rosario and Pike (258)).

### **1.10.3. Copper and cancer pathogenesis**

Both serum and tissue levels of copper in cancer patients are elevated (data summarized in *Tables 1.2* and *1.3*). These altered copper levels can be related to disease progression and, therefore, prognosis. For example, serum copper levels of patients with hematological malignancies either in a disease progression or relapse phase were elevated, whereas those in a stable disease state or remission had normal copper levels (259). This could implicate copper as an important diagnostic marker in cancer. Indeed copper levels have been determined as a useful biomarker in order to assess the response of tumours to chemo- and radio-therapy (260, 261).

Cancer	Normal patients copper levels ( $\mu\text{g/g} \pm \text{SD}$ )	Cancer patients copper levels ( $\mu\text{g/g} \pm \text{SD}$ )	Number of subjects (significance compared to control)
Breast cancer	6.13 $\pm$ 4.32 (normal) 6.51 $\pm$ 5.33 (Benign)	11.08 $\pm$ 4.98 (Stage I) 10.10 $\pm$ 5.61 (Stage II) 17.18 $\pm$ 11.83 (Stage III)	25
Breast cancer	9.3 $\pm$ 2.3	21.0 $\pm$ 10.7	22 ( $p < 0.0001$ )
Ovarian cancer	0.2–0.9	0.4–2.8	10
Colorectal cancer	1.79 $\pm$ 0.57	2.78 $\pm$ 0.84	30 ( $p < 0.001$ )
Breast cancer	2.38	3.25	20
Breast cancer	0.29 $\pm$ 0.29 ppm	0.89 $\pm$ 0.56 ppm	40
Large bowel	1.53 $\pm$ 0.35	1.90 $\pm$ 0.6	24 ( $p < 0.05$ )
Stomach	1.44 $\pm$ 0.38	2.09 $\pm$ 0.52	7 ( $p < 0.02$ )
Ovarian	1.26 $\pm$ 0.45	2.16 $\pm$ 0.63	5 ( $p < 0.01$ )
Breast	1.58 $\pm$ 0.62	1.91 $\pm$ 0.56	8
Kidney	1.80 $\pm$ 0.42	1.61 $\pm$ 0.25	3
Bladder	1.54	2.80 $\pm$ 0.3	2
Testis	1.48 $\pm$ 0.7	1.43	1
Hodgkin's	1.42 $\pm$ 0.44	3.18	1
Total cases	1.42 $\pm$ 0.44	2.08 $\pm$ 0.76	53 ( $p < 0.001$ )
Breast cancer	1.47 ppm	5.12 ppm	15 ( $p < 0.01$ )
Stomach cancer	1.1 $\pm$ 0.4	1.7 $\pm$ 0.1	18 ( $p < 0.01$ )
Ovarian cancer	1.95 $\pm$ 0.64	2.17 $\pm$ 0.64	40
Leukemia	15 $\pm$ 4 $\mu\text{g}/10^6$ cells	52 $\pm$ 16 $\mu\text{g}/10^6$ cells	12 ( $p < 0.01$ )

**Table 1.2. Tissue copper levels in cancer.** Taken from Gupte *et al.* (262). In all but 2 studies cancer patients have elevated tissue copper levels in comparison to normal patients.

Cancer	Normal patients copper levels ( $\mu\text{g}/\text{dL} \pm \text{SD}$ )	Cancer patients copper levels ( $\mu\text{g}/\text{dL} \pm \text{SD}$ )	Number of subjects (significance compared to control)
Acute lymphocytic leukemia	114 $\pm$ 29	328 $\pm$ 74	21 ( $p < 0.01$ )
Breast cancer	115 $\pm$ 20	131 $\pm$ 20	35 ( $p < 0.01$ )
Cervical	92.9	129.3	19 ( $p < 0.001$ )
Ovarian	92.9	139.5	4 ( $p < 0.001$ )
Non-Hodgkin's lymphoma	120.4 $\pm$ 23.3	134.9 $\pm$ 42.4 (Stage I) 176.1 $\pm$ 66.3 (Stage II) 176.9 $\pm$ 37.5 (Stage III) 157.7 $\pm$ 49.6 (Stage IV)	
Breast cancer	122.4 $\pm$ 15.8	222.7 $\pm$ 44.4 (Stage I) 203.9 $\pm$ 31.3 (Stage II) 238.1 $\pm$ 36.8 (Stage III) 228.4 $\pm$ 38.0 (Total)	35
Lung cancer	100 $\pm$ 18.2	125 $\pm$ 20.2 (Stage I and II) 150 $\pm$ 33.8 (Stage III)	65 ( $p < 0.001$ )
Prostate cancer	84.1 $\pm$ 6.27	124 $\pm$ 8.3	44 ( $p < 0.01$ )
Reticulo-endothelial system	115.8 $\pm$ 13.9 (males) 118.9 $\pm$ 17.1 (females)	228.0 $\pm$ 52.4 (males) 225.4 $\pm$ 61.8 (females)	70 ( $p < 0.001$ )
(1) Lung cancer	143.0 $\pm$ 3.2	188.2 $\pm$ 14.8 (Lung)	20 ( $p < 0.01$ )
(2) Stomach cancer		171.9 $\pm$ 7.3 (Stomach)	33 ( $p < 0.01$ )
(3) Large intestine		164.7 $\pm$ 13.4 (large intestine)	22 ( $p < 0.05$ )
Colorectal cancer	98.8 $\pm$ 24.3	165 $\pm$ 33.9	30 ( $p < 0.001$ )
Leukemia	86.7 $\pm$ 25.3	132.8 $\pm$ 50.6 (Acute leukemia) 129.1 $\pm$ 49.8 (acute lymphoid leukemia) 139.9 $\pm$ 51.2 (acute non-lymphoid leukemia) 109.2 $\pm$ 45.4 (Chronic myelogeneous leukemia)	41 ( $p < 0.01$ ) 7 ( $p < 0.01$ ) 34 ( $p < 0.001$ ) 8 ( $p < 0.05$ )
(1) Oral leukoplakia	66.9 $\pm$ 22.0 (male)	(1) Oral leukoplakia 89.6 $\pm$ 19.0 (male) 95.2 $\pm$ 17.0 (female)	21 25 ( $p < 0.001$ )
(2) Squamous cell carcinoma	66.8 $\pm$ 14.0 (female)	(2) Oral cancer 108.9 $\pm$ 17.0 (male) 107.8 $\pm$ 12.0 (female)	22 ( $p < 0.001$ ) 20 ( $p < 0.001$ )
Ovarian cancer	133 $\pm$ 17.0 (Benign, $n = 42$ )	160 $\pm$ 17.0 (Stage I) 190 $\pm$ 6.0 (Stage II) 179 $\pm$ 18.0 (Stage III) 210 $\pm$ 23.0 (Stage IV)	2 4 19 ( $p < 0.001$ ) 11
Breast cancer	96.5 $\pm$ 7.3 (control) $n = 26$ 103.8 $\pm$ 8.3 (Benign) $n = 43$	125.2 $\pm$ 15.0	25 ( $p < 0.01$ )
Breast cancer	100.7 $\pm$ 40.5	172.8 $\pm$ 12.2	50 ( $p < 0.01$ )

Table 1.3. Serum copper levels in cancer. Taken from Gupte *et al.* (262). All studies demonstrate elevated copper levels in cancer patients.

As elevated copper levels have been associated with cancer progression, the use of copper chelators in the treatment of cancers has been assessed. Trial of treatment using the copper chelator, tetrathiomolybdate, with women possessing a high chance of breast cancer recurrence was carried out. It demonstrated that if copper-depletion was successful, the number of bone marrow-derived endothelial progenitor cells (EPCs) in circulation was maintained below baseline, reducing the risk of recurrence (263). This suggests that copper may assist with the survival of the risk enhancing EPCs. Not only do copper chelators alone appear to have benefits associated with reducing cancer burden, but these chelators can also enhance cancer treatment with Herpes simplex virus-derived oncolytic viruses and cisplatin (264, 265).

Interestingly, even though cancer pathogenesis correlates with elevated copper levels, it has also been associated with decreases in antioxidant activity, with catalase and superoxide dismutase (SOD) exhibiting decreased activity in colorectal cancer patients (266). This effect could imply that the reduced activity of SOD may be due to the liberation of its copper cofactor into serum/tissue, leaving SOD inactive, or that elevating copper levels may be a physiological mechanism employed to try and enable SOD to regain its antioxidative capacity.

The role of copper in the stimulation of angiogenesis has been known for some time, and is comprehensively reviewed in Gupte *et al.* (262). However, more recently, the metal has been linked to the stimulation of shedding of key cell surface proteins involved in cancer pathogenesis and to the invasion of PCa cells. Parr-Sturgess *et al.* (267) demonstrated that the metal can stimulate the shedding of the Notch ligand, Jagged1 and the cell adhesion protein, E-cadherin in the PCa cell line, PC3. This elevated shedding correlated with an enhanced invasive potential of the cells.

Whilst elevated serum and tissue copper is associated with various cancers, the link between dietary intake of the metal and cancer is less clear. Certain studies suggest that enhanced dietary copper may be beneficial in the prevention of cancer. Mahabir *et al.* (268) related an increase in dietary copper to a reduced risk of lung cancer in humans. Furthermore, supplementing the diet of rats with cupric acetate has been shown to prevent the induction of hepatoma formation by ethionine (269). Similarly, tumour incidence and burden were increased in a murine model of intestinal cancer when the animals were fed a copper deficient diet (270). Studies in rats also showed that low copper intake resulted in elevated dimethylhydrazine -induced colon tumour formation, the effect of which may have been due to the reduced activity of Cu antioxidant enzymes (271, 272). Conversely, Senesse *et al.* (273) correlated high levels of dietary copper with an increased risk of colorectal cancer in humans, and Nicodemus *et al.* (274) found that postmenopausal women who had taken copper supplements were at increased risk of getting kidney cancer. Therefore, there appears to be a relationship between copper intake and cancer risk; however this risk is likely related to the type and location of the cancer.

### **1.11. Aims of the current project**

APP and copper, individually, appear to have pivotal roles to play in both Alzheimer's disease and PCa. However, whether these roles are mutually exclusive or connected in the two conditions is less clear.

The overarching aim of the current project is to examine the relationship between APP and copper in two distinct cell models; SH-SY5Y neuroblastoma cells (in relation to AD) and Du145 cells (in relation to brain metastatic PCa). Specifically, the effects of APP over-expression and depletion on cell viability in the presence of copper are examined and the molecular pre-requisites underlying such effects are elucidated.

Firstly, I will characterize the expression and proteolysis of APP in a range of prostate cancer cell lines, and in a neuroblastoma cell line. This analysis aims to determine whether there is a pattern relating APP expression or proteolysis to cancer stage. Additionally, it will investigate the appropriateness of a range of cell lines for the general analysis of the molecular biology of APP.

Next, I will examine the effect of copper on the viability of these prostate cancer cell lines. I will also investigate the effect of copper on APP expression and proteolysis in these cell lines. This analysis will begin to investigate the relationship between copper and APP in a range of cell models.

Then, using the Du145 cell system, I will study the effect of full-length (isoform-specific) APP expression on Du145 cell viability in the presence of copper. Assuming that APP influences the viability of Du145 cells, I will express a range of APP constructs in this cell line in order to elucidate which regions of the protein are involved in this activity. These APP constructs will investigate the roles of the APP cytosolic domain, the APP  $\alpha$ - and  $\beta$ -ectodomains, the N-terminal APP copper binding domain, and the specific histidine residues within it, in this action.

An additional aim, which arose as the project developed, concerns the influence of APP on Du145 cell morphology. APP appeared to induce a morphological change in Du145 cells, and therefore I also used the constructs developed for the above analysis to determine which regions of the APP molecule are involved in this activity.

In order to consolidate the results from the above studies, a similar analysis was carried out in the SY-SY5Y cell system. In addition, the histidine residues located within an additional copper binding region (in the E2 domain) of the protein, were examined in this cell line.

Such studies of APP and copper have relevance to both neuronal viability in AD and the survival of brain metastatic PCa cells.

# 2. Materials and Methods

---

The following text is extremely faint and illegible, appearing to be a list of references or a detailed methodology section. It contains numerous small, scattered characters and words that are not readable.

## 2.1. Materials

Du145 cells were a gift from Alix Bee (University of Liverpool, UK). PC-3 and SH-SY5Y cells were purchased from the American Type Culture Collection (ATCC). LNCaP cells were a gift from Caroline Dalgliesh (Newcastle University, UK).

The anti- $\beta$ -actin monoclonal antibody, the anti-APP C-terminal polyclonal antibody and the anti-FLAG M2 monoclonal antibody were from Sigma-Aldrich (Poole, UK). The anti-APP 6E10 monoclonal antibody was from Covance (California, USA). The anti-ADAM10 (C-terminal) polyclonal antibody and the anti-ADAM17 (amino acids 807-823 of human ADAM-17) polyclonal antibody were from Merck (Nottingham, UK). The anti-sAPP $\beta$  (1A9) antibody was kindly provided by Ishrut Hussain (GlaxoSmithKline, Harlow, U.K.). The anti-APP (amino acids 66-81 of the N-terminus on the pre-A4 molecule) monoclonal antibody 22C11 was from Millipore (Watford, UK). The anti-neuron specific enolase mouse monoclonal antibody, NSE-P2 was from Abcam (Cambridge, UK). The anti-ERK1 polyclonal antibody, the anti-E-cadherin polyclonal antibody and the anti-vimentin polyclonal antibody were from R&D systems (Minneapolis, USA). The anti-caveolin polyclonal antibody was from BD biosciences (San Jose, California). All Secondary antibody peroxidase conjugates were from Sigma-Aldrich (Poole, UK).

Unless otherwise stated all tissue culture reagents were purchased from Lonza (Basel, Switzerland), all molecular biology reagents from New England Biolabs (Ipswich, UK), and all other reagents from Sigma-Aldrich (Poole, UK).

## 2.2. Molecular biology

### 2.2.1. Preparation of agar plates

Both serum and Agar (7.5 g) was added to 500 ml of 2% (w/v) liquid broth (LB) (low salt granulated) and the solution was autoclaved. Once the agar solution was cooled to 45 °C, ampicillin was added to a final concentration of 0.1 mg/ml before pouring the plates.

### 2.2.2. Bacterial transformation

XL-1 Competent *E.coli* (Agilent, California, USA) cells were thawed on ice and combined with DNA at a volume ratio of 20:1 (bacteria:DNA). The mixture was then incubated on ice for 30 min before heat shocking at 42 °C for 45 seconds and then returning to ice for another 2 min. LB (9 volumes) was added and the samples were incubated on a carousel for 1h at room temperature. The samples were then centrifuged at 3500 *g* for 1 min before removing all but 100 µl of the supernatant. The bacteria were then resuspended in the remaining sample volume, spread on agar plates and incubated at 37°C overnight.

### 2.2.3. Bacterial suspension cultures

Bacterial suspension cultures were grown in either 5 ml mini-cultures or 50 ml midi-cultures. In each case a single bacterial colony was stabbed into the cognate volume of LB containing 0.1 mg/ml final concentration of ampicillin. Cultures were then grown overnight on an orbital incubator at 37 °C.

### 2.2.4. DNA purification

DNA was extracted and purified from mini- and midi-suspension cultures using QIAGEN Plasmid Mini and Midi kits (Qiagen, Crawley, UK) according to the manufacturer's

instructions. DNA was eluted from mini- and midi-prep columns in final distilled water volumes of 50 and 300  $\mu$ l, respectively.

### **2.2.5. Spectrophotometric quantification of DNA**

DNA concentrations were determined using a Nanodrop 2000c spectrophotometer reading at a wavelength of 260 nm (Thermo Scientific, St Leon-Rot, Germany).

### **2.2.6. Agarose gel electrophoresis**

Agarose or NUsieve GTG agarose (Lonza, Basel, Switzerland) (1-3% (w/v)) was dissolved by microwaving in Tris acetate EDTA (TAE) buffer (0.8 mM Tris, 0.4 mM acetic acid, 0.02 mM EDTA, pH 8.0). After cooling to 40°C in a water bath for 30 min, ethidium bromide was added to a final concentration of 1 $\mu$ g/ml (alternatively gels were post-stained with GelRed (Biotium, Hayward, California). Gels were then poured and allowed to set for at least 30 min before transferring to a running kit containing TAE. DNA samples were prepared by diluting 1 in 6 with 6 x loading buffer (0.25% (w/v) bromophenol blue, 1 mM EDTA, 30% (v/v) glycerol, 0.25% (w/v) xylene cyanol FF, pH 8.0). Samples were loaded onto gels alongside an appropriate DNA standard (either 1 kB standards (Invitrogen, Paisley, UK) or 100 bp standards (New England Biolabs, Herts, UK)). Gels were run at 90 volts for 30-90 min. If post-staining was required, the gel was incubated in GelRed solution (1:5000, GelRed: TAE) for 30 min at room temperature on a rotating platform. The results were documented using a BioDoc-It Transilluminator and Sony Video Graphic Printer UP895MD.

## 2.2.7. Site-directed mutagenesis polymerase chain reaction (PCR)

Primers were designed and ordered from Sigma-Aldrich (Poole, UK) and resuspended according to the manufacturer's instructions in distilled water. The following reaction mixture was then prepared:

DNA (54.5 ng/ $\mu$ l)	- 1 $\mu$ l
5 x high fidelity buffer	- 10 $\mu$ l
2mM dNTPs	- 5 $\mu$ l
Forward primer (1 $\mu$ g/ $\mu$ l)	- 1 $\mu$ l
Reverse primer (1 $\mu$ g/ $\mu$ l)	- 1 $\mu$ l
Sterile dH <sub>2</sub> O	- 31.5 $\mu$ l
Phusion DNA polymerase	- 0.5 $\mu$ l

The PCR reactions were then performed in a Techne TC-312 thermal cycler (Techne Inc, New Jersey, USA) using the conditions below:

98 °C	30 sec	
98 °C	30 sec	} loop x 16
72 °C	30 sec	
72 °C	2 min	
72 °C	7 min	
10 °C	Soak	

Dpn1 (0.5  $\mu$ l) was then added to the samples followed by an additional incubation at 37 °C for 1 h.

## 2.2.8. Restriction enzyme digests / DNA linearization

DNA digest reactions were made up as shown below and incubated at 37°C overnight:

10 x restriction enzyme buffer	- 5 µl
BSA (10 µg/µl 10 x stock)	- 0.5 µl
Restriction enzyme	- 1 µl
DNA	- 0.5-2 µg
Sterile H <sub>2</sub> O	- make up to 50 µl

## 2.2.9. Ethanol precipitation of plasmid DNA

The required amount of DNA (either linearized or non-linearized) was combined with 1/10 volume of filter-sterilised 3M sodium acetate (pH 5.2) and 2 volumes of cold absolute ethanol. Samples were then mixed and incubated at -20°C for 1 h. DNA was pelleted by centrifuging for 20 min at top speed in a microfuge (4°C). The supernatant was removed and 300 µl of cold 80% (v/v) ethanol was added to the pellet before centrifuging once more at top speed in a microfuge (4°C). The supernatant was removed from the DNA pellet under aseptic conditions and the DNA was resuspended in filter-sterilized distilled water to the required concentration.

## 2.3. Mammalian cell culture

### 2.3.1. Growth incubations

SH-SY5Y cells were cultured in Dulbecco's modified Eagle's medium (DMEM) supplemented with 25 mM glucose, 4 mM L-glutamine, 10% (v/v) fetal bovine serum (FBS), penicillin (50 U/ml), streptomycin (50 µg/ml) and fungizone (2.5 µg/ml). Du-145, LNCaP and PC-3 cells were cultured in Roswell Park Memorial Institute (RPMI) 1640 medium containing the same supplements. All cells were grown at 37 °C in 5 % (v/v) CO<sub>2</sub>. For splitting, confluent flasks of cells were trypsinised and centrifuged for 3 min (1500 g) after first neutralising the trypsin by the addition of growth medium. The resultant pellets were resuspended routinely in 1 ml of growth medium for every subsequent culture to be seeded.

### 2.3.2. Freezing down cell stocks

The protocol above (section 2.3.1.) was followed but, instead of seeding cells into a fresh flask, the pellet was resuspended in 1.5 ml of 10% (v/v) dimethyl sulfoxide (DMSO) (made up in growth medium). Samples were transferred to cryovials and frozen at -80 °C for approximately 24 h before transferring to liquid nitrogen.

### 2.3.3. Cell counting

The haemocytometer and cover slip were rinsed in 70 % (v/v) ethanol then dried. The cell suspension was then loaded into the 'V' notch of the haemocytometer slide to load the sample via capillary action; this was done on both sides of the haemocytometer. The number of cells in each counting area was counted and an average taken. The average was then multiplied by 10,000 to give the number of cells per ml.

#### **2.3.4. Transient transfection using lipofectamine**

Mammalian cells were grown to approximately 80% confluence in T75 cm<sup>2</sup> flasks before removing the growth medium and replacing with a fresh 10 ml of OptiMEM (Invitrogen, Paisley, UK). The cells were then placed back in the growth incubator during preparation of DNA: lipofectamine complexes. Ethanol precipitated non-linearized DNA (8 µg) (section 2.2.9.) was resuspended in 30 µl of sterile distilled water and diluted with 470 µl of OptiMEM. In a second tube, 20 µl lipofectamine 2000 (Invitrogen, Paisley, UK) was added to 480 µl OptiMEM. Following 5 min incubation at room temperature, the DNA and lipofectamine solutions were combined and incubated for a further 20 min at room temperature. During this incubation the cells were removed from the incubator and the OptiMEM was replaced with a fresh 2 ml of the same medium. The DNA: lipofectamine complexes were then added, drop-wise, to the OptiMEM bathing the cells and the transfections were incubated for 5 h (37 °C, 5 % (v/v) CO<sub>2</sub>). DMEM or RPMI (according to the cell type used; section 2.3.1.) (5 ml) containing 30 % (v/v) FBS was then added to the flask and the cells were grown for an additional 24 h. The medium was then removed and replaced with a fresh 10 ml of complete growth medium (section 2.3.1.) before a final 24 h incubation period prior to assessing protein expression.

#### **2.3.5. Stable transfection using lipofectamine**

The protocol described above (section 2.3.4.) was performed but using 15-30 µg of linearized DNA. Stable transfectants were then selected using 150 µg/ml or 200 µg/ml final concentrations of Hygromycin B (Invitrogen, Paisley, UK) for SH-SY5Y and Du145 cells, respectively.

### **2.3.6. Stable transfection of Du145 cells using nucleofection**

The Amaxa cell line nucleofector kit L employed (Lonza, Basel, Switzerland) consists of two components; cell line nucleofector solution L (2.25 ml) and supplement (0.5 ml). The two components were combined to form the working reagent. Linearized ethanol precipitated DNA (2.5 µg) (section 2.2.9.) was resuspended in 4 µl of distilled water and combined with 100 µl of the nucleofector kit L working reagent. Du145 cells cultured to confluence in 6-well plates were harvested as described in section 2.3.1. and any residual growth medium was removed from the cell pellets using a Gilson pipette. The cell pellet was then resuspended directly in the nucleofector kit L working reagent/DNA solution and transferred into an Amaxa certified kit cuvette. The cuvette was placed in the Nucleofector 2b device (Lonza, Basel, Switzerland) and program A-23 was run. The cells were then gently transferred from the cuvette into the wells of a 6-well plate containing 2 ml of pre-equilibrated (37°C) growth medium. Cells were then incubated under normal growth conditions (37 °C, 5 % (v/v) CO<sub>2</sub>) for 48 h before stable transfectants were selected using a 200 µg/ml final concentration of Hygromycin B.

### **2.3.7. Stable transfection using electroporation**

Linearized DNA (30 µg for SH-SY5Y cells and 20 µg for Du145 cells) was ethanol precipitated (section 2.2.9.) and resuspended in 30 µl of sterile distilled water. A T75 cm<sup>2</sup> flask of cells was then harvested (section 2.3.1.) and the cell pellet was resuspended in 800 µl of OptiMEM and transferred, along with the 30 µl of DNA to an electroporation cuvette (Fisher, Loughborough, UK). The cuvette was then incubated on ice for 10 min before electroporating the cells in a gene pulser Xcell electroporator (Bio-Rad, Hertfordshire, UK). The following electroporation parameters were utilised:

- SH-SY5Y cells - 'square wave' program
- 120 V
- 25 ms
- 0.2 cm cuvette width

- Du145 cells - 'square wave' program
- 200 V
- 50 ms
- 0.2 cm cuvette width

Following electroporation, the cuvette was incubated on ice for a further 10 min.

The transfected cells were then transferred to 5 ml of complete growth medium in a 50 ml Falcon tube to allow effective resuspension by repeated pipetting before adding the mixture to another 10 ml of complete growth medium in a T75 cm<sup>2</sup> flask. The cells were then incubated under normal growth conditions (37 °C, 5 % (v/v) CO<sub>2</sub>) for 24 h after which the medium was removed and replaced with a fresh 10 ml of complete growth medium. The selection of stable transfectants was commenced 48-72 h post-transfection using 150 µg/ml and 200 µg/ml final concentrations of Hygromycin B for SH-SY5Y and Du145 cells, respectively.

### **2.3.8. Small interfering RNA (siRNA) transfection of Du145 cells**

Du145 cells were seeded at  $6.6 \times 10^4$  cells per well of a 6-well plate in antibiotic and fungizone free RPMI containing 10% (v/v) FBS and grown overnight. The growth medium was then replaced with 2 ml of UltraMEM (Lonza, Basel, Switzerland) and the cells were subsequently incubated for an additional 30 min.

Smart pool siRNA was purchased from Thermo Scientific Dharmacon (St Leon-Rot, Germany) and consisted, specifically, of non-targeting #1 siRNA control pool (Cat. No. D-001206-13-05) and human APP targeting siRNA SMARTpool (Cat. No. M-003731-00). The siRNA's were reconstituted in RNase-free water to a 5  $\mu$ M stock. For each transfection, the siRNA stock (2.5  $\mu$ l) was then diluted with 47.5  $\mu$ l UltraMEM. In a separate tube, Dharmafect 1 reagent (1  $\mu$ l) (Thermo Scientific, St Leon-Rot, Germany) was diluted with 49  $\mu$ l UltraMEM. Both tubes were incubated at room temperature for 5 min and then combined prior to a further 20 min incubation at room temperature. The Dharmafect: siRNA complexes were then diluted by the addition of 400  $\mu$ l of antibiotic and fungizone free RPMI containing 10% (v/v) FBS.

The previously equilibrated Du145 cells were removed from the incubator and the existing medium discarded prior to transferring a 500  $\mu$ l aliquot of Dharmafect: siRNA complexes to each well. The cells were grown for 24 h prior to the start of copper treatments.

For the copper treatment of siRNA-transfected Du145 cells copper: glycine complexes were prepared by dissolving solid  $\text{CuCl}_2 \cdot 2\text{H}_2\text{O}$  to a final 10 mM concentration in a 100 mM glycine solution. This copper: glycine stock solution (or 100 mM glycine alone as a control) was added directly to the existing 500  $\mu$ l of Dharmafect: siRNA complexes on cells to achieve final metal concentrations of 0 or 200  $\mu$ M. The treated cells were then incubated for an additional 48 h before analysing cell proliferation or harvesting cells and medium for protein analysis.

## 2.4. Protein analysis

### 2.4.1. Preparation of concentrated conditioned medium samples and cell lysates

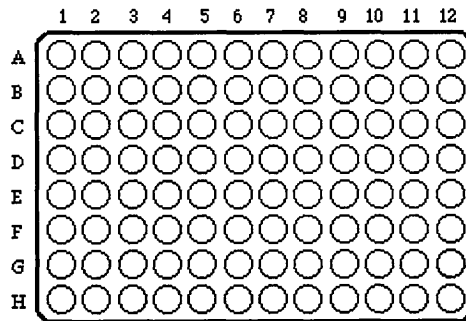
Conditioned medium was removed from cells and centrifuged at 1500 *g* for 5 min in order to remove cell debris. The supernatants were then concentrated in centrifugal concentrators (Sartorius, Epsom, UK) to a final volume of 200-500  $\mu$ l before, where required, determining total protein concentrations (section 2.4.2.) and equalizing protein levels between samples before freezing at -20°C pending further analysis.

The cell monolayers were then washed *in situ* with 20 ml of PBS. The initial PBS was then removed and the cells were scraped into a fresh 10 ml of the same buffer before transferring them into a 50 ml Falcon tube. Residual cells were washed from the culture flask in a further 10 ml of PBS and transferred into the same Falcon tube. Cells were pelleted by centrifugation at 1500 *g* for 3 min then resuspended in 1-2 ml of lysis buffer (0.1 M Tris, 0.15 M NaCl, 1% (v/v) Triton X-100, 0.1% (v/v) Nonidet P-40, 10 mM 1, 10-phenanthroline, pH 7.4). Resuspensions were then sonicated on half power for 30 seconds using a probe sonicator (MSE, Crawley, UK). An aliquot (1 ml) of sample was then transferred to an eppendorf tube and centrifuged at 11,600 *g* for 10 min. The supernatant constituting the cell lysate was transferred to a fresh eppendorf tube and total protein concentrations determined (section 2.4.2.) before equalizing protein levels between samples and freezing at -20 °C pending further analysis.

## 2.4.2. Bicinchoninic acid (BCA) protein assay

Bovine serum albumin (BSA) protein standards were prepared and 10  $\mu$ l of each was standard pipetted into the wells of a 96-well plate (Corning, New York, USA) as indicated below:

- Standard A: 0.2 mg/ml Wells A1 and A2
- Standard B: 0.4 mg/ml Wells A3 and A4
- Standard C: 0.6 mg/ml Wells A5 and A6
- Standard D: 0.8 mg/ml Wells A7 and A8
- Standard E: 1.0 mg/ml Wells A9 and A10



<b>Solution</b>	<b>% Gel</b>	
	<b>7%</b>	<b>17%</b>
Sucrose	-	0.37 g
1 M Tris/HCl pH 8.8	1.39 ml	1.39 ml
1.5 M Tris/HCl pH 8.8		-
30% acrylamide 0.8% Bis (Universal Biologicals, Cambridge, UK)	0.88 ml	2.10 ml
1.5% (w/v) ammonium persulphate	100 $\mu$ l	220 $\mu$ l
Distilled water	1.36 ml	-
10% (w/v) SDS	37 $\mu$ l	37 $\mu$ l

**Table 2.1. The composition of resolving gels used in SDS-PAGE**

<b>Solution</b>	<b>Volume</b>
1 M Tris/HCl pH 6.8	1.25 ml
30% acrylamide 0.8% Bis (Universal Biologicals, Cambridge, UK)	1.00 ml
1.5% (w/v) ammonium persulphate	0.50 ml
Distilled water	7.65 ml
10% (w/v) SDS	100 $\mu$ l

**Table 2.2. The composition of stacking gel used in SDS-PAGE**

Distilled water (10  $\mu$ l) was included in wells A11 and A12 as a blank control and cell lysate and conditioned medium samples (3  $\mu$ l) were placed in duplicate wells starting at B1. BCA working reagent (a 50:1 ratio of BCA stock solution (Pierce, Illinois, USA) and 4% (w/v)  $\text{CuSO}_4 \cdot 5\text{H}_2\text{O}$ ) was added to all wells in 200  $\mu$ l volumes. The plate was gently tapped to mix and remove air bubbles and subsequently incubated for 30 min at 37 °C. Absorbance readings at 570 nm were then taken using a plate reader (Anthos 2020 microtiter plate photometer, version 2.0.5 or Victor<sup>2</sup> 1420 multilabel counter, PerkinElmer, Waltham, Massachusetts). Concentration calibration curves were constructed using the BSA standards and concentrations of the samples were extrapolated.

### **2.4.3. Sodium dodecylsulphate - polyacrylamide gel electrophoresis (SDS-PAGE)**

Unless otherwise stated, SDS-PAGE was performed using 7-17 % acrylamide resolving gels made up as detailed in Table 2.1. N,N,N',N'-Tetramethylethylenediamine (TEMED) (3  $\mu$ l) was added to both solutions followed by gentle mixing by inversion. Resolving gels were poured using a gradient mixer and peristaltic pump. A layer of water-saturated isobutanol was applied to the gel and polymerisation was allowed to proceed for 30 min, after which the water-saturated isobutanol was removed from the resolving gel surface. The stacking gel (Table 2.2.) was poured and allowed to set for a further 30 min.

Protein samples were diluted at a ratio of 2:1 sample to dissociation buffer (3.5 ml 1 M Tris/HCl pH 6.8, 10% (w/v) SDS, 80 mM dithiothreitol, 20% (v/v) glycerol, 0.05 mg bromophenol blue, diluted to a total volume of 25 ml using distilled water) and boiled for 3 min. Samples were then loaded into gel wells in 30  $\mu$ l volumes. Low or high molecular weight standards (GE Healthcare, Buckinghamshire, UK) were prepared and loaded in the same way.

Gels were then run in running buffer (1 × Tris/glycine/SDS, Geneflow Ltd, Fradley, UK) at 45 mA per gel (constant current) for approximately 1h.

#### 2.4.4. Immunoblotting

Following SDS-PAGE, proteins were transferred from the gel to an Immobilon-P transfer membrane (Millipore, Massachusetts, USA) in Towbin buffer (20 mM Tris, 150 mM glycine, 20% (v/v) methanol) at 115 V for 1 h. The membrane was then washed for 5 min in PBS and blocked by incubation in 5% (w/v) skimmed milk powder in PBS-T (PBS + 0.1% (v/v) Tween-20) for 1 h at room temperature on a rotating platform. The membrane was then washed for a further 5 min in PBS-T prior to an overnight incubation with primary antibody at 4 °C (Table 2.3). The following morning the membrane was washed for 3 x 10 min in PBS-T.

Antibody	Dilution
Anti-β-actin	1/5000
Anti-APP 6E10	1/2500
Anti-ADAM10	1/2000
Anti-ADAM17	1/2000
Anti-APP (C-terminal)	1/7500
Anti-sAPPβ	1/3000
Anti-FLAG M2	1/2000
Anti APP 22C11	1/1000
Anti-neuron specific enolase NSE-P2	1/2000
Anti-ERK1	1/10,000
Anti-E-cadherin	1/2000
Anti-Vimentin	1/2000
Anti-Caveolin	1/2000

Table 2.3. Primary antibody dilutions

The membrane was then incubated with the secondary peroxidase-conjugated antibody for a further 1 h at room temperature. It was then washed for 3 x 10 min with PBS prior to development using Enhanced Chemiluminescence (ECL) reagents (Pierce, Illinois, USA) according to the manufacturer's instructions.

All primary antibodies were diluted in PBS-T containing 2 % (w/v) BSA unless otherwise stated. The concentrations of primary antibodies used are detailed in Table 2.3. All Secondary antibody peroxidase conjugates were also diluted in PBS-T containing 2 % (w/v) BSA. Rabbit anti-mouse and goat anti-rabbit secondary were both used at 1/4000. The rabbit anti-goat secondary antibody was used at 1/10,000.

#### **2.4.5. Immunoblotting Stripping and re-probing Western Blots**

After initial antigen detection, the Immobilon-P transfer membrane was submerged in stripping buffer (100 mM  $\beta$ -mercaptoethanol, 2% (w/v) SDS, 62.5 mM Tris, pH 7) and incubated at 50 °C for 30 min with occasional mixing. The membranes were then washed in PBS-T for 2 x 10 min at room temp. Finally, the membrane was blocked and the immunoblotting protocol repeated as already described (section 2.4.4.).

#### **2.4.6. Amido black staining**

Membranes were stained with amido black solution (0.1% (w/v) amido black, 1% (v/v) acetic acid, 40% (v/v) methanol) for 2 min or until protein bands became visible. Membranes were destained by running under cold water for 30 seconds.

## 2.5. Lipid raft isolation

Cells were grown to confluence in T75 cm<sup>2</sup> flasks and then harvested as described in section 2.4.1. but using Mes-buffered saline (MBS; 25 mM Mes, 0.15 M NaCl, pH 6.5) in place of PBS. Any excess liquid was removed from the resultant cell pellets by inverting the tubes for 30 min before tapping out the remaining liquid. The pellet was then incubated on ice for 30 min in the cold room and the remaining steps were performed at 4 °C. The pellet was resuspended in 2 ml of MBS containing 0.5% (v/v) Triton X-100. The cells were then homogenised by passing through a 21G needle 15 times. Solubilized cells (2 ml) were combined with 2.2 ml of 90% sucrose (w/v) in MBS and mixed well by inversion. A 2 ml aliquot of 5% (w/v) sucrose in MBS was then placed in an ultracentrifuge tube before injecting 2 ml of 35% (w/v) sucrose in MBS beneath the initial sucrose layer. The solubilized cell sample (now in approximately 45% (w/v) sucrose) (1 ml) was then injected beneath the sucrose gradient and the gradients were centrifuged at 140,000 *g* for 18-24 h (4°C) in an SW-55Ti rotor. Individual fractions (0.5 ml) were then harvested from the gradients from the base upwards using a 1 ml syringe and a 21G needle.

## 2.6. Cell viability and morphology analysis

### 2.6.1. Methanethiosulfonate (MTS) cell viability assay

CellTiter 96<sup>®</sup> AQueous One Cell Proliferation Assay (methanethiosulfonate; MTS) solution (Promega, Wisconsin, USA) 20 µl) was added to each cell culture plate well. The plate was wrapped in foil and returned to the incubator for 30 min – 2 h. The absorbance readings at 492 nm were then taken using a plate reader (Anthos 2020 microtiter plate photometer, version 2.0.5 or Wallac Victor<sup>2</sup> 1420 multilabel counter, PerkinElmer, Waltham, Massachusetts).

## **2.6.2. Cell morphology documentation using optical microscopy**

The Nikon eclipse TE200 optical microscope (Surrey, UK) was used in conjunction with a Nikon COOLPIX P6000 digital camera (Surrey, UK) to take photographs of cell morphology. Dendricity factor analysis was performed by calculating the area and perimeter of ten randomly selected cells (using points of a superimposed grid to choose individual cells for analysis) from two individual T75 cm<sup>2</sup> cell culture flasks, using image J software. These 20 data points for each cell type were then utilised to calculate dendricity (Inverse shape) factor using the following equation:  $P^2/4\pi A$  when P = perimeter of cell and A = area of cell.

## **2.7. Immobilized metal chelate affinity chromatography**

### **(IMAC)**

Chelating sepharose fast flow resin (GE Healthcare, Buckinghamshire, UK) slurry was resuspended by shaking the container for 10 seconds and transferred into plastic mini columns (1.5 ml) (Jena Bioscience, Jena, Germany) so that the meniscus was located 0.5 cm above the filter giving a column volume of approximately 192  $\mu$ l. The column was then washed with 4 x 1 ml volumes of distilled water and primed with 2 x 1ml volumes of 0.2 M CuSO<sub>4</sub>.5H<sub>2</sub>O or 0.2 M MnCl<sub>2</sub>.4H<sub>2</sub>O. Unbound metal was then washed from the columns with 4 x 1 ml volumes of distilled water, 4 x 1 ml volumes of wash buffer (0.02 M sodium acetate, 0.5 M NaCl, pH 4) and 4 x 1 ml volumes of binding buffer (0.15 M NaCl, 10 mM sodium phosphate, pH 7). Sample (100  $\mu$ l) was then applied to the column, from which point the run-through was collected. Columns were washed with 2 x 770  $\mu$ l volumes of binding buffer and a total of 1.4 ml run through was collected. The remaining binding buffer was discarded and then 2 x 770  $\mu$ l volumes of elution buffer (0.15 M NaCl, 10 mM sodium phosphate, 10 mM imidazole, 50 mM EDTA, pH 7) were applied to the column. Eluate (1.4 ml) was collected from this point.

## 2.8. Statistical analysis

Statistical significance was determined using Microsoft Excel to perform Students *t*-tests. Results shown are either standard deviation or standard error of the mean (as indicated in the Figure legends). Sample population numbers are also indicated in the Figure legends.

# 3. Characterisation of constitutive wild-type APP expression and proteolysis in cell lines

### 3.1. Introduction

The overarching aim of this project was to investigate the relationships between APP and copper in the ageing brain. In this respect, the protein was to be studied in relation to two conditions associated with the ageing brain; Alzheimer's disease and brain metastatic prostate cancer. Thus, the initial part of the project involved the characterisation of APP expression and proteolysis in cell models relevant to the two disease conditions.

In relation to Alzheimer's disease, the key cell line used was the human neuroblastoma line, SH-SY5Y, originally isolated from a bone marrow neuroblastoma metastasis of a 4 year old female (275-277). As far as prostate cancer was concerned, three parent cell lines were employed. LNCaP cells are an androgen sensitive PCa cell line originally isolated in 1977 from the left supraclavicular lymph node of a 50 year old Caucasian male with confirmed PCa metastasis (277, 278). Du145 cells are a hormone insensitive metastatic PCa cell line derived from the brain of a Caucasian male (277, 279) and PC-3 cells, which are also hormone insensitive, are derived from a bone metastasis of a prostate adenocarcinoma in a 62 year old Caucasian male (277, 280).

### 3.2. APP expression and proteolysis

In order to investigate APP expression in cells and the release of its proteolytic fragments, cells were grown to confluence and incubated in reduced serum (OptiMEM) medium in order to allow the release of proteolytically cleaved proteins into conditioned medium. Cell lysates and concentrated conditioned medium samples were then prepared and subjected to immunoblotting with the indicated antibodies as described in the Materials and Methods section. In addition to the various parent cell lines, SH-SY5Y and Du145 cells stably transfected with APP<sub>695</sub> were incorporated into the analysis in order to gain an indication of which APP isoforms were expressed endogenously in the cells (and because

later studies would require the over-expression of the protein). The wild-type (WT)-APP<sub>695</sub> construct has been characterised previously (281) and Du145 and SH-SY5Y cells were stably transfected with the construct using the lipofectamine and electroporation methods described in the Materials and Methods section.

First, lysates from the various cell lines were equalised in terms of protein content before analysing APP holoprotein expression levels. Equal amounts of protein from each cell type were immunoblotted with a commercial anti-APP C-terminal antibody (Sigma-Aldrich, Poole, UK) raised against a synthetic immunogen corresponding to amino acids 676-695 of the APP cytosolic domain. The results (*Fig. 3.1A*) revealed multiple bands around the 110 kDa region probably corresponding to multiple APP isoforms and glycoforms. APP was highly expressed in all three untransfected PCa cell lines being detected at the highest level in PC-3 lysates. In fact, the protein was detected at higher endogenous levels in the three PCa cell lines than in the SH-SY5Y lysates. APP<sub>695</sub> in stably-transfected Du145 cells was clearly detected at a lower molecular weight than the bulk of the endogenous protein suggesting that the latter was constituted primarily by the larger KPI-containing APP isoforms. The same was true for the APP<sub>695</sub>-transfected SH-SY5Y cells except that levels of endogenous APP<sub>695</sub> were more prevalent in these cells than in the Du145 cell line. Equal protein loading of lysates was confirmed by an actin immunoblot (*Fig. 3.1B*).

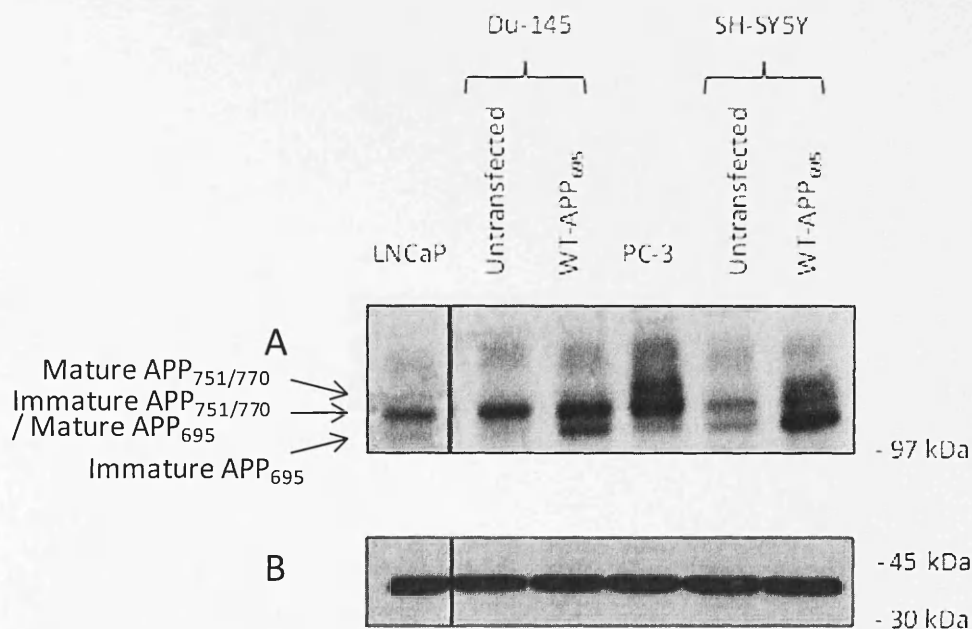


**Figure 3.1. APP expression levels in cell lysates.** Equal amounts of proteins from cell lysates were resolved by SDS-PAGE and immunoblotted according to the Materials and Methods section. **A.** Detection of APP in cell lysates using the anti-APP C-terminal antibody. **B.** Detection of  $\beta$ -actin in cell lysates using the anti- $\beta$ -actin antibody. The vertical lines on blots indicate alignment of samples from distal lanes run on the same immunoblot. The results are representative of three repeat experiments.

Next the non-amyloidogenic processing of APP was examined by analysing the amount of sAPP $\alpha$  released into conditioned medium using the monoclonal anti-APP 6E10 antibody which recognises an epitope within amino acids 3-8 (EFRHDS) of the A $\beta$  domain. The results (*Fig. 3.2*) show that sAPP $\alpha$  was detected as two bands in the conditioned medium from untransfected SH-SY5Y cells. The fact that the lower of these two bands represented sAPP<sub>695</sub> $\alpha$  was verified by the enhanced intensity of this band in medium from the APP<sub>695</sub>-transfected SH-SY5Y cells.

The endogenous sAPP $\alpha$  released from all three PCa cell lines was clearly derived from the larger KPI-containing isoforms (APP<sub>751</sub> and APP<sub>770</sub>) as the bands were larger than the sAPP<sub>695</sub> $\alpha$  band detected in the medium from both Du145 and SH-SY5Y cells stably transfected with the latter APP isoform. When comparing the levels of sAPP $\alpha$  generated from endogenous APP between the PCa cell lines, the LNCaP cells clearly produced the

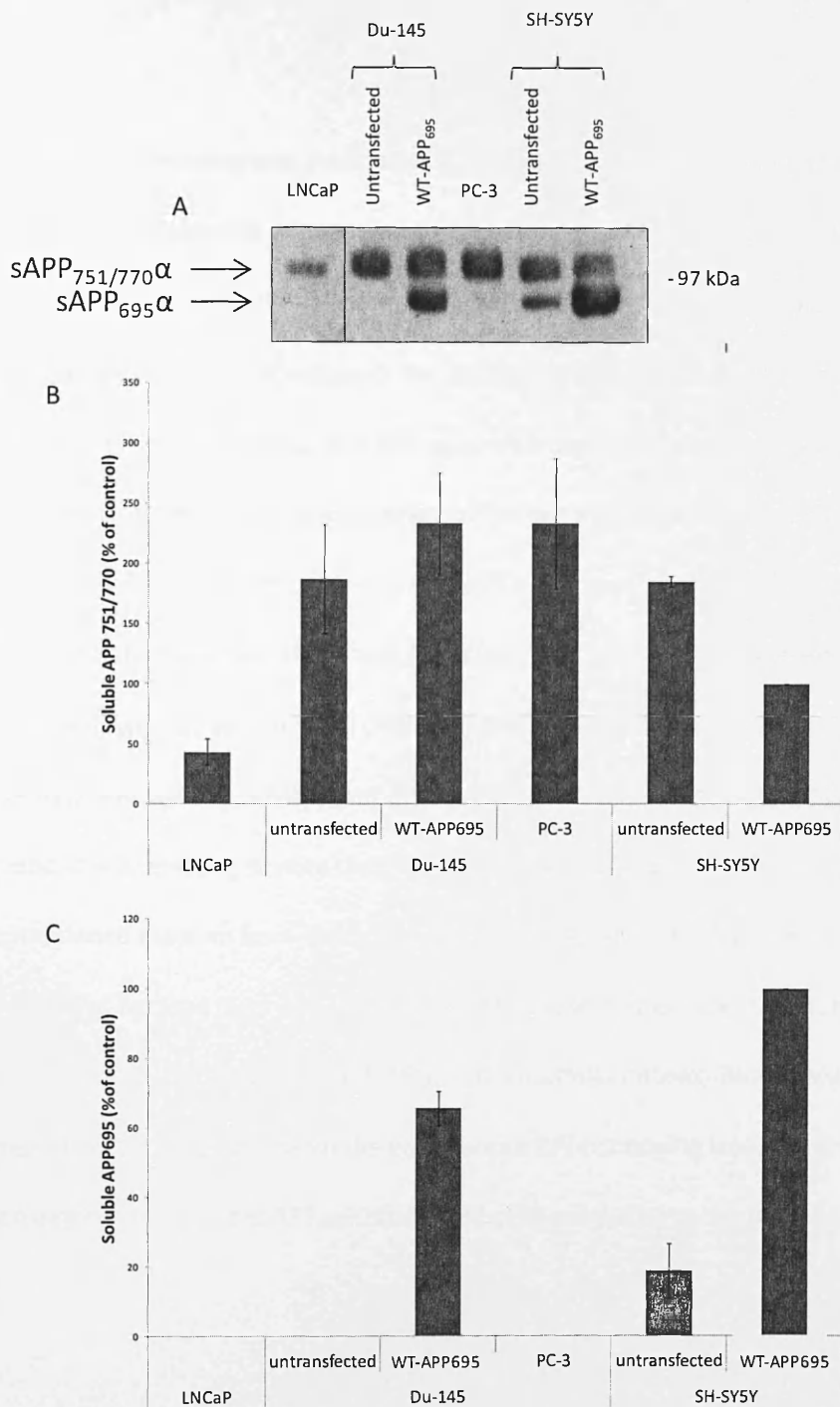


**Figure 3.2. sAPP $\alpha$  shedding into conditioned culture medium.** Cells were grown to confluence and the medium replaced with serum free medium for 24 hours. Conditioned medium was collected and concentrated (Materials and Methods). SDS-PAGE and immunoblots were then performed (Materials and Methods). **A.** Detection of sAPP $\alpha$  in conditioned media using the anti-APP 6E10 antibody. **B** and **C.** Multiple immunoblots were quantified and the levels of sAPP<sub>751/770</sub> $\alpha$  (**B**) and sAPP<sub>695</sub> $\alpha$  (**C**) are expressed relative to the amounts of soluble APP released from the WT-APP<sub>695</sub> over-expressing SH-SY5Y cells. Results are means  $\pm$  S.D. (n=3). The vertical line on the blot indicates alignment of samples from distal lanes run on the same immunoblot.

lowest levels of this fragment with PC3 and Du145 cells both generating considerably higher levels.

Next, the amyloidogenic processing of APP was examined by immunoblotting the conditioned medium samples with antibody 1A9 which specifically detects the C-terminal neoepitope generated on sAPP $\beta$  following  $\beta$ -secretase cleavage of the holoprotein (282). The results (*Fig. 3.3*) show that, in the case of the SH-SY5Y cells, sAPP $\beta$  was generated at roughly equivalent levels from both APP<sub>695</sub> and APP<sub>751/770</sub> with the identity of the former being verified by a massive increase in the intensity of this band in conditioned medium from the APP<sub>695</sub>-transfected SH-SY5Y cells. In terms of the PCa cell lines, sAPP $\beta$  was virtually absent from the conditioned medium of untransfected Du145 and PC-3 cells. However, small amounts of sAPP<sub>695</sub> $\beta$  did appear to be present in the medium from LNCaP cells. As expected, the same fragment was detected, albeit at low levels, in the medium from APP<sub>695</sub>-transfected Du145 cells. It is interesting to note that, whilst comparable levels of sAPP<sub>695</sub> $\alpha$  were detected in the conditioned medium from stably transfected Du145 and SH-SY5Y cells (*Fig. 3.2*), the level of sAPP $\beta$  generated from APP<sub>695</sub> in the Du145 cells was much lower than that seen in medium from the SH-SY5Y transfectants (*Fig. 3.3*). Of similar noteworthiness was the fact that levels of sAPP $\beta$  generated from the endogenous KPI-containing isoforms in Du145 cells were actually increased in the APP<sub>695</sub>-transfected cells compared to the untransfected cells.

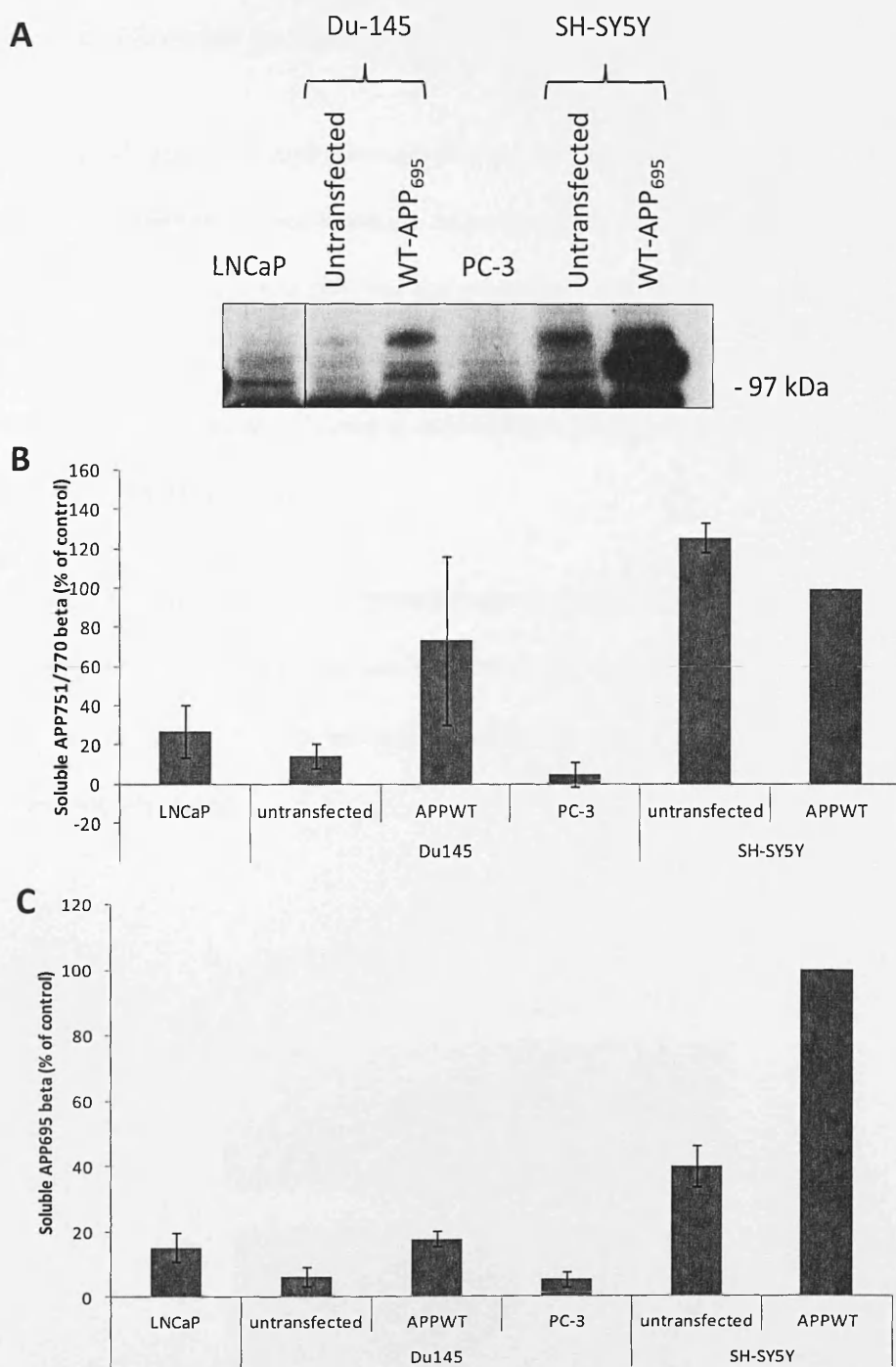


**Figure 3.3. sAPP $\beta$  in conditioned cell culture medium.** Cells were grown to confluence and the medium replaced with serum free medium for 24 hours. Conditioned medium was collected and concentrated (Materials and Methods). SDS-PAGE and immunoblots were then performed (Materials and Methods). **A.** Detection of sAPP $\beta$  in conditioned medium was achieved using the anti-sAPP $\beta$  antibody, 1A9. Multiple immunoblots were quantified and the levels of sAPP<sub>751/770</sub> $\beta$  (**B**) and sAPP<sub>695</sub> $\beta$  (**C**) are expressed relative to the amounts of soluble APP $\beta$  released from the WT-APP<sub>695</sub> over-expressing SH-SY5Y cells. Results are means  $\pm$  S.D. (n=3). The vertical line on the blot indicates alignment of samples from distal lanes run on the same immunoblot.

### 3.3. The effect of dihydrotestosterone on APP expression and proteolysis in LNCaP cells

LNCaP cells are an androgen sensitive cell line in which various PCa-associated proteins have been shown to increase in response to hormone treatment (278). As such, the effect of dihydrotestosterone (DHT) on the expression and proteolysis of APP in this cell line was also examined. Confluent cells were incubated with the indicated concentrations of DHT for 24 h and cell lysates and concentrated conditioned medium prepared as described in the Materials and Methods section.

Initially, equal amounts of protein from cell lysates were immunoblotted with the anti-APP C-terminal antibody. The results show an apparent dose-dependent increase in APP expression (Fig. 3.4A). Equal protein loading of lysates was confirmed by an actin immunoblot (Fig. 3.4B).

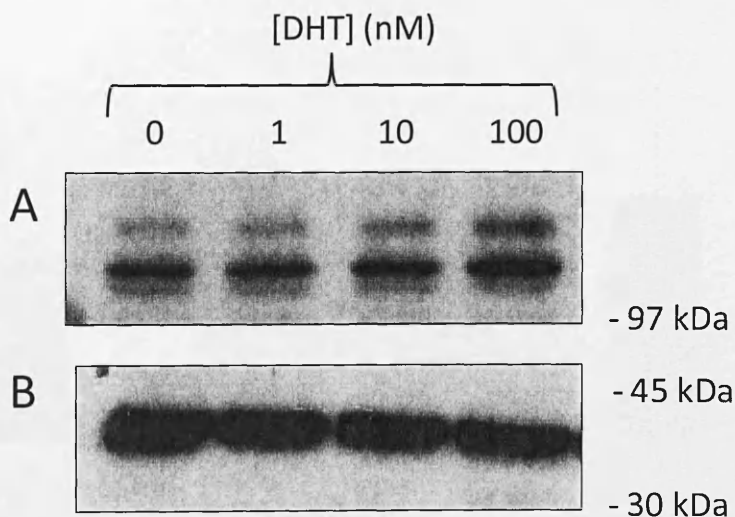


**Figure 3.4. The effect of DHT on APP expression in LNCaP cells.** Cells were grown to confluence and the medium was replaced with serum free medium, containing 0, 1, 10 or 100 nM DHT, for 24 hours. Cells were harvested and lysates prepared (Materials and Methods). SDS-PAGE and immunoblots were then performed (Materials and Methods). **A.** Detection of APP in cell lysates using the anti-APP C-terminal antibody. **B.** Detection of β-actin in cell lysates using the anti-β-actin antibody. The results are representative of three repeat experiments.

The conditioned medium from the control and DHT-treated cells was then immunoblotted with antibody 6E10 in order to determine the levels of shed sAPP $\alpha$ . However, no significant alterations in the levels of sAPP $\alpha$  following DHT treatment could be determined (Fig. 3.5). Similarly, no differences in the levels of sAPP $\beta$  in conditioned medium were observed following DHT treatment when the samples were immunoblotted with antibody 1A9 (Fig. 3.6).

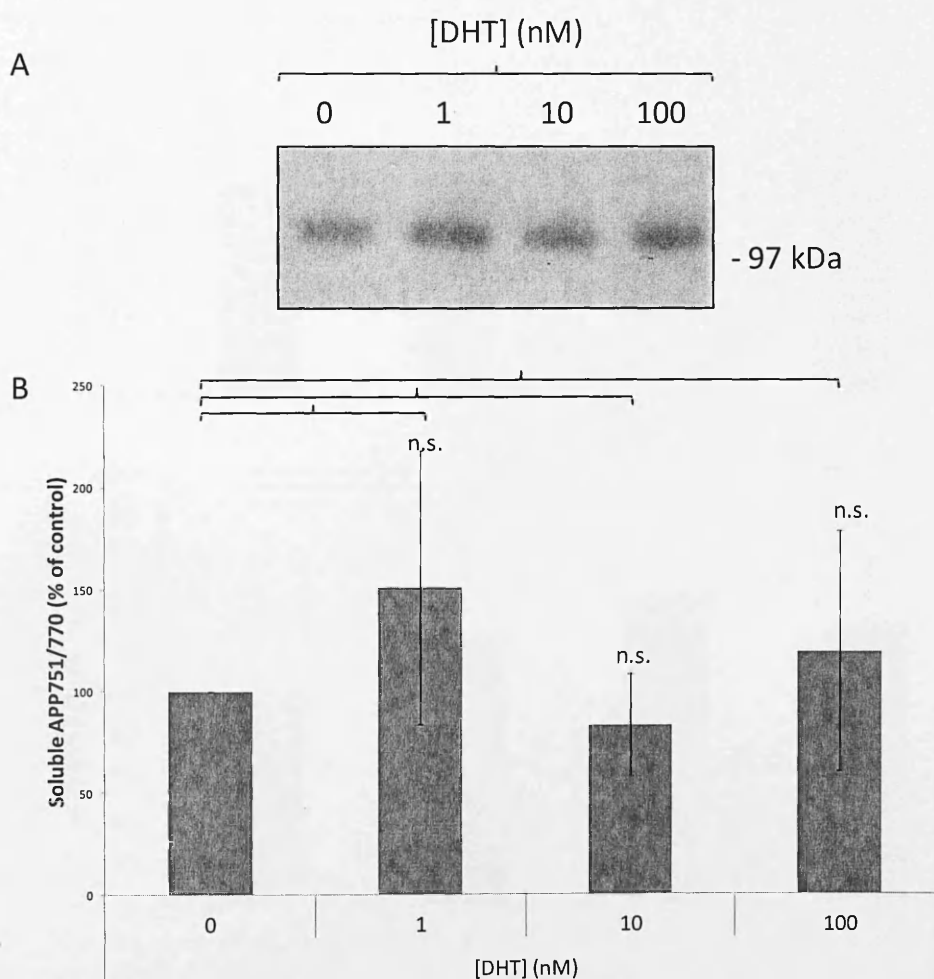


**Figure 3.5. The effect of DHT on sAPP $\alpha$  shedding from LNCaP cells.** Cells were grown to confluence and the medium was replaced with serum free medium, containing 0,1,10 or 100 nM DHT, for 24 hours. Conditioned medium was collected and concentrated (Materials and Methods). SDS-PAGE and immunoblots were then performed (Materials and Methods). **A.** Detection of sAPP $\alpha$  in conditioned media using the anti-APP 6E10 antibody. **B.** Multiple immunoblots were quantified and the results expressed relative to the untreated control. Results are means  $\pm$  S.D. (n=3). n.s. = not significant.

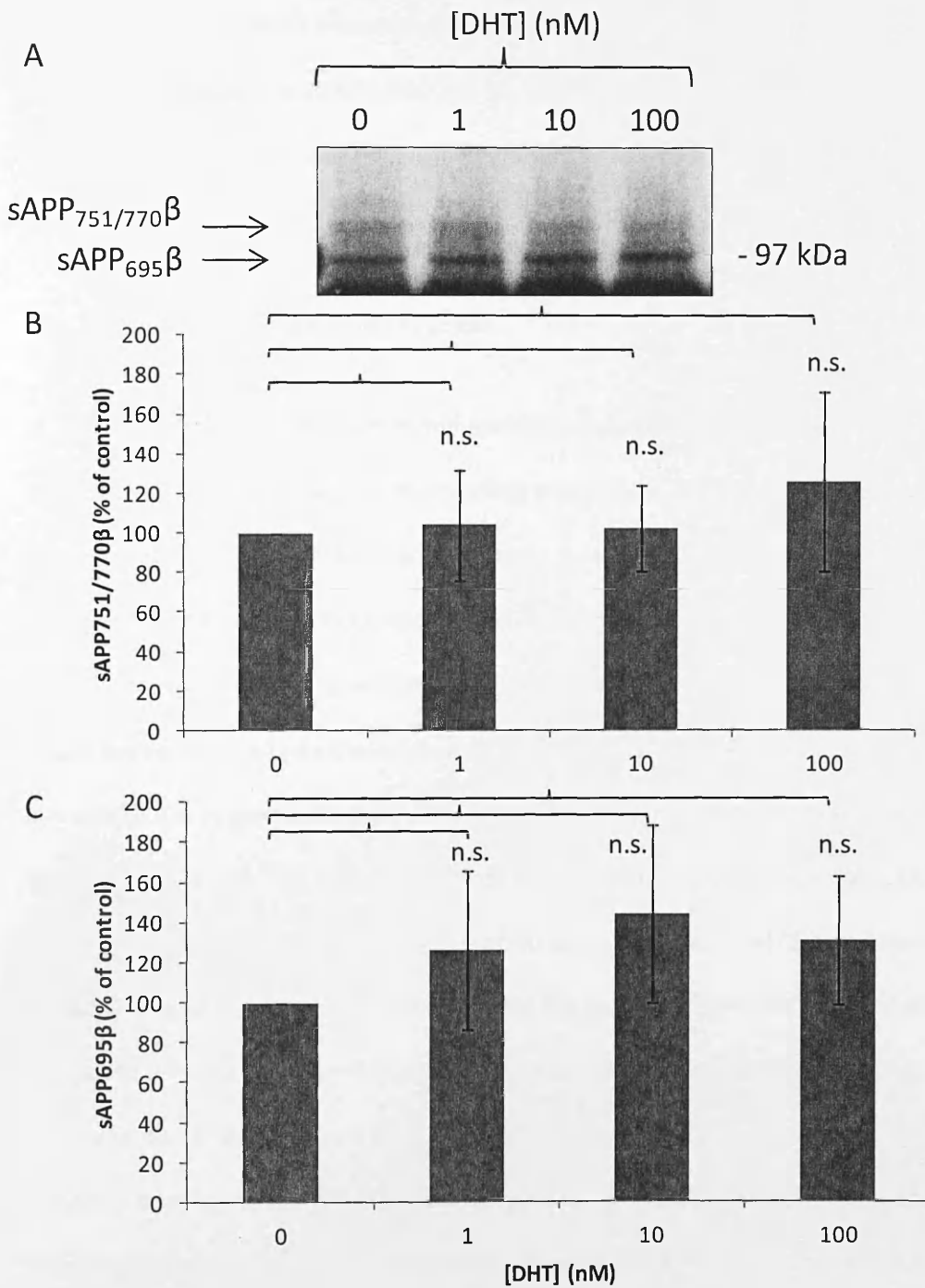


**Figure 3.6. The effect of DHT on sAPP $\beta$  release from LNCaP cells.** Cells were grown to confluence and the medium was replaced with serum free medium containing 0,1,10 or 100 nM DHT, for 24 hours. Conditioned medium was collected and concentrated (Materials and Methods). SDS-PAGE and immunoblots were then performed (Materials and Methods). **A.** Detection of sAPP $\beta$  in the conditioned medium was achieved using the anti-sAPP $\beta$  antibody, 1A9. Multiple immunoblots were quantified and the levels of sAPP<sub>751/770</sub> $\beta$  (**B**) and sAPP<sub>695</sub> $\beta$  (**C**) are expressed relative to the amounts in the untreated controls. Results are means  $\pm$  S.D. (n=3); n.s. = not significant.

### 3.4. $\alpha$ -secretase expression

In order to further understand the proteolysis of APP in the various cell lines employed and because both ADAM10 and ADAM17 have previously been implicated in both AD and prostate cancer (283-286) the levels of these proteins were next analysed in cell lysates.

#### 3.4.1. ADAM10 expression

Initially the cell lysates were immunoblotted with a commercial ADAM10 antibody raised against a synthetic peptide representing amino acids 735-749 in the C-terminal region of murine ADAM10 (see Materials and Methods). As such, this antibody should detect both the immature, prodomain containing form of ADAM10 and the mature form of the enzyme. The samples were run against a positive control of HEK cells transiently transfected with full-length bovine ADAM10 (see Materials and Methods) which was detected as two bands at 98 kDa and 70 kDa as previously observed (287) (*Fig. 3.7*). Immature ADAM10 was barely detectable in SH-SY5Y and PC3 cells but was clearly present in lysates from both LNCaP and Du145 cells. Interestingly, when APP<sub>695</sub> was over-expressed in the Du145 cells, levels of ADAM10 were seen to decrease. Mature ADAM10 was only detected at appreciable levels in the lysates of the untransfected Du145 cells (*Fig. 3.7*). Notably, both the immature and mature forms of ADAM10 were slightly smaller in the sample cell lysates than in the bovine ADAM10- transfected HEK cell lysate control perhaps due to differences in the molecular weight of the protein between species or to differences in glycosylation. Note that these samples were the same ones as used earlier in this chapter; the corresponding actin control is therefore shown in *Fig. 3.1*.

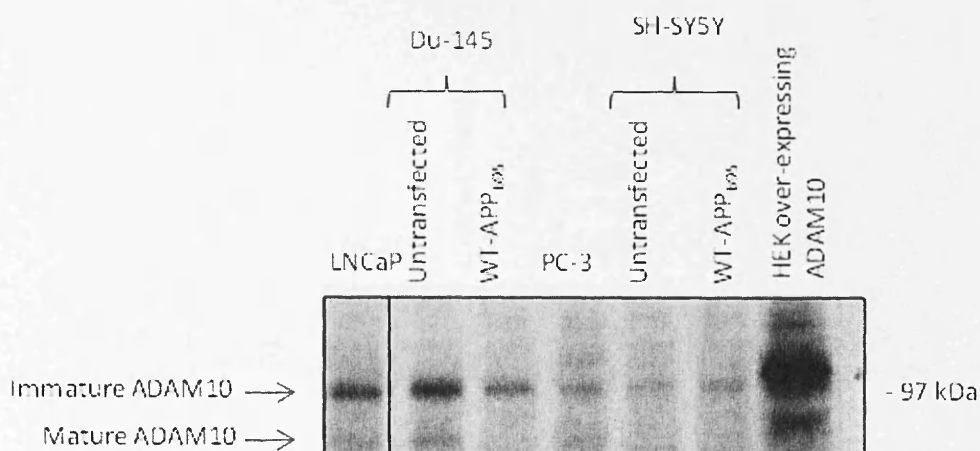


**Figure 3.7. ADAM10 expression in cell lysates.** Cells were grown to confluence and the medium was replaced with serum free medium for 24 hours. Cells were harvested and cell lysates prepared (Materials and Methods). SDS-PAGE and immunoblots were then performed (Materials and Methods). Detection of ADAM10 in cell lysates was achieved using the anti-ADAM10 C-terminal antibody. The vertical line on the blot indicates alignment of samples from distal lanes run on the same immunoblot.

### 3.4.2. ADAM17 expression

Next, the lysates were immunoblotted using a commercial anti-ADAM17 antibody raised against a synthetic peptide corresponding to amino acids 807-823 of the human protein. Similarly to ADAM10, the samples were run alongside HEK cells over-expressing ADAM17 as a positive control in which the protein was detected as a 110 kDa immature form and ~100 kDa mature form consistent with previous findings (288) (Fig. 3.8). Mature ADAM17 was detectable in all of the cell lines, with a particularly high abundance in the hormone-insensitive PC-3 cells (Fig. 3.8). Similarly, immature ADAM17 was present in all of the cell lines examined with the exception of the hormone-sensitive LNCaP cells. Again, the corresponding actin control is shown in Fig. 3.1.

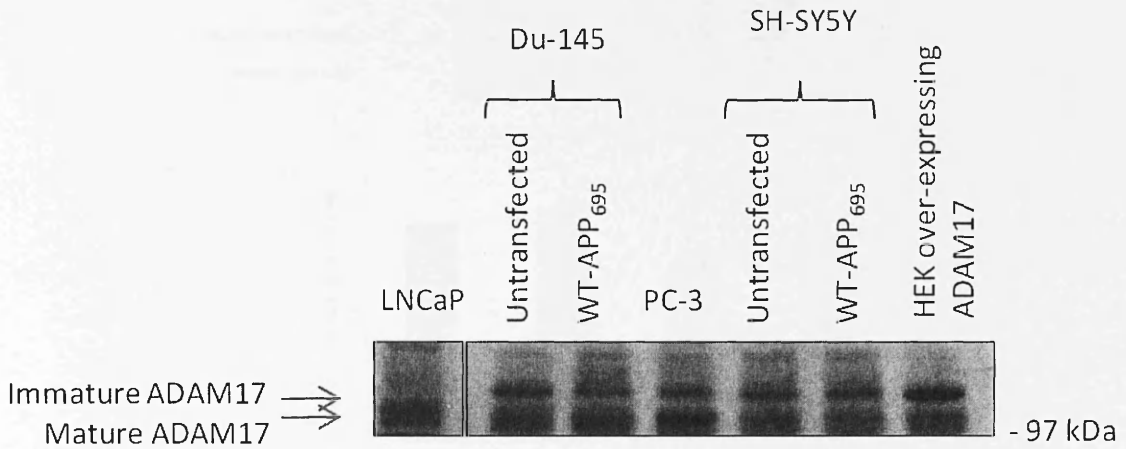


**Figure 3.8. ADAM17 expression in cell lysates.** Cells were grown to confluence and the medium was replaced with serum free medium for 24 hours. Cells were harvested and cell lysates prepared (Materials and Methods). SDS-PAGE and immunoblots were then performed (Materials and Methods). Detection of ADAM17 in cell lysates was achieved using the anti-ADAM17 antibody. The vertical line on the blot indicates alignment of samples from distal lanes run on the same immunoblot.

### 3.4.3. The effect of dihydrotestosterone on ADAM10 and ADAM17 expression in LNCaP cells

Next, the possible effects of DHT on ADAM expression were examined in the hormone sensitive LNCaP cells. The cell lysate samples from *Fig. 3.4.* were initially immunoblotted with the ADAM10 antibody. However, no detectable change in ADAM10 expression levels was observed (*Fig. 3.9.*). Similar results were observed when the samples were immunoblotted with the anti-ADAM17 antibody (*Fig. 3.10.*).

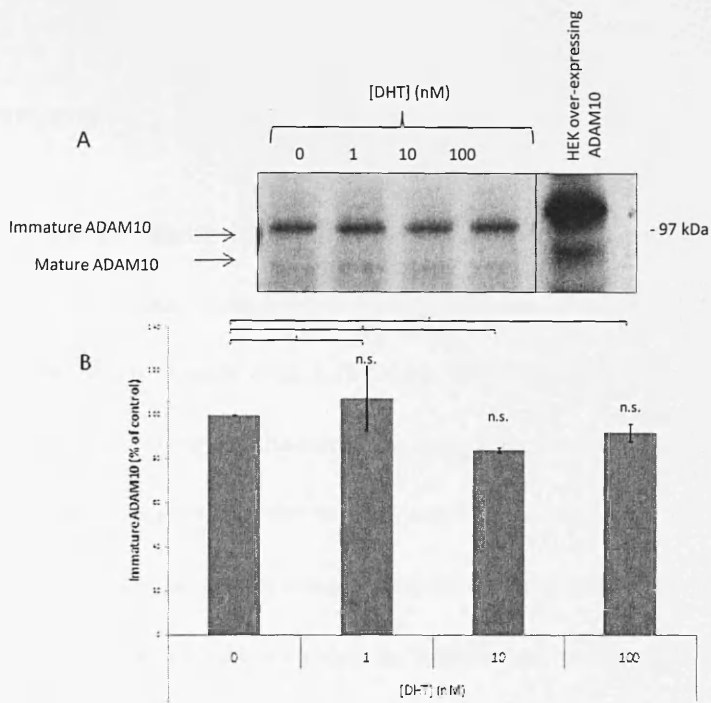


**Figure 3.9. The effect of DHT on ADAM10 expression in LNCaP cells.** Cells were grown to confluence and the medium was replaced with serum free medium, containing 0, 1, 10 or 100 nM DHT, for 24 hours. Cells were harvested and cell lysates prepared (Materials and Methods). SDS-PAGE and immunoblots were then performed (Materials and Methods). **A.** Detection of ADAM10 in cell lysates using the anti-ADAM10 C-terminal antibody. The vertical line on the blot indicates alignment of samples from distal lanes run on the same immunoblot. **B.** Multiple immunoblots were quantified and the results expressed relative to the untreated control. Results are means  $\pm$  S.D. (n=3). n.s. = not significant.

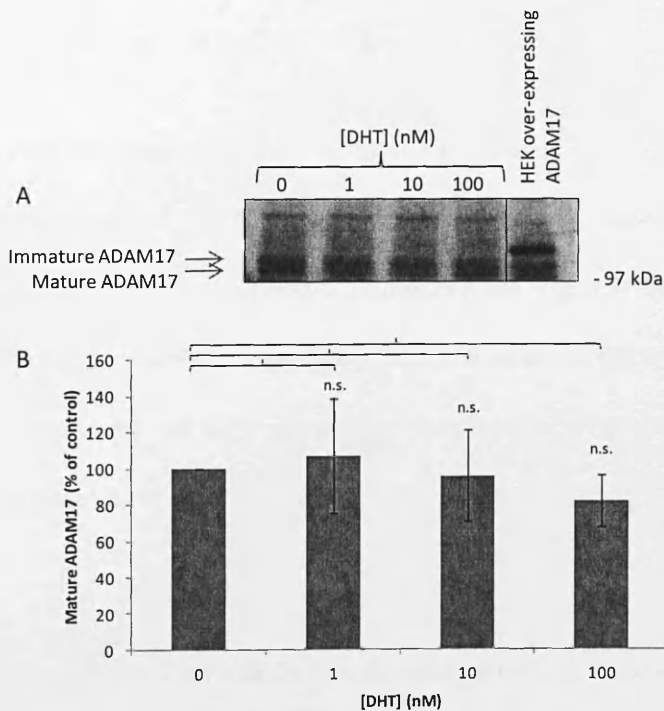


**Figure 3.10. The effect of DHT on ADAM17 expression in LNCaP cells.** Cells were grown to confluence and the medium was replaced with serum free medium, containing 0, 1, 10 or 100 nM DHT, for 24 hours. Cells were harvested and cell lysates prepared (Materials and Methods). SDS-PAGE and immunoblots were then performed (Materials and Methods). **A.** Detection of ADAM17 in the cell lysates was achieved using the anti-ADAM17 C-terminal antibody. The vertical line on the blot indicates alignment of samples from distal lanes run on the same immunoblot. **B.** Multiple immunoblots were quantified and the results expressed relative to the untreated control. Results are means  $\pm$  S.D. (n=3). n.s. = not significant.

### 3.5. Summary

The human neuroblastoma, SH-SY5Y cells, expressed both endogenous APP<sub>695</sub> and APP<sub>751/770</sub> whereas the endogenous expression in the PCa cell lines was restricted to the KPI-containing isoforms of the protein (*Fig. 3.1*). Of the three PCa cell lines studied, APP expression was particularly high in the hormone-insensitive Du145 and PC3 cells. However, in the LNCaP cells the expression of the protein was further increased following DHT treatment (*Fig. 3.4*). The constitutive shedding of sAPP $\alpha$  from the various cell lines largely reflected the expression levels of the various isoforms in cell lysates, with LNCaPs clearly shedding the lowest amount of the protein amongst the PCa cell lines (*Fig. 3.2*). Notably, however, whilst the expression of the APP holoprotein appeared hormone sensitive in the LNCaP cells, its shedding into conditioned medium was not (*Figs. 3.5 and 6*). sAPP $\beta$  generation by the various PCa cells was notably very low and was not responsive to DHT treatment in LNCaP cells (*Figs. 3.3 and 6*).

In terms of ADAM expression, ADAM10 was detected in all of the cell lines studied and was most highly expressed in LNCaP and Du145 cells (*Fig. 3.7*). However, the expression of the enzyme was not affected by DHT in the former cell line (*Fig. 3.9*). Immature and mature ADAM17 were detected at relatively high levels in all of the cell lines studied with the exception that the immature form was notably absent in LNCaP cells (*Fig. 3.8*). Like ADAM10, the expression of ADAM17 in LNCaP cells was not affected by DHT treatment (*Fig. 3.10*).

Collectively, these data provided a firm foundation for future experiments designed to investigate the link between APP and copper in the various cell lines and confirmed that the stable expression of APP<sub>695</sub> in both SH-SY5Y and Du145 cells had been successful.

# 4. The effects of copper on endogenous APP expression and proteolysis in prostate cancer epithelial cells

## 4.1. Introduction

Copper has previously been shown to influence the expression, trafficking and ADAM-mediated proteolysis of APP in various cell lines (163, 168, 289). Furthermore, APP and copper have both, independently, been positively associated with the propensity for prostate cancer epithelial cells to metastasize (2, 267). Thus, in the current study, the potential relationships between copper levels and APP expression/proteolysis in the prostate cancer cell lines LNCaP, PC-3 and Du145 were investigated.

LNCaP, PC-3 and Du145 cells were grown to confluence before being washed *in situ* with OptiMEM (10 ml). The cells were then incubated in copper chloride diluted in OptiMEM (10 ml) to the concentrations stated. After 24 h, the cells were harvested and lysates and concentrated conditioned medium were prepared as described in the Materials and Methods section. The samples were then immunoblotted for full-length APP and its proteolytic fragments. The effect of copper on cell viability was also monitored using the MTS assay as described in Materials and Methods.

## 4.2. The effect of copper on LNCaP cell viability

Initially, the effect of copper on the viability of LNCaP cells was examined. Cells were grown to confluence and then incubated for 24 h in the presence of 0-500  $\mu\text{M}$  copper chloride after which cell viability was determined using the MTS assay. The results (*Fig. 4.1*) show that copper concentrations up to 50  $\mu\text{M}$  were not cytotoxic. However, at 200  $\mu\text{M}$  copper there was a dramatic decrease in cell viability to  $25.52 \pm 1.27\%$  of control levels whilst, at 500  $\mu\text{M}$  copper, cell survival was a mere  $11.35 \pm 0.42\%$  of the untreated control (*Fig. 4.1*).

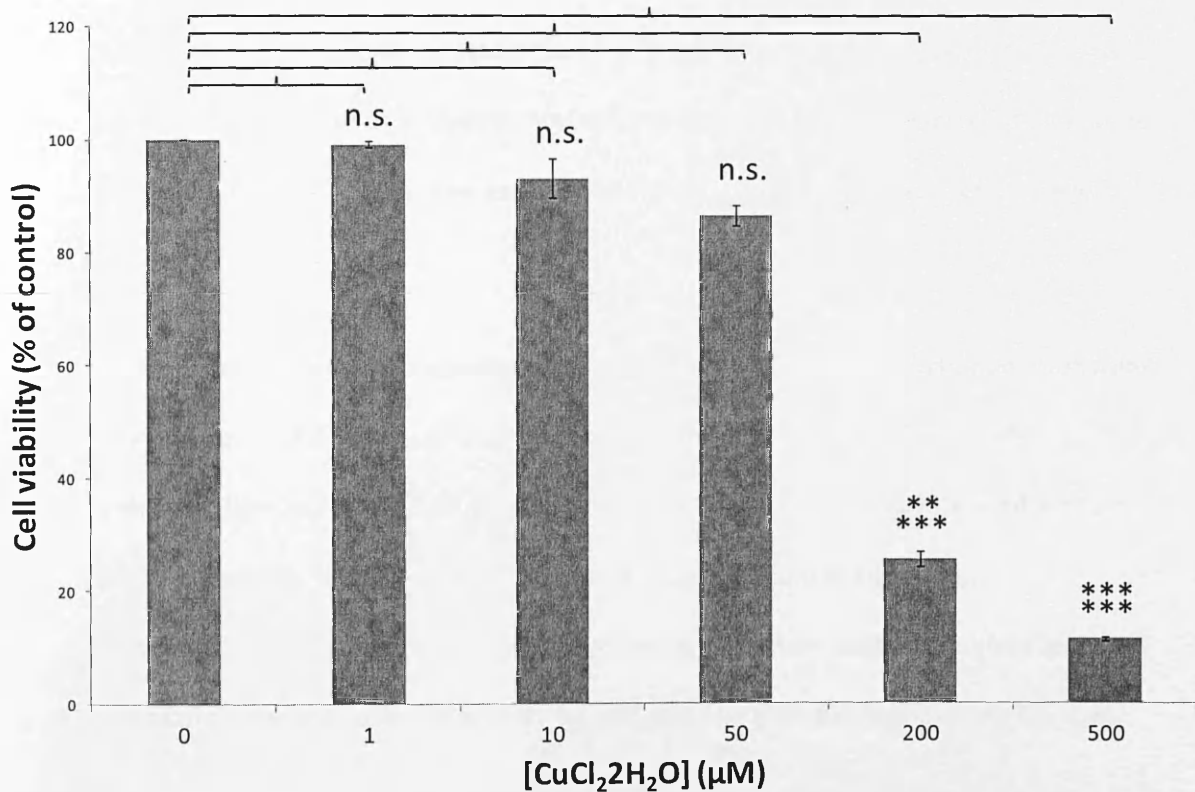


**Figure 4.1. The effect of copper on LNCaP cell viability.** Cells were seeded at 2000 cells per well and grown to confluence. CuCl<sub>2</sub>·2H<sub>2</sub>O was added at 0, 1, 10, 50, 200 or 500 µM concentrations, and the cells were further incubated for 24 hours. Cell viability was then determined using the MTS assay (see Materials and Methods). Results are expressed relative to the viability of the untreated controls and are means ± S.D. (n=3). \*\*\*\* = p≤0.0005; \*\*\*\*\* = p≤0.00001; n.s. = not significant.

### 4.3. The effect of copper on the expression and shedding of endogenous APP in LNCaP cells

Next, the copper treatment of LNCaP cells described in the preceding section was repeated but, this time, the cells and conditioned medium were analysed in terms of APP expression and proteolysis. Due to the massive decreases in cell viability observed at higher copper concentrations (*Fig. 4.1*) very little protein was detected in cell lysates prepared from the 200 and 500  $\mu\text{M}$  copper-treated cells. Thus, it was not feasible to adjust all of the lysate samples on the basis of equal protein. Instead, the cells from the first four treatments were equalised on a protein basis, whereas the 200 and 500  $\mu\text{M}$  copper treated cells were left unequalised.

Initially, equal lysate volumes were resolved by SDS-PAGE and immunoblotted using the APP C-terminal antibody in order to detect the full-length protein. The results, (*Fig. 4.2A*) revealed a slight increase in APP expression in lysates prepared from cells treated with 10 and 50  $\mu\text{M}$  copper. However, APP expression was not detected at higher metal concentrations due to considerable decreases in overall protein levels as a consequence of increased copper-mediated cytotoxicity (as evidenced by the actin immunoblot; *Fig. 4.2B*).

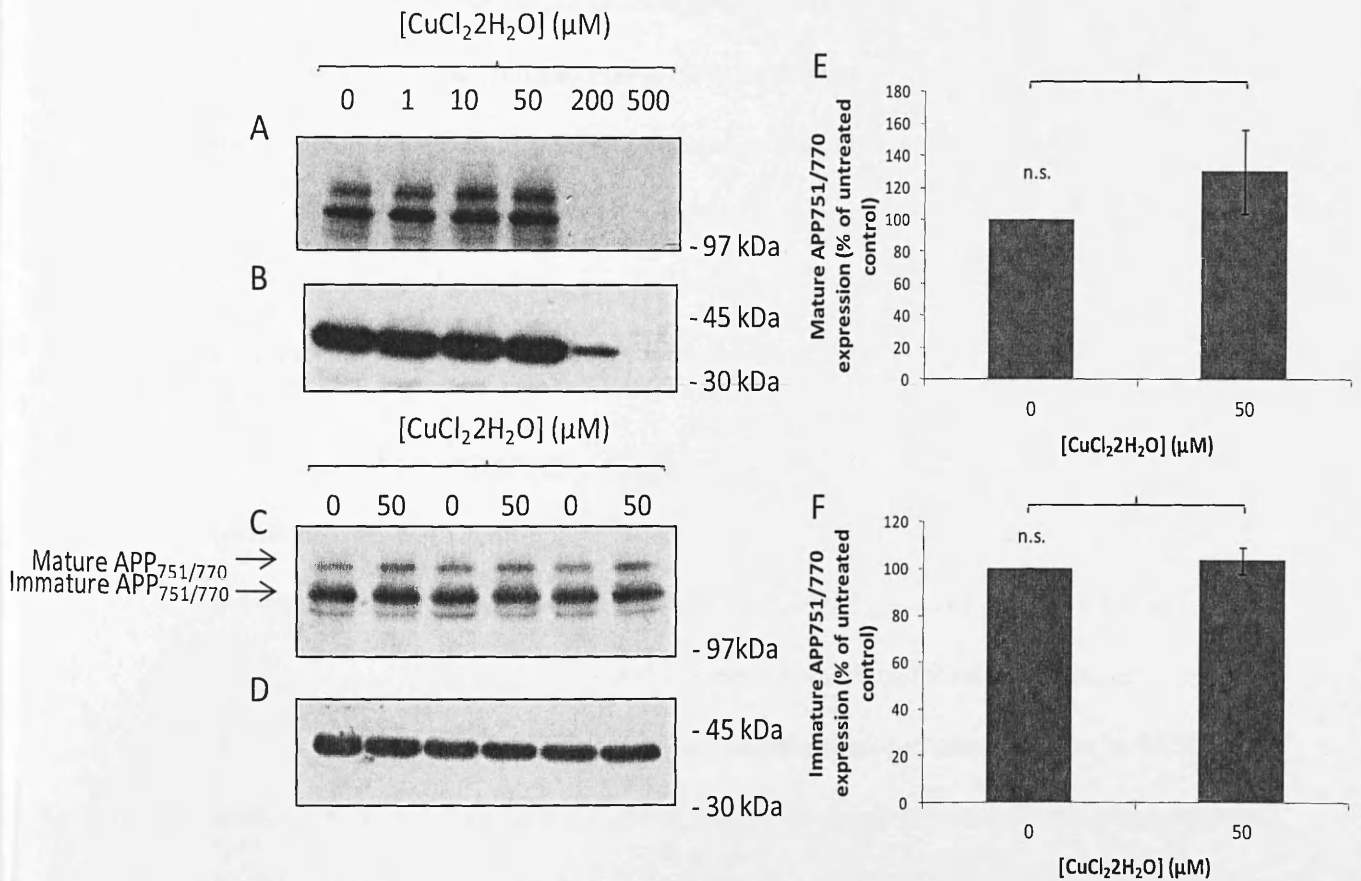


**Figure 4.2. The effect of copper on APP expression in LNCaP cells.** Cells were grown to confluence and the medium was replaced with serum free medium containing 0, 1, 10, 50, 200 or 500 μM CuCl<sub>2</sub>H<sub>2</sub>O. After 24 h, the cells were harvested and lysates prepared (Materials and Methods). Equal volumes of the lysates were then resolved by SDS-PAGE and immunoblotted (Materials and Methods). **A** and **C**. Detection of full-length APP in cell lysates using the anti-APP C-terminal antibody. **B** and **D**. Detection of β-actin in cell lysates using the anti-β-actin antibody. **E** and **F**. Quantification of mature APP<sub>751/770</sub> (**E**) and immature APP<sub>751/770</sub> (**F**) levels from control and copper (50 μM) treated cells. Results are means ± S.D. (n=3). n.s. = not significant.

Due to copper concentrations of 10 and 50  $\mu\text{M}$  initially appearing to enhance APP expression in LNCaP cells (*Fig. 4.2A*), a further experiment was conducted in an attempt to validate this result. Here, confluent flasks of cells were treated in triplicate with 0 or 50  $\mu\text{M}$  copper concentrations and the cell lysates were subsequently immunoblotted once more with the anti-APP C-terminal antibody. The results (*Fig. 4.2C*) initially appeared to show an increase in the levels of mature KPI-containing APP isoforms following copper treatment (note that LNCaP cells primarily express KPI-containing APP isoforms and not APP<sub>695</sub> so immunoblots of cell lysates are not confused by the presence of multiple molecular weight APP isoforms). However, when these changes were quantified, they were deemed not significant (*Fig. 4.2E*). Similarly, no changes in the cell-associated levels of immature KPI-containing APP isoforms were observed following copper treatment (*Figs. 4.2C and 2F*).

Next the conditioned medium samples from cells treated with 0-500  $\mu\text{M}$  copper concentrations were immunoblotted with the anti-APP antibody 6E10 in order to determine the effect of the metal on APP shedding from LNCaP cells. The results (*Fig. 4.3A*) appear once more to show a slight increase in sAPP $\alpha$  levels in conditioned medium at copper concentrations of 10 and 50  $\mu\text{M}$  (note that the conditioned medium samples in this instance were loaded in terms of equal volume as opposed to equal protein levels). When a further experiment was conducted using triplicate treatments of 0 and 50  $\mu\text{M}$  copper, there again appeared to be a slight increase in sAPP $\alpha$  generation in the presence of copper (*Fig. 4.3B*). However, these changes could not be deemed significant (*Fig. 4.3C*).

These data suggest that, at sub-toxic copper concentrations, there may be marginal increases in either the expression or maturation of APP in LNCaP cells, resulting in enhanced shedding of the protein from the cell surface over a 24 h period. However, any such changes were clearly of borderline significance.

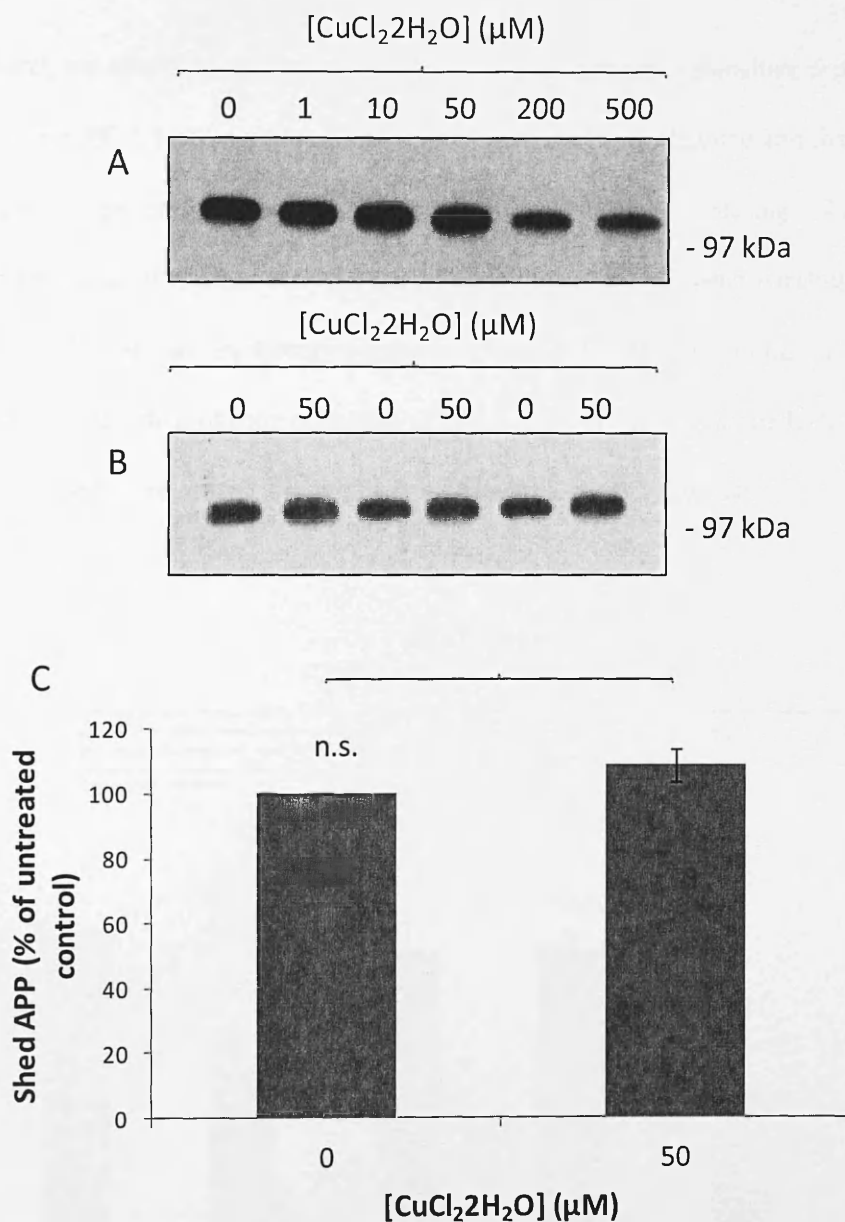


**Figure 4.3. The effect of copper on soluble APP production from LNCaP cells.** Cells were grown to confluence and the medium was replaced with serum free medium containing 0, 1, 10, 50, 200 or 500 μM CuCl<sub>2</sub>·2H<sub>2</sub>O. After 24 h, the conditioned medium was collected and concentrated (Materials and Methods). Equal volumes of the medium samples were then resolved by SDS-PAGE and immunoblotted (Materials and Methods). **A** and **B**. Detection of soluble APP in conditioned medium using the anti-APP antibody 6E10. **C**. Quantification of soluble APP levels in medium from control and copper (50 μM) treated cells. Results are means ± S.D. (n=3). n.s. = not significant.

#### 4.4. The effect of copper on PC-3 cell viability

Next, the effects of copper on the viability of the hormone-insensitive prostate cancer cell line, PC-3, were examined. The cells were grown to confluence and then treated for 24 h with copper concentrations ranging from 0-500  $\mu\text{M}$  before analysing cell viability using the MTS assay (Materials and Methods). The results (Fig. 4. 4) demonstrated a dramatic reduction in PC-3 cell viability following treatment with 200 or 500  $\mu\text{M}$  copper ( $32.75 \pm 9.71\%$  and  $18.31 \pm 3.14\%$  of control viability levels, respectively). As observed previously with LNCaP cells, copper concentrations of 50  $\mu\text{M}$  and lower were not cytotoxic.

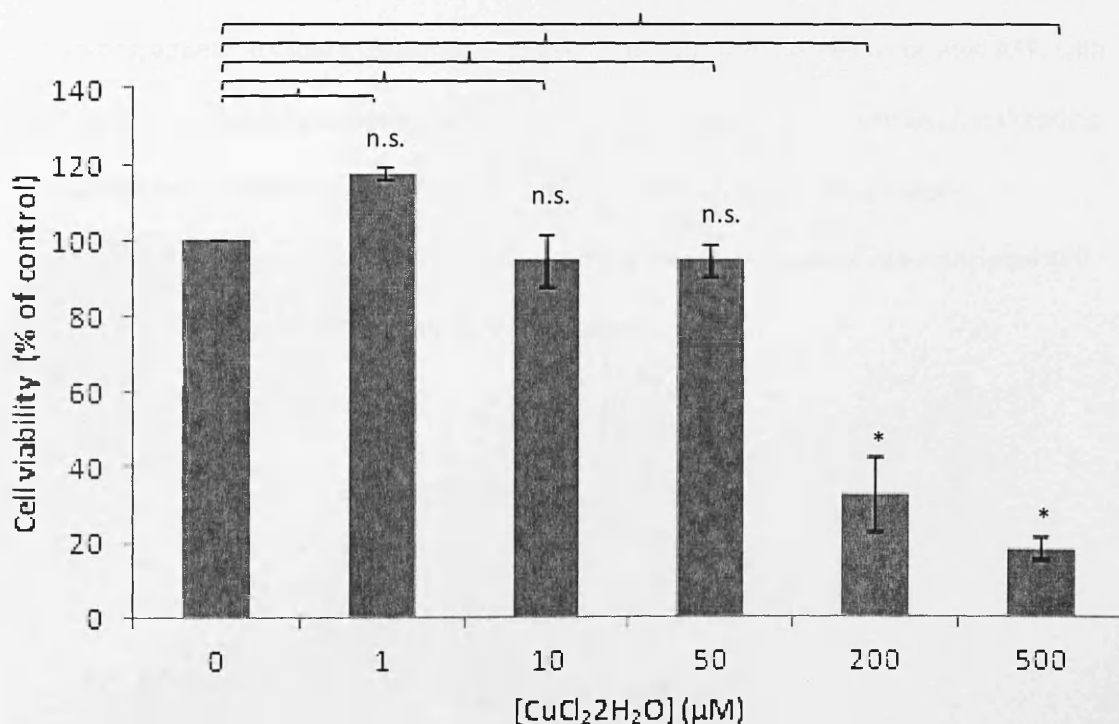


**Figure 4.4. The effect of copper on PC-3 cell viability.** Cells were seeded at 2000 cells per well and grown to confluence.  $\text{CuCl}_2 \cdot 2\text{H}_2\text{O}$  was added at 0, 1, 10, 50, 200 or 500  $\mu\text{M}$  concentrations, and the cells were further incubated for 24 hours. Cell viability was then determined using the MTS assay (see Materials and Methods). Results are expressed relative to the viability of the untreated controls and are means  $\pm$  S.D. ( $n=3$ ). \* =  $p \leq 0.05$ ; n.s. = not significant.

#### 4.5. The effect of copper on the expression and shedding of endogenous APP in PC-3 cells

As with the LNCaP cells previously, PC-3 cells were grown to confluence and then treated for 24 h with 0-500  $\mu$ M copper concentrations. The effects of the metal on APP expression and proteolysis were then examined by immunoblotting. In this case, as protein levels in those cells treated with the highest copper concentrations were detectable, lysates were all equalised on a protein basis.

One of the key limitations with this section of the study is that this particular experiment was only performed on one occasion, with limited replicates, making it difficult to draw any firm conclusions from the data. However, the results (*Fig. 4.5A*) do, in this instance, appear to show a copper-related decrease in the levels of cell-associated APP, with the actin immunoblot confirming equal protein loading (*Fig. 4.5B*). Conversely, the shedding of sAPP $\alpha$  into conditioned medium appeared to increase with increasing copper concentration (*Fig. 4.6*) perhaps suggesting that the decreased levels of cell-associated APP might result from enhanced shedding of the protein.

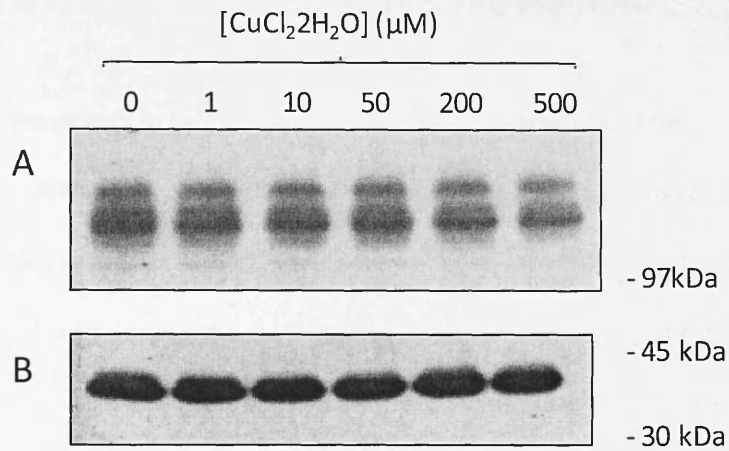


**Figure 4.5. The effect of copper on APP expression in PC-3 cells.** Cells were grown to confluence and the medium was replaced with serum free medium containing 0, 1, 10, 50, 200 or 500 μM CuCl<sub>2</sub>·2H<sub>2</sub>O. After 24 h, the cells were harvested and lysates prepared (Materials and Methods). Equal volumes of the lysates were then resolved by SDS-PAGE and immunoblotted (Materials and Methods). **A.** Detection of full-length APP in cell lysates using the anti-APP C-terminal antibody. **B** Detection of β-actin in cell lysates using the anti-β-actin antibody.

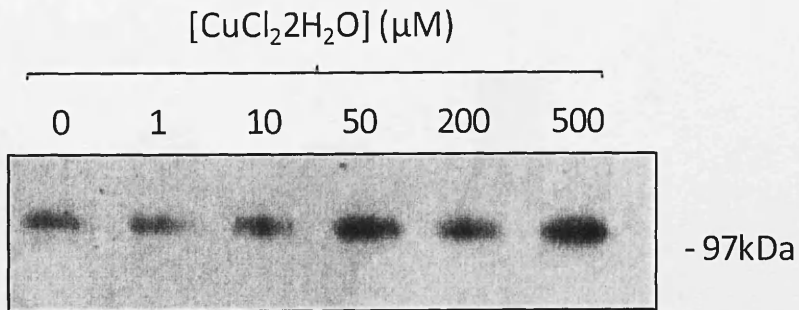


**Figure 4.6. The effect of copper on soluble APP production from PC-3 cells.** Cells were grown to confluence and the medium was replaced with serum free medium containing 0, 1, 10, 50, 200 or 500 μM CuCl<sub>2</sub>·2H<sub>2</sub>O. After 24 h, the conditioned medium was collected and concentrated (Materials and Methods). Equal volumes of the medium samples were then resolved by SDS-PAGE and immunoblotted using the anti-APP antibody 6E10 (Materials and Methods).

#### 4.6. The effect of copper on Du145 cell viability

Next, the effects of copper on the viability and endogenous APP expression/proteolysis of Du145 cells was examined. The viability assay results (Fig. 4.7) clearly show that, as for LNCaP and PC-3 cells no copper-associated cytotoxicity was observed at concentrations of the metal below 200  $\mu\text{M}$ . However, once this metal concentration was reached, there was a drastic drop in cell viability ( $43.24 \pm 18.44\%$  the level of the untreated control). At 500  $\mu\text{M}$  copper, cell viability was a mere  $17.77 \pm 5.81\%$  of the untreated control.

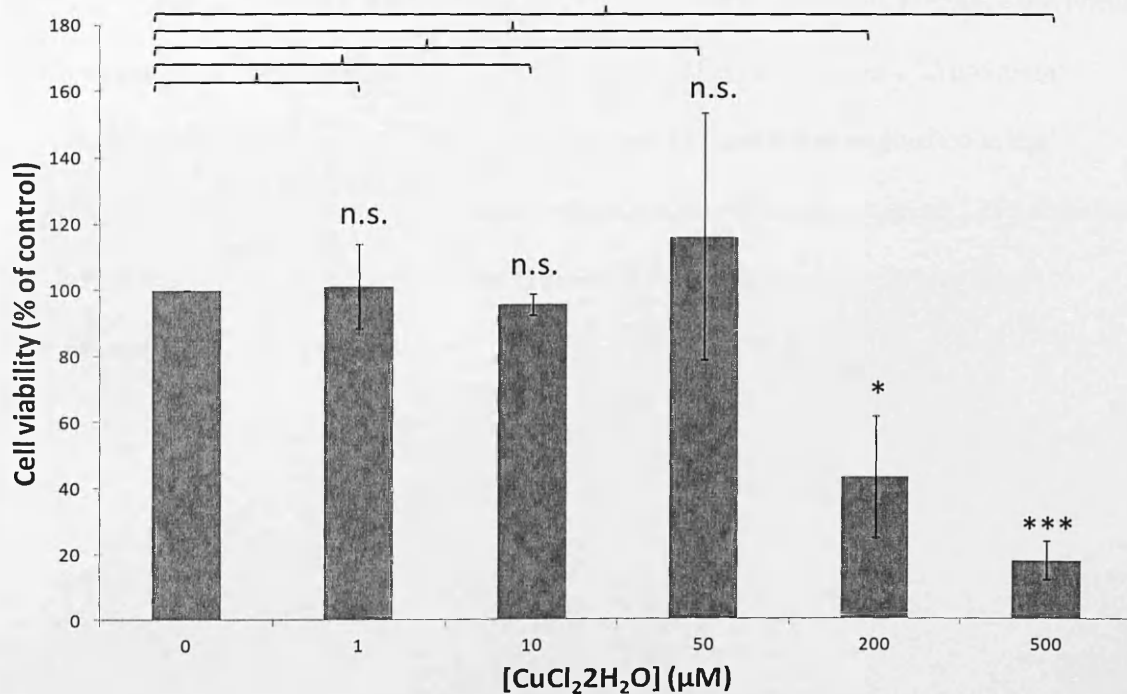


**Figure 4.7. The effect of copper on Du145 cell viability.** Cells were seeded at 2000 cells per well and grown to confluence.  $\text{CuCl}_2 \cdot 2\text{H}_2\text{O}$  was added at 0, 1, 10, 50, 200 or 500  $\mu\text{M}$  concentrations, and the cells were further incubated for 24 hours. Cell viability was then determined using the MTS assay (see Materials and Methods). Results are expressed relative to the viability of the untreated controls and are means  $\pm$  S.D. ( $n=3$ ). \* =  $p \leq 0.05$ ; \*\*\* =  $p \leq 0.005$ ; n.s. = not significant.

#### 4.7. The effect of copper on the expression and shedding of endogenous APP in Du145 cells

Du145 cells were, once more, grown to confluence and then treated with copper for 24 h. However, on this occasion, the cells and conditioned medium were harvested and immunoblotted in order to determine the effects of the metal on APP expression and proteolysis. Initially, equal volumes of cell lysates (equal protein content) were immunoblotted using the anti-APP C-terminal antibody. The results (*Fig. 4.8A*) show an increase in APP expression at metal concentrations of 10, 50 and 200  $\mu\text{M}$  (relative to the untreated control). However, at 200  $\mu\text{M}$  copper, levels of the APP holoprotein appeared to tail off, perhaps consistent with the decreased cell viability observed at these metal concentrations (*Fig. 4.7*). As this initial experiment was only performed on a single occasion, and in order to confirm a copper-associated increase in APP expression, a repeat experiment was performed using multiple cultures treated with either no copper or a 50  $\mu\text{M}$  metal concentration. The results (*Fig. 4.8C-F*) show a clear increase in APP expression in the presence of copper. The levels of mature cell-associated APP were enhanced  $2.74 \pm 0.49$ -fold whilst the increase in immature APP expression in the presence of copper was less pronounced at  $1.29 \pm 10.5$ -fold.

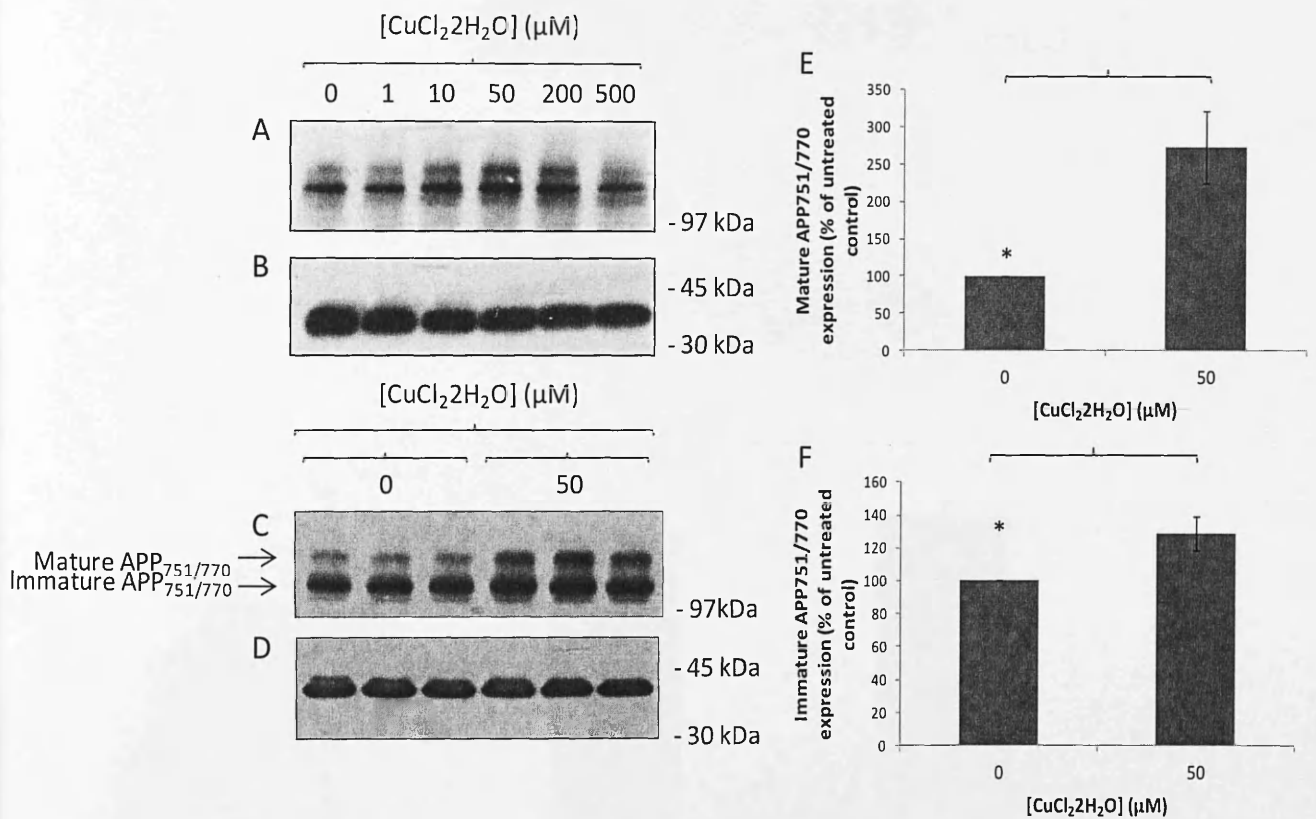


**Figure 4.8. The effect of copper on APP expression in Du145 cells.** Cells were grown to confluence and the medium was replaced with serum free medium containing 0, 1, 10, 50, 200 or 500 μM CuCl<sub>2</sub>·2H<sub>2</sub>O. After 24 h, the cells were harvested and lysates prepared (Materials and Methods). Equal volumes of the lysates were then resolved by SDS-PAGE and immunoblotted (Materials and Methods). **A** and **C**. Detection of full-length APP in cell lysates using the anti-APP C-terminal antibody. **B** and **D**. Detection of β-actin in cell lysates using the anti-β-actin antibody. **E** and **F**. Quantification of mature APP<sub>751/770</sub> (**E**) and immature APP<sub>751/770</sub> (**F**) levels from control and copper (50 μM) treated cells. Results are means ± S.D. (n=3). \* = p ≤ 0.05.

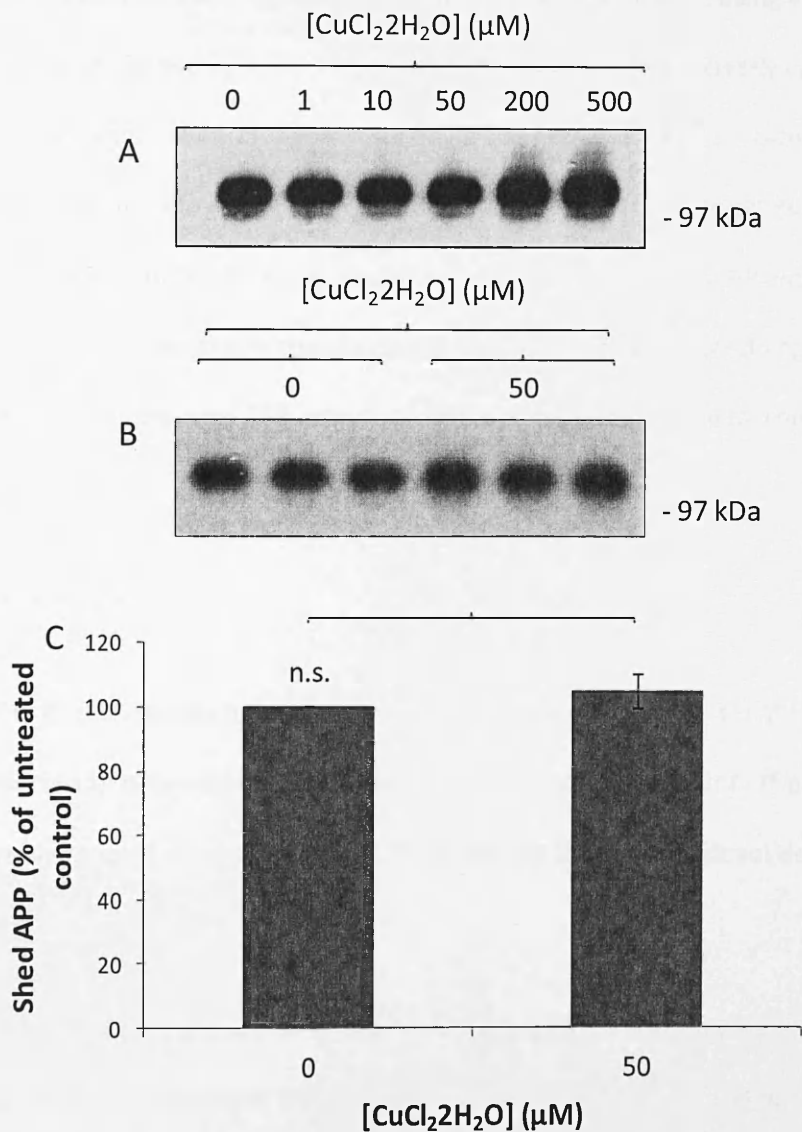


**Figure 4.9.** The effect of copper on soluble APP production from Du145 cells. Cells were grown to confluence and the medium was replaced with serum free medium containing 0, 1, 10, 50, 200 or 500 μM CuCl<sub>2</sub>·2H<sub>2</sub>O. After 24 h, the conditioned medium was collected and concentrated (Materials and Methods). Equal volumes of the medium samples were then resolved by SDS-PAGE and immunoblotted (Materials and Methods). **A** and **B**. Detection of soluble APP in conditioned medium using the anti-APP antibody 6E10. **C**. Quantification of soluble APP levels in medium from control and copper (50 μM) treated cells. Results are means ± S.D. (n=3). n.s. = not significant.

Next, the conditioned medium from Du145 cells treated with the initial 0-500  $\mu\text{M}$  copper concentration range was immunoblotted with antibody 6E10 in order to detect sAPP $\alpha$ . The results (*Fig. 4.9A*) appeared to show an increase in APP shedding at copper concentrations of 200 and 500  $\mu\text{M}$ . These metal concentrations were clearly cytotoxic (*Fig. 4.7*) and so, in order to confirm that APP shedding was not enhanced at sub-toxic copper concentrations, a further experiment was conducted whereby triplicate cell cultures were treated with either 0 or 50  $\mu\text{M}$  metal concentrations. The results (*Fig. 4.9B and 9C*) confirmed that sub-toxic copper concentrations did not enhance APP shedding despite the previously observed elevated APP expression levels at this particular metal concentration (*Fig. 4.8C-F*).

#### 4.8. Summary

The first conclusion to be drawn from this section of the study is that LNCaP, PC-3 and Du145 cells all demonstrated identical susceptibility to copper toxicity (*Figs. 4.1, 4.4 and 4.7*) with only copper concentrations of 200 and 500  $\mu\text{M}$  showing significant decreases in cell viability.

The LNCaP cells showed no change in APP expression when they were treated with sub-toxic copper concentrations (*Fig. 4.2*) with a corresponding lack of change in APP shedding (*Fig. 4.3*). In contrast, PC-3 cells showed a copper-associated decrease in APP expression (*Fig. 4.5*) possibly resulting from enhanced shedding of the protein (*Fig. 4.6*).

In complete contrast to both of the aforementioned cell lines, Du145 cells were the only cell type to show a clear and highly significant increase in APP expression in response to copper (*Fig. 4.8*). Interestingly, this change was not reflected in APP shedding (*Fig. 4.9*).

Notably, however, sAPP $\beta$  levels were not determined, raising the possibility of enhanced APP

processing via the amyloidogenic pathway due to increased APP expression in the presence of copper.

Collectively, these data show that the brain metastatic prostate cancer epithelial cell line, Du145, was the only one of the three lines studied to respond to copper by increasing APP expression. This observation is of particular note given the fact that the brain exhibits particularly high copper concentrations compared to all organs other than the liver (290, 291), raising the possibility that these cells might use APP as a defence against copper toxicity in the former organ.

# 5. The effect of full-length APP construct expression on Du145 cell viability in the presence of copper

## 5.1. Introduction

APP has previously been shown to bind copper at a site within the E1 domain (292) and, more recently, within the E2 domain (159) of the protein. In addition, free A $\beta$ -peptides bind copper (293), although it is not known whether the same domain within intact APP can also bind the metal. Previous research has demonstrated that this copper binding propensity of APP may be involved in copper efflux from cells (156, 170) and, therefore, may be protective against copper-induced cytotoxicity.

As prostate cancer cells metastasizing to the brain will, no doubt, encounter much higher copper concentrations within this organ (290, 291) than those at their point of origin in the prostate gland. The current study examined the ability of APP to protect brain metastatic Du145 cells against copper toxicity. Specifically, this chapter examines the effect of full-length APP isoform expression levels on the viability of Du145 cells in the presence of copper.

## 5.2. Endogenous APP transcript analysis in Du145 cells

Previous data (Chapter 3) established that Du145 cells endogenously expressed detectable (by immunoblotting) levels of only the larger KPI-containing APP isoforms. However, APP<sub>751</sub> and APP<sub>770</sub> co-migrated on gels during the aforementioned immunoblotting experiments and, therefore, could not be identified independently. Thus, in order to further elucidate endogenous APP isoform expression in this cell line, an RT-PCR analysis of endogenous APP transcript expression was performed.

**Table 5.1. RT-PCR primers employed in the current study**

<b>Transcript Analysed</b>	<b>Forward Primer</b>	<b>Reverse Primer</b>
APP	5'-TGAAGACAAAGTAGTAGAAGT-3'	5'-ACCTGGGACATTCTCTCGGTGCTTGGC-3'
Actin	5'-TGAAGTGTGTGACGTGGACATCCG-3'	5'-GCTGTCACCTTCACCGTTCCAG-3'

Du145 cells were grown to ~80% confluence and RNA was subsequently extracted as described in Materials and Methods. RT-PCR was carried out using the primers detailed in *Table 5.1*. The APP primers had previously been shown to amplify the three major APP isoform transcripts (294) producing fragments of 337, 505 and 562 base pairs for APP<sub>695</sub>, APP<sub>751</sub> and APP<sub>770</sub>, respectively.

The results (*Fig. 5.1*) clearly show that, as expected, the major endogenous APP transcripts in Du145 cells were APP<sub>751</sub> and APP<sub>770</sub> constituting  $31.28 \pm 2.67\%$  and  $65.1 \pm 2.43\%$  of the total APP transcripts, respectively. Minor amounts of APP<sub>695</sub> were also detected as confirmed by the co-migration of a faint band in the untransfected samples with a much more intense band at around 337 base pairs in samples extracted from APP<sub>695</sub> over-expressing cells (*Fig. 5.1A*). In fact, the APP<sub>695</sub> transcripts represented  $3.62 \pm 1.87\%$  of the total APP transcripts in Du145 cells (*Fig. 5.1B*). Equal levels of RNA in the untransfected and APP<sub>695</sub> over-expressing samples were confirmed by performing an actin RT-PCR (*Fig. 5.1C*) which generated the expected 449 base pair fragment.

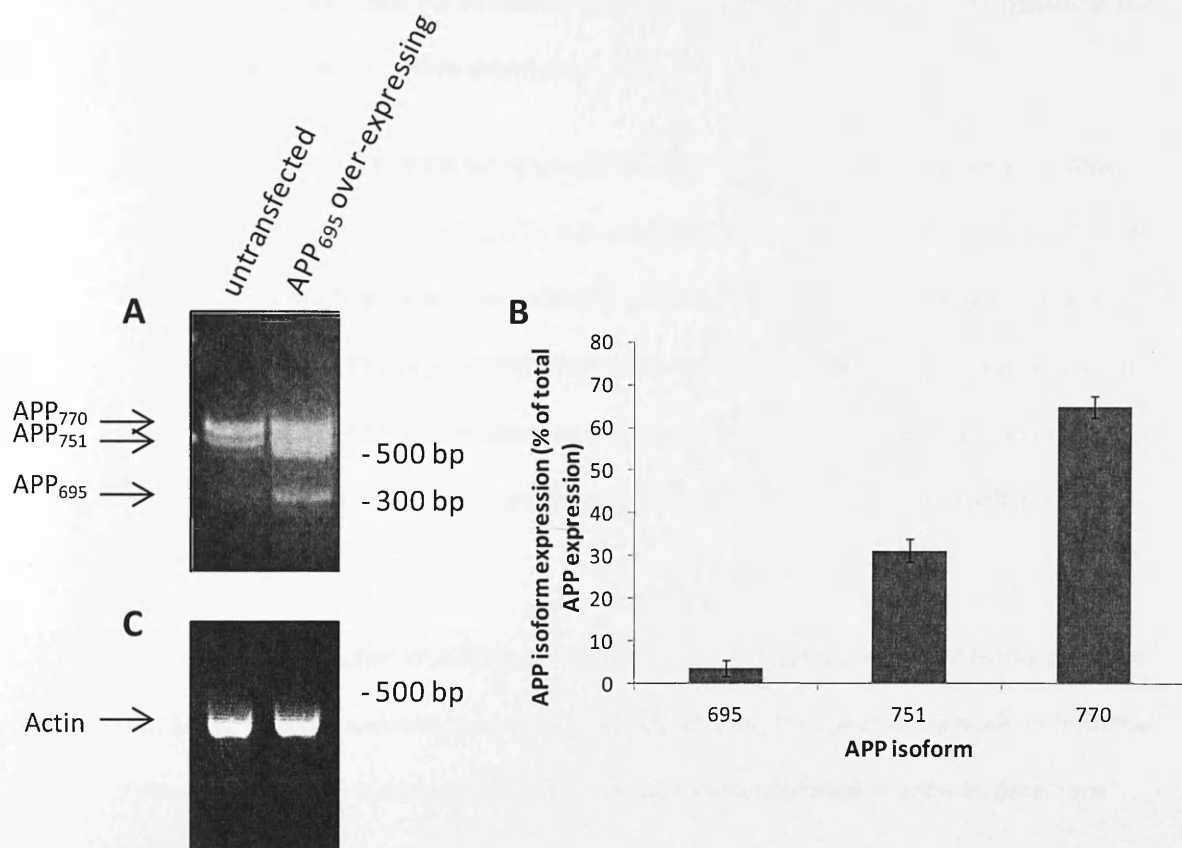


**Figure 5.1. Endogenous APP transcript expression in Du145 cells.** Cells were grown to 80% confluence and harvested for mRNA extraction (see Materials and Methods). RT-PCR was then performed using the APP and actin primers detailed in *Table 5.1* and the reaction products were resolved by agarose gel electrophoresis. **A.** APP transcript expression in untransfected and APP<sub>695</sub> over-expressing cells. **B.** Multiple APP RT-PCR gels were quantified by densitometric analysis. **C.** Actin RT-PCR analysis.

### 5.3. Over-expression of APP isoform constructs in Du145 cells

Having confirmed that all three major APP isoform transcripts were endogenously expressed in Du145 cells, the effects of over-expressing these isoforms on cell viability in the presence of copper were then examined.

Du145 cells were first stably transfected with pRES hyg plasmid containing cDNA encoding APP<sub>695</sub>, APP<sub>751</sub> or APP<sub>770</sub> (Fig. 5.2) using the Nucleofector 2b device as described in Materials and Methods. Following antibiotic selection, cell lysates were prepared and equal amounts of protein from each transfectant were resolved by SDS-PAGE and immunoblotted with the anti-APP C-terminal antibody in order to detect full-length APP. The results (Fig. 5.3) clearly show that all three APP isoforms were successfully over-expressed albeit at varying levels.

As the detection of different APP isoforms in cell lysates is confused by the presence not just of multiple isoforms but also multiple glycoforms, the conditioned medium from the various APP isoform-transfected cell lines was also immunoblotted in order to detect the

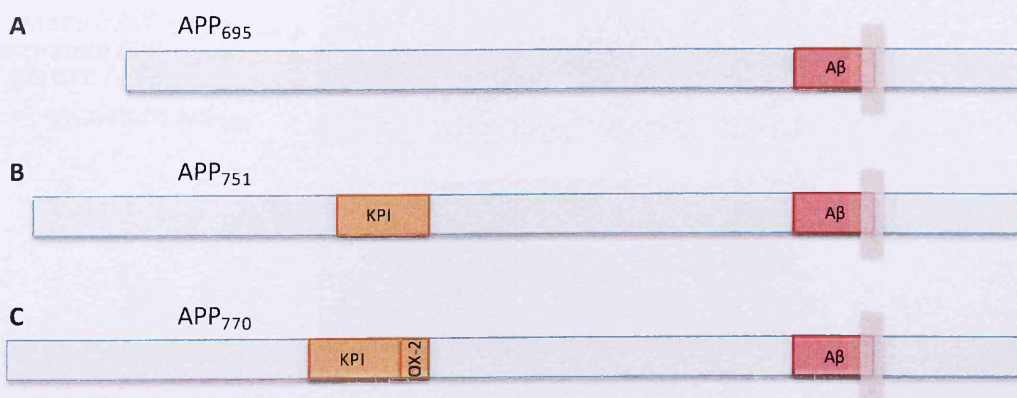


**Figure 5.2. Schematic showing the APP isoform constructs used in the current study.** A. APP<sub>695</sub> contains neither the KPI domain nor the OX-2 domain. B. APP<sub>751</sub> does not contain the OX-2 domain. C. APP<sub>770</sub> possesses both the KPI and the OX-2 domain.

soluble APP ectodomain fragments which consist almost exclusively of fully glycosylated APP isoforms. Initially the medium samples were immunoblotted with antibody 6E10 in order to detect sAPP $\alpha$ . The results (Fig. 5.4A) show that the APP-transfected cells produced significantly more total sAPP $\alpha$  than the mock-transfected cells. The same samples were also immunoblotted with antibody 1A9 in order to detect sAPP $\beta$  (Fig. 5.4B). Whilst there was a significant increase in total sAPP $\beta$  levels shed from the APP<sub>695</sub>-transfected cells, it is interesting to note that sAPP $\beta$  originating from the endogenous KPI-containing isoforms was actually reduced in these cells relative to the mock-transfected cells, perhaps suggesting a competition between isoforms for the active site of BACE1. Also of interest was the fact that the levels of sAPP $\beta$  shed from APP<sub>751</sub>- or APP<sub>770</sub>-transfected cells were much greater (between 10- and 20-fold higher) than those shed from either the mock- or APP<sub>695</sub>-transfected cells.

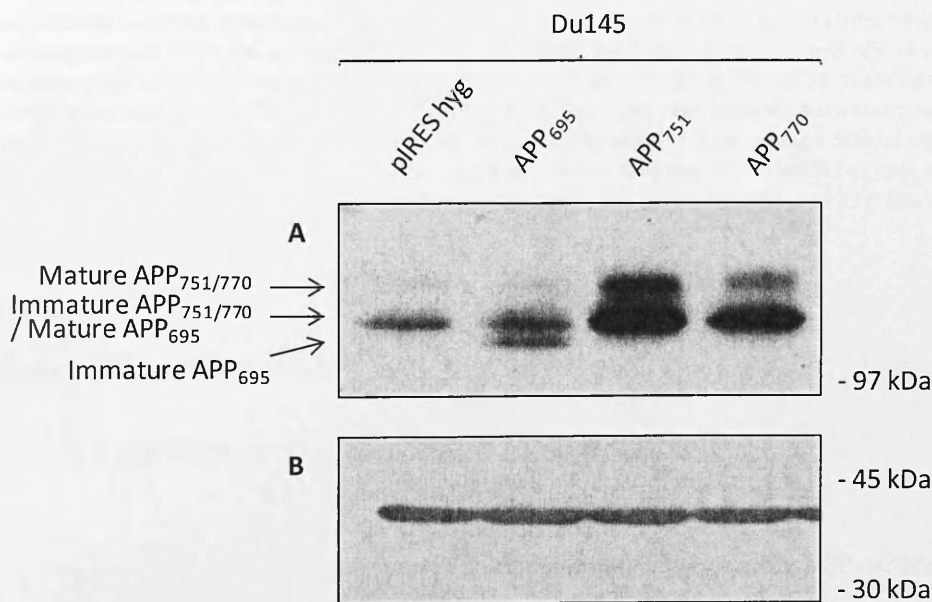


**Figure 5.3. APP isoform over-expression in Du145 cells.** Cells were grown to confluence and the medium was replaced with serum free medium for 24 h. The cells were then harvested and lysates prepared (Materials and Methods). SDS-PAGE and immunoblots were then performed (Materials and Methods). **A.** Detection of full length APP in cell lysates using the anti-APP C-terminal antibody. **B.** Detection of  $\beta$ -actin in cell lysates using the anti- $\beta$ -actin antibody. The results shown are representative of three repeat experiments.

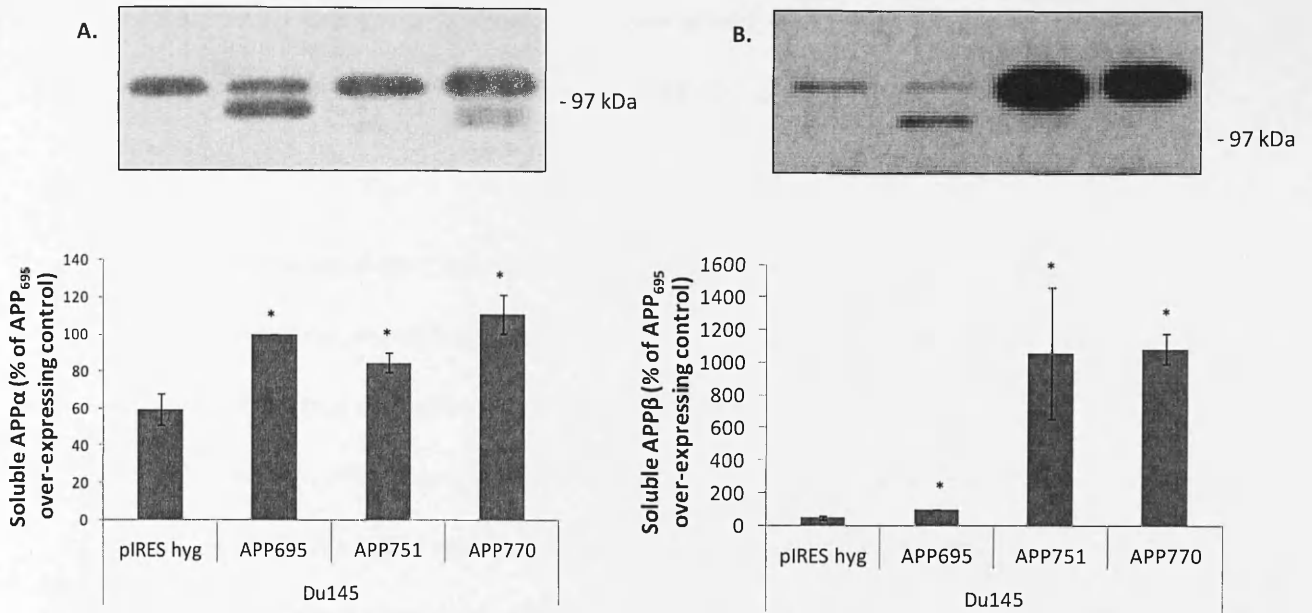


**Figure 5.4. Soluble APP produced by Du145 cells over-expressing APP isoform constructs.** Cells were grown to confluence and the medium was replaced with serum free medium for 24 h. Concentrated conditioned medium samples were prepared and subjected to SDS-PAGE and immunoblotting as described in Materials and Methods. **A.** Detection of sAPP $\alpha$  in conditioned media using the anti-APP 6E10 antibody. Multiple 6E10 immunoblots were quantified and displayed graphically. **B.** Detection of sAPP $\beta$  in conditioned media using the anti-APP 1A9 antibody. Multiple 1A9 immunoblots were also quantified and displayed graphically. Results are means  $\pm$  S.D. (n=3) and displayed as a percentage of total sAPP produced by Du145 APP<sub>695</sub> cells, due to low (and variable) levels produced by the Du145 pIRES hyg cells creating large error. Significance was tested against the Du145 pIRES hyg control. \* = significant at  $p \leq 0.05$ .

#### 5.4. The effect of APP isoform over-expression on Du145 cell viability in the presence of copper

Having analysed the expression and proteolysis of the various APP isoform constructs, their effects on Du145 cell viability in the presence of the various copper concentrations were then examined. Mock- or APP isoform-transfected cells were seeded at 2000 cells per well and equilibrated overnight before adding glycine-complexed copper at metal concentrations ranging from 0-200  $\mu$ M. These copper concentrations are physiologically relevant in the brain as synaptic copper levels are estimated to be 100-250

$\mu\text{M}$  (295, 296). The Du145 cells were then cultured for 7 days with the medium being replaced with fresh copper-containing medium on day 4. MTS cell viability assays were performed on day 0 (5 h after initial copper addition) and day 7 as described in Materials and Methods.

The results from these viability experiments (*Fig. 5.5*) are expressed as percentage viability of the non-metal-treated controls. As would be expected, there was no difference in viability regardless of whether or not the cells had been treated with copper at day 0 (*Fig. 5.5A*). However, after seven days of growth, the viability of the mock-transfected cells was reduced to  $65.42 \pm 3.26\%$  and  $51.72 \pm 4.54\%$  of the untreated cells in the presence of 150 and 200  $\mu\text{M}$  copper respectively (*Fig. 5.5B*). When the cells were stably transfected with APP<sub>695</sub>, this decrease in viability was largely ablated with viability being  $97.13 \pm 1.33\%$  and  $93.45 \pm 2.34\%$  of the untreated controls in the presence of 150 and 200  $\mu\text{M}$  copper respectively. In fact, at a copper concentration of 150  $\mu\text{M}$ , all three of the major APP isoforms significantly enhanced the viability of the Du145 cells relative to the mock-transfected cell viability at the same metal concentration (*Fig. 5.5B*). The pattern was also similar at 200  $\mu\text{M}$  copper, except that APP<sub>770</sub> did not improve viability at this metal concentration. Notably, APP<sub>695</sub> was clearly the most effective isoform in terms of preventing a copper-induced reduction in cell viability.

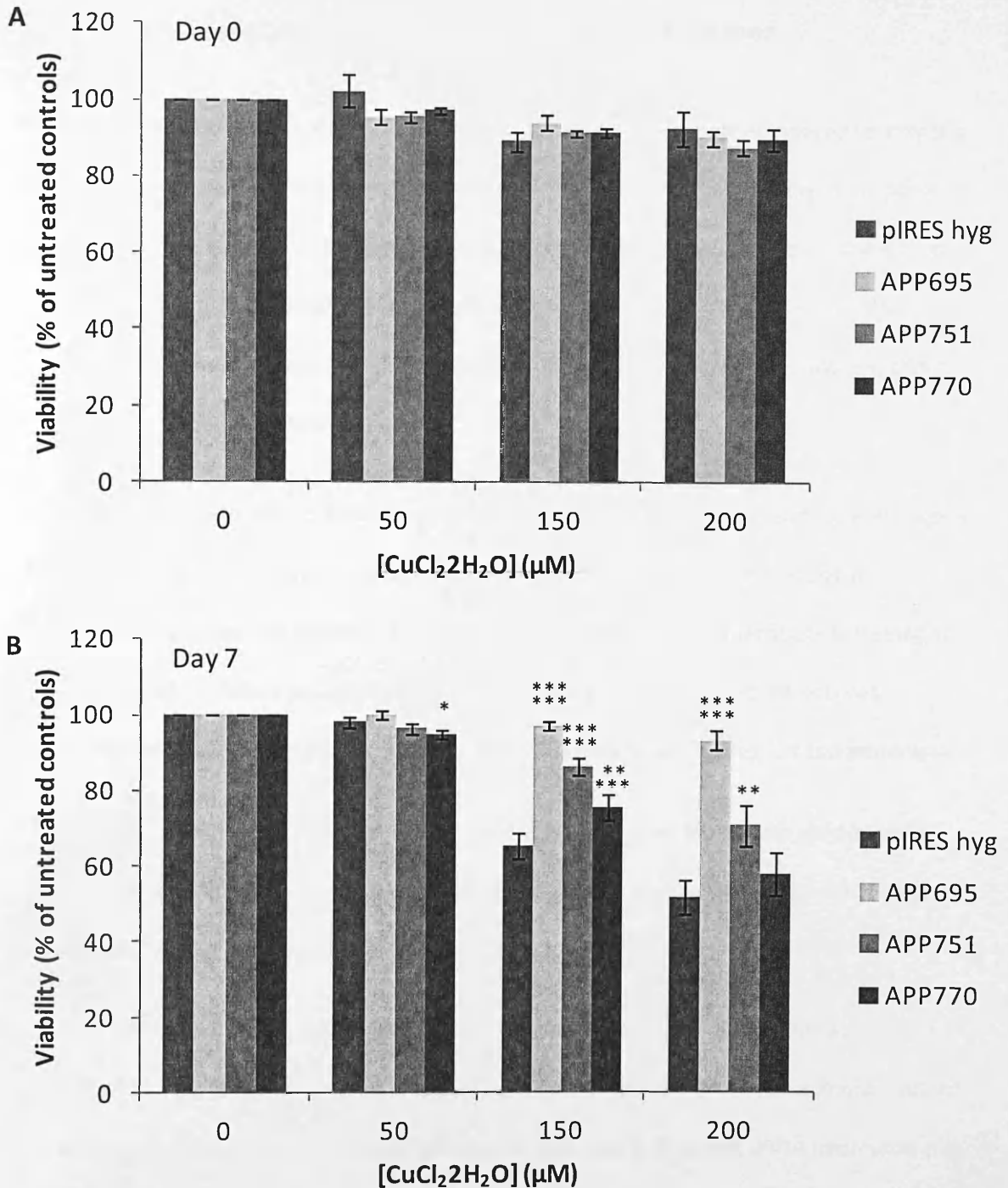


**Figure 5.5. The effects of APP isoform construct over-expression on Du145 cell viability in the presence of copper.** Cells were seeded at 2000 cells per well and equilibrated overnight under normal growth conditions (37 °C, 5% CO<sub>2</sub>). Glycine-complexed copper was added to final metal concentrations of 0, 50, 150 and 200 μM in 100 μl of complete RPMI; the cells were then grown over a 7 day period with medium being replaced with fresh metal-containing medium at day 4. The MTS cell viability assay was performed on day 0 (within 5 h of adding the metal) (A) and on day 7 (B). Results are means ± S.E. (n=12). Significance was tested against the Du145 pIRES hyg control. \* = significant at  $p \leq 0.05$ ; \*\* - significant at  $p \leq 0.01$ ; \*\*\*\* = significant at  $p \leq 0.0005$ ; \*\*\*\*\* =  $p \leq 0.0001$ . Unless otherwise stated, differences were not significant.

## 5.5. The effect of ablating endogenous APP expression on Du145 cell viability in the presence of copper

As over-expression of APP<sub>695</sub> protected Du145 cells from copper induced toxicity (*Fig. 5.5*), the effect of knocking down endogenous APP expression on cell viability in the presence of copper was also examined. For this purpose the following siRNA's were purchased from Thermo Scientific Dharmacon (St Leon-Rot, Germany) and employed in the study: Non-targeting #1 siRNA control pool (Cat. No. D-001206-13-05) and human APP targeting siRNA SMARTpool (Cat. No. M-003731-00).

Cells were seeded in complete growth medium in 24-well plates and allowed to grow overnight. siRNA transfections were commenced the following morning and glycine-complexed copper was added 24 h post transfection (Materials and Methods). Following an additional 48 h culture period, MTS cell viability assays were performed. Parallel cell incubations were performed for the immunoblot analysis of APP expression and proteolysis.

As these experiments were performed in 24 well plates the protein yield in lysate and conditioned medium samples was too low to quantify and, as such, equal volumes of samples (rather than equal protein amounts) were resolved on gels.

The results (*Fig. 5.6A*) show that the APP siRNA treatment reduced the expression of APP to  $23.21 \pm 4.85$  % that of the control siRNA treatment. A similar decrease in the levels of sAPP $\alpha$  was observed in conditioned medium ( $31.15 \pm 3.45$ % of control siRNA treatment) (*Fig. 5.6C*). The corresponding MTS assays (*Fig. 5.7*) showed that depleting APP levels in the presence of copper reduced cell viability by  $9.6 \pm 1.76$ % compared to the control siRNA-treated cells.

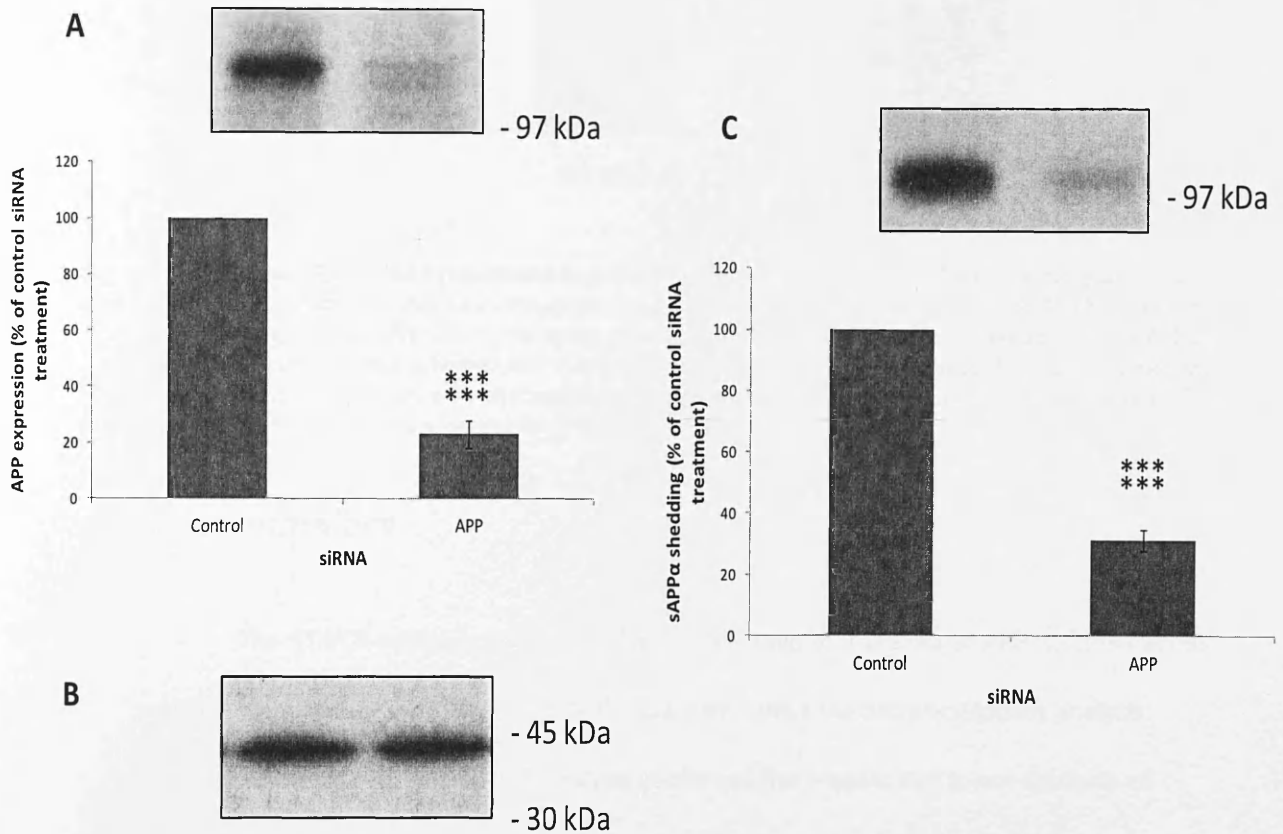


**Figure 5.6. APP expression and proteolysis in siRNA transfected Du145 cells.** Cells were seeded into a 24-well plate as stated in Materials and Methods. After an overnight growth period, the cells were transfected with 25 nM control or APP-targeting siRNA (Materials and Methods). Glycine-complexed copper (200  $\mu$ M) was added to wells 24 h post-transfection. Following further 48 h incubation, cells and conditioned medium were harvested and prepared for immunoblotting as per Materials and Methods. **A.** Detection of APP in lysates using the anti-APP C-terminal antibody. **B.** Detection of  $\beta$ -actin in lysates using the anti- $\beta$ -actin antibody. **C.** Detection of sAPP $\alpha$  in conditioned medium using the anti-APP 6E10 antibody. Immunoblots were quantified and the results expressed relative to the control siRNA treatment. Results are means  $\pm$  S.E. (n=12) from 4 independent experiments. \*\*\*\*\* = significant at  $p \leq 0.0001$ .

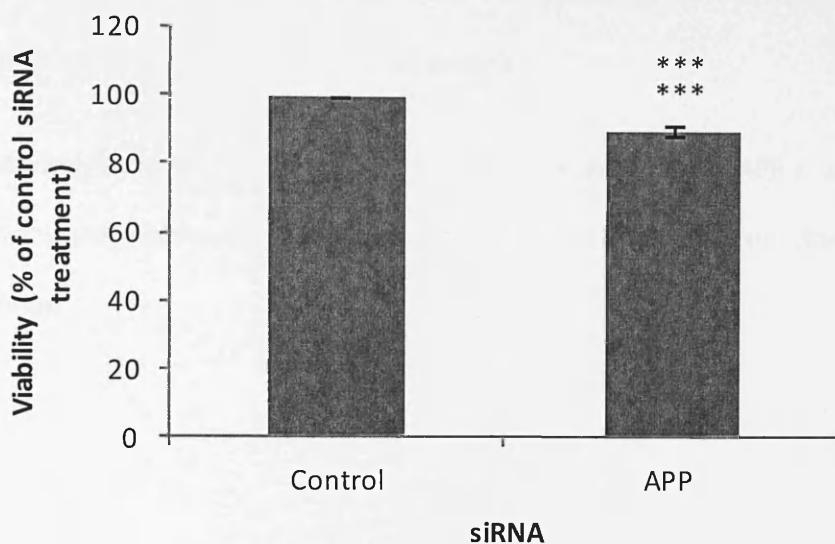


**Figure 5.7. Viability of siRNA transfected Du145 cells.** Cells were seeded into a 24-well plate as stated in Materials and Methods. After an overnight growth period, the cells were transfected with 25 nM control or APP-targeting siRNA (Materials and Methods). Glycine-complexed copper (200  $\mu$ M) was added to wells 24 h post-transfection. Following further 48 h incubation, MTS assays were carried out as stated in Materials and Methods. MTS assay results were analysed relative to the control siRNA treatment. Results are means  $\pm$  S.E. (n=15) from 3 independent experiments. \*\*\*\*\* = significant at  $p \leq 0.0001$ .

## 5.6. Summary

The RT-PCR analysis of Du145 cell RNA confirmed that the major APP isoforms in this cell line were APP<sub>751</sub> and APP<sub>770</sub> (Fig. 5.1). However, unlike the immunoblotting analysis performed previously, the RT-PCR analysis confirmed the presence of minor amounts of APP<sub>695</sub> transcripts in Du145 cells.

The three major APP isoforms were then successfully stably over-expressed in Du145 cells and their effects on cell viability in the presence of copper were monitored. The results (Fig. 5.5) clearly show that all three isoforms were capable of enhancing viability in the presence of the metal, with APP<sub>695</sub> being clearly the most effective isoform in this respect. When siRNA was used to deplete the endogenous expression of APP in Du145 cells, their viability in the presence of copper was slightly decreased (Fig. 5.7). Notably, the decrease in cell viability associated with the depletion of endogenous APP was nowhere near the

increase in viability observed when the protein was over-expressed, perhaps suggesting a degree of redundancy of APP in this functional capacity.

Collectively, these data confirm that Du145 cells are able to utilise APP in order to enhance their viability in the presence of physiologically relevant (to the brain) copper concentrations.

6. The APP cytosolic domain is a prerequisite for enhanced Du145 cell viability in the presence of copper

## 6.1. Introduction

The results presented in the previous chapter clearly demonstrate that APP<sub>695</sub> was able to enhance the viability of the brain metastatic prostate cancer cell line, Du145, in the presence of copper. The current chapter begins to examine the prerequisites within the APP molecule necessary for this effect. Specifically, the role played by the cytosolic domain of the protein is examined. This part of the APP molecule contains a YENPTY motif which is typical of tyrosine kinase receptors and has been shown to interact with a range of intracellular adaptor proteins, some of which elicit downstream signalling events such as the MAPK pathway (reviewed in (50)). The effects of deleting or mutating this part of the molecule on the viability of Du145 cells in the presence of copper are examined.

## 6.2. The expression and proteolysis of APP cytosolic domain mutant constructs in Du145 cells

In order to investigate the role of the APP cytosolic domain in enhancing the viability of Du145 cells in the presence of copper, a range of cytosolic domain mutant constructs were designed and stably expressed in the cell line (*Fig. 6.1*). The APP<sub>695</sub>ΔICD construct (*Fig. 6.1B*) lacked the cytosolic domain of the protein being truncated C-terminally to L648. A series of tyrosine point mutation constructs were also generated (APP<sub>695</sub>-682, APP<sub>695</sub>-687 and APP<sub>695</sub>-682/687) in order to examine the effects of phosphorylation within the YENPTY motif on cell viability (*Figs. 6.1C-E*).

The various APP constructs were stably transfected into Du145 cells (see Materials and Methods) and their expression and proteolysis were subsequently monitored by immunoblotting. Initially, equal amounts of protein from cell lysates were resolved by SDS-PAGE and immunoblotted using the anti-APP antibody 6E10 (APP<sub>695</sub>ΔICD does not possess the intracellular domain epitope recognised by the APP C-terminal antibody used in previous

chapters). The results (Fig. 6.2) clearly show that all of the constructs were successfully expressed albeit that the APP<sub>695</sub>ΔICD construct was expressed at a significantly lower level than the other constructs. Interestingly, the over-expression of the APP<sub>695</sub> constructs appeared to affect the expression of the two larger endogenous isoforms indicating that APP may have the ability to up regulate its own expression as demonstrated previously (297).

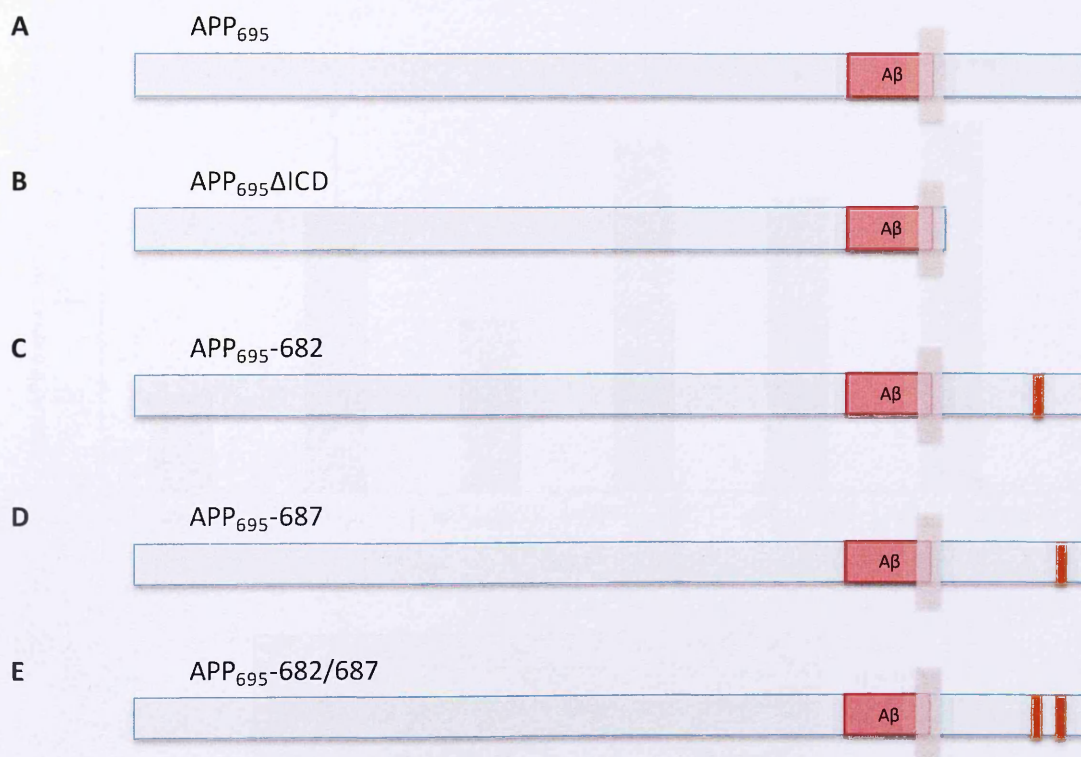


**Figure 6.1. Schematic representing APP intracellular domain mutant constructs.** A. Wild-type APP<sub>695</sub>. B. APP<sub>695</sub>ΔICD was truncated C-terminally to L648 and, therefore, lacks the cytosolic domain of its wild-type counterpart. C-E. Single or double tyrosine to glycine mutations were introduced at positions 682 and/or 687.

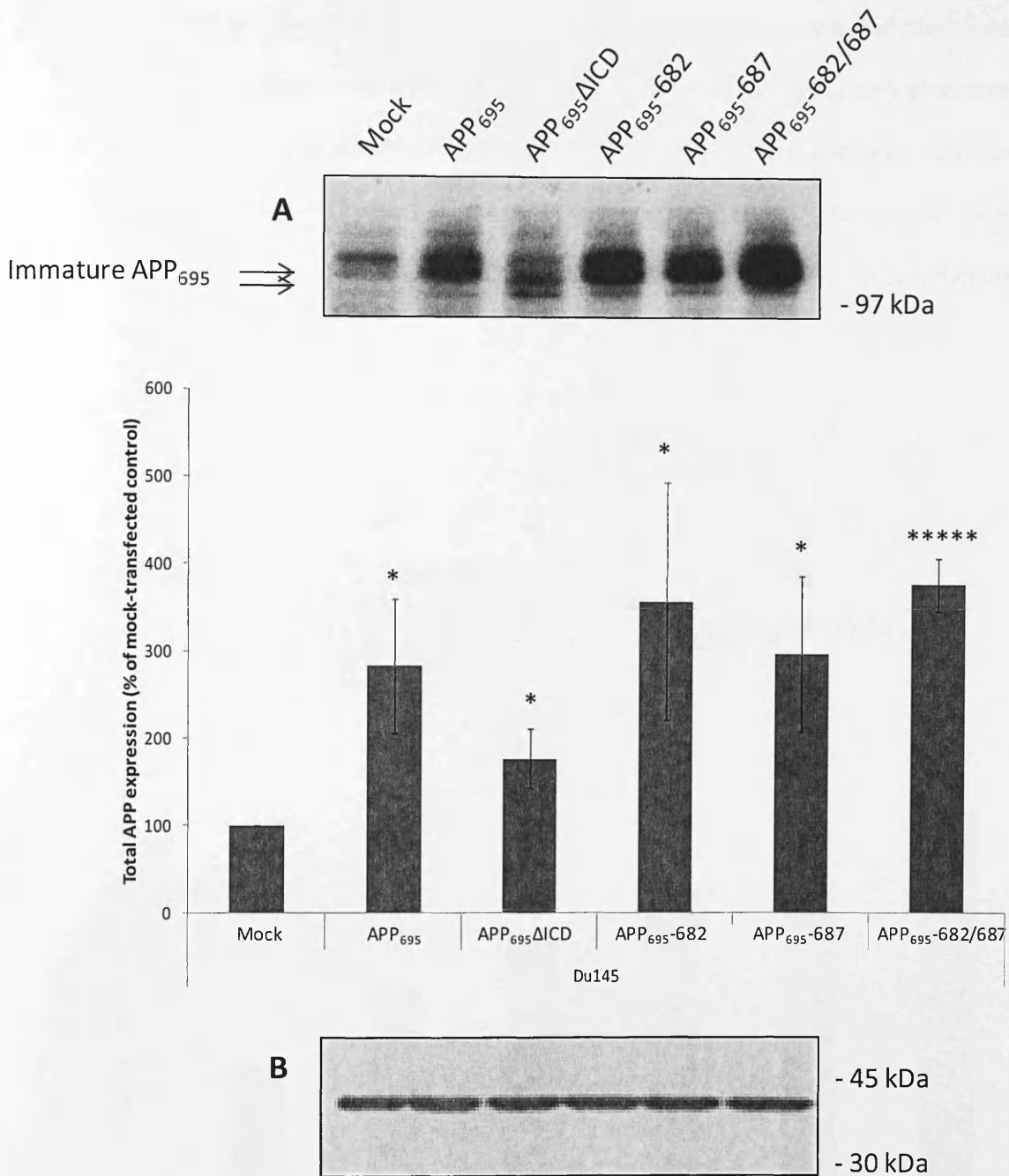


**Figure 6.2. APP intracellular domain mutant over-expression in Du145 cells.** Stably transfected cells were grown to confluence and the medium was replaced with serum free medium for 24 h. Lysates were subsequently prepared and equal amounts of protein from each were immunoblotted (Materials and Methods). **A.** Detection of APP in cell lysates using the anti-APP antibody, 6E10. Multiple 6E10 immunoblots were quantified by densitometric analysis and the results shown are means  $\pm$  S.D. (n=3). Significance was tested against the mock-transfected control. \* = significant at  $p \leq 0.05$ ; \*\*\*\*\* = significant at  $p \leq 0.0005$ . Unless otherwise indicated, the results are not significantly different. **B.** Detection of  $\beta$ -actin in cell lysates using the anti- $\beta$ -actin antibody.

Next, the generation of soluble APP from the various cytosolic domain mutant constructs was examined by immunoblotting equal volumes of concentrated conditioned medium with the anti-APP antibody 6E10 (Fig. 6.3). The wild-type APP<sub>695</sub> cells generated significantly more total sAPP $\alpha$  than the mock-transfected cells, as would be expected, and the generation of this proteolytic fragment was largely unaffected by the removal of the entire APP cytosolic domain (APP<sub>695</sub> $\Delta$ ICD) or the mutation of tyrosine residues within the YENPTY cytosolic motif.

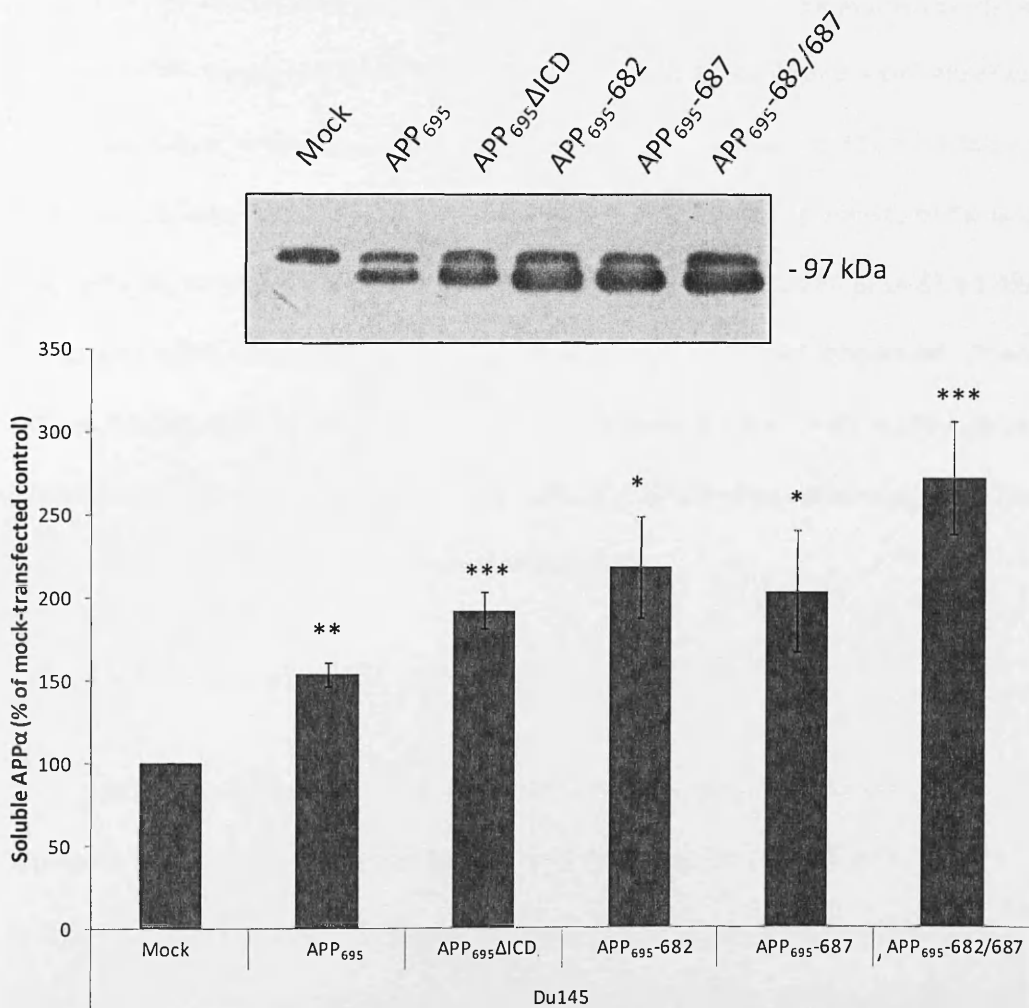


**Figure 6.3. Soluble APP generation by Du145 cells over-expressing APP intracellular domain mutants.** Stably transfected cells were grown to confluence and the medium was replaced with serum free medium for 24 h. Conditioned medium was subsequently prepared and equal volumes of each sample were immunoblotted using the anti-APP antibody 6E10 (Materials and Methods). Multiple 6E10 immunoblots were quantified by densitometric analysis and the results shown are means  $\pm$  S.D. (n=3). Significance was tested against the mock-transfected control. \* = significant at  $p \leq 0.05$ ; \*\* = significant at  $p \leq 0.01$ ; \*\*\* = significant at  $p \leq 0.001$ . Unless otherwise indicated, the results are not significantly different.

### 6.3. The effects of APP cytosolic domain mutations on the viability of Du145 cells in the presence of copper

In order to examine the role played by the APP cytosolic domain in the enhancement of Du145 cell viability in the presence of copper, the stably transfected cells were seeded out and cultured overnight before adding glycine-complexed metal at concentrations of 0-200  $\mu\text{M}$ . MTS viability assays were performed at both 5 h and 7 days after the addition of copper. The results (*Fig. 6.4A*) show a slight initial drop in viability following the addition of copper to the various APP-transfected cells. However, after seven days (*Fig. 6.4B*) the viability of mock-transfected cells treated with 150 and 200  $\mu\text{M}$  copper had decreased to  $63.25 \pm 3.38\%$  and  $49.98 \pm 3.33\%$ , respectively, of the untreated controls. In contrast, the viability of the wild-type APP<sub>695</sub>-transfected cells at the same metal concentrations remained at  $94.88 \pm 1.43\%$  and  $91.48 \pm 3.42\%$ , respectively, of the untreated controls. Thus, the wild-type APP clearly enhanced cell viability in the presence of copper. However, in the case of the APP<sub>695</sub> $\Delta$ ICD mutant and all of the tyrosine mutants, the ability of APP to protect against copper-induced reductions in cell viability was clearly ablated (*Fig. 6.4B*).

### 6.4. APP regulates the raft association of caveolin-1

APP proteolysis is linked to the association of the protein with cholesterol and sphingolipid-rich lipid rafts (87). It is possible that removing the cytosolic domain of APP, as in the case of the APP<sub>695</sub> $\Delta$ ICD construct, would alter its raft association. In order to investigate this possibility, mock-, APP<sub>695</sub>- and APP<sub>695</sub> $\Delta$ ICD-transfected Du145 cells were grown to confluence and solubilised in Triton X-100 at 4 °C. Lipid rafts were subsequently prepared using buoyant sucrose density gradient centrifugation as described in Materials and Methods. After harvesting, the individual gradient fractions were analysed in terms of

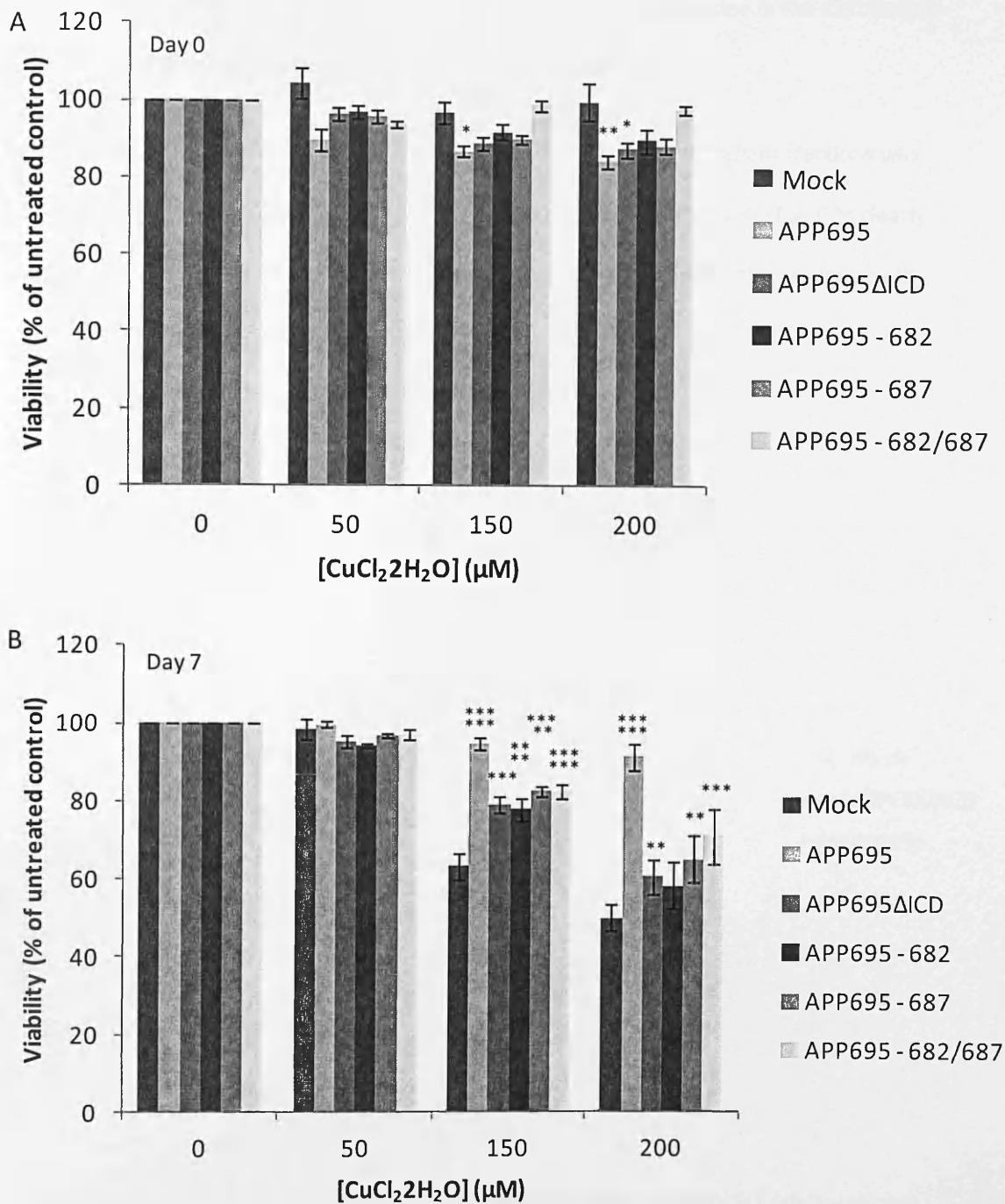


**Figure 6.4. The effects of APP intracellular domain mutant over-expression on Du145 cell viability in the presence of copper.** Cells were seeded at 2000 cells per well and equilibrated overnight under normal growth conditions (37 °C, 5% CO<sub>2</sub>). Glycine-complexed copper was added to final metal concentrations of 0, 50, 150 and 200 μM in 100 μl of complete RPMI; the cells were then grown over a 7 day period with medium being replaced with fresh metal-containing medium at day 4. The MTS cell viability assay was performed on day 0 (within 5 h of adding the metal) (A) and on day 7 (B). Results are means ± S.E. (n=9). Significance was tested against the mock-transfected control. \* = significant at  $p \leq 0.05$ ; \*\* = significant at  $p \leq 0.01$ ; \*\*\* = significant at  $p \leq 0.005$ ; \*\*\*\* = significant at  $p \leq 0.001$ ; \*\*\*\*\* = significant at  $p \leq 0.0001$ . Unless otherwise stated, differences were not significant.

their protein content. The results (Fig. 6.5) are expressed in terms of a percentage distribution of protein throughout the gradients and show no difference in the distribution regardless of which protein was over-expressed in the cells.

Next, the distribution of APP itself throughout the sucrose gradient fractions was determined by immunoblotting with anti-APP antibody, 6E10. The results (Fig. 6.6) clearly show that all forms of the protein were distributed equally throughout the gradients with none being detected in the raft fractions.

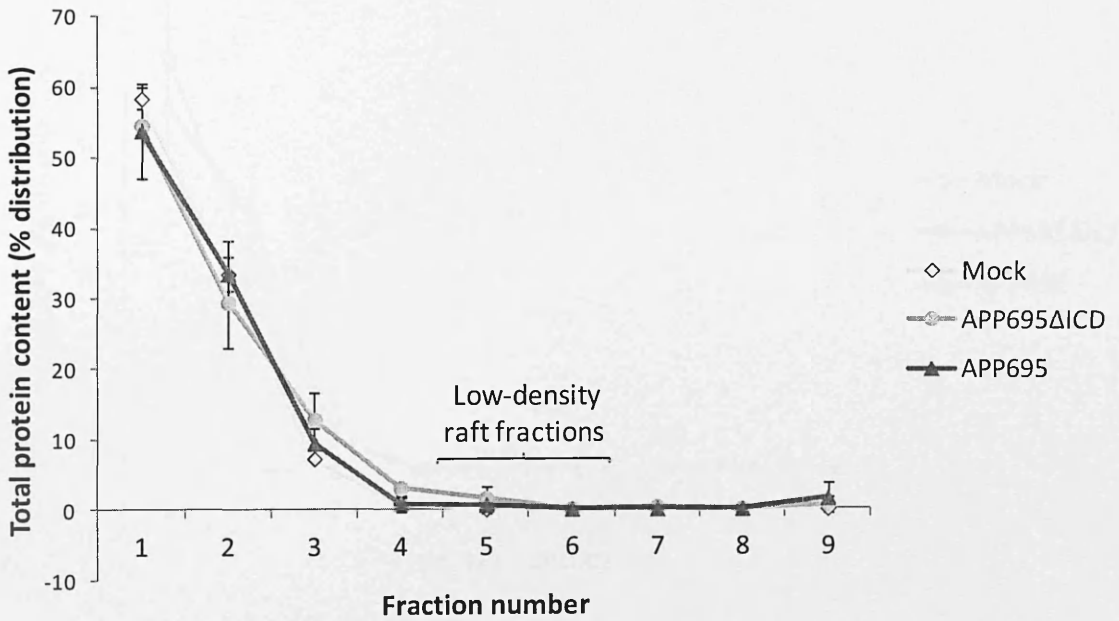


**Figure 6.5. Analysis of protein distribution in sucrose gradients prepared from Du145 cells transfected with either vector alone, wild-type APP<sub>695</sub> or APP<sub>695</sub>ΔICD.** Lipid rafts were prepared as described in Materials and Methods and individual fractions were harvested (1 – bottom of gradient, 9 – top of gradient). Protein concentrations within the fractions were determined using the BCA assay (Materials and Methods). The results are expressed in terms of percentage distribution throughout the gradients and are means ± S.D. (n=3).

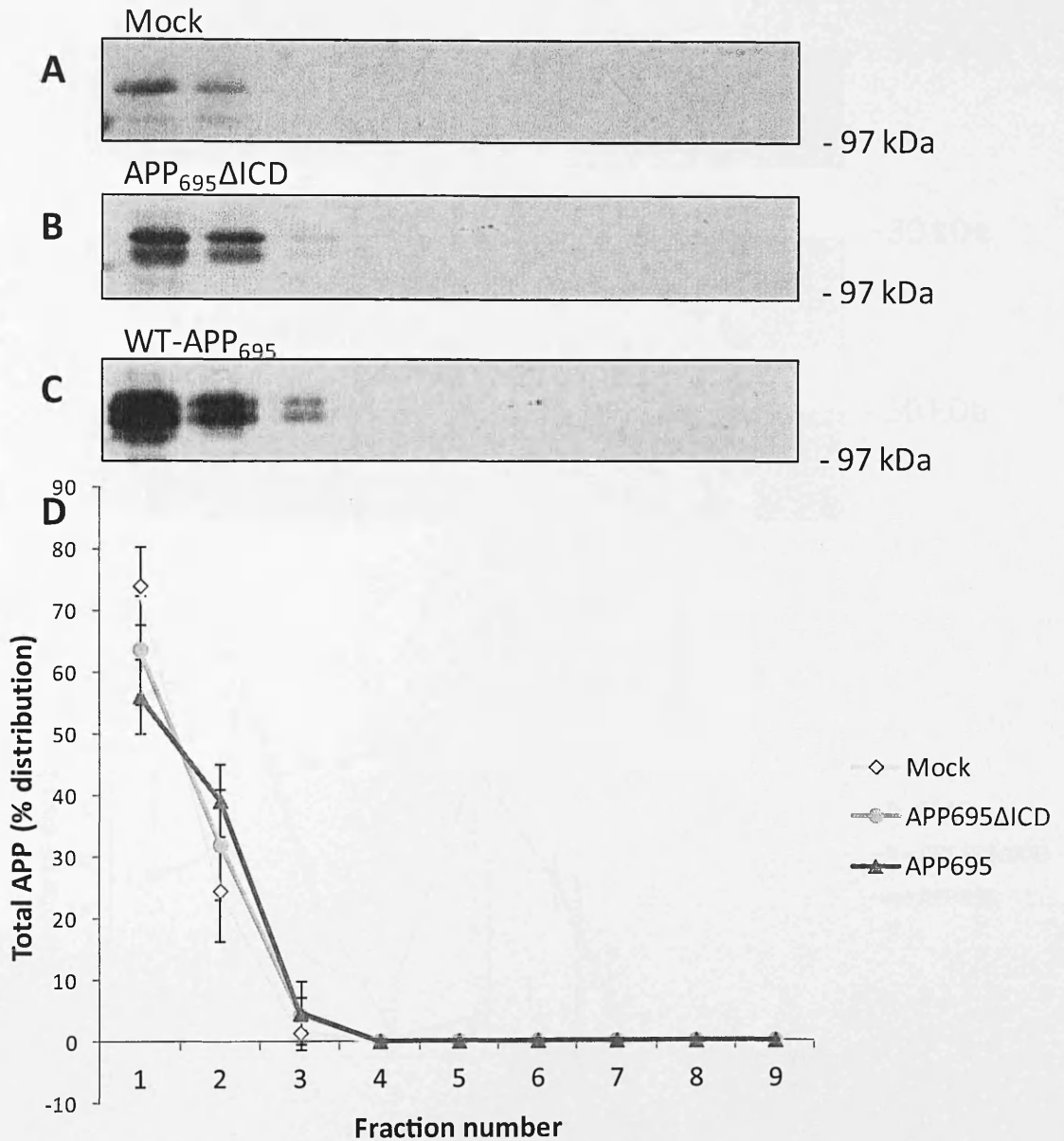


**Figure 6.6.** Analysis of APP distribution in sucrose gradients prepared from Du145 cells transfected with either vector alone, wild-type APP<sub>695</sub> or APP<sub>695</sub>ΔICD. Lipid rafts were prepared as described in Materials and Methods and individual fractions were harvested (1 – bottom of gradient, 9 – top of gradient). Fractions were resolved by SDS-PAGE and subsequently immunoblotted with anti-APP antibody, 6E10 (Materials and Methods) (A-C). Multiple immunoblots from each cell type were quantified by densitometric analysis (D) and the results are expressed in terms of percentage distribution throughout the gradients and are means ± S.D. (n=3).

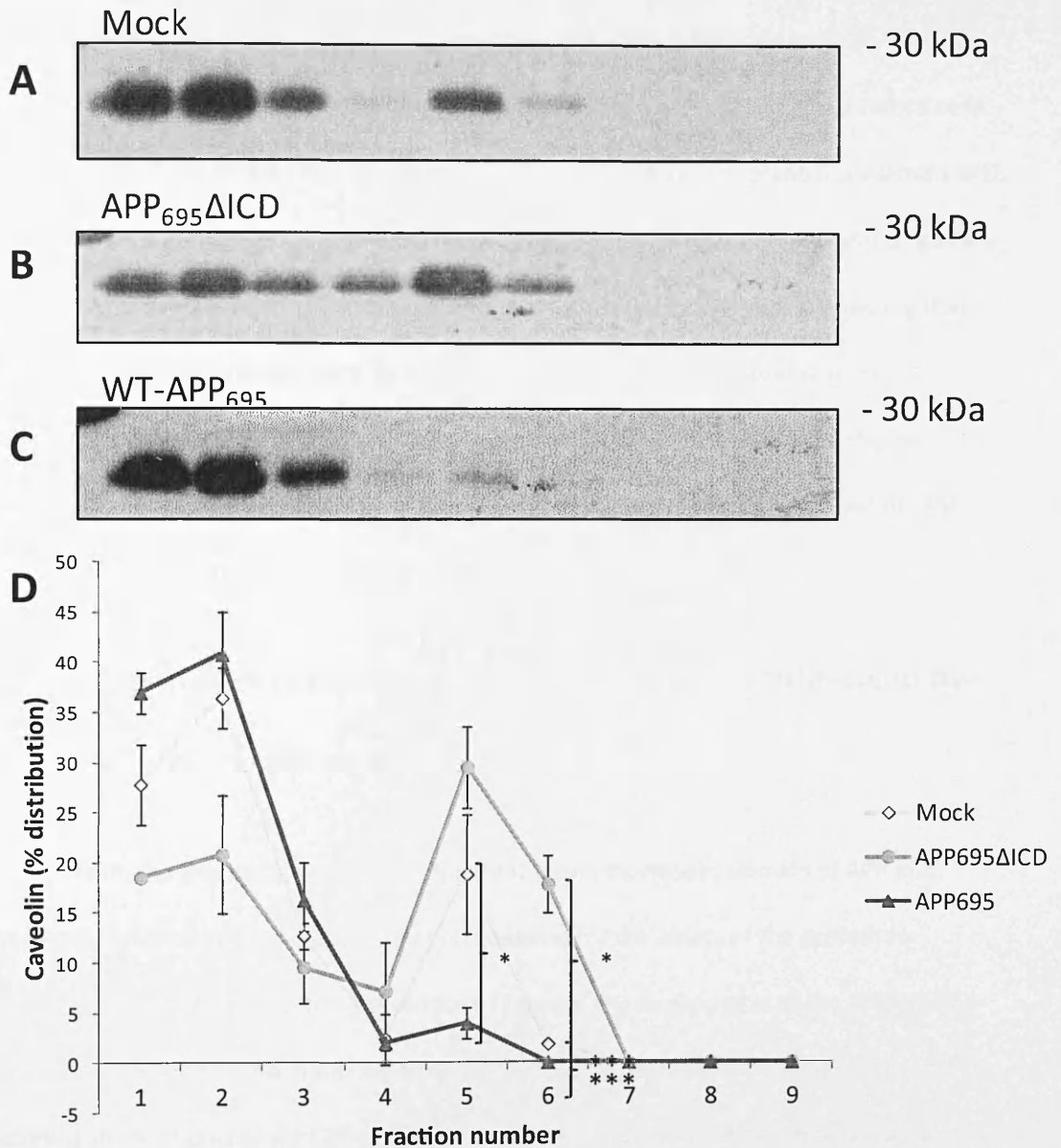


**Figure 6.7.** Analysis of caveolin-1 distribution in sucrose gradients prepared from Du145 cells transfected with either vector alone, wild-type APP<sub>695</sub> or APP<sub>695</sub>ΔICD. Lipid rafts were prepared as described in Materials and Methods and individual fractions were harvested (1 – bottom of gradient, 9 – top of gradient). Fractions were resolved by SDS-PAGE and subsequently immunoblotted with anti-caveolin-1 antibody (Materials and Methods) (A-C). Multiple immunoblots from each cell type were quantified by densitometric analysis (D) and the results are expressed in terms of percentage distribution throughout the gradients and are means ± S.D. (n=3). Significance was tested against the mock transfected control. \* = significant at  $p \leq 0.05$ ; \*\*\*\*\* = significant at  $p \leq 0.0001$ . Unless otherwise stated, differences were not significant.

Finally, the individual sucrose gradient fractions were immunoblotted with an antibody against the raft marker protein, caveolin-1 (83, 298). Whilst the majority of caveolin-1 was actually found in the non-raft fractions of the mock-transfected Du145 cells (*Fig. 6.7A and C*),  $20.64 \pm 6.04\%$  was present, collectively, in fractions 5 and 6 consistent with a low-density raft localisation. However, in the case of the wild-type APP<sub>695</sub>-transfected cells, only  $3.91 \pm 1.55\%$  of caveolin-1 was located in these low-density fractions suggesting that APP may actually disrupt lipid rafts in Du145 cells. Conversely, cells expressing the APP<sub>695</sub>ΔICD construct exhibited more caveolin (relative to the mock transfectants) in fractions 5 and 6 suggesting that the ectodomain and/or transmembrane domain of APP might actually serve to enhance the raft association of caveolin-1.

## 6.5. Potential intracellular signalling pathways influenced by APP over-expression

From the preceding work it was apparent that the cytosolic domain of APP and, specifically tyrosines 682 and 687, were prerequisites for the ability of the protein to enhance Du145 cell viability in the presence of copper. The same region of the protein has previously been implicated in the regulation of various kinase-mediated signalling cascades including those of Erk1 and 2 (299). Thus, in the current study, the effect of over-expressing wild-type APP and the various cytosolic domain mutants on Erk1 expression was examined.

The results (*Fig. 6.8A*) demonstrate a  $58.97 \pm 6.5\%$  reduction in Erk1 monomer expression in the wild-type APP<sub>695</sub>-transfected Du145 cells relative to mock transfectants. This affect was ablated in cells transfected with the APP<sub>695</sub>ΔICD construct and those transfected with any of the three tyrosine mutant constructs. An actin immunoblot confirmed equal protein loading (*Fig. 6.8B*).

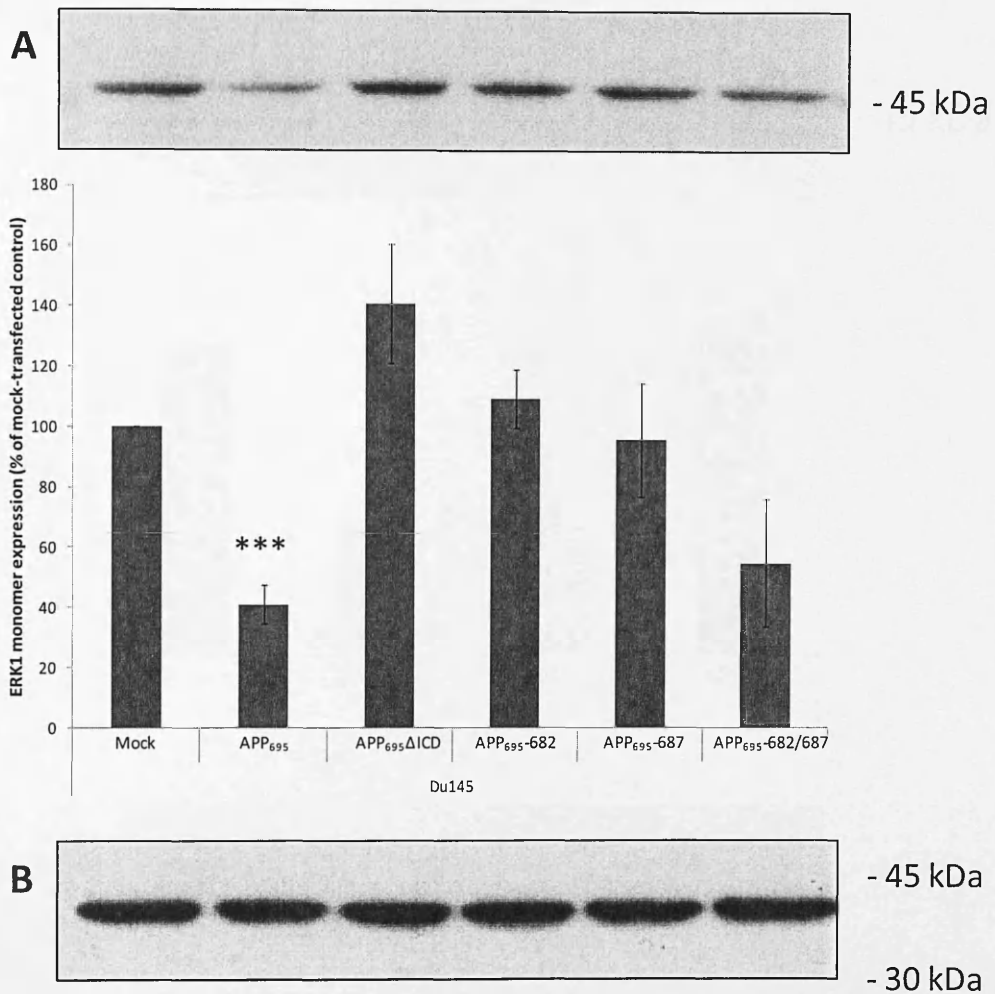


**Figure 6.8. ERK1 expression in Du145 cells over-expressing APP intracellular domain mutants.** Stably transfected cells were grown to confluence and the medium was replaced with serum free medium for 24 h. Lysates were subsequently prepared and equal amounts of protein from each were immunoblotted (Materials and Methods). **A.** Detection of Erk1 in cell lysates. Multiple Erk1 immunoblots were quantified by densitometric analysis and the results shown are means  $\pm$  S.D. ( $n=3$ ). Significance was tested against the mock-transfected control. \*\*\* = significant at  $p \leq 0.005$ . Unless otherwise indicated, the results are not significantly different. **B.** Detection of  $\beta$ -actin in cell lysates using the anti- $\beta$ -actin antibody.

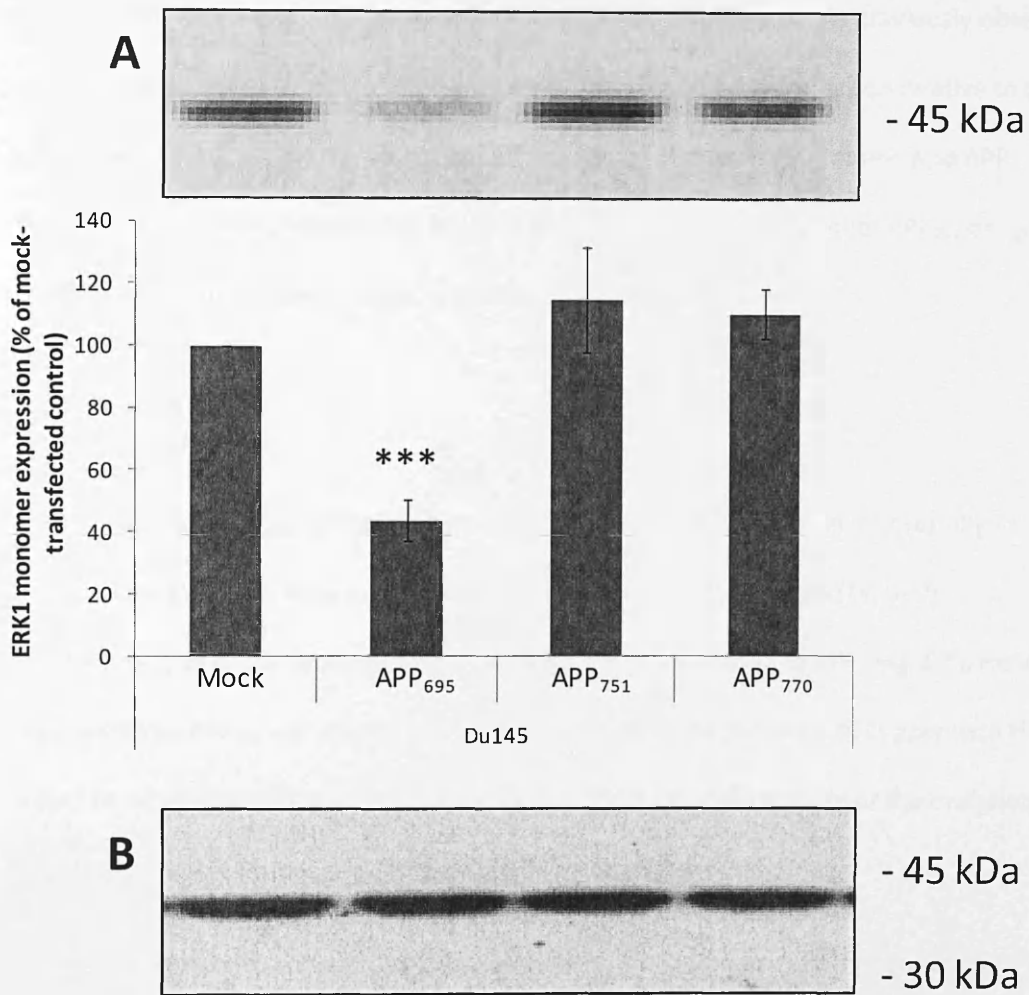


**Figure 6.9. ERK1 expression in Du145 cells over-expressing APP isoforms.** Stably transfected cells were grown to confluence and the medium was replaced with serum free medium for 24 h. Lysates were subsequently prepared and equal amounts of protein from each were immunoblotted (Materials and Methods). **A.** Detection of Erk1 in cell lysates. Multiple Erk1 immunoblots were quantified by densitometric analysis and the results shown are means  $\pm$  S.D. (n=3). Significance was tested against the mock-transfected control. \*\*\* = significant at  $p \leq 0.005$ . Unless otherwise indicated, the results are not significantly different. **B.** Detection of  $\beta$ -actin in cell lysates using the anti- $\beta$ -actin antibody.

Following the observed reduction in Erk1 monomer expression in APP<sub>695</sub>-transfected Du145 cells, and because the ability of the latter protein to enhance viability in the presence of copper was specific to the 695 amino acid isoform, the effect of the larger KPI-containing APP isoforms on Erk1 expression was also subsequently investigated. As previously observed, the results (*Fig. 6.9A*) show that wild-type APP<sub>695</sub> decreased Erk1 expression relative to the mock-transfected control. However, this effect was specific to the 695 amino acid APP isoform with no such change being observed in cells over-expressing either APP<sub>751</sub> or <sub>770</sub>. An actin immunoblot confirmed equal protein loading (*Fig. 6.9B*).

## 6.6. Summary

All of the APP<sub>695</sub> cytosolic domain mutants were over-expressed successfully in Du145 cells, albeit the APP<sub>695</sub>ΔICD construct at a noticeably lower level (*Fig. 6.2*). Furthermore, all of the constructs yielded similar amounts of soluble APP (*Fig. 6.3*). However, only wild-type APP<sub>695</sub> was able to promote cell viability in the presence of copper with this effect being ablated by either complete deletion of the cytosolic domain or the mutation of individual tyrosine residues within the YENPTY motif (*Fig. 6.4*).

Interestingly, whilst the removal of the APP cytosolic domain did not alter the association of APP itself with lipid rafts, the wild-type protein actually prevented caveolin-1 association with these membrane structures with the APP<sub>695</sub>ΔICD construct exhibiting the opposite effect (*Fig. 6.7*).

Finally, the cytosolic domain of APP and the tyrosine residues within the YENPTY motif appear to be involved in the expression of Erk1 in Du145 cells with the expression of the latter protein being impaired by this region of the APP molecule (*Fig. 6.8*); an effect which was also specific to the 695 amino acid isoform of APP (*Fig. 6.9*).

Collectively, these data show that the YENPTY motif within the cytosolic domain of APP is linked to the ability of the protein to enhance Du145 cell viability in the presence of copper and that the regulation of Erk1 expression may be linked to this ability.

# 7. The APP ectodomain and enhanced Du145 cell viability in the presence of copper

## 7.1. Introduction

The data in the preceding chapter indicate that the APP cytosolic domain is a prerequisite for the ability of the protein to enhance Du145 cell viability in the presence of copper. In the current chapter, the role of the APP ectodomain in this phenomenon was investigated.

First, the role of the N-terminal copper binding site in the E1 domain of the APP ectodomain (45) was examined. Metal binding within this copper binding domain (CuBD) has previously been implicated in the reduction of intracellular copper levels in yeast (156) and in protection against copper-mediated neurotoxic effects in mice following intrahippocampal injection of peptides mimicking this region of APP (172). Histidine residues at positions 147, 149 and 151 of the APP protein have been specifically implicated in the co-ordination of copper and the mutation of these residues has previously been shown to ablate the functions related to its metal binding capacity (156). In the current study, the effect of histidine to alanine mutations at these sites on the ability of APP to enhance Du145 cell viability in the presence of copper was examined.

Second, the ability of the soluble APP ectodomain (as opposed to the membrane-anchored full-length protein) to enhance Du145 cell viability in the presence of copper was examined. The soluble APP ectodomain has previously been shown to exhibit functions independent of the cytosolic domain of the protein, including growth promoting activity (124). Furthermore, most of the detrimental effects seen in APP knockout cells can be reversed by application of sAPP $\alpha$  suggesting that this fragment carries the major molecular prerequisites for APP functional activity (121).

## 7.2. The expression and proteolysis of the APP copper binding domain construct in Du145 cells

In order to investigate the role of the N-terminal APP CuBD in enhancing the viability of Du145 cells in the presence of copper, an APP construct which should, in theory, be deficient in metal binding at this site, was designed. The APP<sub>695</sub>ΔCuBD construct contained three histidine to alanine mutations at positions 147, 149 and 151 (*Fig. 7.1*). This construct, along with wild-type APP<sub>695</sub>, was stably transfected into Du145 cells (see Materials and Methods) and the expression and proteolysis of the constructs were subsequently monitored by immunoblotting analysis. Initially, equal amounts of protein from cell lysates were resolved by SDS-PAGE and immunoblotted using the anti-APP C-terminal antibody. The results (*Fig. 7.2*) confirmed that both constructs were successfully over-expressed with wild-type APP<sub>695</sub> being detected at an  $8.51 \pm 2.45$ -fold higher level than the endogenous protein. Notably, however, the level of APP<sub>695</sub>ΔCuBD detected in cell lysates was significantly lower than that of the over-expressed wild-type APP<sub>695</sub> protein ( $5.52 \pm 1.34$ -fold higher level than the endogenous protein).

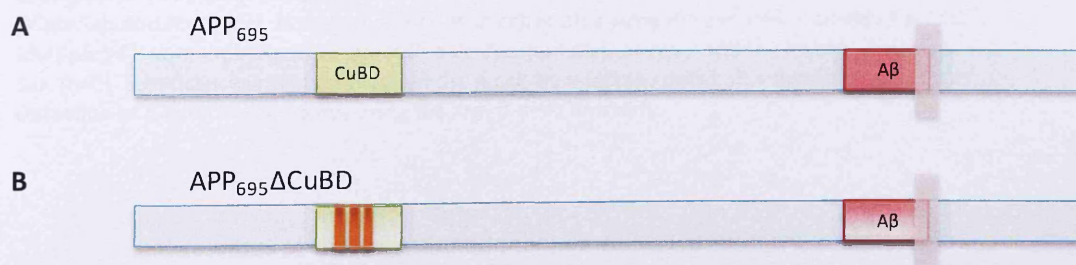


**Figure 7.1. Schematic representing the APP N-terminal copper binding domain deficient construct. A.** Wild-type APP<sub>695</sub>. **B.** The APP<sub>695</sub>ΔCuBD construct contained three histidine to alanine mutations at positions 147, 149 and 151.

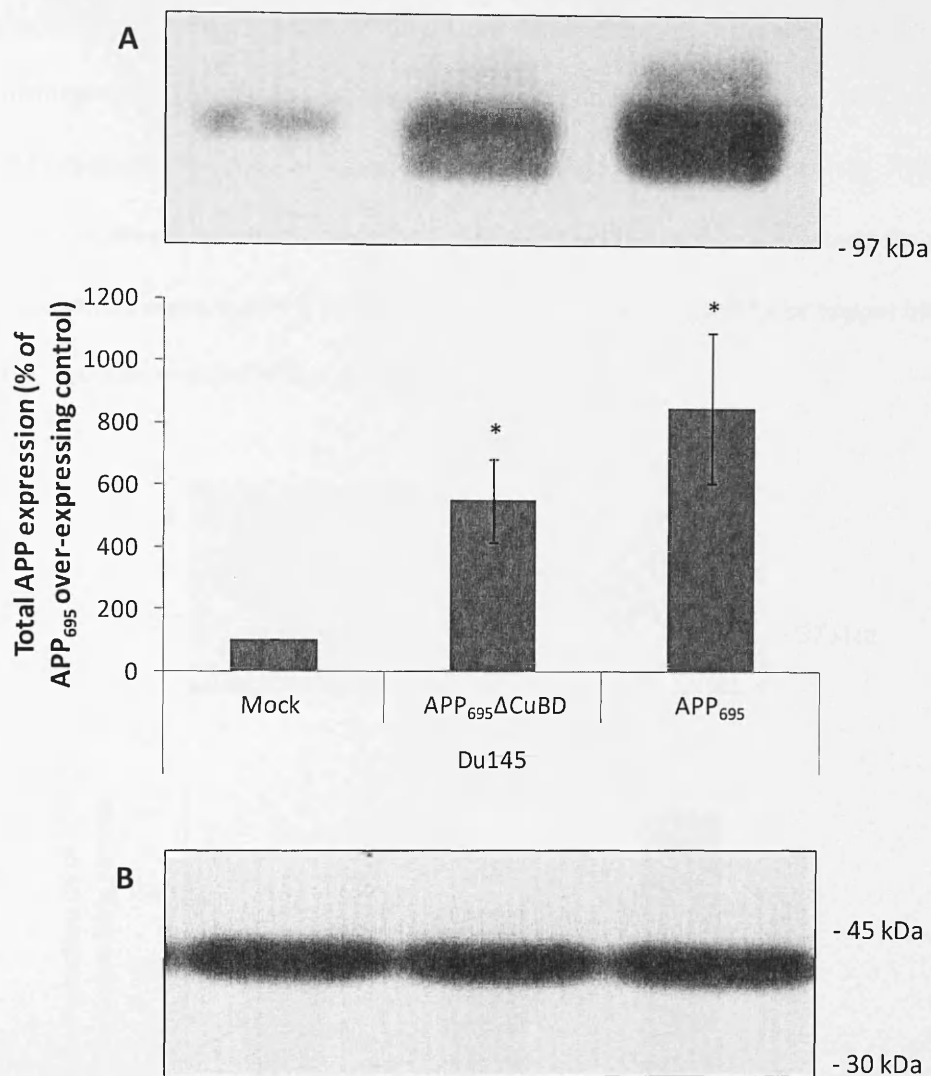


**Figure 7.2. APP N-terminal copper binding domain mutant over-expression in Du145 cells.** Stably transfected cells were grown to confluence and the medium was replaced with serum free medium for 24 h. Lysates were subsequently prepared and equal amounts of protein from each were immunoblotted (Materials and Methods). **A.** Detection of APP in cell lysates using the anti-APP C-terminal antibody. Multiple APP immunoblots were quantified by densitometric analysis and the results shown are means  $\pm$  S.D. (n=3). Significance was tested against the mock-transfected control. \* = significant at  $p \leq 0.05$ . **B.** Detection of  $\beta$ -actin in cell lysates using the anti- $\beta$ -actin antibody.

Equal volumes of the conditioned medium collected from these cell types was then immunoblotted and analysed for production of soluble APP metabolites, using the anti-APP 6E10 and 1A9 antibodies as probes for sAPP $\alpha$  and sAPP $\beta$ , respectively. The results (Fig. 7.3A) show that the wild-type APP<sub>695</sub> and APP<sub>695</sub>ΔCuBD transfected cells produced  $2.04 \pm 0.27$ - and  $1.35 \pm 0.28$ -fold more sAPP $\alpha$ , respectively, than the mock-transfected cells; perhaps

reflecting the elevated full-length protein expression observed in the wild-type APP<sub>695</sub>-transfected cells (Fig. 7.2A). The level of sAPP $\beta$  produced by the wild-type APP<sub>695</sub>-transfected Du145 cells was massively increased compared to the mock transfectants (Fig. 7.3B). Notably, however, the mutation of the CuBD in the APP<sub>695</sub> $\Delta$ CuBD-transfected cells appeared to completely prevent sAPP $\beta$  generation (Fig. 7.3B), suggesting a role for copper binding in the production of this APP metabolite.

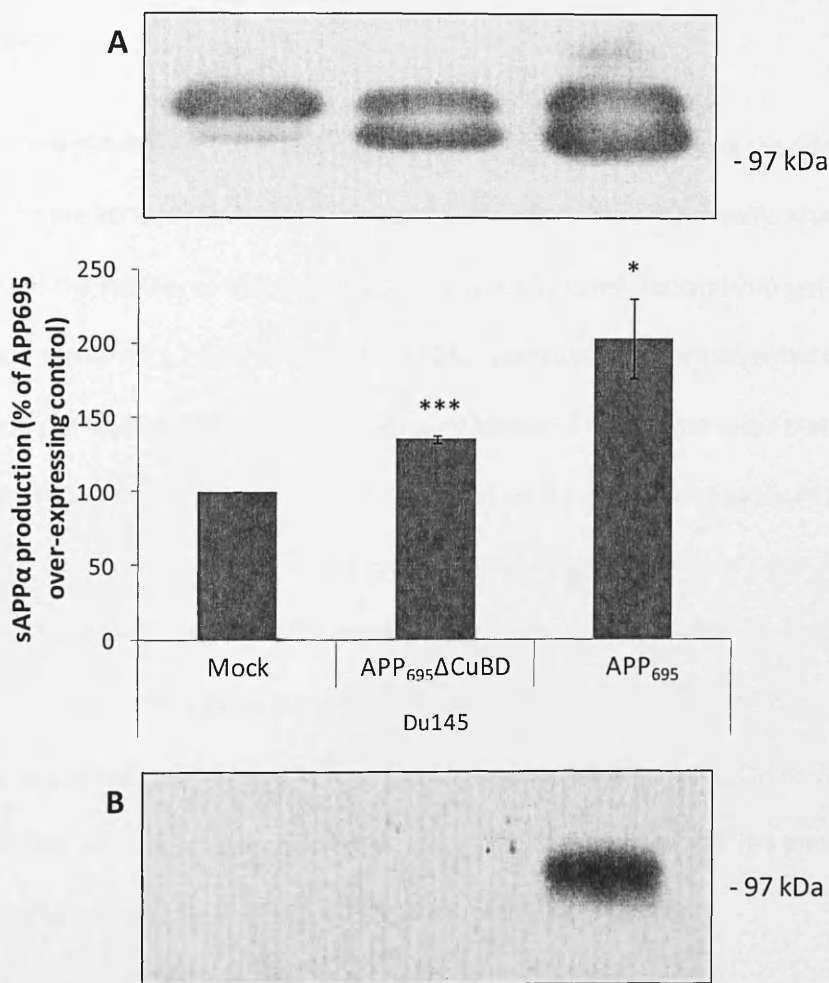


**Figure 7.3. Soluble APP generation by Du145 cells over-expressing the APP<sub>695</sub> $\Delta$ CuBD construct.** Stably transfected cells were grown to confluence and the medium was replaced with serum free medium for 24 h. Conditioned medium was subsequently prepared and equal volumes of each sample were immunoblotted. **A.** Detection of sAPP $\alpha$  in conditioned medium using the anti-APP antibody, 6E10. Multiple 6E10 immunoblots were quantified by densitometric analysis and the results shown are means  $\pm$  S.D. (n=3). Significance was tested against the mock-transfected control. \* = significant at  $p \leq 0.05$ ; \*\*\* = significant at  $p \leq 0.005$ . **B.** Detection of sAPP $\beta$  in conditioned medium using antibody 1A9.

### 7.3. The effect of E1 copper binding domain mutations on the viability of Du145 cells in the presence of copper

In order to examine the role of the APP E1 copper binding domain in maintaining Du145 cell viability in the presence of copper, the stably transfected cells were seeded out and cultured overnight before adding glycine-complexed metal at concentrations of 0, 150 and 200  $\mu\text{M}$ . MTS viability assays were performed at both 5 h and 7 days after the addition of copper.

The results (*Fig. 7.4A*) show an initial drop in viability following the addition of copper to the various cell types, particularly in the mock-transfected cells. After seven days (*Fig. 7.4B*) the viability of mock-transfected cells treated with 150 and 200  $\mu\text{M}$  copper had decreased to  $40.45 \pm 2.56\%$  and  $15.46 \pm 0.32\%$ , respectively, of the untreated controls. In contrast, the viability of the wild-type APP<sub>695</sub>-transfected cells at the same metal concentrations remained at  $68.38 \pm 1.08\%$  and  $51.06 \pm 1.89\%$ , respectively, of the untreated controls. These initial data confirmed the previously observed ability of wild-type APP<sub>695</sub> to promote Du145 cell viability in the presence of copper. Notably, however, at seven days, the mutation of the APP E1 CuBD partially ablated the effect of the wild-type protein at 200  $\mu\text{M}$  copper and completely ablated its effect at 150  $\mu\text{M}$  copper (*Fig. 7.4B*). These data clearly indicate that an intact copper binding domain in the E1 domain of APP is a prerequisite for its ability to promote Du145 cell viability in the presence of copper.

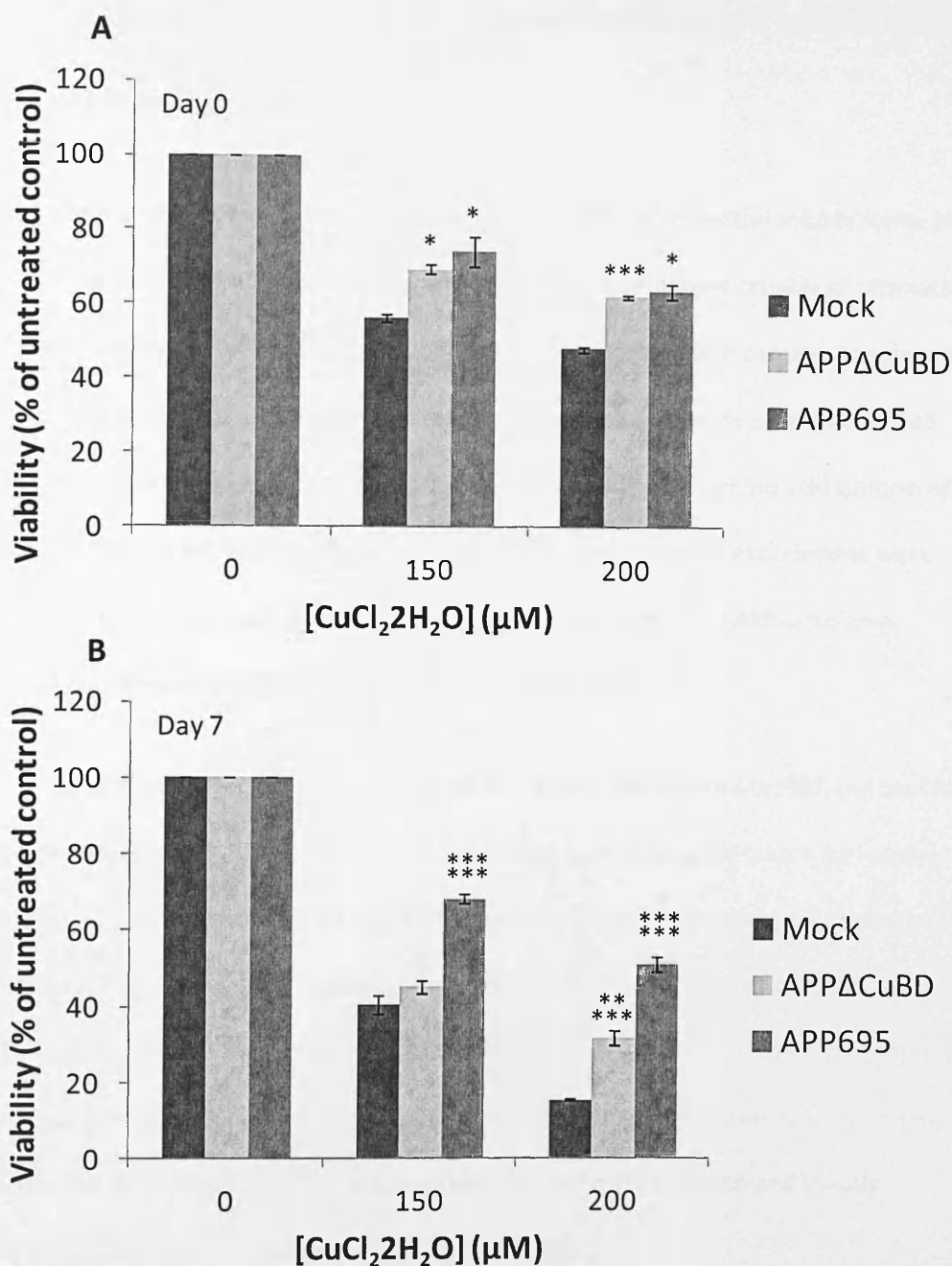


**Figure 7.4.** The effect of APP<sub>695</sub>ΔCuBD mutant over-expression on Du145 cell viability in the presence of copper. Cells were seeded at 2000 cells per well and equilibrated overnight under normal growth conditions (37 °C, 5% CO<sub>2</sub>). Glycine-complexed copper was added to final metal concentrations of 0, 150 and 200 μM in 100 μl of complete RPMI; the cells were then grown over a 7 day period with medium being replaced with fresh metal-containing medium at day 4. The MTS cell viability assay was performed on day 0 (within 5 h of adding the metal) (A) and on day 7 (B). Results are means ± S.E. (n=9). Significance was tested against the mock-transfected control. \* = significant at  $p \leq 0.05$ ; \*\*\* = significant at  $p \leq 0.005$ ; \*\*\*\*\* = significant at  $p \leq 0.0005$ ; \*\*\*\*\* = significant at  $p \leq 0.0001$ . Unless otherwise stated, differences were not significant.

#### 7.4. The role of the soluble APP ectodomain in promoting Du145 cell viability in the presence of copper; stable over-expression of sAPP $\alpha$

These studies were performed in order to determine whether the soluble forms of APP (as opposed to the full-length membrane-anchored protein) were capable of promoting Du145 cell viability in the presence of copper. Initially, a truncated APP construct analogous to sAPP $\alpha$  was generated with a view to over-expressing this form of the protein in Du145 cells. The construct generated in this instance was based on the 770 amino acid isoform of APP, and in this respect it should be noted that, chronologically, these experiments were performed before the data in Chapter 5 was obtained pertaining to an APP<sub>695</sub> isoform-specific enhancement of cell viability in the presence of copper.

In full length APP<sub>770</sub>, the alpha cleavage site is between residues Lys687 and Leu688 (300). The soluble APP<sub>770</sub> construct (APP<sub>770S</sub>) was made by mutating the codon for residue Leu688 (which was originally 'TTG') into a 'TAG' stop codon and was subsequently stably expressed in Du145 cells using lipofectamine transfection as described in Materials and Methods. It should be noted that the original full-length APP<sub>770</sub> construct used to generate the APP<sub>770S</sub> construct also possessed a FLAG epitope tag immediately C-terminal to the signal sequence (i.e. after Ala17) thereby enabling detection of both full-length and soluble derivatives of the construct using an anti-FLAG antibody.

Following transfection, the secretion of soluble APP into conditioned medium from Du145 cells was compared to that in medium conditioned on SH-SY5Y cells previously also stably transfected with the APP<sub>770S</sub> construct in our laboratory. Immunoblotting the conditioned medium with the anti-FLAG antibody (*Fig. 7.5A*) detected a band at approximately 106 kDa in the SH-SY5Y conditioned medium as would be expected for the

molecular mass of sAPP $\alpha$ . However, the same band was absent from medium conditioned on the APP<sub>770</sub>S-transfected Du145 cells. Instead, an extremely intense band was detected in this conditioned medium at 25 kDa and, notably, the same band was completely absent from mock-transfected Du145 cells (Fig. 7.5A).

When the cell lysates from the various transfectants were immunoblotted with the anti-FLAG antibody (Fig. 7.5B) a lesser amount of the 25 kDa protein fragment was also detected in the APP<sub>770</sub>S-transfected Du145 cells and was, again, absent from the mock-transfected Du145 cell lysates.

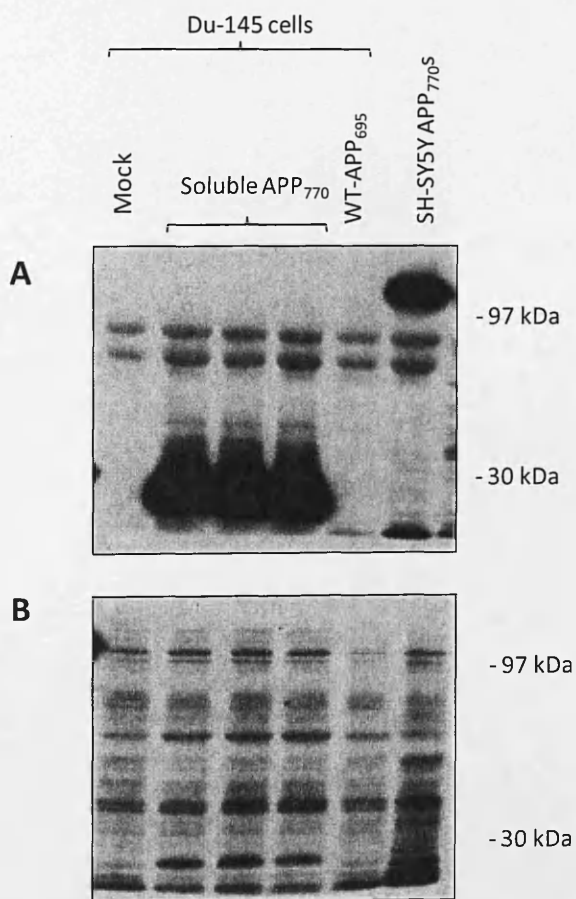


**Figure 7.5. Detection of the soluble APP<sub>770</sub> construct using the anti-FLAG antibody.** Du145 cells were transfected using the lipofectamine technique (Materials and Methods). Cells were grown to confluence and the medium was replaced with serum free medium for 24 h. Conditioned medium and cell lysates were prepared and SDS-PAGE and immunoblotting performed according to Materials and Methods. **A.** Detection of the FLAG tag in conditioned medium. **B.** Detection of the FLAG tag in cell lysates.

In order to further characterise the 25 kDa fragment detected in the APP<sub>770S</sub>-transfected Du145 cells, the same conditioned medium and lysate samples were immunoblotted using the anti-APP antibody, 22C11 (Millipore, Watford, UK) which specifically recognises amino acids 66-81 within the APP ectodomain. The results (Fig. 7.6A) show that 22C11 also detected an intense 25 kDa fragment in medium conditioned on the APP<sub>770S</sub>-transfected Du145 cells. As observed previously using the anti-FLAG antibody, lower levels of this fragment were also detected in lysates of the same cell line (Fig. 7.6B).

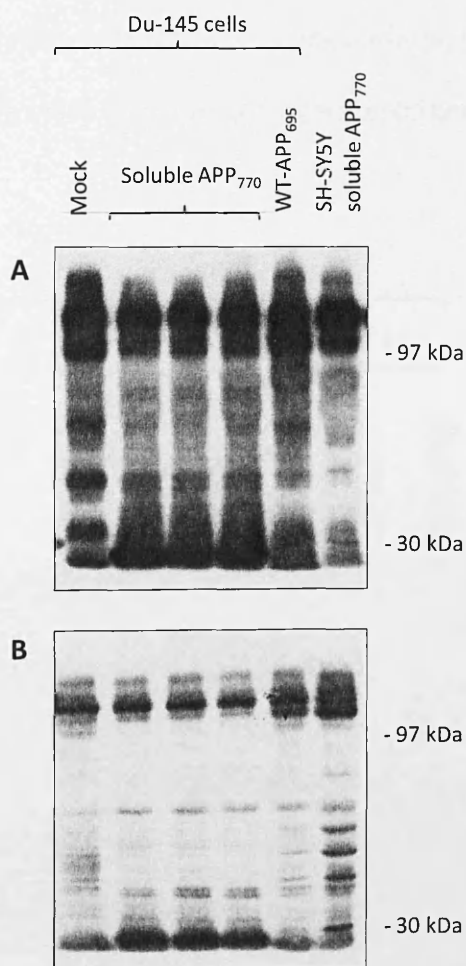


**Figure 7.6. Detection of the soluble APP<sub>770</sub> construct using the antibody 22C11.** Du145 cells were transfected using the lipofectamine technique (Materials and Methods). Cells were grown to confluence and the medium was replaced with serum free medium for 24 h. Conditioned medium and cell lysates were prepared and SDS-PAGE and immunoblotting performed according to Materials and Methods. **A.** Detection of APP in conditioned medium using antibody 22C11. **B.** Detection of APP in cell lysates using antibody 22C11.

From the data shown in *Figs. 7.5 and 7.6* it was apparent that, although the APP<sub>770S</sub> construct behaved as expected in SH-SY5Y cells, a truncated version of the construct, possibly derived by proteolytic digestion, was detected in Du145 cells. Thus, in order to determine whether proteolytic digestion was involved, a degradation assay was performed. Cell lysate from untransfected Du145 cells was prepared in the absence of protease inhibitors and was subsequently incubated at 37°C over a 24 h time course with conditioned medium containing the 106 kDa APP<sub>770S</sub> construct from SH-SY5Y cells. Incubations were performed with both boiled and unboiled lysates in order to detect any inactivation of endogenous Du145 cell proteolytic activity. The results, however, (*Fig. 7.7*) showed no degradation of the 106 kDa sAPP $\alpha$  band over the experimental time course.

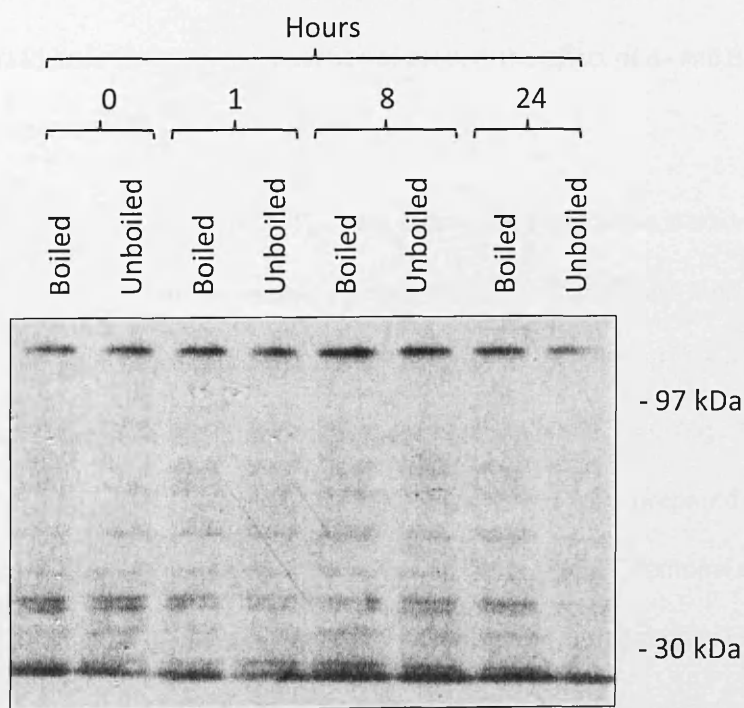


**Figure 7.7. Lack of soluble APP<sub>770</sub> degradation by Du145 cell lysates.** Lysates were prepared from untransfected Du145 cells and aliquots of this lysate (boiled and unboiled) were incubated at 37 °C for the indicated times with concentrated conditioned medium from APP<sub>770S</sub>-transfected SH-SY5Y cells. The FLAG tag in the sAPP $\alpha$  present in the SH-SY5Y conditioned medium was then detected with the anti-FLAG antibody (Materials and Methods).

Collectively, the data presented in this section show that the APP<sub>770S</sub> construct, although behaving as expected in SH-SY5Y cells, was aberrantly processed in Du145 cells to produce a 25 kDa N-terminal fragment. How, exactly, this fragment was generated remains to be determined. However, in the context of the current study, the use of the APP<sub>770S</sub> construct to determine the effect of the soluble APP ectodomain on Du145 cell viability in the presence of copper was clearly not a viable approach.

## 7.5. The role of the soluble APP ectodomain in promoting Du145 cell viability in the presence of copper; inhibition of endogenous ectodomain generation

As an alternative approach to investigate the involvement of soluble APP in promoting Du145 cell viability in the presence of copper, the effect of  $\alpha$ - and  $\beta$ -secretase inhibitors was investigated.

Initially, confluent wild-type APP<sub>695</sub> over-expressing Du145 cells were incubated for 24 h in serum free medium in the presence or absence of the  $\alpha$ -secretase inhibitor G1254023X (A gift from Ishrut Hussain, GlaxoSmithKline, Harlow) (20  $\mu$ M) in order to demonstrate effective shedding inhibition by the compound. The results (*Fig. 7.8A*) showed no significant change in cell-associated APP levels when lysates were prepared from inhibitor treated and untreated cells and immunoblotted using the anti-APP C-terminal antibody. When the conditioned medium from cells was immunoblotted with antibody 6E10 (*Fig. 7.8B*) a reduction in sAPP $\alpha$  generation to  $73.79 \pm 9.84\%$  that of controls was observed in the medium of G1254023X-treated cells, consistent with a partial inhibition of  $\alpha$ -secretase activity. A reciprocal increase in sAPP $\beta$  generation by the inhibitor-treated cells was also

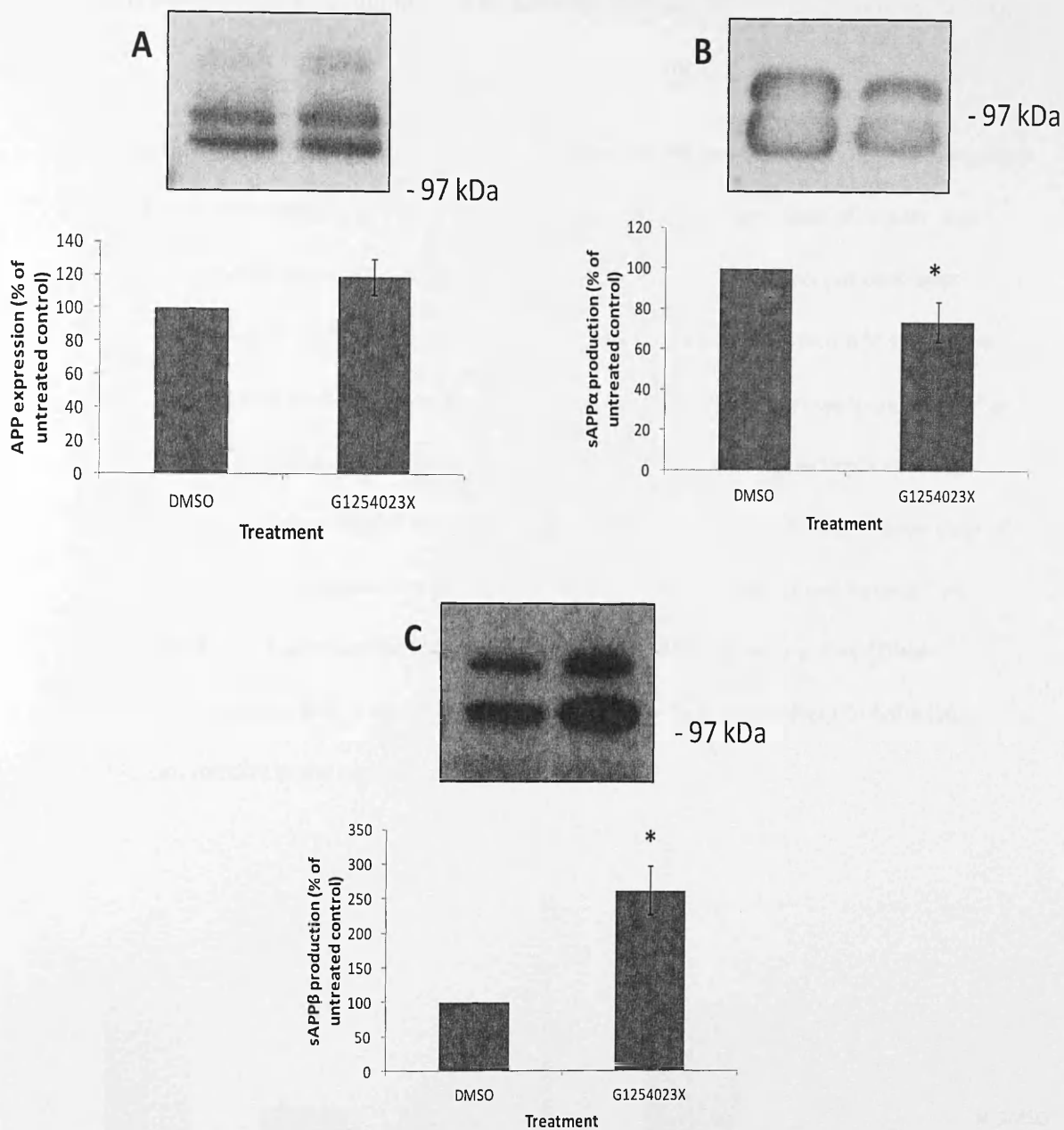


**Figure 7.8. Inhibition of APP  $\alpha$ -secretase activity by G1254023X in wild-type APP<sub>695</sub>-transfected Du145 cells.** Du145 cells were transfected with the wild-type APP<sub>695</sub> construct using the lipofectamine technique (Materials and Methods). Cells were grown to confluence and the medium was replaced with serum free medium and incubated in the absence or presence of G1254023X (20  $\mu$ M) for 24 hours. Conditioned medium and cell lysates were prepared and SDS-PAGE and immunoblotting performed according to Materials and Methods. **A.** Detection of APP in cell lysates using anti-APP C-terminal antibody. **B.** Detection of sAPP $\alpha$  in conditioned medium samples using anti-APP antibody, 6E10. **C.** Detection of sAPP $\beta$  in conditioned medium samples using the antibody 1A9. Immunoblots were quantified and the results expressed relative to the DMSO treated control. Results are means  $\pm$  S.D. (n=3). \* = significant at  $p \leq 0.05$ . Unless otherwise stated, differences were not significant.

observed following immunoblotting of conditioned medium samples with antibody 1A9 (Fig. 7.9C).

Having established that G1254023X inhibited sAPP $\alpha$  generation in Du145 cells (albeit only partially), the viability of APP<sub>695</sub> over-expressing cells in the presence of copper was examined in the absence or presence of the inhibitor. The stably transfected cells were seeded and cultured overnight in the absence/presence of inhibitor before adding glycine-complexed metal at concentrations of 0 or 200  $\mu$ M. MTS viability assays were performed at both 5 h and 7 days after the addition of copper and the inhibitor was incorporated into medium where required for the duration of these incubations (Fig. 7.9). After seven days of growth, only minor changes in cell viability in the presence of copper could be detected between the inhibitor treated and untreated cells (Fig. 7.9B), suggesting that ADAM-mediated cleavage of APP is not a prerequisite for the ability of the protein to enhance Du145 cell viability in the presence of copper.

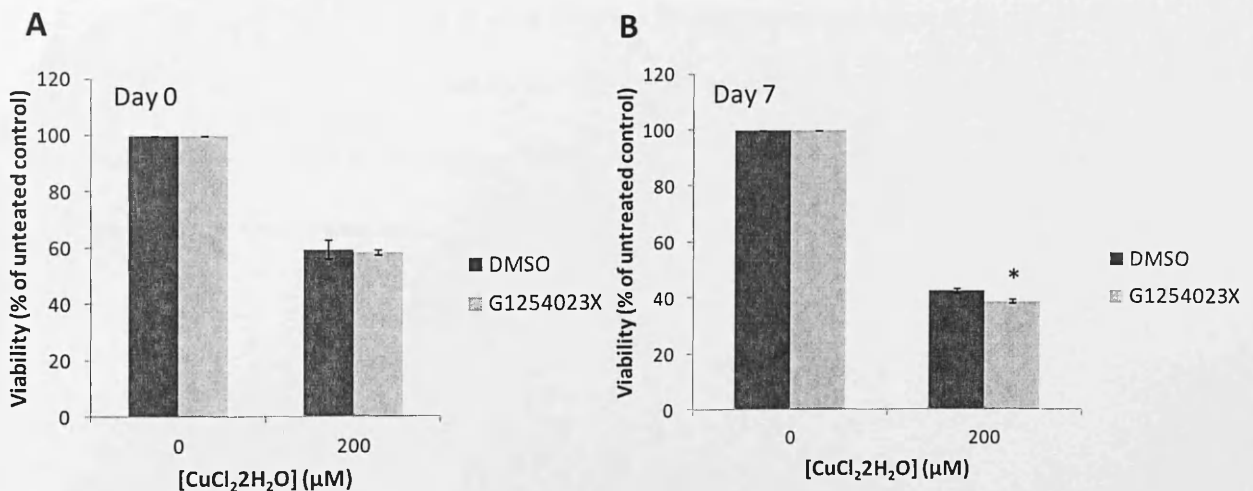


**Figure 7.9. The effect of APP  $\alpha$ -secretase inhibition on the viability of APP<sub>695</sub>-transfected Du145 cells in the presence of copper.** Cells were seeded at 2000 cells per well and equilibrated overnight under normal growth conditions (37  $^{\circ}$ C, 5% CO<sub>2</sub>) in the absence or presence of G1254023X (20  $\mu$ M). Glycine-complexed copper and of G1254023X (20  $\mu$ M) was added to final metal concentrations of 0 and 200  $\mu$ M in 100  $\mu$ l of complete RPMI; the cells were then grown over a 7 day period with medium being replaced with fresh metal- and inhibitor- containing medium at day 4. The MTS cell viability assay was performed on day 0 (within 5 h of adding the metal) (A) and on day 7 (B). Results are means  $\pm$  S.D. (n=3). \* = significant at  $p \leq 0.05$ . Unless otherwise stated, differences were not significant.

Next, the effect of  $\beta$ -secretase inhibition on the ability of APP to enhance Du145 cell viability in the presence of copper was investigated. The ability of  $\beta$ -secretase inhibitor IV (Calbiochem, Merck-Millipore, Darmstadt, Germany) to effectively inhibit  $\beta$ -secretase activity in wild-type APP<sub>695</sub>-transfected Du145 cells was initially investigated by incubating confluent cells in serum free medium for 24 h in the absence or presence of the compound (100 nM). Subsequent immunoblotting of cell lysates (*Fig. 7.10A*) with the anti-APP C-terminal antibody showed no change in full-length cell-associated APP levels following inhibitor treatment. Similarly, no changes in the level of sAPP $\alpha$  in conditioned medium were detected using antibody 6E10 (*Fig. 7.10B*). However, blotting conditioned medium samples with antibody 1A9 (*Fig. 7.10C*) showed an  $85.9 \pm 7.35\%$  decrease in sAPP $\beta$  generation following inhibitor treatment.

Having clearly established that  $\beta$ -secretase inhibitor IV virtually ablated sAPP $\beta$  generation in wild-type APP<sub>695</sub> over-expressing Du145 cells, the effect of the compound on the viability of these cells in the presence of copper was then examined. These experiments were performed (with the exception of different inhibitor concentrations) in an identical manner to that already described for the G1254023X inhibitor. The results (*Fig. 7.11*) showed no change in cell viability regardless of whether the  $\beta$ -secretase inhibitor was present or absent from the incubations.

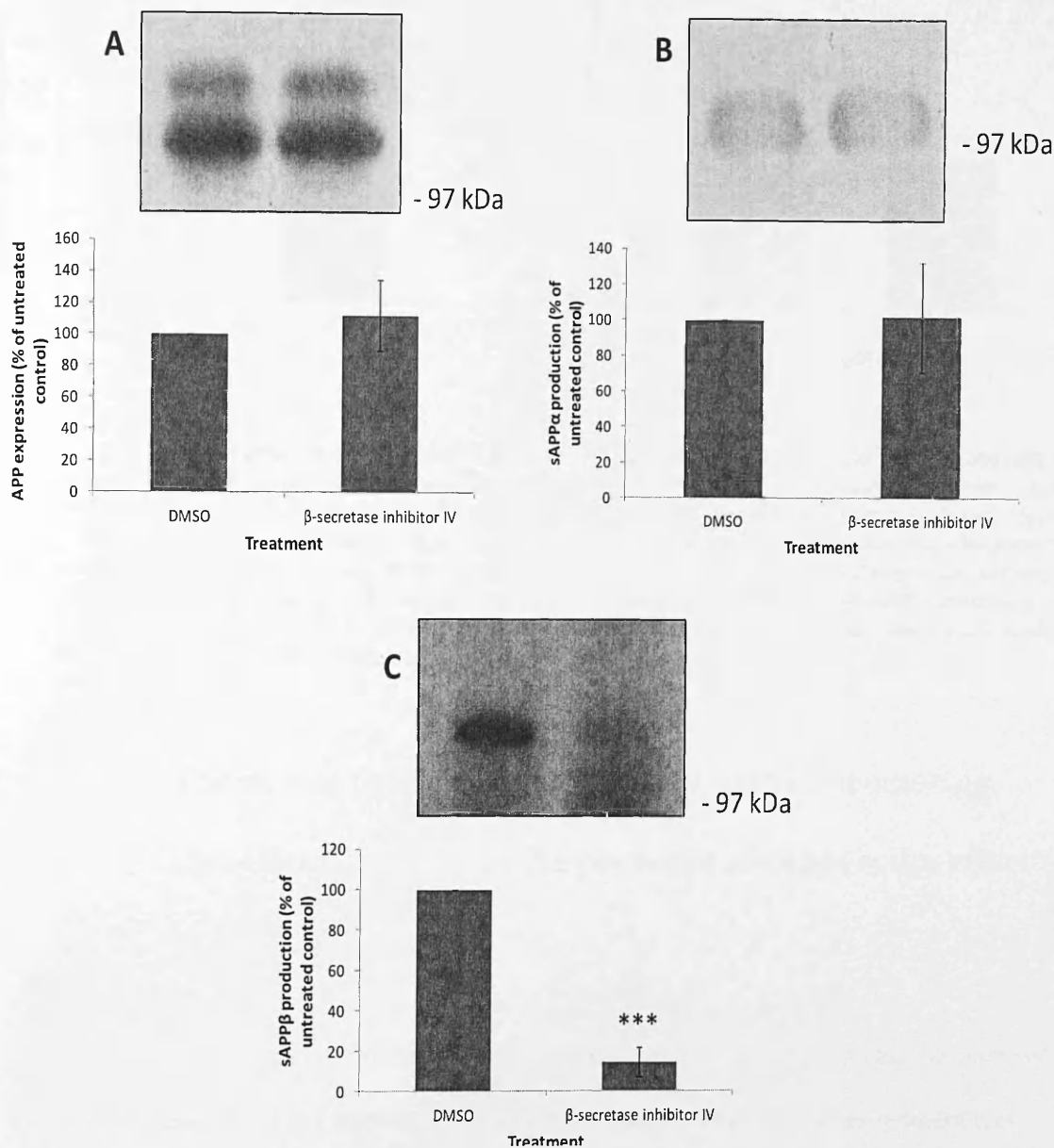


**Figure 7.10. Inhibition of APP  $\beta$ -secretase activity by  $\beta$ -secretase inhibitor IV in Du145 cells.** Cells were grown to confluence and the medium was replaced with serum free medium and incubated in the absence or presence of  $\beta$ -secretase inhibitor IV (100 nM) for 24 h. Conditioned medium and cell lysates were prepared and SDS-PAGE and immunoblotting performed according to Materials and Methods. **A.** Detection of APP in cell lysates using anti-APP C-terminal antibody. **B.** Detection of sAPP $\alpha$  in conditioned medium samples using anti-APP antibody, 6E10. **C.** Detection of sAPP $\beta$  in conditioned medium samples using antibody 1A9. Immunoblots were quantified and the results expressed relative to the DMSO treated control. Results are means  $\pm$  S.D. (n=3). \*\*\* = significant at  $p \leq 0.005$ . Unless otherwise stated, differences were not significant.

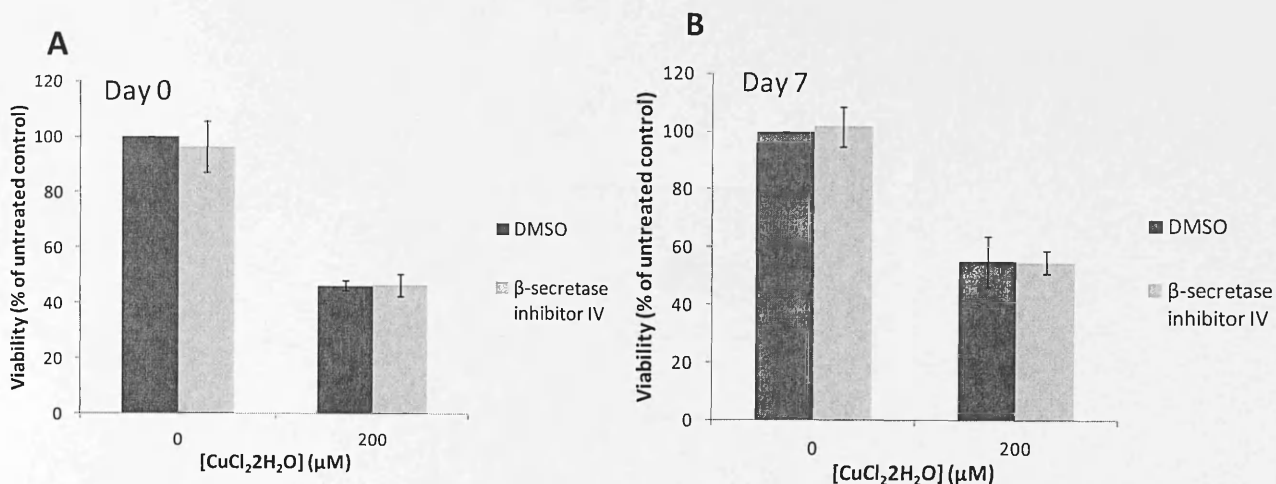


**Figure 7.11. The effect of APP β-secretase inhibition on the viability of APP<sub>695</sub>-transfected Du145 cells in the presence of copper.** Cells were seeded at 2000 cells per well and equilibrated overnight under normal growth conditions (37 °C, 5% CO<sub>2</sub>) in the absence or presence of β-secretase inhibitor IV (100 nM). Glycine-complexed copper was added to final metal concentrations of 0 and 200 μM with β-secretase inhibitor IV (100 nM) in 100 μl of complete RPMI; the cells were then grown over a 7 day period with medium being replaced with fresh metal- and inhibitor- containing medium at day 4. The MTS cell viability assay was performed on day 0 (within 5 h of adding the metal) (A) and on day 7 (B). Results are means ± S.D. (n=3). Unless otherwise stated, differences were not significant.

## 7.6. The role of the soluble APP ectodomain in promoting Du145 cell viability in the presence of copper; the effect of recombinant sAPPβ

In order to confirm that sAPPβ generation was not a prerequisite for the ability of APP<sub>695</sub> to enhance cell viability in the presence of copper an additional experiment was conducted. Here, a truncated APP<sub>695</sub> construct analogous to sAPPβ was utilised in which the codon encoding D597 (C-terminal to the β-secretase cleavage site) was mutated to a stop codon. As soluble APP had previously been shown to be aberrantly processed in Du145 cells (section 7.4) the sAPPβ<sub>695</sub> construct was initially stably transfected into HEK cells and its secretion into conditioned medium monitored by immunoblotting. The results (Fig. 7.12A) show that the construct was clearly detected in conditioned medium using antibody 1A9 and

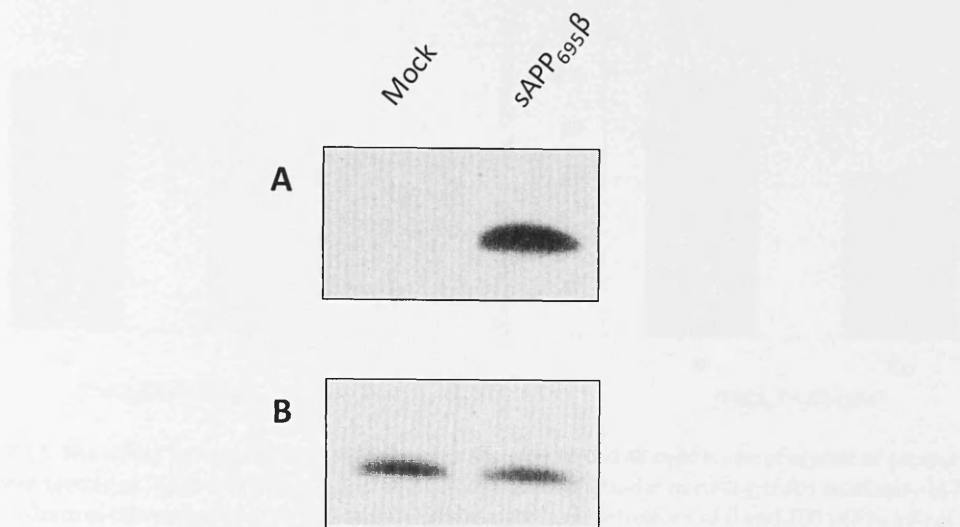


**Figure 7.12. Detection of soluble APP derivatives in conditioned medium from mock- and APP<sub>695</sub>β-transfected HEK cells.** HEK cells were stably transfected using the lipofectamine method (Materials and Methods). Confluent cells were then incubated for 24 h in serum free medium. Conditioned medium samples were prepared and immunoblotted as described in Materials and Methods. **A.** Detection of sAPPβ in conditioned medium using antibody 1A9. **B.** Detection of sAPPα in conditioned medium using anti-APP antibody, 6E10.

the same band was absent from mock-transfected cells. When the same conditioned medium samples were immunoblotted with anti-APP antibody 6E10 in order to detect sAPPα, no difference was detected between the mock- and sAPP<sub>695</sub>β-transfected cells (Fig. 7.12B).

Having confirmed that the sAPP<sub>695</sub>β construct was secreted into the conditioned medium of HEK cells and could be detected using antibody 1A9, similar batches of medium from both mock- and sAPP<sub>695</sub>β-transfected HEK cells were concentrated 50-fold by centrifugal filtration and then re-diluted to their original volume in order to neutralise the acidity of the medium and in order to remove any low molecular weight toxins. This rediluted medium was then used to culture untransfected Du145 cells during their treatment with copper as previously described. In this way the effect of copper on cells grown in the presence of background or high levels of sAPPβ could be studied. However, the resultant

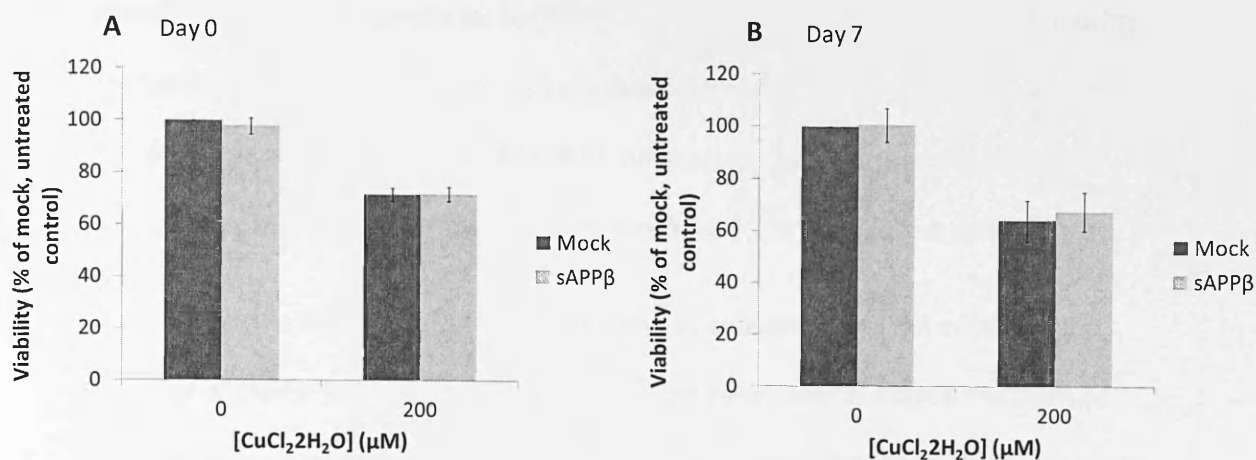


**Figure 7.13. The effect of recombinant sAPP $\beta$  on the viability of Du145 cells in the presence of copper.** Cells were seeded at 2000 cells per well and equilibrated overnight under normal growth conditions (37 °C, 5% CO<sub>2</sub>). Glycine-complexed copper was added to final metal concentrations of 0 and 200 μM in 100 μl of complete RPMI; the cells were then grown over a 7 day period with medium pre-conditioned on either mock- or sAPP $\beta_{695}$ -transfected HEK cells. The medium was replaced with fresh pre-conditioned, metal-containing medium at day 4. The MTS cell viability assay was performed on day 0 (within 5 h of adding the metal) (A) and on day 7 (B). Results are means  $\pm$  S.D. (n=3). Unless otherwise stated, differences were not significant.

MTS assay data (Fig. 7.13), again, showed no effect of sAPP $\beta$  on the viability of cells in the presence of copper.

## 7.7. Summary

The over-arching aim of the work presented in the current chapter was to investigate the potential role played by the APP ectodomain in the enhancement of Du145 cell viability in the presence of copper. Initially, the role of the E1 copper binding domain of APP was examined in this respect. The APP<sub>695</sub>CuBD construct generated for this purpose was successfully over-expressed in Du145 cells (Fig. 7.2) and appeared to be processed by  $\alpha$ -secretase in a manner analogous to its wild-type counterpart (Fig. 7.3A). However, notably, the mutation of the E1 CuBD clearly prevented  $\beta$ -secretase-mediated processing of the protein (Fig. 7.3B). It was subsequently demonstrated that, whereas wild-type APP<sub>695</sub> clearly enhanced Du145 cell viability in the presence of copper, the mutation of the E1 CuBD prevented this phenomenon (Fig. 7.4). It is therefore clear that copper binding to the E1

domain of APP is a prerequisite for the ability of the protein to enhance Du145 cell viability. The later experiments in this chapter clearly show that sAPP $\beta$  had no impact on cell viability. This precludes the possibility that the lack of sAPP $\beta$  and/or A $\beta$  generated from the APP<sub>695</sub>CuBD construct was responsible for its lack of ability to promote cell viability.

Next, the ability of soluble APP derivatives to enhance Du145 cell viability in the presence of copper was examined. Initially, attempts were made to address this point by over-expressing a truncated APP construct analogous to sAPP $\alpha$  in Du145 cells. However, the resultant protein was aberrantly processed in Du145 cells to generate a 25 kDa N-terminal fragment (which could be detected using antibody 22C11) (*Fig. 7.6*) despite the construct being secreted as the expected 106 kDa fragment in SH-SY5Y cells (*Fig. 7.5*).

As an alternative approach to examining the role of soluble APP derivatives,  $\alpha$ - and  $\beta$ -secretase inhibitors were employed. However, despite these compounds effectively inhibiting sAPP $\alpha$  or sAPP $\beta$  generation (to differing degrees) (*Figs. 7.8 and 7.10*) little or no effect of these compounds on the viability of wild-type APP<sub>695</sub> over-expressing Du145 cells was observed in the presence of copper. Similarly, recombinant sAPP $\beta$  was unable to promote the viability of Du145 cells in the presence of copper (*Fig. 7.13*).

In summary, it is clear that, whilst an intact APP E1 CuBD is a prerequisite for the protein to enhance Du145 cell viability in the presence of copper, the generation of soluble, secretase-cleaved, APP derivatives is quite clearly not a requirement in this respect.

# 8. APP-induced morphological changes in Du145 cells

## 8.1. Introduction

During the preceding research it was noted that, when Du145 cells were transfected with the APP<sub>695</sub> isoform, a morphological change was observed, clearly distinguishing them from mock-transfected cells. The current chapter investigates the biological basis for these morphological changes and how they might relate to prostate cancer pathogenesis.

## 8.2. The effect of APP<sub>695</sub> over-expression on Du145 cell morphology

Du145 cells were stably transfected with either vector alone (mock) or APP<sub>695</sub> and cell morphology was subsequently visualised at 35% confluency. Parallel cultures were also grown in order to confirm APP over-expression by immunoblotting. The results (*Fig. 8.1A-D*) confirm that the APP<sub>695</sub>-transfected Du145 cells over-expressed the desired protein and that they generated more sAPP $\alpha$  and sAPP $\beta$  than the mock-transfected cells. In terms of cell morphology, the mock-transfected Du145 cells had a flat epithelial type morphology, tending to grow in small focal groups (*Fig. 8.1E*), whereas the APP<sub>695</sub>-transfected cultures contained cells with several neurite-like extensions (*Fig. 8.1F*). Thus, it was apparent that APP<sub>695</sub> was capable of inducing clear morphological changes in Du145 cells.

## 8.3. APP<sub>695</sub>-induced morphological changes in Du145 cells are not associated with neuroendocrine differentiation

Having shown that APP<sub>695</sub> was capable of inducing morphological changes in Du145 cells, experiments were then conducted with a view to determining the biological basis for these changes.

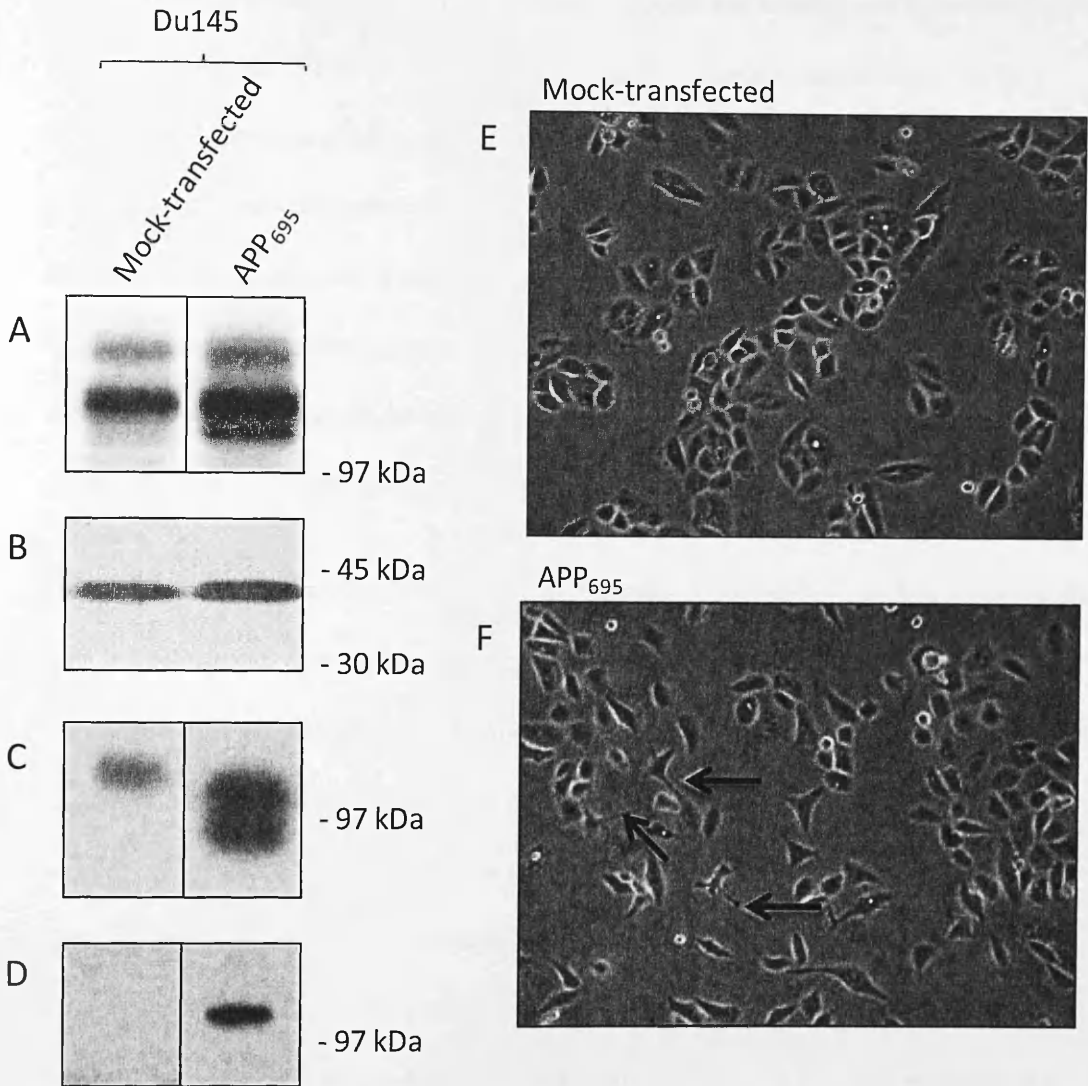


**Figure 8.1. APP<sub>695</sub>- induced morphological changes in Du145 cells.** A-D. Du145 cells stably transfected with either vector alone (mock) or APP<sub>695</sub> were grown to confluence and the medium was replaced with serum free medium for 24 h. Cells and conditioned medium were then harvested and prepared for immunoblotting as described in Materials and Methods. **A.** Detection of the APP holoprotein in cell lysates using the anti-APP C-terminal antibody. **B.** Detection of  $\beta$ -actin in cell lysates using the anti- $\beta$ -actin antibody. **C.** Detection of sAPP $\alpha$  in conditioned medium using the anti-APP 6E10 antibody. **D.** Detection of sAPP $\beta$  in conditioned medium using the antibody 1A9. The vertical lines on blots indicate alignment of samples from distal lanes run on the same immunoblot. **E** and **F.** Light microscopy images at 35% confluency of (A) mock-transfected and (B) APP<sub>695</sub>-transfected cells. Arrows indicate neurite-like extensions. The results are representative of three repeat experiments.

Neuroendocrine (NE) differentiation is the process by which prostate cancer cells differentiate into a cell type capable of the generation and secretion of multiple neuropeptides. Prostatic NE cells may, therefore, support the androgen-independent growth of tumour cells (301). Focal NE differentiation of cells in prostatic carcinomas is fairly common (302) and is positively associated with tumour progression (303) making this process directly relevant to the progression of prostate cancer. One subtype of NE differentiated prostatic cells is characterised by cells having a multipolar appearance with long processes and beaded varicosities (304) similar to the morphology of the APP<sub>695</sub> over-expressing Du145 cells in the current study. Amongst other proteins, NE differentiation is associated with the increased expression of neuron-specific enolase (NSE) (302).

In order to determine whether the APP<sub>695</sub>-induced morphological changes in Du145 cells represented NE differentiation, mock- and APP<sub>695</sub>-transfected cells were grown to confluence and cell lysates and conditioned medium samples were immunoblotted in order to determine NSE expression and secretion levels, respectively. The target of the NSE-P2 antibody employed is a homodimer, the expression of which is enhanced in cells which have undergone neuroendocrine differentiation (302). The results from the current study (*Fig. 8.2*) actually show a decrease in the expression of NSE dimer ( $55.71 \pm 4.07\%$  of mock-transfected control) and monomer ( $10.21 \pm 2.06\%$  of mock-transfected control) in lysates prepared from APP<sub>695</sub>-transfected cells (*Fig. 8.2A and B*). The level of NSE secreted into the conditioned medium of APP<sub>695</sub>-transfected cells was also dramatically decreased.

Thus, it would appear that the morphological changes brought about by APP<sub>695</sub> in Du145 cells do not correspond with a classical protein marker of neuroendocrine differentiation.

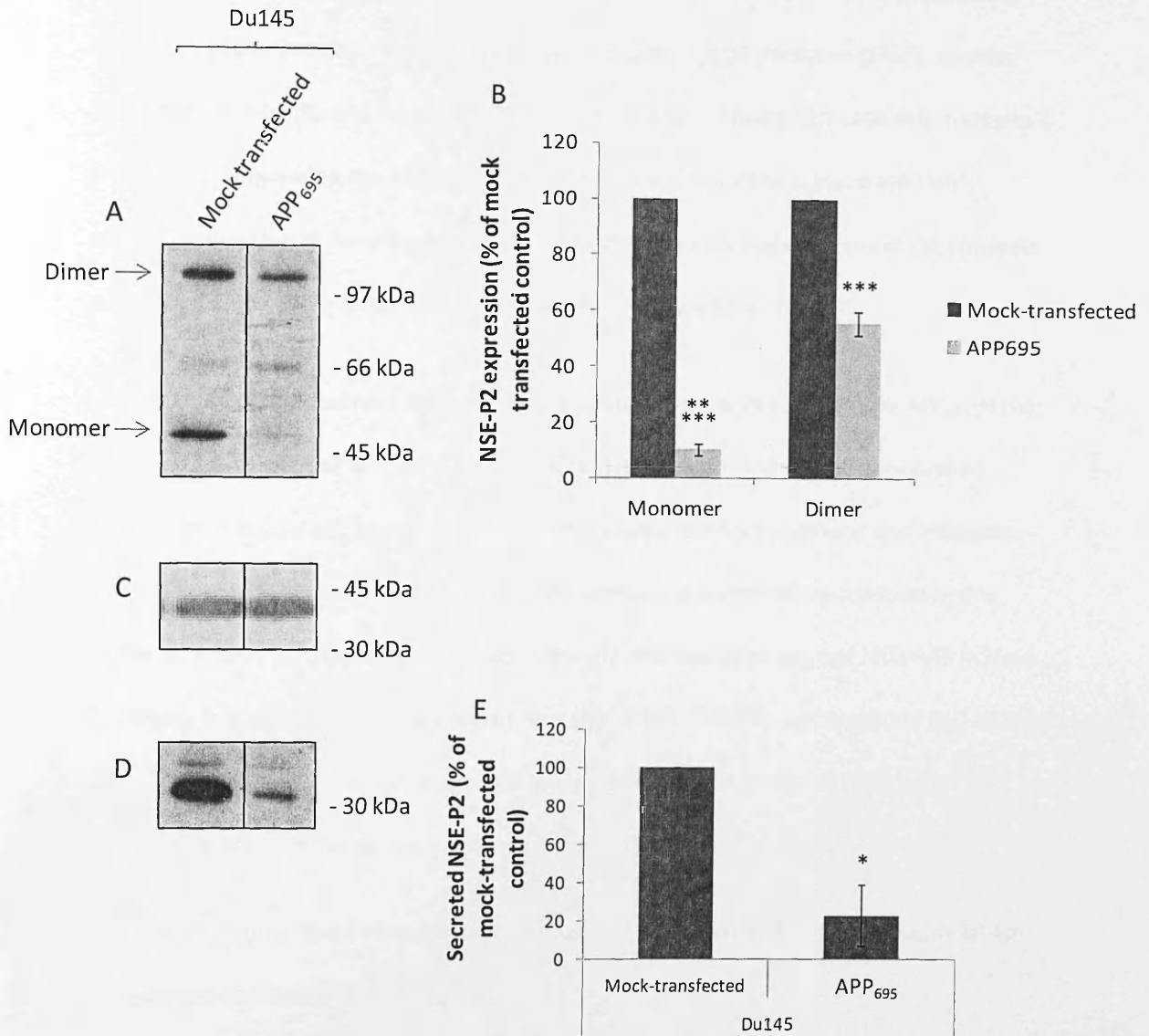


**Figure 8.2. Decreased NSE expression and secretion in APP<sub>695</sub>-transfected Du145 cells.** Du145 cells (mock) or Du145 cells stably transfected with APP<sub>695</sub> were grown to confluence and the medium was replaced with serum free medium for 24 h. Cells and conditioned medium were then harvested and prepared for immunoblotting as described in Materials and Methods. **A.** Detection of NSE in cell lysates using the anti-NSE-P2 antibody. **B.** Quantification of multiple NSE lysate blots showing relative levels of both monomeric and dimeric forms of the protein. **C.** Detection of  $\beta$ -actin in cell lysates using the anti- $\beta$ -actin antibody. **D.** Detection of NSE in conditioned medium using the NSE-P2 antibody. **E.** Quantification of multiple NSE blots showing relative levels of the secreted form of the protein. Results are means  $\pm$  S.D. (n=3). \* = significant at  $p \leq 0.05$ ; \*\*\* = significant at  $p \leq 0.005$ ; \*\*\*\*\* = significant at  $p \leq 0.0005$ .

#### 8.4. APP<sub>695</sub>-induced morphological changes in Du145 cells are associated with epithelial-to-mesenchymal transition

The transition of adherent epithelial cells to non-polar mesenchymal cells lacking their intercellular junctions through epithelial-to-mesenchymal transition (EMT), permits enhanced cell mobility and invasion (305). Therefore, EMT of malignant cells aids metastasis and disease progression resulting in a poorer prognosis (306). EMT is associated with reduced expression of the adhesion protein E-cadherin and a converse increase in vimentin expression which, in turn, correlates with increased disease severity (307).

In order to determine whether the morphological changes induced by APP<sub>695</sub> in the current study correlated with EMT marker protein expression, lysates and conditioned medium from the Du145 transfectants were immunoblotted for E-cadherin and vimentin. The results (*Fig. 8.3A*) showed a  $59.53 \pm 2.29\%$  decrease in E-cadherin expression in the lysates of the APP<sub>695</sub>-transfected cells. Interestingly, this decrease was not reflected in shed E-cadherin in the conditioned medium of cells (*Fig. 8.3B*). The APP<sub>695</sub>-transfected Du145 cells also expressed significantly more vimentin with a  $4.46 \pm 0.9$ -fold increase in levels of the protein in lysates relative to the mock-transfected cell lysates (*Fig. 8.3C*).

Collectively, these changes indicate that APP<sub>695</sub> is capable of inducing epithelial-to-mesenchymal transition in Du145 cells.

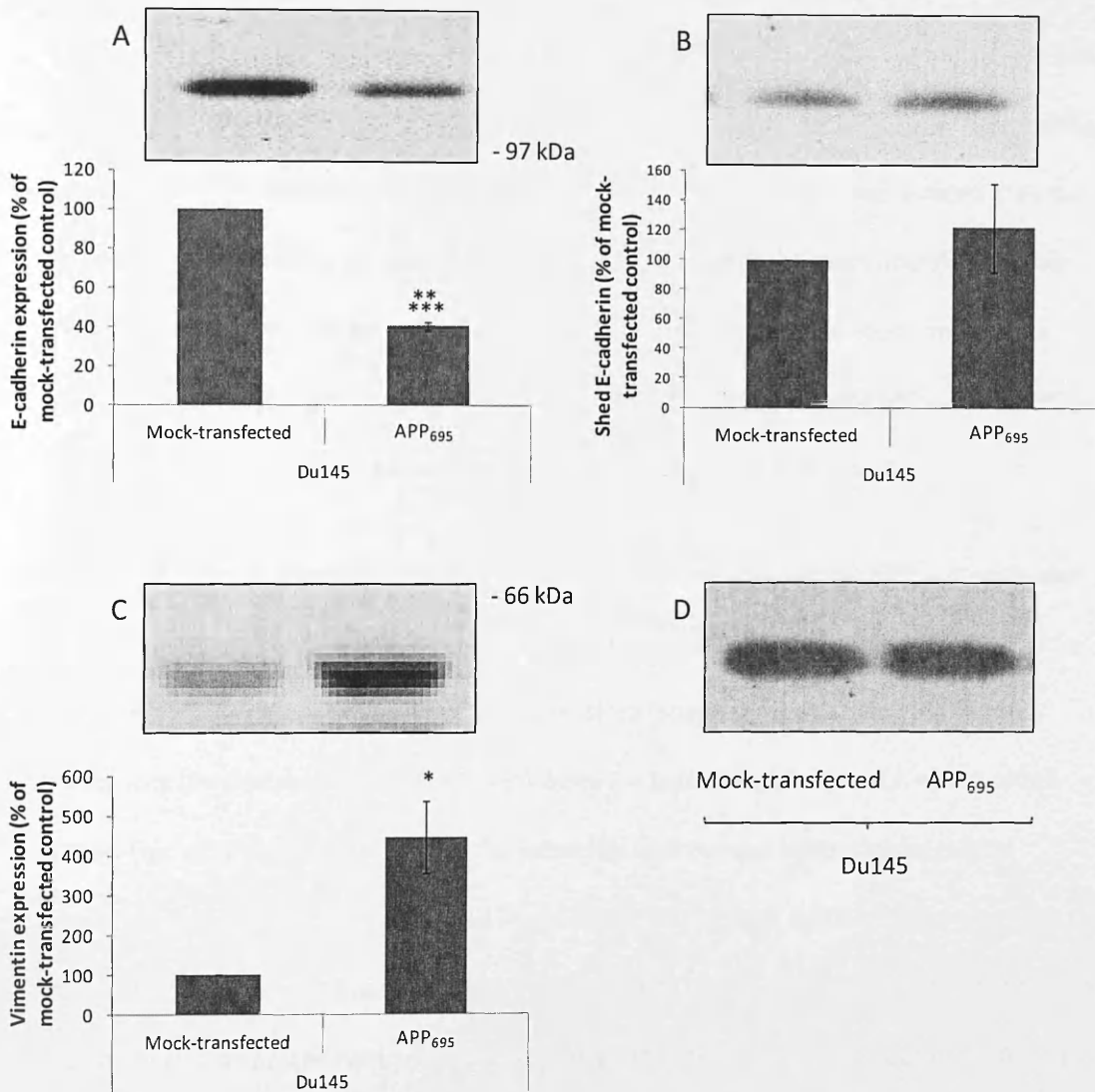


**Figure 8.3. APP<sub>695</sub>-transfection is associated with epithelial-to-mesenchymal transition in Du145 cells.**

Mock Du145 cells or cells stably transfected with APP<sub>695</sub> were grown to confluence and the medium was replaced with serum free medium for 24 h. Cells and conditioned medium were then harvested and prepared for immunoblotting as described in Materials and Methods. **A.** Detection of E-cadherin in cell lysates. **B.** Detection of E-cadherin in conditioned medium. **C.** Detection of vimentin in cell lysates. **D.** Detection of β-actin in cell lysates. Multiple immunoblots were quantified by densitometric analysis and the results are means ± S.D. (n=3). Significance was tested against the mock-transfected control. \* = significant at  $p \leq 0.05$ ; \*\*\*\* = significant at  $p \leq 0.0005$ . When significance is not indicated, results are not significantly different.

## 8.5. APP-induced epithelial-to-mesenchymal transition in Du145 cells is isoform specific

In order to determine whether all isoforms of APP were capable of inducing EMT in Du145 cells, the morphology of stable transfectants over-expressing APP<sub>695</sub>, APP<sub>751</sub> or APP<sub>770</sub> was examined by light microscopy. The results (*Fig. 8.4*) once more demonstrated that the APP<sub>695</sub>-transfected cells had an altered morphology relative to the mock-transfected cells (*Fig. 8.4A and B*) with the former cell type having more apparent extensions and a more elongated cell body, indicative of EMT. In contrast, the visual analysis of APP<sub>751</sub>- and APP<sub>770</sub>-transfected cells suggested a lesser change in morphology (*Fig. 8.4C and D*).

In order to quantify the morphological changes occurring in the APP<sub>695</sub>-transfected cells, a dendricity factor analysis of the light microscope images was performed. Dendricity factor is a mathematical measure of a 2-dimensional shape using the following formula: Dendricity (Inverse shape) factor =  $P^2/4\pi A$  when P = perimeter of cell and A = area of cell (308). This arbitrary value quantifies the extension of processes which causes cells to develop a more complex/less rounded shape (309). This analysis demonstrated that the APP<sub>695</sub>-transfected Du145 cells exhibit a  $1.54 \pm 0.39$ -fold increase in dendricity factor relative to the mock-transfected controls (*Fig. 8.4E*). However, there was no increase in dendricity factor when cells were transfected with KPI-containing isoforms of APP (*Fig. 8.4E*). Thus, it appears that APP-induced EMT in Du145 cells is specific to the 695 amino acid isoform of the protein.

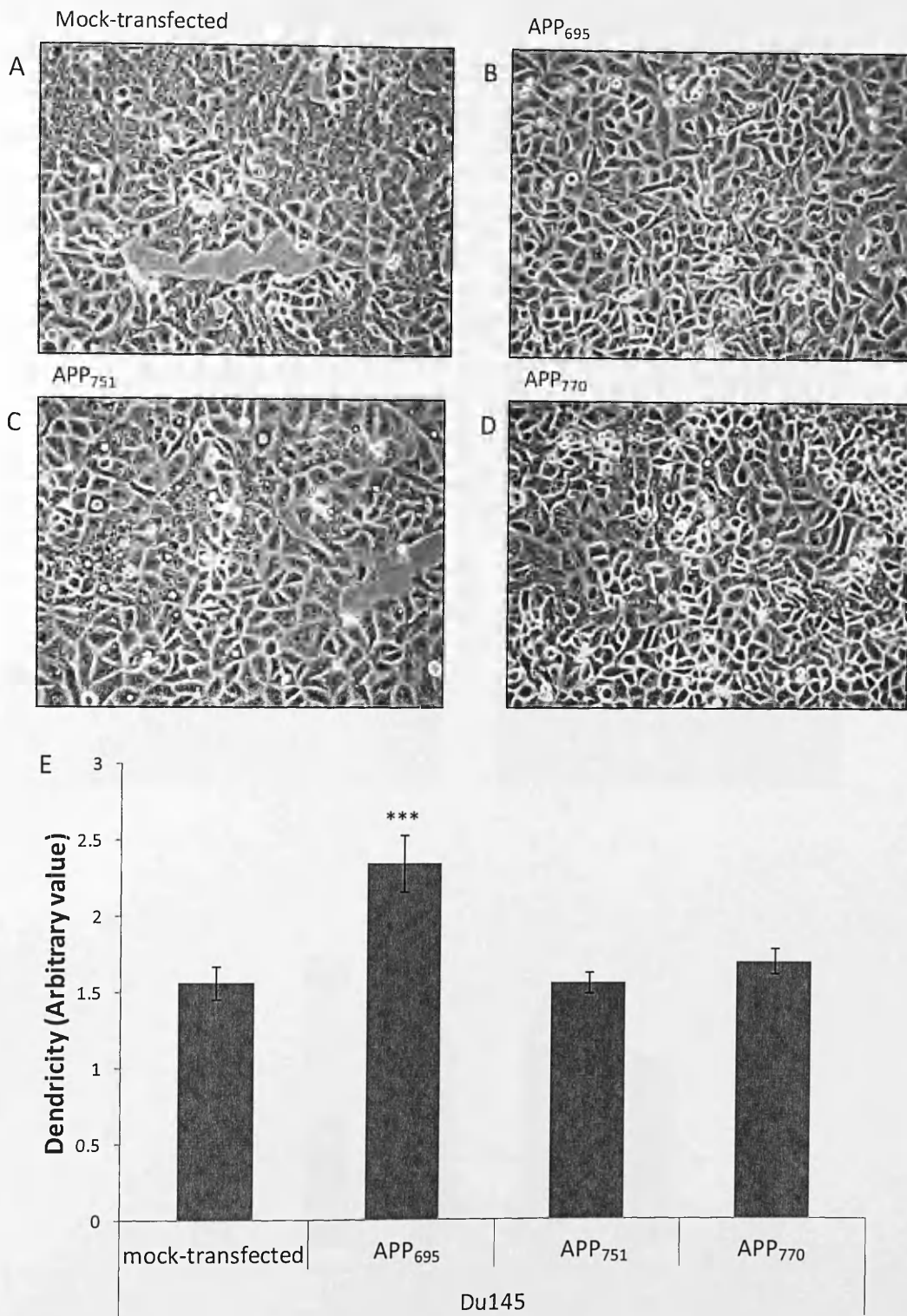


**Figure 8.4. The effect of APP isoforms on EMT in Du145 cells.** Du145 cells stably transfected with either vector alone or the APP isoforms indicated were visualised by light microscopy as described in Materials and Methods (A-D). A dendricity factor analysis was then performed on multiple images (E) and results are means  $\pm$  S.E. ( $n=20$ ). Significance was tested against the mock-transfected control. \*\*\* = significant at  $p \leq 0.005$ . No indication of significance means results are not significantly different.

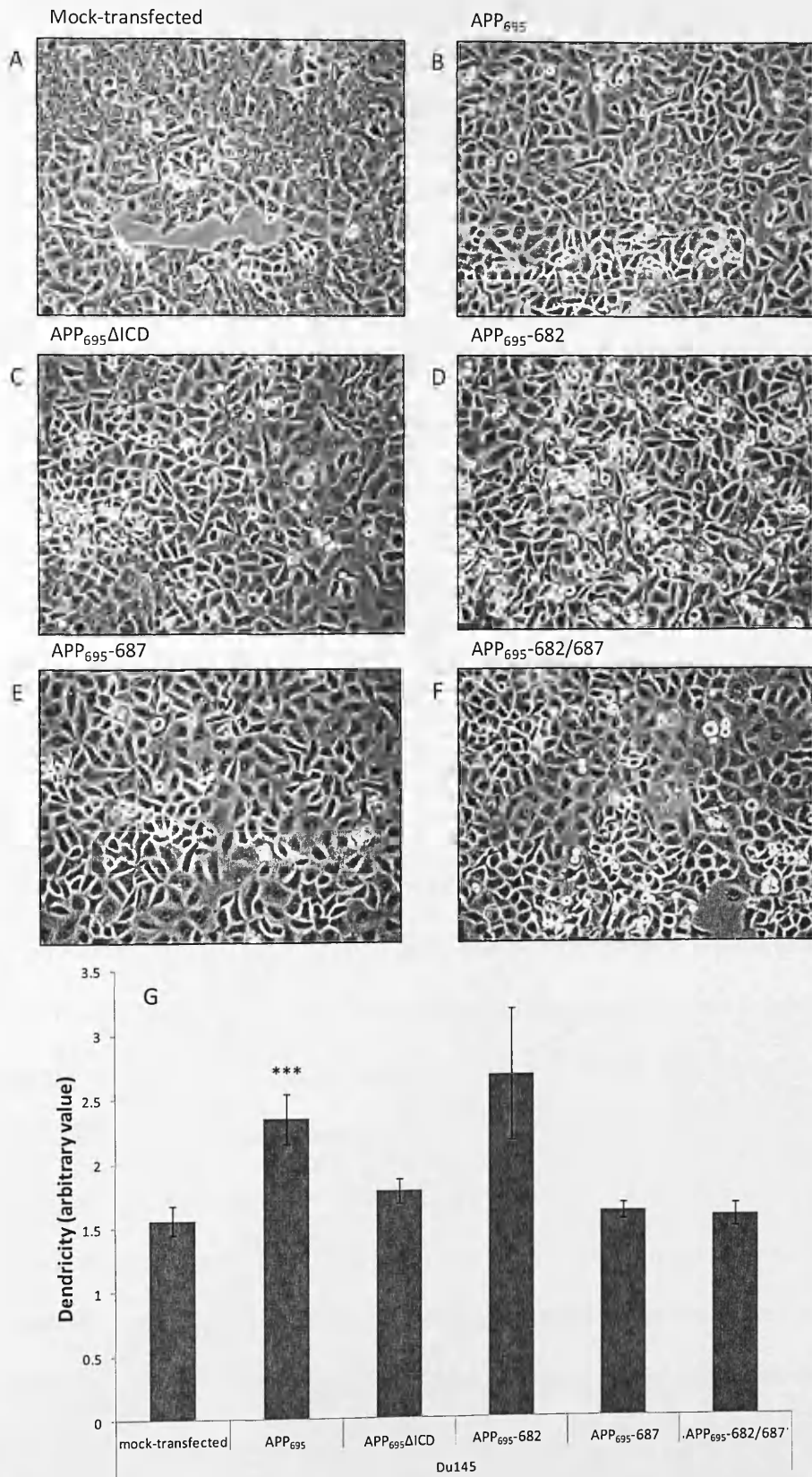


**Figure 8.5. The effect of APP C-terminal constructs on EMT in Du145 cells.** Du145 cells stably transfected with either vector alone or the APP C-terminal constructs indicated were visualised by light microscopy as described in Materials and Methods (A-F). A dendricity factor analysis was then performed on multiple images (G) and results are means  $\pm$  S.E. (n=20). Significance was tested against the mock-transfected control. \*\*\* = significant at  $p \leq 0.005$ . No indication of significance means results are not significantly different.

## 8.6. The APP<sub>695</sub> cytosolic domain is involved in epithelial-to-mesenchymal transition in Du145 cells

Having determined that the ability to induce EMT in Du145 cells was specific to the APP<sub>695</sub> isoform, the molecular determinants within the APP molecule contributing to these morphological changes were next examined. Initially, the involvement of the APP cytosolic domain was examined by comparing the morphology of wild-type APP<sub>695</sub>-transfected cells with that of the cytosolic-domain lacking mutant, APP $\Delta$ ICD (described previously in Chapter 6). The results (*Fig. 8.5A-C and G*) clearly show that, whilst wild-type APP<sub>695</sub> induced EMT, no change in morphology or dendricity factor was observed in the APP $\Delta$ ICD-transfected cells.

Next, the potential involvement in EMT of phosphorylatable tyrosine residues in the APP<sub>695</sub> cytosolic domain was examined. The APP<sub>695</sub> tyrosine 682 residue has an essential role in development and regulating APP function (310, 311) and has been shown to exhibit elevated phosphorylation in an AD brain (312). This tyrosine residue has also been previously shown to be both involved in the phosphorylation of the protein (313) and to interact with specific proteins only when phosphorylated, such as GRB2 and shc, which upon binding can influence downstream signalling pathways (109, 299). The APP<sub>695</sub> tyrosine 687 residue has been identified as a regulator of APP processing (314) and has also been found to exhibit elevated phosphorylation in AD brains (315). A range of proteins interact with the Y<sup>682</sup>ENPTY<sup>687</sup> motif of APP, such as the shc family (316) and Grb2 (317) which are involved in signalling intracellularly. Mutation of the tyrosine residue at position 687 to glycine (APP<sub>695</sub>-687) ablated the ability of wild-type APP<sub>695</sub> to induce EMT in Du145 cells (*Fig. 8.5D, E and G*) as did the mutation of both residues together (APP<sub>695</sub>-682/687) (*Fig. 8.5F and G*), however mutation of the tyrosine residue at 682 (APP<sub>695</sub>-682) caused cells to exhibit an EMT-like morphology, which was not significantly different from the control when carrying out dendricity analysis due to variation (*Fig. 8.5A, B, D, and G*). Thus, it is apparent that specific

tyrosine residues within the cytosolic domain of APP are required as a prerequisite for the ability of the protein to induce epithelial-to-mesenchymal transition.

### **8.7. The E1 copper binding domain is a prerequisite for APP<sub>695</sub>-induced epithelial-to-mesenchymal transition in Du145 cells**

In order to further elucidate the molecular determinants within the APP<sub>695</sub> molecule contributing to EMT, the morphology of mock-transfected Du145 cells was compared with that of cells stably transfected with either wild-type APP<sub>695</sub> or the previously described E1 copper-binding domain deficient construct, APP<sub>695</sub>ΔCuBD. Visual analysis (*Fig. 8.6A-C*) confirmed that the disruption of the E1 copper binding domain prevented the morphological changes associated with wild-type APP<sub>695</sub>. These results were confirmed when a dendricity analysis was performed which, again, showed that only wild-type APP<sub>695</sub> induced EMT-associated morphological changes in Du145 cells (*Fig. 8.6D*). Thus, it would appear that copper binding within the E1 domain of APP is also a prerequisite for epithelial-to-mesenchymal transition in Du145 cells.

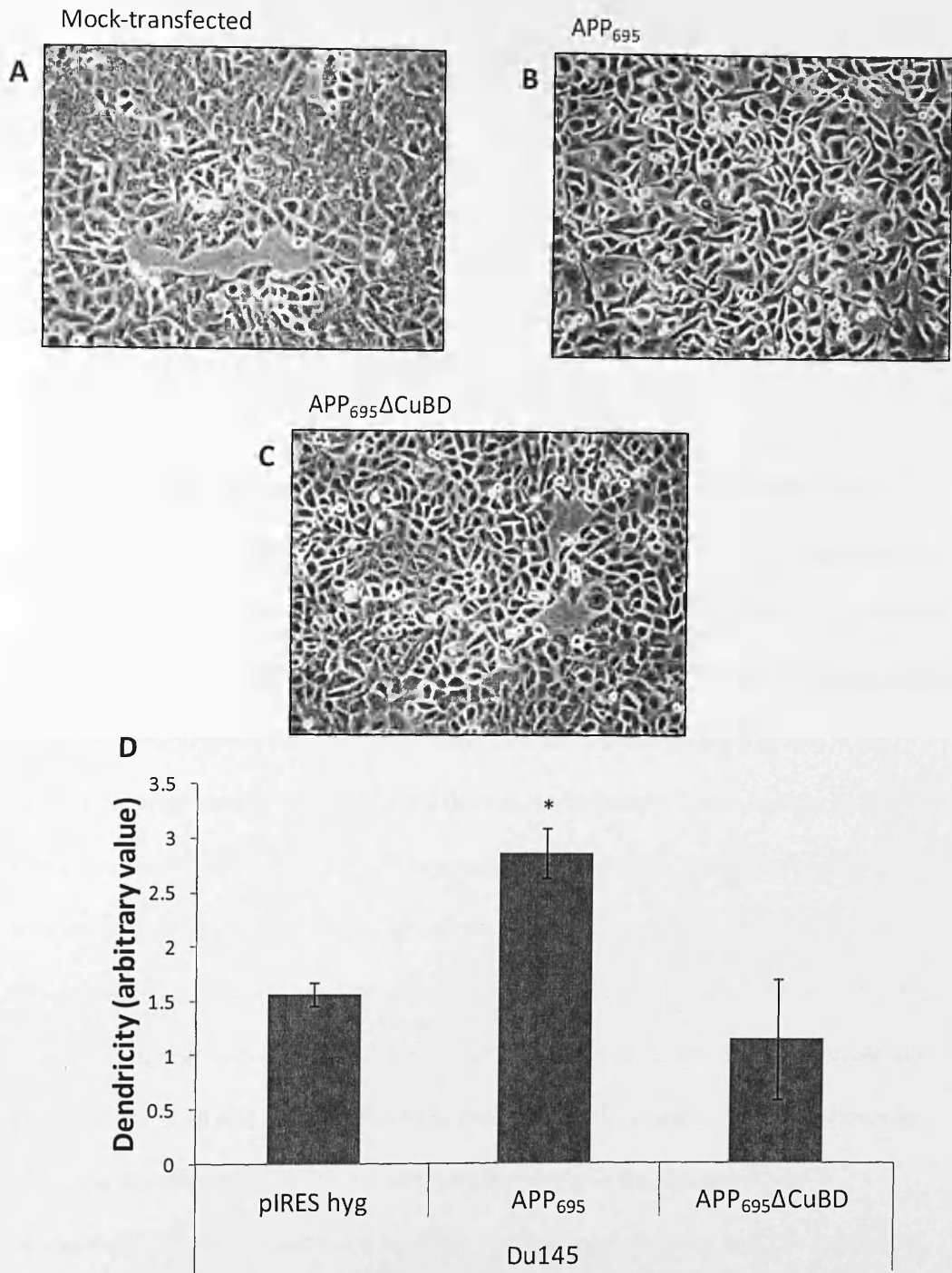


**Figure. 8.6.** The effect of APP E1 domain copper binding ablation on EMT in Du145 cells. Du145 cells stably transfected with either vector alone or the APP constructs indicated were visualised by light microscopy as described in Materials and Methods (A-C). A dendricity factor analysis was then performed on multiple images (D) and results are means  $\pm$  S.E. (n=20). Significance was tested against the mock transfected control. \* = significant at  $p \leq 0.05$ . When no significance is indicated, results are not significantly different.

## 8.8. Attempted artificial induction of epithelial-to mesenchymal transition by enhancing endogenous APP expression

Having established that the artificial over-expression of APP<sub>695</sub> could induce EMT in Du145 cells, attempts were then made to stimulate expression of the endogenous protein with a view to initiating EMT.

Nerve growth factor (NGF) is a neurotrophin present in the brain involved in promoting survival, growth and differentiation of neurons (318) and has previously been shown to increase APP mRNA levels in hamster brain and PC12 cells (319, 320). As Du145 cells are a brain metastatic prostate cancer cell line, the effect of NGF on APP expression in these cells was examined in the current study. Untransfected cells were grown in the absence or presence of a range of NGF- $\beta$  (human, recombinant, Sigma-Aldrich, Poole, UK) concentrations and the effect on APP expression and proteolysis was subsequently monitored by immunoblot analysis. Initial results (*Fig. 8.7A*) appeared to show an increase in the expression of endogenous APP when cells were treated with NGF- $\beta$  in the concentration range 3-20 ng/ml. Such changes were not mirrored in conditioned medium when the anti-APP antibody 6E10 was used to detect the shed form of the protein (*Fig. 8.7C*). However, when the experiment was repeated in triplicate using only 0 and 3 ng/ml NGF- $\beta$  concentrations no significant increase in APP expression or shedding could be confirmed (*Fig. 8.7D-H*).

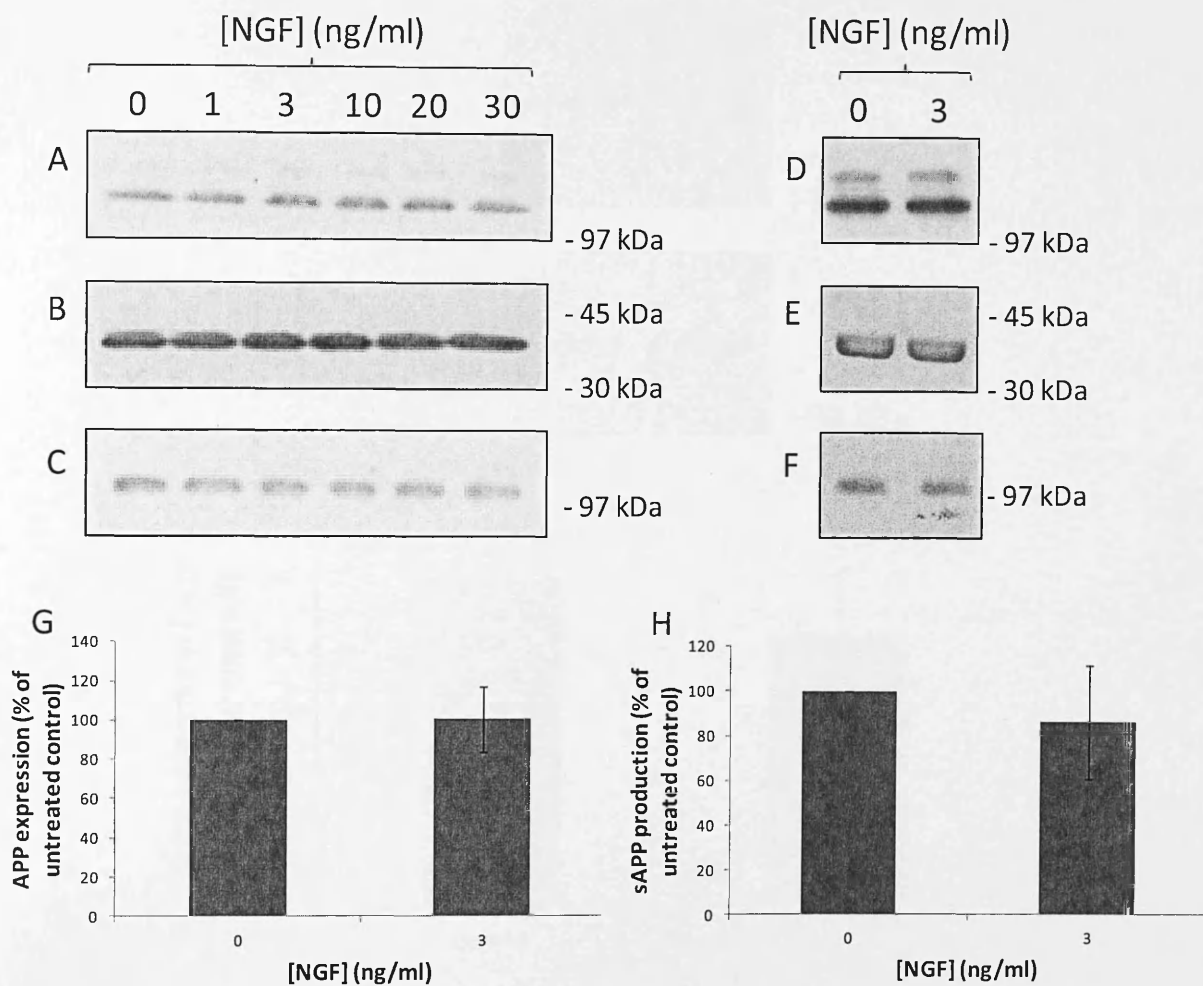


**Figure 8.7. The effect of NGF-β on APP expression and proteolysis in Du145 cells.** Cells were grown in the absence or presence of NGF-β (Materials and Methods) and cell lysates and conditioned medium were subsequently prepared and subjected to immunoblotting (Materials and Methods). **A-C.** Cells were treated with the indicated range of NGF-β concentrations and cell lysates were subsequently immunoblotted with anti-APP C-terminal antibody (**A**) and anti-β-actin antibody (**B**). The conditioned medium samples were immunoblotted with anti-APP antibody, 6E10 (**C**). **D-H.** Cells were grown in the absence or presence of 3 ng/ml NGF-β and lysates were immunoblotted with anti-APP C-terminal antibody (**D**), anti-β-actin antibody (**E**) or anti-APP antibody 6E10 (**F**). Multiple APP-CT antibody (**G**) and anti-APP 6E10 antibody (**H**) blots, respectively, were quantified by densitometric analysis and the results are means ± S.D. (n=5). Significance was tested against the untreated control. Unless otherwise indicated, the results are not significantly different.

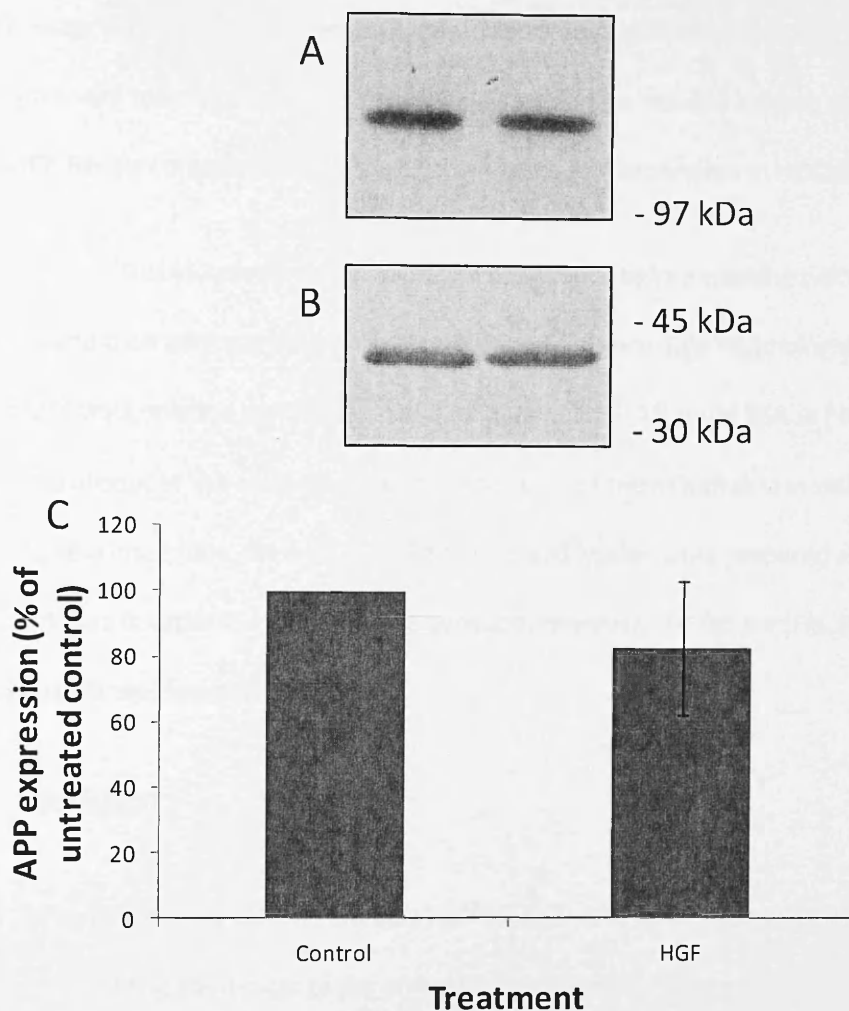


**Figure 8.8. The effect of HGF on APP expression in Du145 cells.** Cells were grown in the absence or presence of HGF (Materials and Methods) and cell lysates were subsequently prepared and subjected to immunoblotting (Materials and Methods). **A.** Detection of APP in cell lysates using the anti-APP C-terminal antibody. **B.** Detection of  $\beta$ -actin in cell lysates using the anti- $\beta$ -actin antibody. **C.** APP C-terminal antibody immunoblots were quantified and the results expressed relative to the untreated control. Results are means  $\pm$  S.D. (n=3). Significance was tested against the untreated control. Unless otherwise indicated, the results are not significantly different.

As NGF treatment of Du145 cells did not have the desired effect, a second compound was tested for its ability to enhance endogenous APP expression. Hepatocyte growth factor (HGF) has been linked to prostate cancer disease progression (321) and has also been linked to brain tumour growth, angiogenesis and a reduced disease prognosis (322). HGF has also previously been shown to enhance APP expression in HEK293 cells (323).

Du145 cells were grown to 80% confluence before washing twice in OptiMEM and then adding a fresh 10 ml OptiMEM. HGF (Gibco, Life Technologies Ltd., Paisley, UK) stock solution was made up at 0.33  $\mu\text{g}/50 \mu\text{l}$  of 0.1% (w/v) BSA in PBS and a single 50  $\mu\text{l}$  aliquot of this stock was added to the 10 ml of fresh OptiMEM in cell cultures. Following 48 h incubation, the cells were harvested and lysates were prepared and immunoblotted in order to examine APP expression. However, the results (*Fig. 8.8*) showed no HGF-associated change in APP levels.

## 8.9. Summary

In the current chapter the effects of APP<sub>695</sub> on Du145 cell morphology have been characterised. Stable expression of the protein induced neurite-like extensions at the cell periphery (*Fig. 8.1*) and these changes were shown to be associated not with neuroendocrine differentiation (*Fig. 8.2*) but with epithelial-to-mesenchymal transition (*Fig. 8.3*).

The induction of EMT by APP in Du145 cells was specific to the smaller 695 amino acid isoform (*Fig. 8.4*) and to a specific tyrosine residue in the cytosolic domain of the protein (*Fig. 8.5*). An intact E1 copper binding domain (*Fig. 8.6*) was also shown to be a prerequisite for the effect.

# 9. The role of copper binding in APP proteolysis and the viability of SH- SY5Y cells

## 9.1. Introduction

The preceding chapters have largely focused on the potential role of APP in regulating the viability of prostate cancer cells upon metastasis to the brain. In this respect it is apparent that the E1 copper binding domain of APP was a prerequisite for the enhanced viability of Du145 cells observed in the presence of copper.

In the current chapter, the role of APP copper binding in relation to Alzheimer's disease rather than brain metastatic prostate cancer is examined. Specifically, the effects of histidine to alanine mutations within the E1 CuBD or the putative copper binding sites within the A $\beta$  domain, on the proteolysis of APP and cell viability within the neuroblastoma cell line SH-SY5Y are examined.

## 9.2. The expression and proteolysis of APP<sub>695</sub> copper binding mutants in SH-SY5Y cells

As APP<sub>695</sub> is the major isoform of the protein expressed in neurons (324), SH-SY5Y cells were initially stably transfected with a range of APP<sub>695</sub> copper binding mutant constructs (*Fig. 9.1*). The E1 copper binding domain mutant, APP<sub>695</sub> $\Delta$ CuBD (*Fig. 9.1B*) has been described previously (Chapter 7). In addition, three further constructs were employed, each with a single histidine to alanine mutation within the A $\beta$  domain at positions 602, 609 or 610 (*Fig 9.1C-E*).

The various APP constructs were stably transfected into SH-SY5Y cells (see Materials and Methods) and their expression and proteolysis were subsequently monitored by immunoblotting. Initially, equal amounts of protein from cell lysates were resolved by SDS-PAGE and immunoblotted using the anti-APP C-terminal antibody. The results (*Fig. 9.2*) were expressed relative to the levels of APP detected in lysates from the wild-type APP<sub>695</sub> over-

expressing cells as the level of endogenous APP in the mock-transfected cells was extremely low relative to the APP-transfected cell lines. The data clearly show that, in all of the transfectants, APP was dramatically over-expressed and no significant difference could be determined between the expression levels of the individual constructs.

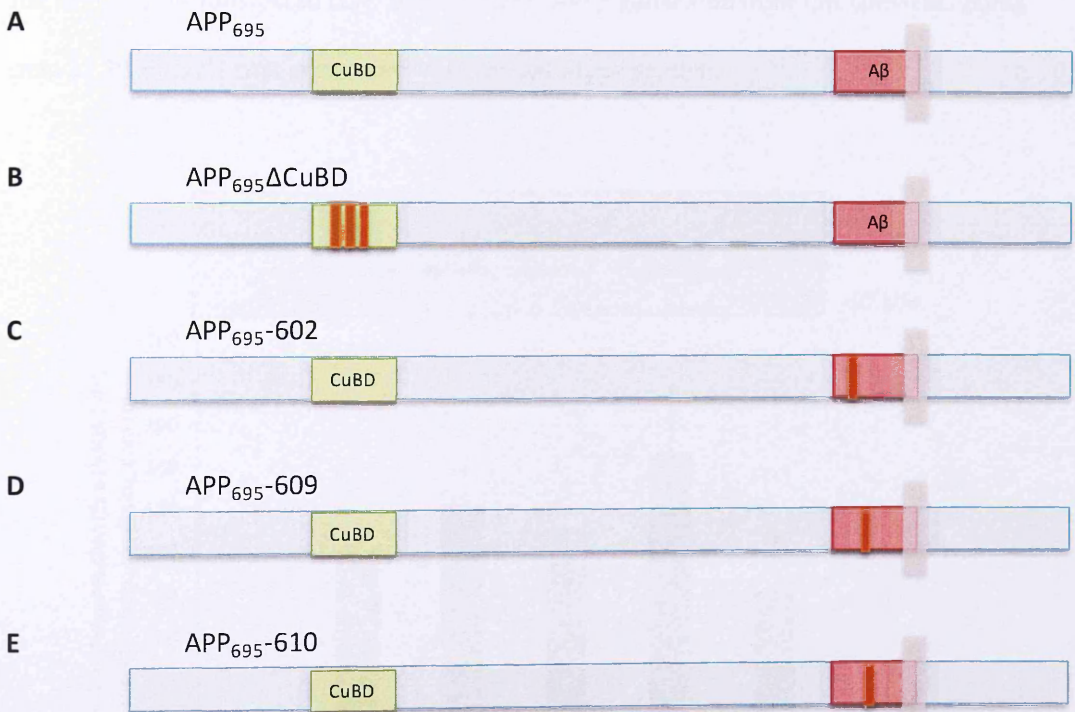


**Figure 9.1. Schematic representing APP<sub>695</sub> copper binding mutant constructs.** A. Wild-type APP<sub>695</sub>. B. The APP<sub>695</sub>ΔCuBD construct contained three histidine to alanine mutations at positions 147, 149 and 151. C-E. Three additional constructs were employed, each one containing a single histidine to alanine mutation at position 602, 609 or 610.

Next, the generation of soluble APP from the various APP<sub>695</sub> copper binding mutant proteins was examined by immunoblotting equal volumes of concentrated conditioned medium. Immunoblotting the samples with anti-APP antibody 22C11 (*Fig. 9.3A*) revealed that the generation of sAPP from the various APP constructs was identical. However, when the samples were immunoblotted using antibody 1A9, a clear decrease in the levels of sAPP $\beta$  generated from all of the histidine to alanine mutants was detected relative to the wild-type APP<sub>695</sub>-transfected cells (*Fig. 9.3B*). This difference was particularly pronounced in the APP<sub>695</sub>-610-transfected cells with levels of sAPP $\beta$  generated from this construct being only  $37.86 \pm 4.77\%$  that generated from the wild-type protein.

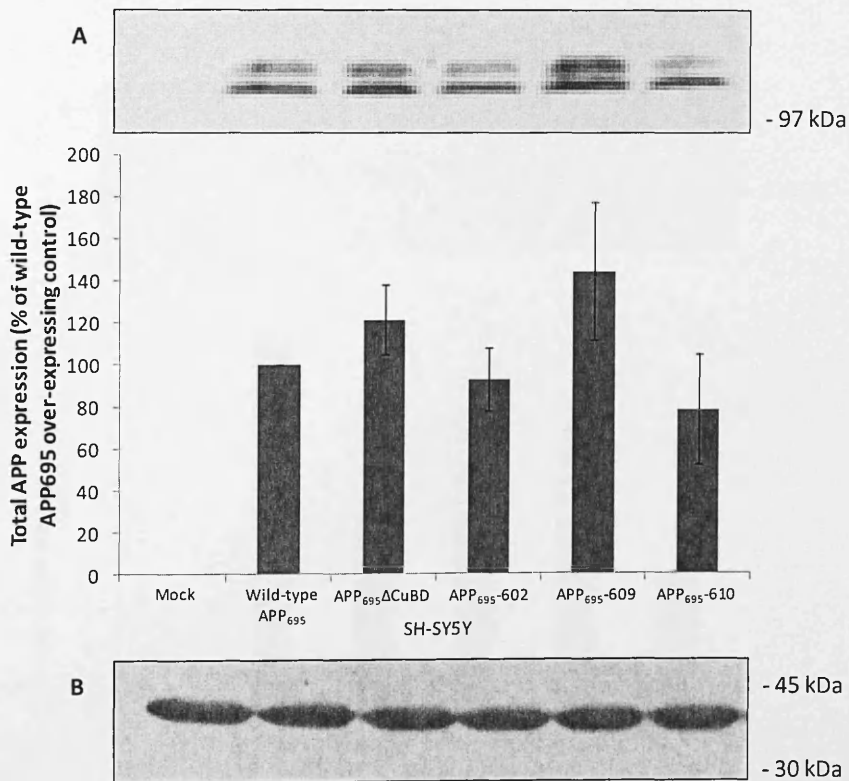


**Figure 9.2.** APP<sub>695</sub> copper binding domain mutant over-expression in SH-SY5Y cells. Stably transfected cells were grown to confluence and the medium was replaced with serum free medium for 24 h. Lysates were subsequently prepared and equal amounts of protein from each were immunoblotted (Materials and Methods). **A.** Detection of APP in cell lysates using the anti-APP C-terminal antibody. Multiple APP immunoblots were quantified by densitometric analysis and the results shown are expressed relative to the wild-type APP<sub>695</sub>-transfected cells and are means  $\pm$  S.D. (n=3). Unless otherwise indicated, the results are not significantly different. **B.** Detection of  $\beta$ -actin in cell lysates using the anti- $\beta$ -actin antibody.

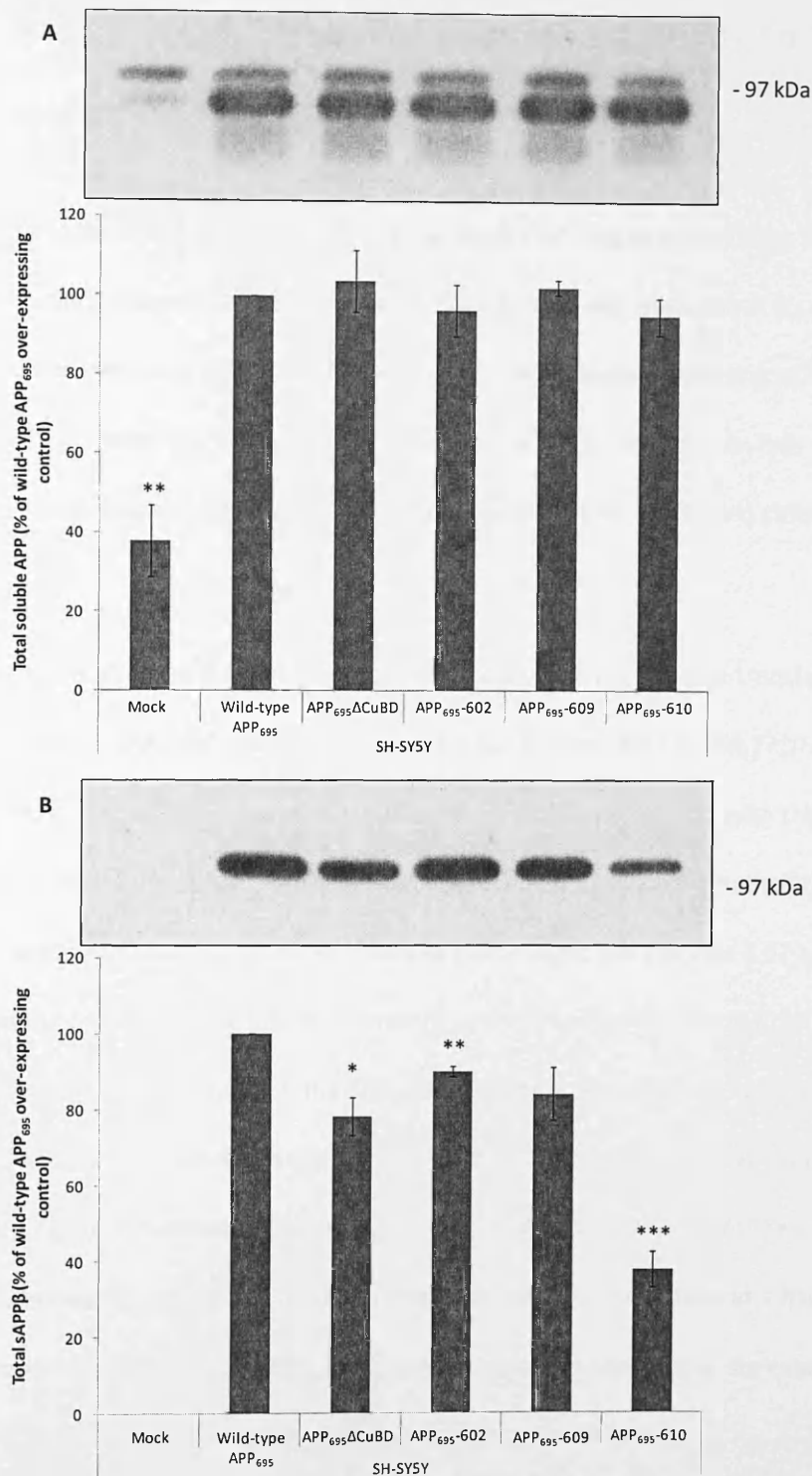


**Figure 9.3. Soluble APP generation by SH-SY5Y cells over-expressing the APP<sub>695</sub> copper binding constructs.** Stably transfected cells were grown to confluence and the medium was replaced with serum free medium for 24 h. Conditioned medium was subsequently prepared and equal volumes of each sample were immunoblotted. **A.** Detection of sAPP in conditioned medium using the anti-APP antibody, 22C11. **B.** Detection of sAPPβ in conditioned medium using antibody 1A9. Multiple immunoblots were quantified by densitometric analysis and the results shown are means ± S.D. (n=3). Significance was tested against the wild-type APP<sub>695</sub>-transfected cells. \* = significant at  $p \leq 0.05$ ; \*\* = significant at  $p \leq 0.01$ ; \*\*\* = significant at  $p \leq 0.005$ . Unless otherwise indicated, the results are not significantly different.

### 9.3. The effects of APP<sub>695</sub> copper binding mutants on the viability of SH-SY5Y cells in the presence of copper

In order to examine the role of APP<sub>695</sub> copper binding in maintaining SH-SY5Y cell viability in the presence of copper, the stably transfected cells were grown for 72 h in serum-free medium containing a range of copper concentrations before analysing cell viability using the MTS assay (Materials and Methods). Note that, in these experiments, free copper was employed as opposed to the glycine-complexed metal used for the Du145 cells in Chapters 5-7.

The results (*Fig. 9.4*) show that, after 72 h, the viability of mock-transfected cells treated with 100, 200 and 250  $\mu\text{M}$  copper had decreased to  $83.27 \pm 3.29$ ,  $77.76 \pm 2.98$  and  $68.3 \pm 3.91\%$ , respectively, that of the untreated controls. However, as with the Du145 cells (Chapter 5), wild-type APP<sub>695</sub> generally enhanced SH-SY5Y cell viability in the presence of copper, particularly at metal concentrations of 100 and 200  $\mu\text{M}$  ( $95.28 \pm 3.67$  and  $98.84 \pm 2.52\%$  of the untreated controls, respectively). As with the Du145 cells, the disruption of copper binding by the E1 CuBD in the APP<sub>695</sub>CuBD mutant prevented the ability of APP to enhance SH-SY5Y cell viability in the presence of copper (*Fig. 9.4*). However, mutating individual histidine residues within the A $\beta$  domain of APP did not prevent the ability of the protein to enhance cell viability at lower copper concentrations. In fact, at a higher metal concentration of 250  $\mu\text{M}$ , the APP<sub>695</sub>-602 mutant construct appeared to be even more effective in promoting cell viability than its wild-type counterpart.

Collectively, these data indicate that copper binding within the E1 domain of APP<sub>695</sub> as opposed to the A $\beta$  domain is a prerequisite for the ability of the protein to enhance SH-SY5Y cell viability in the presence of copper.

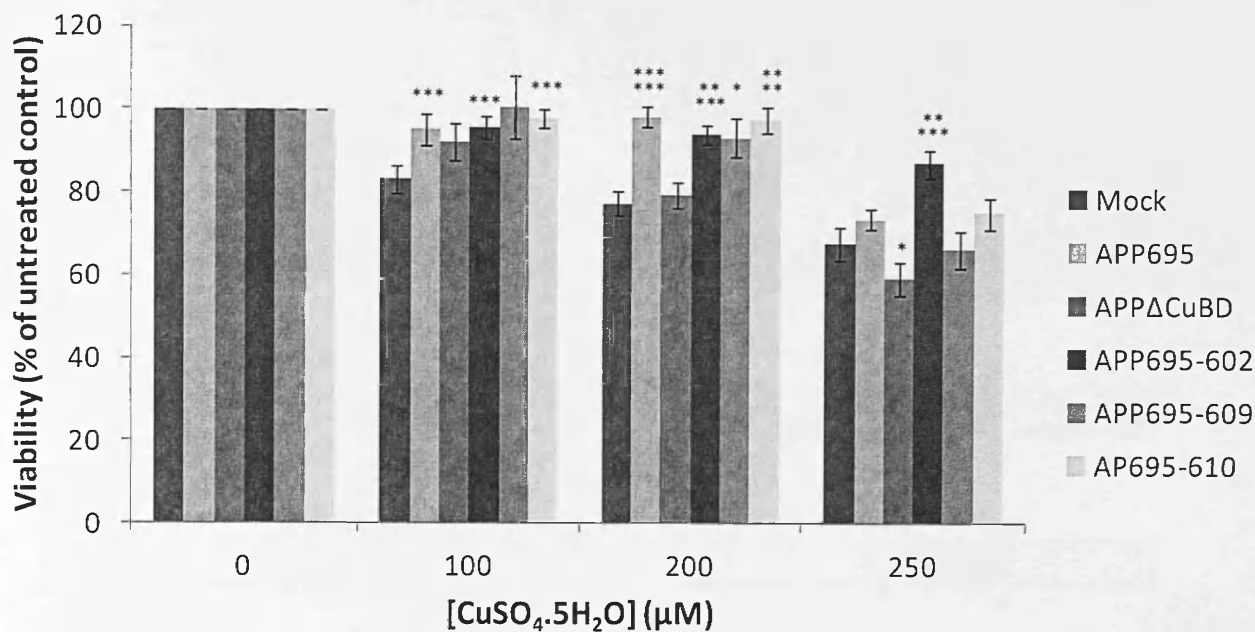


**Figure 9.4.** The effect of APP<sub>695</sub> copper binding mutant over-expression on SH-SY5Y cell viability in the presence of copper. Cells were seeded from an 'ultraconfluent' T75 flask into a 24-well plate after diluting 1 in 150 in DMEM and equilibrated overnight under normal growth conditions (37 °C, 5% CO<sub>2</sub>). The following day, the medium was replaced with 100 µl of serum free medium containing the indicated concentrations of CuSO<sub>4</sub>.5H<sub>2</sub>O and cells were grown for a further 72 h before conducting an MTS viability assay (Materials and Methods). Results are means ± S.E. (n=15). Significance was tested against the mock-transfected control. \* = significant at  $p \leq 0.05$ ; \*\*\* = significant at  $p \leq 0.005$ ; \*\*\*\* =  $p \leq 0.001$ ; \*\*\*\*\* =  $p \leq 0.0005$ ; \*\*\*\* =  $p \leq 0.0001$ . Unless otherwise stated, differences were not significant.

#### 9.4. The expression and proteolysis of APP<sub>770</sub> copper binding mutants in SH-SY5Y cells

As the ability of APP to enhance Du145 cell viability observed in Chapter 5 was isoform specific, the effect of APP<sub>770</sub> on SH-SY5Y viability in the presence of copper was also investigated in this respect. A range of APP<sub>770</sub> copper binding mutants analogous to those previously generated in APP<sub>695</sub> were designed (Fig. 9.5). The amino acid numbering of the three mutated histidine residues in the APP<sub>770</sub> E1 CuBD construct was the same as that in the analogous APP<sub>695</sub> construct, as the E1 domain precedes the KPI and OX-2 domains in terms of primary sequence. However, the positions of the histidine residues mutated in the APP<sub>770</sub> Aβ

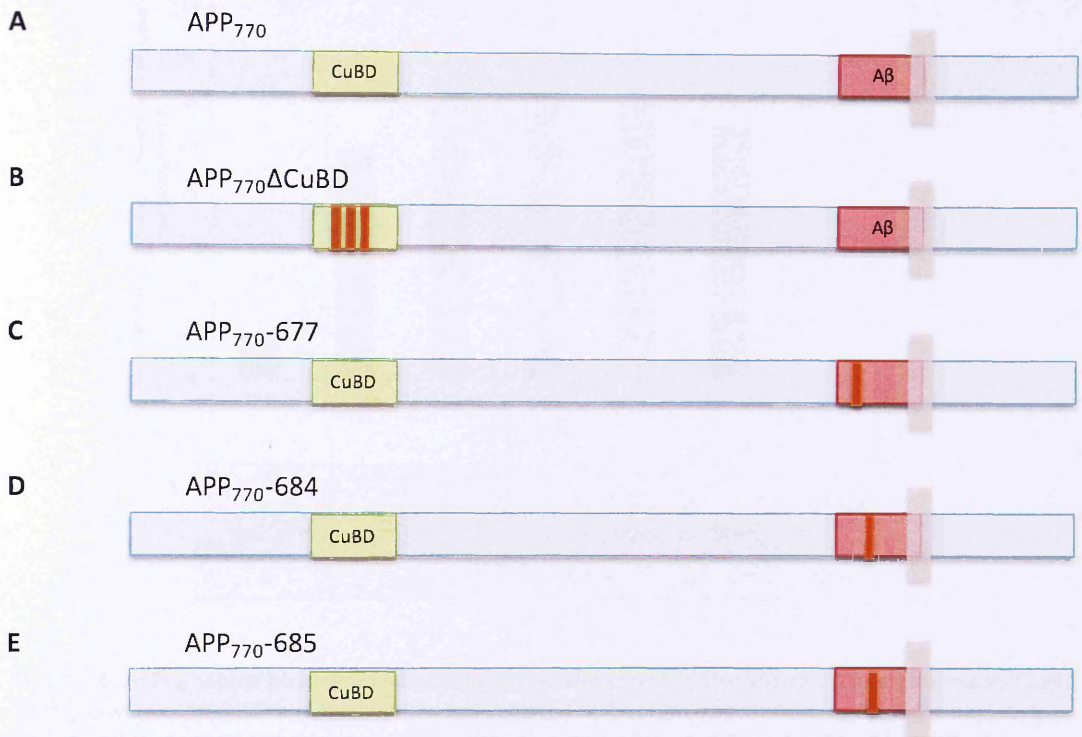


**Figure 9.5. Schematic representing APP<sub>770</sub> copper binding mutant constructs.** A. Wild-type APP<sub>770</sub>. B. The APP<sub>770</sub>ΔCuBD construct contained three histidine to alanine mutations at positions 147, 149 and 151. C-E. Three additional constructs were employed, each one containing a single histidine to alanine mutation at position 677, 684 or 685.

domain constructs were 677, 684 or 685 (as opposed to 602, 609 or 610 in the APP<sub>695</sub> constructs).

Stable over-expression of the APP<sub>770</sub> copper-binding constructs was confirmed by immunoblotting with the anti-APP C-terminal antibody (Fig. 9.6A). Equal protein loading was demonstrated via immunoblotting with the anti-β-actin antibody (Fig. 9.6B).

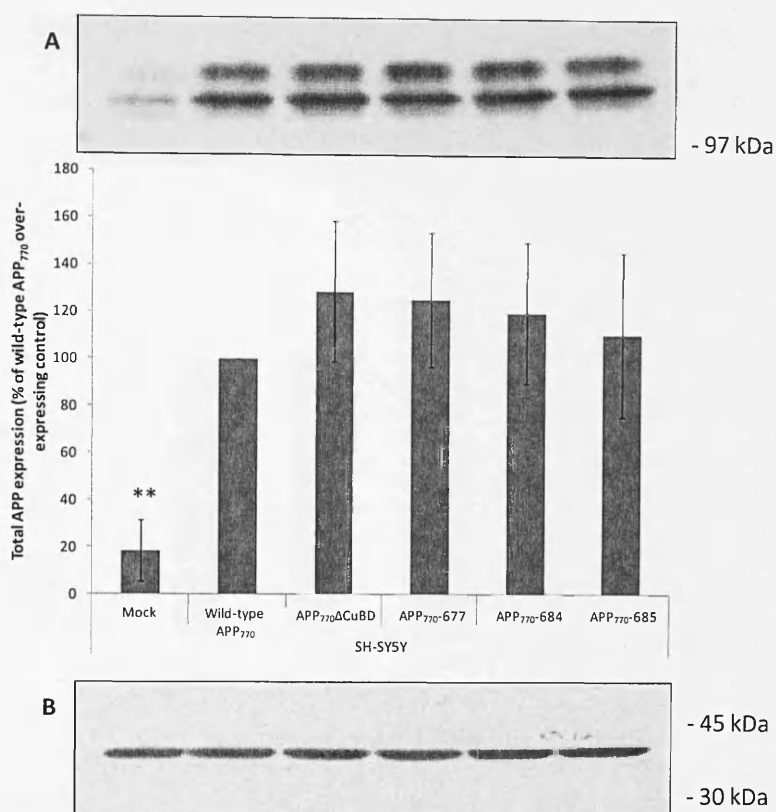


**Figure 9.6. APP<sub>770</sub> copper binding domain mutant over-expression in SH-SY5Y cells.** Stably transfected cells were grown to confluence and the medium was replaced with serum free medium for 24 h. Lysates were subsequently prepared and equal amounts of protein from each were immunoblotted (Materials and Methods). **A.** Detection of APP in cell lysates using the anti-APP C-terminal antibody. Multiple APP immunoblots were quantified by densitometric analysis and the results shown are expressed relative to the wild-type APP<sub>770</sub>-transfected cells and are means  $\pm$  S.D. (n=3). \*\* = significant at  $p \leq 0.01$ . Unless otherwise indicated, the results are not significantly different. **B.** Detection of  $\beta$ -actin in cell lysates using the anti- $\beta$ -actin antibody.

Next, the generation of soluble APP from the various APP<sub>770</sub> copper binding mutant proteins was examined by immunoblotting concentrated conditioned medium.

Immunoblotting the samples with anti-APP antibody 22C11 (*Fig. 9.7A*) revealed that, as for the analogous APP<sub>695</sub> constructs, the generation of sAPP from the various APP<sub>770</sub> constructs was identical. However, when the samples were immunoblotted using antibody 1A9, a clear decrease in the levels of sAPP $\beta$  generated from all of the histidine to alanine mutants was again detected relative to the wild-type APP<sub>770</sub> over-expressing cells (*Fig. 9.7B*). This difference was particularly pronounced in the APP<sub>770</sub>-685-transfected cells with levels of

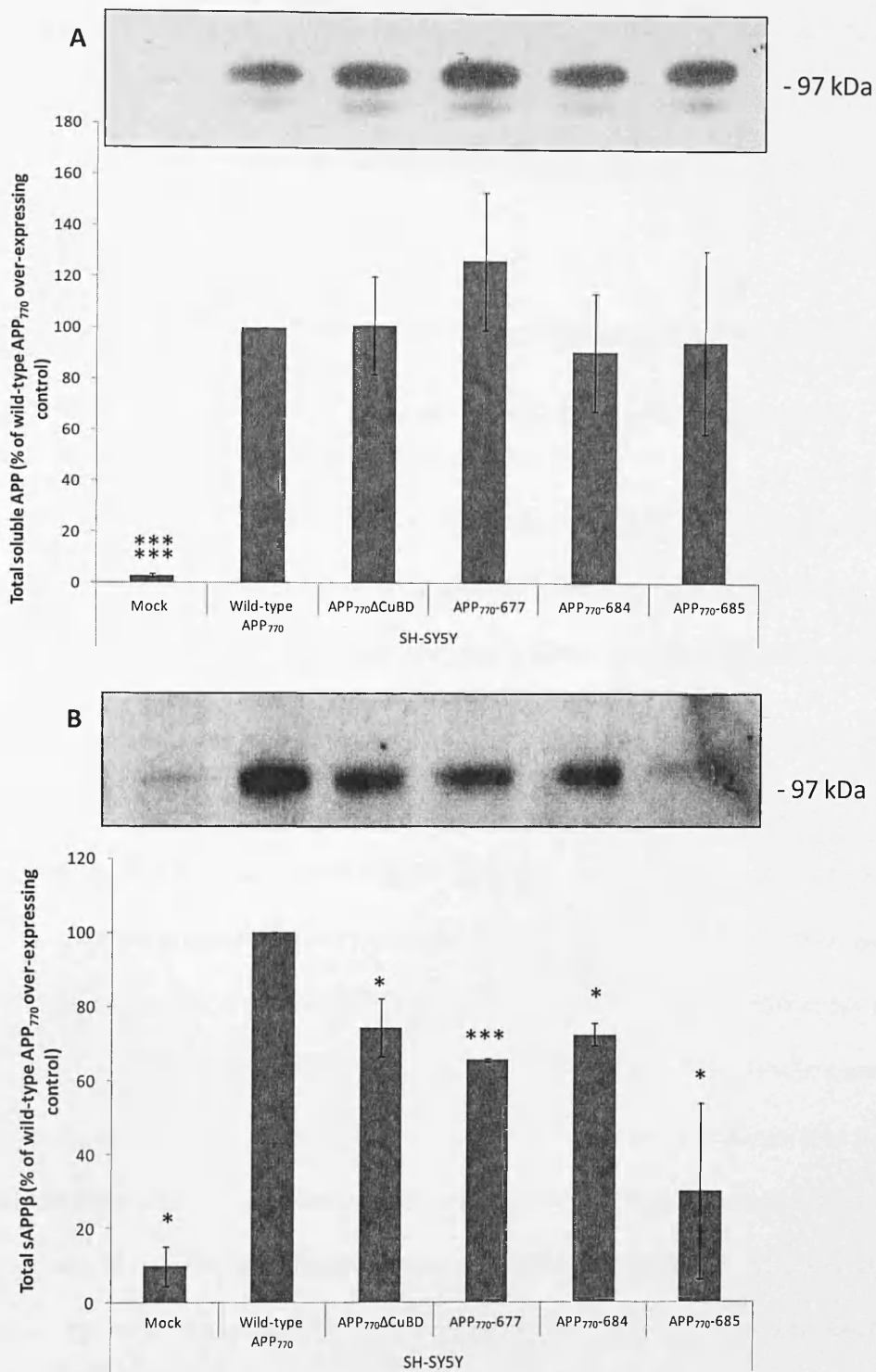


**Figure 9.7. Soluble APP generation by SH-SY5Y cells over-expressing the APP<sub>770</sub> copper binding constructs.** Stably transfected cells were grown to confluence and the medium was replaced with serum free medium for 24 h. Conditioned medium was subsequently prepared and equal volumes of each sample were immunoblotted. **A.** Detection of sAPP $\alpha$  in conditioned medium using the anti-APP antibody, 22C11. **B.** Detection of sAPP $\beta$  in conditioned medium using antibody 1A9. Multiple immunoblots were quantified by densitometric analysis and the results shown are means  $\pm$  S.D. (n=3). Significance was tested against the wild-type APP<sub>770</sub>-transfected cells. \* = significant at  $p \leq 0.05$ ; \*\*\* = significant at  $p \leq 0.005$ . Unless otherwise indicated, the results are not significantly different.

sAPP $\beta$  generated from this construct being only  $29.96 \pm 23.78\%$  that generated from the wild-type protein. It would seem, therefore, that the differences in proteolysis brought about by the various histidine mutations in the current study occur in both APP<sub>695</sub> and APP<sub>770</sub> isoforms of the protein.

## 9.5. The effects of APP<sub>770</sub> copper binding mutants on the viability of SH-SY5Y cells in the presence of copper

In order to examine the role of APP<sub>770</sub> copper binding in maintaining SH-SY5Y cell viability in the presence of copper, the viability experiments previously performed with the analogous APP<sub>695</sub> constructs were repeated for the APP<sub>770</sub> isoform expressing cell lines.

The results (*Fig. 9.8*) show that, after 72 h, the viability of mock-transfected cells treated with 200 and 250  $\mu\text{M}$  copper had decreased to  $79.53 \pm 4.16$ , and  $62.71 \pm 9.64\%$  respectively, that of the untreated controls. However, as with the APP<sub>695</sub> isoform, wild-type APP<sub>770</sub> generally enhanced SH-SY5Y cell viability in the presence of copper, particularly at metal concentrations of 200 and 250  $\mu\text{M}$  ( $110.65 \pm 7.86$  and  $107.35 \pm 9.05\%$  of the untreated controls, respectively). The disruption of the E1 CuBD in the APP<sub>770</sub>CuBD mutant prevented the ability of APP to enhance SH-SY5Y cell viability in the presence of copper (*Fig. 9.8*). As with the analogous APP<sub>695</sub> constructs, the APP<sub>770</sub>-677 and APP<sub>770</sub>-685 constructs had a similar propensity to the wild-type protein to enhance SH-SY5Y cell viability in the presence of copper. However, in the case of the APP<sub>770</sub> isoform, the mutation of His609 to alanine ablated the ability of the protein to maintain cell viability.

Collectively, these data indicate that the roles of the various copper binding histidine residues in the E1 and A $\beta$  domains of APP, in relation to maintaining cell viability, are similar but not identical in the 695 and 770 amino acid isoforms of the protein.

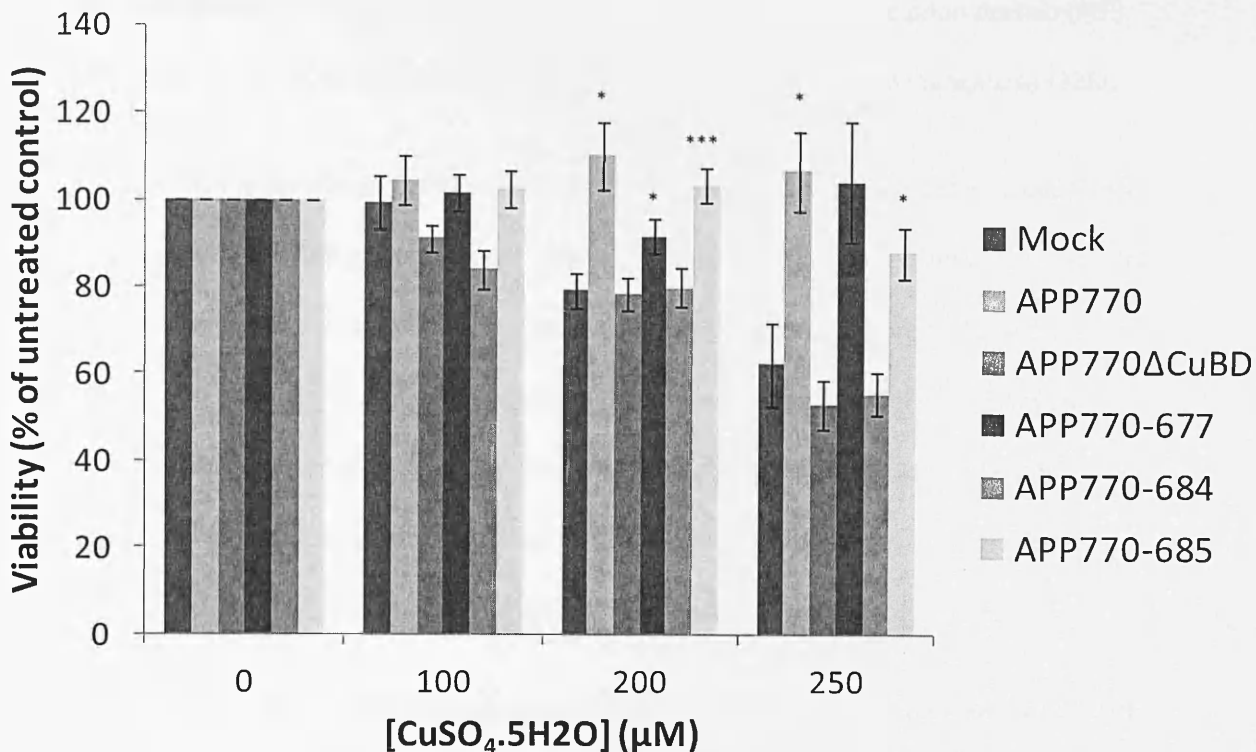


**Figure 9.8. The effect of APP<sub>770</sub> copper binding mutant over-expression on SH-SY5Y cell viability in the presence of copper.** Cells were seeded from an 'ultraconfluent' T75 flask into a 24-well plate after diluting 1 in 150 in DMEM and equilibrated overnight under normal growth conditions (37 °C, 5% CO<sub>2</sub>). The following day, the medium was replaced with 100 µl of serum free medium containing the indicated concentrations of CuSO<sub>4</sub>.5H<sub>2</sub>O and cells were grown for a further 72 h before conducting an MTS viability assay (Materials and Methods). Results are means ± S.E. (n=15). Significance was tested against the mock-transfected control. \* = significant at  $p \leq 0.05$ ; \*\*\* = significant at  $p \leq 0.005$ . Unless otherwise stated, differences were not significant.

## 9.6. APP binds copper despite mutation of the E1 or Aβ copper binding domains

In order to determine whether the histidine mutations in the APP constructs employed affected metal binding, soluble APP<sub>770</sub> shed into the conditioned medium of SH-SY5Y cells expressing the various copper binding domain APP mutants was subjected to metal chelate affinity chromatography (Materials and Methods). The affinity columns were preloaded with either no metal, copper or manganese. The rationale for using manganese

was that there exist many similarities in the cell biology of APP and the prion protein (PrP) (281, 325) the latter of which has been shown to bind both copper and manganese (326).

The results (*Fig. 9.9*) show that, when the affinity columns were not preloaded with metal, the soluble APP generated from all of the constructs, as expected, was detected solely in the column run-through. In fact, the same was true when columns preloaded with manganese were employed, indicating that APP does not bind effectively to this metal. However, soluble APP bound effectively to the affinity columns when they had been preloaded with copper, regardless of any histidine to alanine mutations in either the E1 CuBD or the A $\beta$  domain and was, therefore, only detected in the column eluate.

Thus, whilst the mutation of histidine residues within either the E1 CuBD or the A $\beta$  region might well ablate copper binding in those specific regions of the protein, such mutations do not entirely prevent copper binding of the protein *per se*.

## 9.7. Summary

In the current chapter, the effects of copper binding within the E1 and A $\beta$  domains of APP on the proteolysis of the protein in SH-SY5Y cells and the viability of these cells in the presence of copper have been investigated. The results show that the introduction of histidine to alanine mutations within either the E1 or A $\beta$  domains of both the 695 and 770 amino acid APP isoforms had no effect on the expression of, or  $\alpha$ -secretase-mediated proteolysis of the protein (*Figs. 9.2A, 9.3A, 9.6A and 9.7A*). However, such mutations did significantly reduce the generation of sAPP $\beta$  from both APP isoforms with the introduction of a H610A (APP<sub>695</sub>) or H685A (APP<sub>770</sub>) mutation having a particularly dramatic effect in this respect (*Fig. 9.3B and 9.7B*).

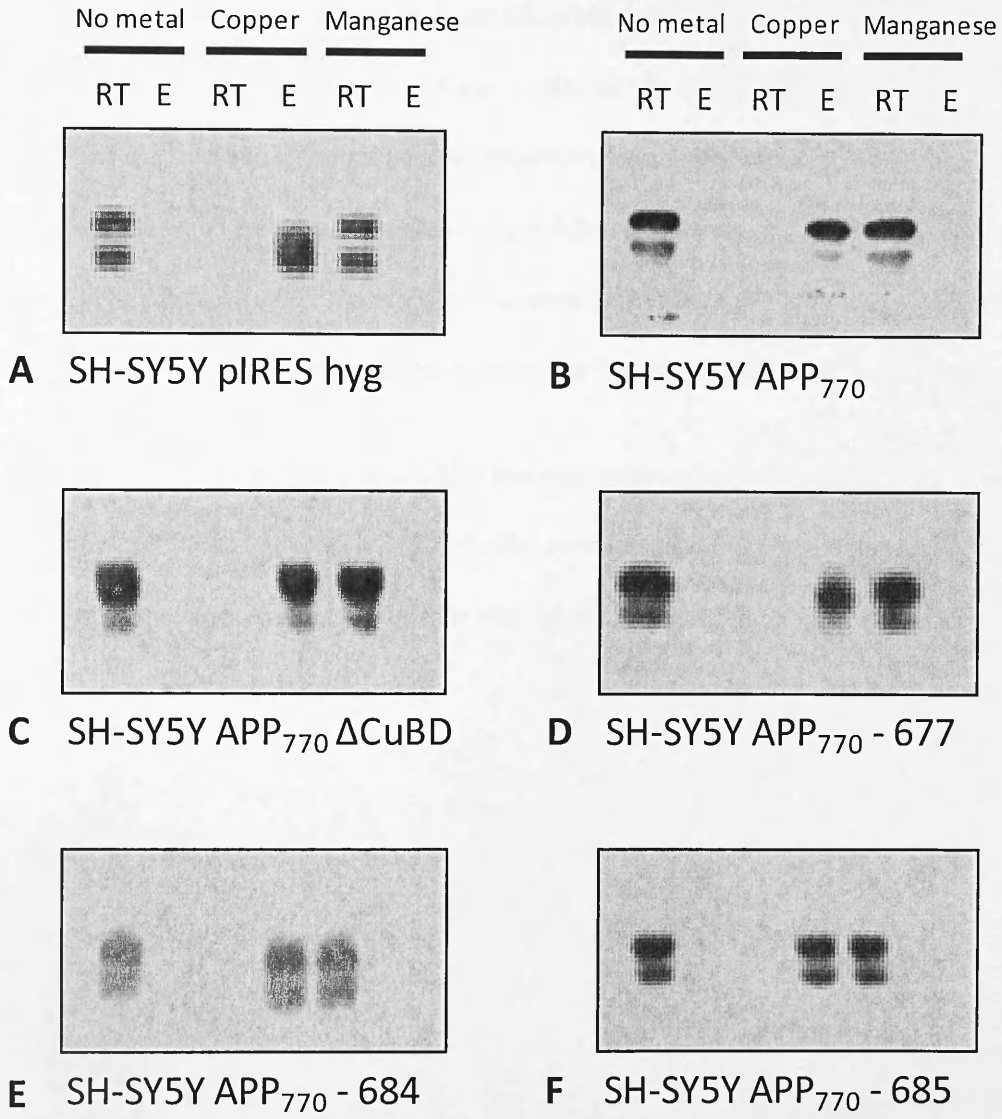


**Figure 9.9. Binding of APP constructs to metal affinity spin columns.** Serum free medium was conditioned for 48 hours on SH-SY5Y cells expressing the indicated APP constructs (A-F). The medium was then concentrated and passed through metal affinity spin columns in the absence of metals, presence of copper or manganese (Materials and Methods). Column run through (RT) and eluate (E) were made up to equal volumes and immunoblotted with the 22C11 antibody in order to detect soluble APP.

Both APP<sub>695</sub> and APP<sub>770</sub> were capable of enhancing the viability of SH-SY5Y cells in the presence of copper and mutation of the E1 CuBD in both isoforms ablated this function (*Fig. 9.4*). In the case of APP<sub>695</sub>, the introduction of histidine to alanine mutations at positions 602, 609 or 610 largely had no effect on the ability of the wild-type protein to enhance viability in the presence of copper. The situation was similar for the APP<sub>770</sub> isoform with mutations at positions 677 and 685 largely having no effect on the ability of the wild-type protein to enhance cell viability in the presence of copper (*Fig. 9.8*). However, the H684A mutation in APP<sub>770</sub> (analogous to H609A in APP<sub>695</sub>) did seem to prevent the ability of the wild-type protein in this respect (thereby differing from the situation with the APP<sub>695</sub> isoform).

Finally, in the current study, APP was able to bind copper regardless of any of the histidine mutations introduced (*Fig. 9.9*). This indicates that the protein was still capable of binding copper to some degree, despite the ablation of particular copper binding residues.

# 10. Discussion

## 10.1. Introduction

The current study has examined the ability of the amyloid precursor protein to promote cell viability within the environment of the brain in two diseases associated with ageing; Alzheimer's disease and prostate cancer. The results are discussed in the context of individual results chapters below.

## 10.2. Characterisation of constitutive wild-type APP expression and proteolysis in cell lines

An analysis of APP expression, its proteolysis and its secretases was performed in various PCa cell lines and in SH-SY5Y neuroblastoma cells. This analysis was carried out in preparation for subsequent use of these cell lines in studies relating to PCa and AD.

Of the PCa cell lines, endogenous APP expression and shedding were lowest in LNCaP cells (*Figs. 3.1A and 3.2*). This observation is interesting given that LNCaPs are an early stage, hormone sensitive, cell line in which APP has previously been shown to be a key androgen receptor target gene and to promote cell proliferation and tumorigenesis (233). The higher APP expression and proteolysis in Du145 and PC3 cells, which are derived from later stage, more aggressive, hormone-insensitive metastases, might add further weight to the argument that APP expression in PCa cells is directly linked to their proliferative capacity. In fact, so high were the levels of APP expression in PC3 and Du145 cells that they were comparable to levels of the over-expressed protein in SH-SY5Y cells (*Fig. 3.1A*). This raises the possibility that, when cells become hormone-insensitive (for example, in the Du145 cells) APP expression gets 'stuck on' regardless of androgen levels and the cells proliferate more aggressively as a consequence.

Levels of sAPP $\alpha$  generated by the various cell lines generally reflected the expression levels of the various APP isoforms (*Fig. 3.2*). However, interestingly, the over-expression of wild-type APP<sub>695</sub> in SH-SY5Y cells resulted in decreased endogenous APP<sub>751/770</sub> shedding in comparison to the mock-transfected controls (*Fig. 3.2A and B*). This could suggest that in SH-SY5Y cells, the secretases regulating APP  $\alpha$ -shedding become saturated when APP<sub>695</sub> is over-expressed, resulting in a decline in endogenous APP shedding. This implies that the over-expressed protein may be competing with endogenous APP for shedding. Interestingly, a similar effect was not observed when APP<sub>695</sub> was over-expressed in Du145 cells (*Fig. 3.2*), a cell line which expressed more endogenous ADAM10 than SH-SY5Y cells (*Fig. 3.7*). However, the ratio of endogenous to over-expressed APP in Du145 cells was also considerably higher than in the SH-SY5Y cells, perhaps creating less competition for this  $\alpha$ -secretase activity.

In terms of the sAPP $\beta$  levels secreted from the PCa cell lines, LNCaP cells produced slightly more than the Du145 and PC-3 cells (*Fig. 3.3*), despite holoprotein expression and sAPP $\alpha$  generation being lowest in the former cell line. This observation raises the possibility that amyloidogenic processing of APP is perhaps associated particularly with the early stages of PCa but decreases as cells become more malignant. This theory would coincide with the data generated in regards to the involvement of sAPP $\alpha$  (and not sAPP $\beta$ ) in cell proliferation (111, 123, 125).

When APP<sub>695</sub> was over-expressed in both the Du145 and SH-SY5Y cell lines, there was an increase in the sAPP<sub>695</sub> $\beta$  production (*Fig. 3.3*). Such an increase was to be expected following the increase in soluble APP substrate presented to BACE1. Interestingly, in the Du145 cells, endogenous sAPP<sub>751/770</sub> $\beta$  production was also elevated (*Fig. 3.3*). APP expression levels have previously been shown to regulate the expression of BACE1 (100), making it possible that over-expressing APP in the Du145 cells in the current study may have increased

BACE1 expression and, consequently, increased the generation of sAPP $\beta$  from endogenous APP.

### 10.3. The effects of copper on endogenous APP expression and proteolysis in prostate cancer epithelial cells

In order to examine the effects of copper on APP expression and proteolysis in PCa cells, LNCaP, Du145 and PC-3 cells were treated with a concentration range of the metal. Copper was not toxic to any of the cell types when used at concentrations of 50  $\mu$ M or lower (Figs. 4.1, 4.4 and 4.7). At metal concentrations of 200  $\mu$ M or higher, all three cell lines exhibited dramatically reduced viability. This was likely due to toxicity rather than decreased proliferation given the short time course employed in these experiments. The toxic effects of copper complexes on cells have previously been attributed to the inhibition of proteasome function and promotion of apoptosis (327). Furthermore, the oxidative capacity of copper may result in oxidative damage to cells (328).

In contrast to LNCaP and PC-3 cells (where copper, at sub-toxic concentrations, had no effect), APP expression was enhanced in Du145 cells following metal treatment (Fig. 4.8). The mechanism behind this increase in APP expression could be via copper binding to a copper responsive regulatory element in the APP promoter (163). However, the oxidative properties of copper alone may enhance APP expression, as this effect has been shown to be ablated using antioxidants (160). Whatever the molecular mechanisms involved, the fact that serum and tissue copper concentrations are elevated in prostate cancer patients (262) raises the possibility that these increased metal concentrations may serve to promote APP expression in these patients. The fact that copper promoted APP expression only in Du145 cells is particularly interesting given the fact that these cells are of a brain metastatic origin (279) and this organ is second only to the liver in terms of copper concentration. Thus, the

copper-induced expression of APP in Du145 cells may play a role in their ability to survive in an organ containing exceptionally high copper concentrations.

#### 10.4. The effect of full-length APP construct expression on Du145 cell viability in the presence of copper

As copper had been shown to promote endogenous APP expression in Du145 cells, it was hypothesized that the protein might be able to promote Du145 cell viability in the presence of the metal. Thus, APP was over-expressed in cells in the form of APP<sub>695</sub>. The migration differences between this isoform and the endogenous protein/proteolytic fragments (APP<sub>751/770</sub>) in Du145 cells made it easier to quantify over-expression of the employed constructs. Although previous sections in the current study had failed to detect any endogenous APP<sub>695</sub> protein in Du145 cells, the RT-PCR data in the current section (*Fig. 5.1*) clearly show that low levels of the RNA transcript of this isoform were present. The fact that the larger KPI-containing isoforms of APP predominated in Du145 cells was not surprising given that whilst APP<sub>695</sub> is the major isoform in neurons (324), the KPI-containing isoforms predominate in other tissues, such as the liver, skeletal muscle, heart and lung (329). These results correlate with the observed APP expression pattern in Du145 cells, which originate in prostate tissue (279).

When APP<sub>695</sub>, <sub>751</sub> or <sub>770</sub> were over-expressed in Du145 cells, it was clear that the former isoform promoted cell viability in the presence of 150 and 200  $\mu$ M copper, whereas the other isoforms were less effective in this respect (*Fig. 5.5*). Previous experiments have demonstrated that Tg2576 mouse primary cortical neurons contain significantly less copper than wild-type mice, whereas APP knockout primary cortical neurons contained significantly more copper than cells from control mice (163). The Tg2576 mice over-express APP<sub>695</sub> (330), rendering this isoform responsible for the observed copper efflux, which could be the

mechanism responsible for the elevated viability of APP<sub>695</sub> over-expressing Du145 cells in the current study.

It might also be possible that the APP<sub>695</sub> over-expressed in Du145 cells in the current study, promotes the uptake and safe sequestration of copper, thereby reducing toxicity of the metal. This theory is supported by the fact that HEK293 cells over-expressing APP have been shown to exhibit enhanced copper uptake and increased levels of metallothionein-I/II expression; a protein which assists cells in the management of intracellular copper ions (175).

Subsequent experiments using siRNA knockdown of endogenous APP in Du145 cells revealed a slight reduction in viability in the presence of copper following APP knockdown (*Fig. 5.7*). However, this change was not in the same order of magnitude as that observed when APP was over-expressed in the same cell line. This discrepancy may be explained by the fact that in the over-expression studies the cells were exposed to copper for 7 days as opposed to only 48 h (due to the transient nature of the APP knockdown). There also exists the possibility that APP may be partially redundant in relation to its ability to enhance cell viability in the presence of copper. Indeed previous studies have shown that a double APP/APLP2 knockout, as opposed to a single APP knockout, was more effective at increasing copper levels in both cortical neurons (331) and in the cerebral cortex and liver of knockout mice (332).

## **10.5. The APP cytosolic domain is a prerequisite for enhanced Du145 cell viability in the presence of copper**

Next, various cytosolic domain APP mutant constructs were over-expressed in Du145 cells, in order to examine the role of this domain in the ability of the molecule to enhance

cell viability in the presence of copper. All of the constructs were successfully expressed, albeit the APP<sub>695</sub>ΔICD construct at a seemingly lower level than the others (*Fig. 6.2*). Notably, the sAPP $\alpha$  produced by the APP<sub>695</sub>ΔICD over-expressing cells was higher than that generated by the wild-type APP<sub>695</sub> over-expressing cells, despite the lower apparent expression level of the former construct (*Fig. 6.3*). This might be the result of increased retention of APP at the cell surface, as the cytosolic domain is thought to be required for endocytosis (53). As  $\alpha$ -secretase cleavage primarily takes place at the cell surface (333), this location is likely to enhance sAPP $\alpha$  generation. The enhanced  $\alpha$ -shedding of the APP<sub>695</sub>ΔICD construct from the cell surface might also explain the seemingly lower levels of this construct detected in cell lysates.

As observed earlier, wild-type APP<sub>695</sub> was able to enhance the viability of Du145 cells in the presence of copper. However, the removal of the cytosolic domain or mutation of individual tyrosine residues within this domain reduced the action of APP in this respect (*Fig. 6.4*). There are several possible explanations for this observation. First, the APP intracellular domain is involved in interactions with G-protein-coupled receptors regulating cellular apoptosis, therefore the deletion/mutation of this region of APP might impede apoptosis (105). The APP intracellular domain also interacts with a wide range of adaptor proteins (108), primarily through the YENPTY motif, the tyrosine residues of which were mutated in the current study. Interactions with these adaptor proteins have been associated with cell growth, proliferation, homeostasis, responses to stress, apoptosis, cell fate determination and in regulation of the cell cycle (*Table 1.1*). Alterations in any of these pathways as a result of impaired APP cytosolic domain function, as in the case of the mutant constructs, might explain the observed decrease in cell viability in the presence of copper relative to wild-type APP-transfected cells. Furthermore, the ability of APP to generate AICD would clearly be prevented in the APP<sub>695</sub>ΔICD construct, thereby preventing the regulation of gene expression by this fragment (121). The genes regulated by the AICD include those involved in cell cycle

regulation and proliferation (discussed in section 1.5.4.), which may explain the impact of this mutation on cell growth. The YENPTY motif in the APP cytosolic domain may be responsible for trafficking the AICD fragment through the cell (93), and for its interaction with adapter proteins to form the complex able to translocate to the nucleus and regulate gene expression (142). These latter points might explain the impact of the tyrosine mutations in the current study on the cell viability results.

In the context of gene expression regulation by the APP cytosolic domain (or the AICD), it is notable that in the current study, the over-expression of wild-type APP<sub>695</sub> in Du145 cells repressed ERK1 expression; an effect that was isoform-specific (*Figs. 6.8 and 6.9*). In contrast, all of the APP cytosolic domain mutants studied failed to elicit a similar effect, raising the possibility of involvement of the YENPTY region of APP in the regulation of ERK1 expression. Although a direct interaction between APP and ERK1 has not been previously demonstrated, soluble APP can activate the ERK pathway (97, 126, 127) and A $\beta$  has been associated with neuroprotection through ERK1 signalling (146). Binding of the SH2 and PTB containing adaptor proteins to the APP intracellular domain is also associated with the ERK signalling pathway (109). The APP<sub>695</sub> induced reduction in ERK1 expression may enable Du145 cells to remain viable in the presence of exogenous copper through altered regulation of cell cycle progression, cell survival, metabolism, proliferation and transcription by the ERK1 signalling pathway (334).

Also of interest in relation to the cytosolic domain of APP, is the observation that wild-type APP appeared to dissociate caveolin-1 from lipid rafts whereas the APP<sub>695</sub> $\Delta$ AICD construct actually appeared to enhance caveolin-1 association with rafts (*Fig. 6.7*). One possible explanation for these contrasting observations is that the APP ectodomain and cytosolic domain have opposing roles in relation to caveolin-1 association with rafts. The ectodomain might promote caveolin-1 raft association, whereas the intracellular domain

might stimulate the dissociation of the protein from rafts, possibly over-riding the former effect of the ectodomain.

## 10.6. The APP ectodomain and enhanced Du145 cell viability in the presence of copper

In this section of the study, the role of the N-terminal copper binding domain of APP in enhancing Du145 cell viability was investigated. When a copper binding APP mutant, APP<sub>695</sub>ΔCuBD, was over-expressed in these cells, the expression and  $\alpha$ -secretase-mediated processing of the protein were similar to that of wild-type APP<sub>695</sub> (Fig. 7.2 and 7.3A). However, the generation of sAPP $\beta$  from APP<sub>695</sub>ΔCuBD was negligible, being the same as that generated by mock-transfected Du145 cells (Fig. 6.3B). This suggests that copper binding in the E1 domain of APP is essential for the production of sAPP $\beta$ . This observation is at odds with previous studies which demonstrated that the addition of copper to cell culture medium reduced cellular A $\beta$  production and, therefore, presumably, sAPP $\beta$  generation (166, 168). Similarly, studies using APP over-expressing mouse models have shown that copper reduces CSF A $\beta$  and A $\beta$  plaque burden (170, 171). However, the exact mechanism of A $\beta$  reduction was not demonstrated in these studies, raising the possibility that enhanced A $\beta$  clearance, as opposed to reduced generation, could have been responsible for the results observed.

Spoerri *et al.* (165) demonstrated that sAPP $\beta$  production was reduced when APP histidine residues 149 and 151 were mutated to asparagines. However, these mutations also resulted in decreased sAPP $\alpha$  generation; something that was not observed in the current study. Moreover, it seems the case that the replacement of histidine residues with asparagines (as opposed to alanines, as in this study) resulted in APP folding and trafficking abnormalities. The reduced generation of both sAPP $\beta$  and sAPP $\alpha$  observed by Spoerri *et al.*

was therefore more likely due to decreased trafficking of APP to the cell surface, which would subsequently reduce endocytosis and access to secretases.

Baumkötter *et al.* (134) demonstrated a reduction in A $\beta$  production with prevention of copper binding at the N-terminal APP CuBD, and this was associated with the prevention of copper/CuBD dependent dimerization. This could therefore be a mechanism behind the observed reduction of sAPP $\beta$  in this study.

In the cell viability studies presented, the mutation of the APP E1 copper binding domain ablated the ability of wild-type APP<sub>695</sub> to enhance Du145 cell viability in the presence of copper (*Fig. 7.4*). This might well indicate that copper binding within this domain is a prerequisite for promoting cell viability. However, the possibility that conformational changes in the APP molecule unrelated to copper binding were induced by the histidine to alanine mutations cannot be entirely excluded. However, this is extremely unlikely given the fact that the maturation and trafficking of APP were unaffected by these mutations (based on the glycosylation banding patterns of the protein, and on the fact that the  $\alpha$ -secretase-mediated shedding of the APP<sub>695</sub> $\Delta$ CuBD construct was similar to that of its wild-type counterpart, meaning that trafficking to the cell surface must not have been affected).

The mechanism by which copper binding to the E1 domain of APP might promote cell viability is unclear. However, it has previously been demonstrated that the E1 copper binding domain sequence is highly specific for Cu(II) and that the geometry of the CuBD is highly unfavourable in relation to Cu(I) binding (335, 336). These observations support the possibility that APP may preferentially transfer redox active Cu(II) to other proteins, facilitating its sequestration and preventing the generation of damaging ROS. Furthermore, a peptide based on the APP E1 CuBD has been shown to promote copper efflux from yeast cells (156); an effect which was ablated following the mutation of histidine residues 147, 149

and 151 to alanines. Similar observations have also been demonstrated in mice. Mice exhibited reduced neurotoxicity when an infused CuBD peptide was administered alongside copper (172); an effect which was dependent on the Cys144 residue responsible for the reduction of Cu(II) to Cu(I). A similar transfer of redox active Cu(II) to other proteins, an APP-mediated efflux of Cu from cells and/or a potential copper detoxification strategy exhibited by APP may have been responsible for the observed enhanced viability of Du145 cells in the presence of the metal.

In the current study, efforts were also made to determine whether soluble APP could enhance Du145 cell viability in the presence of copper in the same way as its full-length counterpart. In this respect, a truncated construct analogous to  $\alpha$ -secretase-cleaved APP<sub>770</sub> was stably transfected into Du145 cells. However, despite the construct being validated in SH-SY5Y cells, the resultant protein was aberrantly expressed and/or processed in Du145 cells (*Fig. 7.5*). The key transfection product in Du145 cells consisted of an approximately 25 kDa fragment arising from the N-terminus of APP, as confirmed by immunoblots using the anti-FLAG and 22C11 antibodies (*Fig. 7.5 and 7.6*). It would seem that this fragment was not generated through the proteolysis of the mature, fully glycosylated sAPP770 $\alpha$  protein, as Du145 cell lysates were incapable of cleaving the latter fragment when secreted into the conditioned medium of SH-SY5Y transfectants (*Fig. 7.7*). In this respect, cleavage of the construct in Du145 cells is likely to take place prior to secretion, possibly as a consequence of the lack of membrane anchorage. This raises the possibility that the small amounts of the endogenous APP 25 kDa fragment observed by other groups (337, 338) result from a minor pool of immature APP cleaved from the membrane in the endoplasmic reticulum (as opposed to the major pool which reaches the cell surface uncleaved).

As the sAPP $\alpha$  construct did not over-express as expected in Du145 cells, the effect of inhibiting endogenous sAPP $\alpha$  generation on cell viability in the presence of copper was

examined instead. As such, cells were incubated in the absence or presence of the ADAM inhibitor, G1254023X whilst treating with copper. However, sAPP $\alpha$  generation was only reduced by approximately one quarter in the inhibitor-treated cells (*Fig. 7.8*) making it difficult to make any definitive conclusions in relation to the observed small changes observed in cell viability (*Fig. 7.9*). Similar experiments using  $\beta$ -secretase inhibitor IV reduced the generation of sAPP $\beta$  by  $85.9 \pm 7.35\%$  (*Fig. 7.10*), but failed to change cell viability in the presence of copper (*Fig. 7.11*). It therefore seems apparent that membrane anchorage of the APP molecule is required in order for the protein to enhance cell viability in the presence of copper. These data are in agreement with earlier results in the current study indicating that the cytosolic domain of APP is required in this respect. However, these results seem to conflict with the studies of other groups which have shown that fragments of the sAPP ectodomain with an intact CuBD protect cells from copper insult (172, 175). This conflicting data in regards to the ability of soluble forms of APP to protect against copper-mediated insult is likely both cell-type and experimental condition- type specific.

## 10.7. APP-induced morphological changes in Du145 cells

The over-expression of APP<sub>695</sub> in Du145 cells led to a change in morphology (*Fig.8.1*), with the cells appearing to have long neuron-like extensions. Such morphological appearance is similar to that seen following neuroendocrine differentiation (NED) (*Fig. 10.1*) (339). NED occurs in more than 50% of malignant prostatic tumours (340), and has been associated with a poorer prognosis in non-organ confined prostate cancer (301). NED is also associated with the increased expression of neuron-specific enolase (NSE) (339). However, in the current study, NSE expression was decreased rather than increased following APP<sub>695</sub> over-expression in Du145 cells (*Fig.8.2*). This would indicate that the morphological changes observed following APP transfection were not linked to NSE.

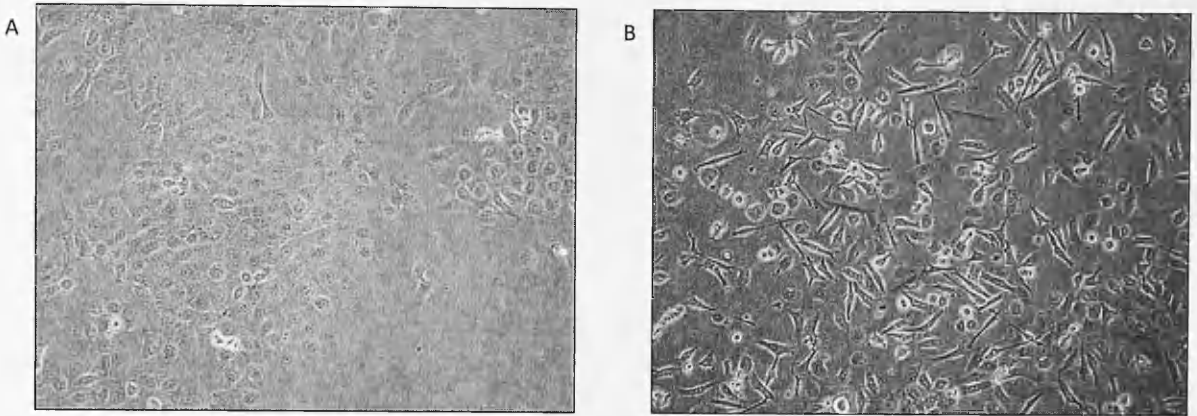


**Figure 10.1. NED in Du145 cells.** A. Normal Du145 cells. B. NED in Du145 cells induced by the addition of 5ng/ml EGF. Image taken and adapted from Humez *et al.* 2006 (339).

Another phenomenon which could potentially explain the morphological changes linked to APP<sub>695</sub> in the current study, is that of epithelial-to-mesenchymal transition (EMT). EMT brings about an elevated population of mesenchymal cells which lack intercellular junctions and therefore exhibit greater mobility and invasion, resulting in a poorer prognosis in cancer (305, 306). EMT is associated with the decreased expression of the cell adhesion molecule, E-cadherin, and conversely an increased expression of vimentin (307). Just such changes in expression were observed in the current study following APP<sub>695</sub> over-expression in Du145 cells (*Fig.8.3*), suggesting that the protein enhances EMT and might well, therefore, lead to a poorer prognosis in PCa. A causal relationship between APP and EMT has not previously been identified. However, it has been shown that human proximal tubular cells undergo suspected EMT, concomitant with a two-fold increase in APP gene expression following cyclosporine A treatment (341). Furthermore, the nuclear translocation of the AICD/binding partner complex can regulate genes such as GSK3 $\beta$  and p53 which have, in turn, been implicated in the regulatory network controlling EMT (342).

Further results in this study showed that both an intact APP cytosolic domain and an E1 CuBD were required in order to induce EMT-like morphological changes; in addition, the effect was specific to the APP<sub>695</sub> isoform (*Figs. 8.4, 8.5 and 8.6*).

## 10.8. The role of copper binding in APP proteolysis and the viability of SH-SY5Y cells

In order to examine the role of APP copper binding and cell viability in relation to AD, several APP constructs were stably over-expressed in SH-SY5Y cells. The E1 CuBD deficient construct, APP $\Delta$ CuBD, has been described previously. However, additional constructs with histidine to alanine mutations within the A $\beta$  domain of the APP molecule were also expressed. These latter mutants were generated following previous evidence that copper binds to the A $\beta$  peptide via these residues (343, 344); it is not known whether the same residues participate in copper co-ordination in the full-length APP molecule.

All of these APP constructs (both the <sub>695</sub> and <sub>770</sub> mutants) expressed at comparable levels in cell lysates and gave rise to the same levels of shed sAPP $\alpha$  (*Figs. 9.2, 9.3, 9.6 and 9.7*). However, lower levels of sAPP $\beta$  were produced by the mutated constructs, particularly the APP $\Delta$ CuBD and APP<sub>695-610</sub>/APP<sub>770-685</sub> constructs (*Fig. 9.3, 9.7*). A reduction in sAPP $\beta$  generation as a consequence of histidine to alanine mutations in the E1 CuBD of APP was also observed earlier in the current study in Du145 cells (discussed in section **10.5**). Notably, the reduction in Du145 cells was more dramatic than that observed in SH-SY5Y cells. The observed reductions in SH-SY5Y cells in relation to the APP<sub>695-610</sub>/APP<sub>770-685</sub> construct indicate the particular importance of copper coordination at His610/685 in  $\beta$ -cleavage of APP. Previous studies have demonstrated that elevated copper concentrations can result in reduced A $\beta$  levels in SH-SY5Y cells (161) and *in vivo* (171). There is therefore a possibility that if the mutated APP histidine residues in this study prevent the relocation of copper, the

resultant elevated local copper concentration may replicate this effect. Examination of local copper levels would enable the testing of this hypothesis.

The molecular mechanisms behind the decreased generation of sAPP $\beta$  from the various copper binding mutants are unclear. Certainly, the decreased sAPP $\beta$  generation from APP<sub>695-610</sub>/APP<sub>770-685</sub> is not likely due to BACE1 being blocked from accessing APP by the amino acid substitution, as this residue is the furthest mutated residue from the  $\beta$ -cleavage site. However, it is possible that copper binding to APP and subsequent homodimerisation might be required for BACE1 cleavage of the protein (154, 345). As BACE1 has been shown to directly interact with copper via its cytoplasmic domain (169), it is also possible that one of the mechanisms employed by BACE1 in order to come into contact with APP, is via interacting with the copper ion bound to the His610/685 residue of the protein; thus when this interaction is prevented, perhaps the association between BACE1 and APP is reduced or weakened, consequently decreasing sAPP $\beta$  production. Further investigation into the conformation and functionality of this APP copper binding region as a component of the holoprotein and into the interactions between copper, the APP His610/685 residues and the APP secretases may provide an explanation for this effect.

The cell viability results generated using the APP<sub>695</sub> copper binding mutants suggest that, as in the Du145 studies (discussed in section 10.5); the APP<sub>695</sub> $\Delta$ CuBD mutant does not enhance the viability of the SH-SY5Y cells, whereas the over-expressed wild-type APP<sub>695</sub> construct does (Fig. 9.4). The single histidine mutations within the A $\beta$  region of the protein, however do not reduce this positive effect (Fig. 9.4). These results therefore suggest that only copper binding in the E1 CuBD of the protein is involved in promoting cell viability, an effect which has previously been discussed in section 10.5.

The cell viability results generated using the APP<sub>770</sub> copper binding mutants assigned another amino acid a role in APP's ability to enhance SH-SY5Y cell viability in the face of

exogenous copper stress. The APP<sub>770</sub> isoform indeed promoted cell viability, whereas the APP $\Delta$ CuBD and the APP<sub>770-684</sub> mutant constructs did not (*Fig. 9.8*). Firstly, this demonstrates that in SH-SY5Y cells, the beneficial role of APP on viability when presented with exogenous copper is not isoform specific. In the Du145 cell studies this effect was limited to the APP<sub>695</sub> isoform (*Fig. 5.5*), demonstrating the variable molecular mechanisms which emerge when using different model cell systems.

Secondly, as independent mutations within the N-terminal and A $\beta$  regions of APP prevent the ability of APP<sub>770</sub> to enhance the viability of SH-SY5Y cells following copper treatment, it suggests that these two regions of the protein may act together in order to coordinate copper and prevent the observed reduction in viability. Previous evidence suggests that a conformational change occurs following copper binding at both the E1 CuBD (292) and within the A $\beta$  peptide (346), which may also take place upon copper binding to the A $\beta$  region of the full length holoprotein. This structural change following binding to one of the domains may bring the copper ion into contact with the other domain, allowing the interaction to take place which results in the SH-SY5Y enhanced viability when treated with copper. These results identify a possible physiological function for APP in the maintenance of cell viability in the presence of high copper concentrations, which depends on its ability to bind copper at both the N-terminal CuBD and within the A $\beta$  domain of the protein.

APP has previously been demonstrated to bind copper at the N-terminal E1 CuBD, the E2 CuBD and via the secreted A $\beta$  peptide (157, 159, 293), giving sufficient evidence to expect that the soluble APP ectodomain collected from SH-SY5Y cell conditioned medium will bind copper. In order to demonstrate whether or not the copper binding constructs used lost their metal binding ability, metal chelate affinity chromatography was employed. None of the constructs (including wild-type APP<sub>770</sub>) were able to bind manganese in these columns.

In terms of copper, none of the constructs lost their ability to bind to the metal (*Fig. 9.9*), suggesting that APP-copper binding sites exhibit a degree of functional redundancy.

## 10.8. Future directions

Future research directions for this work would involve the further elucidation of the specific region of APP which potentially interacts with copper. Additional APP constructs, containing individual amino acid mutations within the E1 copper binding domain of APP, would be developed. These constructs would be examined using the same Du145 and SY-SY5Y cell systems as in this analysis. Furthermore, additional viability assays would be employed in order to determine whether APP promotes cell viability by protecting against cell toxicity, or by directly enhancing cell viability.

Once the exact region of APP which interacts with copper is identified, further investigation into the way in which this interaction between APP and copper promotes cell viability would be carried out. Copper chelation experiments, using the appropriate APP construct fragments, would determine whether the APP constructs which were ineffective at promoting cell viability had lost the ability to bind copper, or whether they had lost their ability to interact with copper in an alternative way. Additional *in vitro* experiments would also be used to examine the APP conformational changes which take place during its interaction with copper. This may provide an explanation as to why both the intracellular and extracellular domains of APP are required in order to promote cell viability during exposure to copper.

Subsequent progression of these experiments into mouse models would assist in determining whether APP promotes cellular viability in the face of copper *in vivo*. If indeed APP does enhance cell viability with elevated copper concentrations *in vivo*, this work could have a major impact on AD, and particularly PCa research.

If APP demonstrates the ability to protect PCa cells against the raised copper levels found in the tissues and serum of cancer patients, then APP could potentially be used as a biomarker for prognosis. In the even distant future, it may become viable to therapeutically target APP in order to reduce cancer cell viability, as part of a personally tailored cancer treatment program. In addition, this further insight into the molecular biology of APP will be invaluable when working towards the development of successful AD treatments.

## 10.9. Summary

In the current study, there seems to be a link between malignancy of PCa cell lines and APP expression, albeit the number of cell lines analysed was limited. There was also some evidence to suggest that APP processing via the non-amyloidogenic pathway may be favoured over the amyloidogenic pathway as the malignancy of cells increases. However, the results also suggest that, if particularly high levels of APP expression are evident, the  $\alpha$ -secretases may become saturated limiting further sAPP $\alpha$  production and, potentially forcing APP down the reciprocal amyloidogenic pathway.

The data presented in the current study also indicate that copper enhances the expression of endogenous APP in Du145 cells. This increased expression may potentially protect these brain metastatic cells from the high levels of metal encountered in this organ. This is supported by the fact that the over-expression of wild-type APP enhanced the viability of Du145 cells in the presence of copper. Furthermore, the over-expression of APP in the same cell line induced EMT-like changes thereby possibly promoting the metastatic potential of this PCa cell line.

In terms of the molecular prerequisites for the ability of APP to enhance Du145 cell viability in the presence of copper and to promote EMT, it is apparent that only the 695 amino acid isoform of the protein induces such changes. Furthermore, an intact E1 CuBD is

required for these abilities, suggesting that copper binding to the molecule plays a direct role in these functional capacities. Membrane anchorage and, in particular, an intact APP cytosolic domain are also required in these respects. More specifically still, it is apparent that specific tyrosine residues within the APP cytosolic domain are required for the protein to exert these effects. The role of the cytosolic domain in this context may well be linked to changes in ERK1 expression.

The ability of APP to promote cell viability in the presence of copper has also been investigated in the context of AD by employing the neuroblastoma cell line, SH-SY5Y. Here, both APP<sub>695</sub> and APP<sub>770</sub> enhance viability following copper treatment. This activity was, again, dependent on intact putative copper binding histidine residues in the E1 CuBD and A $\beta$  domain of the protein.

In conclusion, a possible physiological function for APP has been identified, which involves promoting cell survival in the presence of copper and the induction of EMT-like changes. The former function will, no doubt, be proved to have an important role in both PCa and AD pathogenesis. The latter function may well identify future therapeutic intervention sites for the treatment or prevention of metastatic PCa.

# References

1. Glenner GG, Wong CW. Alzheimers-Disease - Initial Report of the Purification and Characterization of a Novel Cerebrovascular Amyloid Protein. *Biochemical and Biophysical Research Communications*. 1984;120(3):885-90.
2. Takayama KI, Tsutsumi S, Suzuki T, Horie-Inoue K, Ikeda K, Kaneshiro K, et al. Amyloid Precursor Protein Is a Primary Androgen Target Gene That Promotes Prostate Cancer Growth. *Cancer Res*. 2009;69(1):137-42.
3. Hatzoglou V PG, Morris MJ, Curtis K, Zhang Z, Shi W, Huse J, Rosenblum M, Holodny AI, Young RJ. Brain Metastases from Prostate Cancer: An 11-Year Analysis in the MRI Era with Emphasis on Imaging Characteristics, Incidence, and Prognosis. *J Neuroimaging*. 2012.
4. Waldemar G, Burns AS. *Alzheimer's disease*. Oxford: Oxford University Press; 2009.
5. Blennow K, de Leon MJ, Zetterberg H. *Alzheimer's disease*. *Lancet*. 2006;368(9533):387-403.
6. Ferri CP, Prince M, Brayne C, Brodaty H, Fratiglioni L, Ganguli M, et al. Global prevalence of dementia: a Delphi consensus study. *Lancet*. 2005;366(9503):2112-7.
7. Society As. Financial cost of dementia. Available from: [www.alzheimers.org.uk](http://www.alzheimers.org.uk).
8. Society As. What is Alzheimer's disease. Available from: [www.alzheimers.org.uk](http://www.alzheimers.org.uk).
9. Davies L, Wolska B, Hilbich C, Multhaup G, Martins R, Simms G, et al. A4 amyloid protein deposition and the diagnosis of Alzheimers-disease - prevalence in aged brains determined by immunocytochemistry compared with conventional neuropathologic techniques. *Neurology*. 1988;38(11):1688-93.
10. Kawas C, Gray S, Brookmeyer R, Fozard J, Zonderman A. Age-specific incidence rates of Alzheimer's disease - The Baltimore Longitudinal Study of Aging. *Neurology*. 2000;54(11):2072-7.
11. Champion D, Dumanchin C, Hannequin D, Dubois B, Belliard S, Puel M, et al. Early-onset autosomal dominant Alzheimer disease: Prevalence, genetic heterogeneity, and mutation spectrum. *American Journal of Human Genetics*. 1999;65(3):664-70.
12. Corder EH, Saunders AM, Strittmatter WJ, Schmechel DE, Gaskell PC, Small GW, et al. Gene dose of apolipoprotein-E type-4 allele and the risk of Alzheimers-disease in late-onset families. *Science*. 1993;261(5123):921-3.
13. Farrer LA, Cupples LA, Haines J, Hyman B, Kukull W, Mayeux R, et al. Effects of age, gender and ethnicity on the association between APOE genotype and Alzheimer disease. *American Journal of Human Genetics*. 1997;61(4):234.
14. Wang DS, Dickson DW, Malter JS. beta-amyloid degradation and Alzheimer's disease. *J Biomed Biotechnol*. 2006.
15. Hsieh H, Boehm J, Sato C, Iwatsubo T, Tomita T, Sisodia S, et al. AMPAR removal underlies A beta-induced synaptic depression and dendritic spine loss. *Neuron*. 2006;52(5):831-43.
16. Chiang PK, Lam MA, Luo Y. The many faces of amyloid beta in Alzheimer's disease. *Current Molecular Medicine*. 2008;8(6):580-4.
17. Selkoe DJ. Cell biology of protein misfolding: The examples of Alzheimer's and Parkinson's diseases. *Nature Cell Biology*. 2004;6(11):1054-61.
18. Zatta P, Drago D, Bolognin S, Sensi SL. Alzheimer's disease, metal ions and metal homeostatic therapy. *Trends Pharmacol Sci*. 2009;30(7):346-55.
19. Blessed G, Tomlinso.Be, Roth M. Association between quantitative measures of dementia and of senile change in cerebral grey matter of elderly subjects. *British Journal of Psychiatry*. 1968;114(512):797-&.
20. Puglielli L. Aging of the brain, neurotrophin signaling, and Alzheimer's disease: Is IGF1-R the common culprit? *Neurobiology of Aging*. 2008;29(6):795-811.
21. Cowan CM, Chee F, Shepherd D, Mudher A. Disruption of neuronal function by soluble hyperphosphorylated tau in a Drosophila model of tauopathy. *Biochemical Society Transactions*. 2010;38:564-70.

22. Marcello E, Epis R, Di Luca M. Amyloid flirting with synaptic failure: Towards a comprehensive view of Alzheimer's disease pathogenesis. *European Journal of Pharmacology*. 2008;585(1):109-18.
23. Vanderstichele H, Bibl M, Engelborghs S, Le Bastard N, Lewczuk P, Molinuevo JL, et al. Standardization of preanalytical aspects of cerebrospinal fluid biomarker testing for Alzheimer's disease diagnosis: A consensus paper from the Alzheimer's Biomarkers Standardization Initiative. *Alzheimers & Dementia*. 2012;8(1):65-73.
24. Salloway S, Mintzer J, Weiner MF, Cummings JL. Disease-modifying therapies in Alzheimer's disease. *Alzheimers & Dementia*. 2008;4(2):65-79.
25. Etcheberrigaray R, Tan M, Dewachter I, Kuiperi C, Van der Auwera I, Wera S, et al. Therapeutic effects of PKC activators in Alzheimer's disease transgenic mice. *Proceedings of the National Academy of Sciences of the United States of America*. 2004;101(30):11141-6.
26. Pastorino L, Lu KP. Pathogenic mechanisms in Alzheimer's disease. *European Journal of Pharmacology*. 2006;545(1):29-38.
27. Adessi C, Frossard MJ, Boissard C, Fraga S, Bieler S, Ruckle T, et al. Pharmacological profiles of peptide drug candidates for the treatment of Alzheimer's disease. *J Biol Chem*. 2003;278(16):13905-11.
28. Gong CX, Grundke-Iqbal I, Iqbal K. Targeting Tau Protein in Alzheimer's Disease. *Drug Aging*. 2010;27(5):351-65.
29. Caccamo A, Oddo S, Tran LX, LaFerla FM. Lithium reduces tau phosphorylation but not A beta or working memory deficits in a transgenic model with both plaques and tangles. *American Journal of Pathology*. 2007;170(5):1669-75.
30. Sastre M, Klockgether T, Heneka MT. Contribution of inflammatory processes to Alzheimer's disease: molecular mechanisms. *International Journal of Developmental Neuroscience*. 2006;24(2-3):167-76.
31. UK CR. Prostate cancer incidence statistics. Available from: <http://www.cancerresearchuk.org/cancer-info/cancerstats/types/prostate/incidence/>.
32. Sakr WA, Grignon DJ, Haas GP, Heilbrun LK, Pontes JE, Crissman JD. Age and racial distribution of prostatic intraepithelial neoplasia. *European Urology*. 1996;30(2):138-44.
33. Underwood JCE, Cross SS. *General and systematic pathology*. 5th ed. Edinburgh: Churchill Livingstone; 2009.
34. Mason M, Moffat LEF. *Prostate cancer*. 2nd ed. Oxford: Oxford University Press; 2010.
35. Epstein JI, Carmichael M, Walsh PC. Adenocarcinoma of the prostate invading the seminal-vesicle - definition and relation of tumor volume, grade and margins of resection to prognosis. *Journal of Urology*. 1993;149(5):1040-5.
36. Salomon L, Anastasiadis AG, Johnson CW, McKiernan JM, Goluboff ET, Abbou CC, et al. Seminal vesicle involvement after radical prostatectomy: Predicting risk factors for progression. *Urology*. 2003;62(2):304-9.
37. Hall MC, Zagars GK, Troncoso P, Chung LWK, Pollack A, Voneschenbach AC, et al. Significance of tumor angiogenesis in clinically localized prostate carcinoma treated with external-beam radiotherapy. *Urology*. 1994;44(6):869-75.
38. Feldman BJ, Feldman D. The development of androgen-independent prostate cancer. *Nature Reviews Cancer*. 2001;1(1):34-45.
39. Yu H, Bharaj B, Vassilikos EJK, Giai M, Diamandis EP. Shorter CAG repeat length in the androgen receptor gene is associated with more aggressive forms of breast cancer. *Breast Cancer Research and Treatment*. 2000;59(2):153-61.
40. Buhmeida A, Pyrhonen S, Laato M, Collan Y. Prognostic factors in prostate cancer. *Diagnostic Pathology*. 2006;1.
41. Zagars GK. Prostate-specific antigen as a prognostic factor for prostate-cancer treated by external beam radiotherapy. *International Journal of Radiation Oncology Biology Physics*. 1992;23(1):47-53.

42. Daher R, Beaini M. Prostate-specific antigen and new related markers for prostate cancer. *Clinical Chemistry and Laboratory Medicine*. 1998;36(9):671-81.
43. Umbas R, Schalken JA, Aalders TW, Carter BS, Karthaus HFM, Schaafsma HE, et al. Expression of the cellular adhesion molecule e-cadherin is reduced or absent in high-grade prostate-cancer. *Cancer Res*. 1992;52(18):5104-9.
44. Shurbaji MS, Kalbfleisch JH, Thurmond TS. Immunohistochemical detection of p53 protein as a prognostic indicator in prostate-cancer. *Human Pathology*. 1995;26(1):106-9.
45. Jacobsen KT, Iverfeldt K. Amyloid precursor protein and its homologues: a family of proteolysis-dependent receptors. *Cellular and Molecular Life Sciences*. 2009;66(14):2299-318.
46. Yoshikai S. Correction. *Gene*. 1991;102(2):291-2.
47. Hynes TR, Randal M, Kennedy LA, Eigenbrot C, Kossiakoff AA. X-ray crystal-structure of the protease inhibitor domain of Alzheimers amyloid beta-protein precursor. *Biochemistry*. 1990;29(43):10018-22.
48. Kaden D, Munter LM, Reif B, Multhaup G. The amyloid precursor protein and its homologues: Structural and functional aspects of native and pathogenic oligomerization. *European Journal of Cell Biology*. 2012;91(4):234-9.
49. Reinhard C, Hebert SS, De Strooper B. The amyloid-beta precursor protein: integrating structure with biological function. *Embo Journal*. 2005;24(23):3996-4006.
50. Schettini G, Govoni S, Racchi M, Rodriguez G. Phosphorylation of APP-CTF-AICD domains and interaction with adaptor proteins: signal transduction and/or transcriptional role - relevance for Alzheimer pathology. *J Neurochem*. 2010;115(6):1299-308.
51. Cole SL, Vassar R. The Role of Amyloid Precursor Protein Processing by BACE1, the beta-Secretase, in Alzheimer Disease Pathophysiology. *J Biol Chem*. 2008;283(44):29621-8.
52. Tang BL. Neuronal protein trafficking associated with Alzheimer disease From APP and BACE1 to glutamate receptors. *Cell Adhes Migr*. 2009;3(1):118-28.
53. Perez RG, Soriano S, Hayes JD, Ostaszewski B, Xia WM, Selkoe DJ, et al. Mutagenesis identifies new signals for beta-amyloid precursor protein endocytosis, turnover, and the generation of secreted fragments, including A beta 42. *J Biol Chem*. 1999;274(27):18851-6.
54. Kandalepas PC, Vassar R. Identification and biology of ss-secretase. *J Neurochem*. 2012;120:55-61.
55. Cole SL, Vassar R. The Alzheimer's disease beta-secretase enzyme, BACE1. *Mol Neurodegener*. 2007;2.
56. Sathya M, Premkumar P, Karthick C, Moorthi P, Jayachandran KS, Anusuyadevi M. BACE1 in Alzheimer's disease. *Clin Chim Acta*. 2012;414:171-8.
57. St George-Hyslop P, Fraser PE. Assembly of the presenilin -/e-secretase complex. *J Neurochem*. 2012;120:84-8.
58. Thinakaran G, Koo EH. Amyloid Precursor Protein Trafficking, Processing, and Function. *J Biol Chem*. 2008;283(44):29615-9.
59. Takami M, Nagashima Y, Sano Y, Ishihara S, Morishima-Kawashima M, Funamoto S, et al. gamma-Secretase: Successive Tripeptide and Tetrapeptide Release from the Transmembrane Domain of beta-Carboxyl Terminal Fragment. *Journal of Neuroscience*. 2009;29(41):13042-52.
60. Zhao GJ, Mao GZ, Tan JX, Dong YZ, Cui MZ, Kim SH, et al. Identification of a new presenilin-dependent zeta-cleavage site within the transmembrane domain of amyloid precursor protein. *J Biol Chem*. 2004;279(49):50647-50.
61. Kaether C, Haass C, Steiner H. Assembly, trafficking and function of gamma-secretase. *Neurodegener Dis*. 2006;3(4-5):275-83.
62. Sisodia SS. Beta-Amyloid Precursor Protein Cleavage by a Membrane-Bound Protease. *Proceedings of the National Academy of Sciences of the United States of America*. 1992;89(13):6075-9.

63. Tousseyn T, Jorissen E, Reiss K, Hartmann D. (Make) stick and cut loose - Disintegrin metalloproteases in development and disease. *Birth Defects Research*. 2006;78(1):24-46.
64. Endres K, Anders A, Kojro E, Gilbert S, Fahrenholz F, Postina R. Tumor necrosis factor- $\alpha$  converting enzyme is processed by proprotein-convertases to its mature form which is degraded upon phorbol ester stimulation. *European Journal of Biochemistry*. 2003;270(11):2386-93.
65. Endres K, Fahrenholz F. Upregulation of the alpha-secretase ADAM10-risk or reason for hope? *Febs Journal*. 2010;277(7):1585-96.
66. Anders A, Gilbert S, Garten W, Postina R, Fahrenholz F. Regulation of the alpha-secretase ADAM10 by its prodomain and proprotein convertases. *Faseb Journal*. 2001;15(8):1837-+.
67. Karkkainen I, Rybnikova E, Peltö-Huikko M, Huovila APJ. Metalloprotease-disintegrin (ADAM) genes are widely and differentially expressed in the adult CNS. *Molecular and Cellular Neuroscience*. 2000;15(6):547-60.
68. Pruessmeyer J, Ludwig A. The good, the bad and the ugly substrates for ADAM10 and ADAM17 in brain pathology, inflammation and cancer. *Seminars in Cell & Developmental Biology*. 2009;20(2):164-74.
69. Lammich S, Kojro E, Postina R, Gilbert S, Pfeiffer R, Jasionowski M, et al. Constitutive and regulated alpha-secretase cleavage of Alzheimer's amyloid precursor protein by a disintegrin metalloprotease. *Proceedings of the National Academy of Sciences of the United States of America*. 1999;96(7):3922-7.
70. Marcinkiewicz M, Seidah NG. Coordinated expression of beta-amyloid precursor protein and the putative beta-secretase BACE and alpha-secretase ADAM10 in mouse and human brain. *J Neurochem*. 2000;75(5):2133-43.
71. Postina R, Schroeder A, Dewachter I, Bohl J, Schmitt U, Kojro E, et al. A disintegrin-metalloproteinase prevents amyloid plaque formation and hippocampal defects in an Alzheimer disease mouse model. *Journal of Clinical Investigation*. 2004;113(10):1456-64.
72. Vingtdeux V, Marambaud P. Identification and biology of a-secretase. *J Neurochem*. 2012;120:34-45.
73. Arribas J, Esselens C. ADAM17 as a Therapeutic Target in Multiple Diseases. *Current Pharmaceutical Design*. 2009;15(20):2319-35.
74. Buxbaum JD, Liu KN, Luo YX, Slack JL, Stocking KL, Peschon JJ, et al. Evidence that tumor necrosis factor alpha converting enzyme is involved in regulated alpha-secretase cleavage of the Alzheimer amyloid protein precursor. *J Biol Chem*. 1998;273(43):27765-7.
75. Hooper NM, Turner AJ. The search for alpha-secretase and its potential as a therapeutic approach to Alzheimer's disease. *Current Medicinal Chemistry*. 2002;9(11):1107-19.
76. Goddard DR, Bunning RAD, Woodroffe MN. Astrocyte and endothelial cell expression of ADAM 17 (TACE) in adult human CNS. *Glia*. 2001;34(4):267-71.
77. Jolly-Tornetta C, Wolf BA. Protein kinase C regulation of intracellular and cell surface amyloid precursor protein (APP) cleavage in CHO695 cells. *Biochemistry*. 2000;39(49):15282-90.
78. Parkin E, Harris B. A disintegrin and metalloproteinase (ADAM)-mediated ectodomain shedding of ADAM10. *J Neurochem*. 2009;108(6):1464-79.
79. Qi B, Newcomer RG, Sang QXA. ADAM19/Adamalysin 19 Structure, Function, and Role as a Putative Target in Tumors and Inflammatory Diseases. *Current Pharmaceutical Design*. 2009;15(20):2336-48.
80. Zou J, Zhu F, Liu JJ, Wang WY, Zhang RM, Garlisi CG, et al. Catalytic activity of human ADAM33. *J Biol Chem*. 2004;279(11):9818-30.
81. Naus S, Reipschlag S, Wildeboer D, Lichtenthaler SF, Mitterreiter S, Guan ZQ, et al. Identification of candidate substrates for ectodomain shedding by the metalloprotease-disintegrin ADAM8. *Biological Chemistry*. 2006;387(3):337-46.

82. Vetrivel KS, Thinakaran G. Membrane rafts in Alzheimer's disease beta-amyloid production. *Bba-Mol Cell Biol L*. 2010;1801(8):860-7.
83. Riddell DR, Christie G, Hussain I, Dingwall C. Compartmentalization of beta-secretase (Asp2) into low-buoyant density, noncaveolar lipid rafts. *Curr Biol*. 2001;11(16):1288-93.
84. Vetrivel KS, Cheng HP, Kim SH, Chen Y, Barnes NY, Parent AT, et al. Spatial segregation of gamma-secretase and substrates in distinct membrane domains. *J Biol Chem*. 2005;280(27):25892-900.
85. Parvathy S, Hussain I, Karran EH, Turner AJ, Hooper NM. Cleavage of Alzheimer's amyloid precursor protein by alpha-secretase occurs at the surface of neuronal cells. *Biochemistry*. 1999;38(30):9728-34.
86. Vetrivel KS, Cheng HP, Lin W, Sakurai T, Li T, Nukina N, et al. Association of gamma-secretase with lipid rafts in post-golgi and endosome membranes. *J Biol Chem*. 2004;279(43):44945-54.
87. Taylor DR, Hooper NM. Role of lipid rafts in the processing of the pathogenic prion and Alzheimer's amyloid-beta proteins. *Seminars in Cell & Developmental Biology*. 2007;18(5):638-48.
88. Hardy J. Apolipoprotein-E in the Genetics and Epidemiology of Alzheimers-Disease. *Am J Med Genet*. 1995;60(5):456-60.
89. Mahley RW, Innerarity TL, Rall SC, Weisgraber KH. Plasma-Lipoproteins - Apolipoprotein Structure and Function. *J Lipid Res*. 1984;25(12):1277-94.
90. Strittmatter WJ, Saunders AM, Schmechel D, Pericakvance M, Enghild J, Salvesen GS, et al. Apolipoprotein-E - High-Avidity Binding to Beta-Amyloid and Increased Frequency of Type-4 Allele in Late-Onset Familial Alzheimer-Disease. *Proceedings of the National Academy of Sciences of the United States of America*. 1993;90(5):1977-81.
91. Kawarabayashi T, Shoji M, Younkin LH, Lin WL, Dickson DW, Murakami T, et al. Dimeric amyloid beta protein rapidly accumulates in lipid rafts followed by apolipoprotein E and phosphorylated tau accumulation in the Tg2576 mouse model of Alzheimer's disease. *Journal of Neuroscience*. 2004;24(15):3801-9.
92. Herms J, Anliker B, Heber S, Ring S, Fuhrmann M, Kretzschmar H, et al. Cortical dysplasia resembling human type 2 lissencephaly in mice lacking all three APP family members. *Embo Journal*. 2004;23(20):4106-15.
93. Ring S, Weyer SW, Kilian SB, Waldron E, Pietrzik CU, Filippov MA, et al. The secreted beta-amyloid precursor protein ectodomain APPs alpha is sufficient to rescue the anatomical, behavioral, and electrophysiological abnormalities of APP-deficient mice. *Journal of Neuroscience*. 2007;27(29):7817-26.
94. Aydin D, Weyer SW, Muller UC. Functions of the APP gene family in the nervous system: insights from mouse models. *Exp Brain Res*. 2012;217(3-4):423-34.
95. Song P, Pimplikar SW. Knockdown of Amyloid Precursor Protein in Zebrafish Causes Defects in Motor Axon Outgrowth. *Plos One*. 2012;7(4).
96. Ho T, Vessey KA, Cappai R, Dinet V, Mascarelli F, Ciccotosto GD, et al. Amyloid Precursor Protein Is Required for Normal Function of the Rod and Cone Pathways in the Mouse Retina. *Plos One*. 2012;7(1).
97. Kogel D, Deller T, Behl C. Roles of amyloid precursor protein family members in neuroprotection, stress signaling and aging. *Exp Brain Res*. 2012;217(3-4):471-9.
98. Szpankowski L, Encalada SE, Goldstein LSB. Subpixel colocalization reveals amyloid precursor protein-dependent kinesin-1 and dynein association with axonal vesicles. *Proceedings of the National Academy of Sciences of the United States of America*. 2012;109(22):8582-7.
99. Jean-Noel Octave NP, Susana Ferao Santos, Natalia N. Nalivaeva, Anthony J. Turner. From synaptic spines to nuclear signaling: nuclear and synaptic actions of the amyloid precursor protein. *J Neurochem*. 2013;126(2):183-190.

100. Schroetter A, Pfeiffer K, El Magraoui F, Platta HW, Erdmann R, Meyer HE, et al. The Amyloid Precursor Protein (APP) Family Members are Key Players in S-adenosylmethionine Formation by MAT2A and Modify BACE1 and PSEN1 Gene Expression-Relevance for Alzheimer's Disease. *Mol Cell Proteomics*. 2012;11(11):1274-88.
101. Kusiak JW, Lee LL, Zhao BY. Expression of mutant amyloid precursor proteins decreases adhesion and delays differentiation of Hep-1 cells. *Brain Res*. 2001;896(1-2):146-52.
102. Storey E, Beyreuther K, Masters CL. Alzheimer's disease amyloid precursor protein on the surface of cortical neurons in primary culture co-localizes with adhesion patch components. *Brain Res*. 1996;735(2):217-31.
103. Ghiso J, Rostagno A, Gardella JE, Liem L, Gorevic PD, Frangione B. A 109-amino-acid C-terminal fragment of alzhemiers-disease amyloid precursor protein contains a sequence, -RHDS-, that promotes cell-adhesion. *Biochem J*. 1992;288:1053-9.
104. Puig KL, Swigost AJ, Zhou XD, Sens MA, Combs CK. Amyloid Precursor Protein Expression Modulates Intestine Immune Phenotype. *J Neuroimmune Pharm*. 2012;7(1):215-30.
105. Okamoto T, Takeda S, Murayama Y, Ogata E, Nishimoto I. Ligand-Dependent G-Protein Coupling Function of Amyloid Transmembrane Precursor. *J Biol Chem*. 1995;270(9):4205-8.
106. Brouillet E, Trembleau A, Galanaud D, Volovitch M, Bouillot C, Valenza C, et al. The amyloid precursor protein interacts with G(o) heterotrimeric protein within a cell compartment specialized in signal transduction. *Journal of Neuroscience*. 1999;19(5):1717-27.
107. Turner PR, O'Connor K, Tate WP, Abraham WC. Roles of amyloid precursor protein and its fragments in regulating neural activity, plasticity and memory. *Progress in Neurobiology*. 2003;70(1):1-32.
108. Russo C, Venezia V, Repetto E, Nizzari M, Violani E, Carlo P, et al. The amyloid precursor protein and its network of interacting proteins: physiological and pathological implications. *Brain Res Rev*. 2005;48(2):257-64.
109. Russo C, Dolcini V, Salis S, Venezia V, Zambrano N, Russo T, et al. Signal transduction through tyrosine-phosphorylated C-terminal fragments of amyloid precursor protein via an enhanced interaction with Shc/Grb2 adaptor proteins in reactive astrocytes of Alzheimer's disease brain. *J Biol Chem*. 2002;277(38):35282-8.
110. Leyssen M, Ayaz D, Hebert SS, Reeve S, De Strooper B, Hassan BA. Amyloid precursor protein promotes post-developmental neurite arborization in the Drosophila brain. *Embo Journal*. 2005;24(16):2944-55.
111. Chen YN, Tang BL. The amyloid precursor protein and postnatal neurogenesis/neuroregeneration. *Biochemical and Biophysical Research Communications*. 2006;341(1):1-5.
112. Muresan Z, Muresan V. c-Jun NH2-terminal kinase-interacting protein-3 facilitates phosphorylation and controls localization of amyloid-beta precursor protein. *Journal of Neuroscience*. 2005;25(15):3741-51.
113. Ando K, Oishi M, Takeda S, Iijima K, Isohara T, Nairn AC, et al. Role of phosphorylation of Alzheimer's amyloid precursor protein during neuronal differentiation. *Journal of Neuroscience*. 1999;19(11):4421-7.
114. Rogelj B, Mitchell JC, Miller CCJ, McLoughlin DM. The X11/Mint family of adaptor proteins. *Brain Res Rev*. 2006;52(2):305-15.
115. Pilecka I, Banach-Orlowska M, Miaczynska M. Nuclear functions of endocytic proteins. *European Journal of Cell Biology*. 2007;86(9):533-47.
116. Schlatterer SD, Acker CM, Davies P. c-Abl in Neurodegenerative Disease. *J Mol Neurosci*. 2011;45(3):445-52.

117. Wills MKB, Jones N. Teaching an old dogma new tricks: twenty years of Shc adaptor signalling. *Biochem J.* 2012;447:1-16.
118. Koushika SP. "JIP"ing along the axon: the complex roles of JIPs in axonal transport. *Bioessays.* 2008;30(1):10-4.
119. Gulino A, Di Marcotullio L, Screpanti I. The multiple functions of Numb. *Experimental Cell Research.* 2010;316(6):900-6.
120. Giubellino A, Burke TR, Bottaro DP. Grb2 signaling in cell motility and cancer. *Expert Opin Ther Tar.* 2008;12(8):1021-33.
121. Chow VW, Mattson MP, Wong PC, Gleichmann M. An Overview of APP Processing Enzymes and Products. *NeuroMolecular Medicine.* 2010;12(1, Sp. Iss. SI):1-12.
122. Taylor CJ, Ireland DR, Ballagh I, Bourne K, Marechal NM, Turner PR, et al. Endogenous secreted amyloid precursor protein-alpha regulates hippocampal NMDA receptor function, long-term potentiation and spatial memory. *Neurobiology of Disease.* 2008;31(2):250-60.
123. Saitoh T, Sundsmo M, Roch JM, Kimura N, Cole G, Schubert D, et al. Secreted form of amyloid-beta protein-precursor is involved in the growth-regulation of fibroblasts. *Cell.* 1989;58(4):615-22.
124. Ninomiya H, Roch JM, Sundsmo MP, Otero DAC, Saitoh T. Amino-acid- sequence RERMS represents the active domain of amyloid-beta/A4-protein precursor that promotes fibroblast growth. *Journal of Cell Biology.* 1993;121(4):879-86.
125. Caille I, Allinquant B, Dupont E, Bouillot C, Langer A, Muller U, et al. Soluble form of amyloid precursor protein regulates proliferation of progenitors in the adult subventricular zone. *Development.* 2004;131(9):2173-81.
126. Greenberg SM, Koo EH, Selkoe DJ, Qiu WQ, Kosik KS. Secreted Beta-Amyloid Precursor Protein Stimulates Mitogen-Activated Protein-Kinase and Enhances Tau-Phosphorylation. *Proceedings of the National Academy of Sciences of the United States of America.* 1994;91(15):7104-8.
127. Demars MP, Bartholomew A, Strakova Z, Lazarov O. Soluble amyloid precursor protein: a novel proliferation factor of adult progenitor cells of ectodermal and mesodermal origin. *Stem Cell Res Ther.* 2011;2:36.
128. Schmitz A, Tikkanen R, Kirfel G, Herzog V. The biological role of the Alzheimer amyloid precursor protein in epithelial cells. *Histochem Cell Biol.* 2002;117(2):171-80.
129. Corrigan F, Vink R, Blumbergs PC, Masters CL, Cappai R, van den Heuvel C. sAPPa rescues deficits in amyloid precursor protein knockout mice following focal traumatic brain injury. *J Neurochem.* 2012;122(1):208-20.
130. Tyan SH, Shih AYJ, Walsh JJ, Maruyama H, Sarsoza F, Ku L, et al. Amyloid precursor protein (APP) regulates synaptic structure and function. *Molecular and Cellular Neuroscience.* 2012;51(1-2):43-52.
131. Copanaki E, Chang S, Vlachos A, Tschape JA, Muller UC, Kogel D, et al. sAPP alpha antagonizes dendritic degeneration and neuron death triggered by proteasomal stress. *Molecular and Cellular Neuroscience.* 2010;44(4):386-93.
132. Furukawa K, Barger SW, Blalock EM, Mattson MP. Activation of K<sup>+</sup> channels and suppression of neuronal activity by secreted beta-amyloid-precursor protein. *Nature.* 1996;379(6560):74-8.
133. Gralle M, Botelho MG, Wouters FS. Neuroprotective Secreted Amyloid Precursor Protein Acts by Disrupting Amyloid Precursor Protein Dimers. *J Biol Chem.* 2009;284(22):15016-25.
134. Baumkötter F, Wagner K, Eggert S, Wild K, Kins S. Structural aspects and physiological consequences of APP/APLP trans-dimerization. *Exp Brain Res.* 2012;217(3-4):389-95.
135. Li HM, Wang BP, Wang ZL, Guo QX, Tabuchi K, Hammer RE, et al. Soluble amyloid precursor protein (APP) regulates transthyretin and Klotho gene expression without rescuing

the essential function of APP. *Proceedings of the National Academy of Sciences of the United States of America*. 2010;107(40):17362-7.

136. Schreiber G, Richardson SJ. The evolution of gene expression, structure and function of transthyretin. *Comp Biochem Phys B*. 1997;116(2):137-60.

137. Yamamoto M, Clark JD, Pastor JV, Gurnani P, Nandi A, Kurosu H, et al. Regulation of oxidative stress by the anti-aging hormone Klotho. *J Biol Chem*. 2005;280(45):38029-34.

138. Nikolaev A, McLaughlin T, O'Leary DDM, Tessier-Lavigne M. APP binds DR6 to trigger axon pruning and neuron death via distinct caspases. *Nature*. 2009;457(7232):981-U1.

139. Li HL, Roch JM, Sundsmo M, Otero D, Sisodia S, Thomas R, et al. Defective neurite extension is caused by a mutation in amyloid beta/A4 (A beta) protein precursor found in familial Alzheimer's disease. *J Neurobiol*. 1997;32(5):469-80.

140. Freude KK, Penjwini M, Davis JL, LaFerla FM, Blurton-Jones M. Soluble Amyloid Precursor Protein Induces Rapid Neural Differentiation of Human Embryonic Stem Cells. *J Biol Chem*. 2011;286(27):24264-74.

141. Van Gassen G, Annaert W. Amyloid, presenilins, and Alzheimer's disease. *Neuroscientist*. 2003;9(2):117-26.

142. Zheng H, Koo EH. Biology and pathophysiology of the amyloid precursor protein. *Mol Neurodegener*. 2011;6:27.

143. Muller T, Concannon CG, Ward MW, Walsh CM, Tirniceriu AL, Tribl F, et al. Modulation of gene expression and cytoskeletal dynamics by the amyloid precursor protein intracellular domain (AICD). *Molecular Biology of the Cell*. 2007;18(1):201-10.

144. Cao XW, Sudhof TC. A transcriptionally active complex of APP with Fe65 and histone acetyltransferase Tip60. *Science*. 2001;293(5527):115-20.

145. Morley JE, Farr SA. Hormesis and Amyloid-beta Protein: Physiology or Pathology? *J Alzheimers Dis*. 2012;29(3):487-92.

146. Parihar MS, Brewer GJ. Amyloid-beta as a Modulator of Synaptic Plasticity. *J Alzheimers Dis*. 2010;22(3):741-63.

147. Plant LD, Boyle JP, Smith IF, Peers C, Pearson HA. The production of amyloid beta peptide is a critical requirement for the viability of central neurons. *Journal of Neuroscience*. 2003;23(13):5531-5.

148. Whitson JS, Selkoe DJ, Cotman CW. Amyloid-Beta Protein Enhances the Survival of Hippocampal-Neurons *In Vitro*. *Science*. 1989;243(4897):1488-90.

149. Gruhn B, Hafer R, Voigt A, Wittig S, Fuchs D, Hermann J, et al. Prognostic significance of minimal residual disease after hematopoietic stem cell transplantation. *Bone Marrow Transpl*. 2002;29:S124-S.

150. Puzzo D, Privitera L, Leznik E, Fa M, Staniszewski A, Palmeri A, et al. Picomolar Amyloid-beta Positively Modulates Synaptic Plasticity and Memory in Hippocampus. *Journal of Neuroscience*. 2008;28(53):14537-45.

151. Ohm TG, Hamker U, Cedazo-Minguez A, Rockl W, Scharnagl H, Marz W, et al. Apolipoprotein E and beta A4-amyloid: signals and effects. *Biochem Soc Symp*. 2001(67):121-9.

152. Yao ZX, Papadopoulos V. Function of beta-amyloid in cholesterol transport: a lead to neurotoxicity. *Faseb Journal*. 2002;16(10):1677-9.

153. Linder MC, Goode CA. *Biochemistry of copper*. New York: Plenum Press; 1991. xiv, 525.

154. Kong GKW, Miles LA, Crespi GAN, Morton CJ, Ng HL, Barnham KJ, et al. Copper binding to the Alzheimer's disease amyloid precursor protein. *European Biophysics Journal with Biophysics Letters*. 2008;37(3):269-79.

155. Bayer TA, Multhaup G. Involvement of amyloid beta precursor protein (A beta PP) modulated copper homeostasis in Alzheimer's disease. *J Alzheimers Dis*. 2005;8(2):201-6.

156. Treiber C, Simons A, Strauss M, Hafner M, Cappai R, Bayer TA, et al. Clioquinol mediates copper uptake and counteracts copper efflux activities of the amyloid precursor protein of Alzheimer's disease. *J Biol Chem*. 2004;279(50):51958-64.
157. Barnham KJ, McKinstry WJ, Multhaup G, Galatis D, Morton CJ, Curtain CC, et al. Structure of the Alzheimer's disease amyloid precursor protein copper binding domain - A regulator of neuronal copper homeostasis. *J Biol Chem*. 2003;278(19):17401-7.
158. Wang Q, Werstuijk NH, Kramer JR, Bell RA. Effects of Cu Ions and Explicit Water Molecules on the Copper Binding Domain of Amyloid Precursor Protein APP(131-189): A Molecular Dynamics Study. *J Phys Chem B*. 2011;115(29):9224-35.
159. Dahms SO, Konnig I, Roeser D, Guhrs KH, Mayer MC, Kaden D, et al. Metal Binding Dictates Conformation and Function of the Amyloid Precursor Protein (APP) E2 Domain. *J Mol Biol*. 2012;416(3):438-52.
160. Lin RZ, Chen XH, Li WM, Han YF, Liu PQ, Pi RB. Exposure to metal ions regulates mRNA levels of APP and BACE1 in PC12 cells: Blockage by curcumin. *Neuroscience Letters*. 2008;440(3):344-7.
161. Cater MA, McInnes KT, Li QX, Volitakis I, La Fontaine S, Mercer JFB, et al. Intracellular copper deficiency increases amyloid-ss secretion by diverse mechanisms. *Biochem J*. 2008;412:141-52.
162. Armendariz AD, Gonzalez M, Loguinov AV, Vulpe CD. Gene expression profiling in chronic copper overload reveals upregulation of Prnp and App. *Physiological Genomics*. 2004;20(1):45-54.
163. Bellingham SA, Lahiri DK, Maloney B, La Fontaine S, Multhaup G, Camakaris J. Copper depletion down-regulates expression of the Alzheimer's disease amyloid-beta precursor protein gene. *J Biol Chem*. 2004;279(19):20378-86.
164. Mao XX, Ye JT, Zhou SY, Pi RB, Dou J, Zang LQ, et al. The effects of chronic copper exposure on the amyloid protein metabolism associated genes' expression in chronic cerebral hypoperfused rats. *Neuroscience Letters*. 2012;518(1):14-8.
165. Spoerri L, Vella LJ, Pham CLL, Barnham KJ, Cappai R. The Amyloid Precursor Protein Copper Binding Domain Histidine Residues 149 and 151 Mediate APP Stability and Metabolism. *J Biol Chem*. 2012;287(32):26840-53.
166. Hung YH, Robb EL, Volitakis I, Ho M, Evin G, Li QX, et al. Paradoxical Condensation of Copper with Elevated beta-Amyloid in Lipid Rafts under Cellular Copper Deficiency Conditions IMPLICATIONS FOR ALZHEIMER DISEASE. *J Biol Chem*. 2009;284(33):21899-907.
167. Hung YH, Bush AI, La Fontaine S. Links between copper and cholesterol in Alzheimer's disease. *Frontiers in Physiology*. 2013;4:111.
168. Borchardt T, Camakaris J, Cappai R, Masters CL, Beyreuther K, Multhaup G. Copper inhibits beta-amyloid production and stimulates the non-amyloidogenic pathway of amyloid-precursor-protein secretion. *Biochem J*. 1999;344:461-7.
169. Angeletti B, Waldron KJ, Freeman KB, Bawagan H, Hussain I, Miller CCJ, et al. BACE1 cytoplasmic domain interacts with the copper chaperone for superoxide dismutase-1 and binds copper. *J Biol Chem*. 2005;280(18):17930-7.
170. Bayer TA, Schafer S, Simons A, Kemmling A, Kamer T, Tepest R, et al. Dietary Cu stabilizes brain superoxide dismutase 1 activity and reduces amyloid A beta production in APP23 transgenic mice. *Proceedings of the National Academy of Sciences of the United States of America*. 2003;100(24):14187-92.
171. Phinney AL, Drisaldi B, Schmidt SD, Lugowski S, Coronado V, Liang Y, et al. In vivo reduction of amyloid-beta by a mutant copper transporter. *Proceedings of the National Academy of Sciences of the United States of America*. 2003;100(24):14193-8.
172. Cerpa WF, Barria MI, Chacon MA, Suazo M, Gonzalez M, Opazo C, et al. The N-terminal copper-binding domain of the amyloid precursor protein protects against Cu<sup>2+</sup> neurotoxicity in vivo. *Faseb Journal*. 2004;18(12):1701-3.

173. White AR, Multhaup G, Maher F, Bellingham S, Camakaris J, Zheng H, et al. The Alzheimer's disease amyloid precursor protein modulates copper-induced toxicity and oxidative stress in primary neuronal cultures. *Journal of Neuroscience*. 1999;19(21):9170-9.
174. Ruiz FH, Gonzalez Y, Bodini M, Opazo C, Inestrosa NC. Cysteine 144 is a key residue in the copper reduction by the beta-amyloid precursor protein. *J Neurochem*. 1999;73(3):1288-92.
175. Suazo M, Hodar C, Morgan C, Cerpa W, Cambiazo V, Inestrosa NC, et al. Overexpression of amyloid precursor protein increases copper content in HEK293 cells. *Biochemical and Biophysical Research Communications*. 2009;382(4):740-4.
176. Maynard CJ, Cappai R, Volitakis I, Cherny RA, White AR, Beyreuther K, et al. Overexpression of Alzheimer's disease amyloid-beta opposes the age-dependent elevations of brain copper and iron. *J Biol Chem*. 2002;277(47):44670-6.
177. Multhaup G, Ruppert T, Schlicksupp A, Hesse L, Behr D, Masters CL, et al. Reactive oxygen species and Alzheimer's disease. *Biochem Pharmacol*. 1997;54(5):533-9.
178. White AR, Multhaup G, Galatis D, McKinstry WJ, Parker MW, Pipkorn R, et al. Contrasting, species-dependent modulation of copper-mediated neurotoxicity by the Alzheimer's disease amyloid precursor protein. *Journal of Neuroscience*. 2002;22(2):365-76.
179. Multhaup G, Ruppert T, Schlicksupp A, Hesse L, Bill E, Pipkorn R, et al. Copper-binding amyloid precursor protein undergoes a site-specific fragmentation in the reduction of hydrogen peroxide. *Biochemistry*. 1998;37(20):7224-30.
180. Huang XD, Cuajungco MP, Atwood CS, Hartshorn MA, Tyndall JDA, Hanson GR, et al. Cu(II) potentiation of Alzheimer A beta neurotoxicity - Correlation with cell-free hydrogen peroxide production and metal reduction. *J Biol Chem*. 1999;274(52):37111-6.
181. Cuajungco MP, Goldstein LE, Nunomura A, Smith MA, Lim JT, Atwood CS, et al. Evidence that the beta-amyloid plaques of Alzheimer's disease represent the redox-silencing and entombment of A beta by zinc. *J Biol Chem*. 2000;275(26):19439-42.
182. Pramanik D, Ghosh C, Dey SG. Heme-Cu Bound A beta Peptides: Spectroscopic Characterization, Reactivity, and Relevance to Alzheimer's Disease. *J Am Chem Soc*. 2011;133(39):15545-52.
183. Butterfield DA, Galvan V, Lange MB, Tang HD, Sowell RA, Spilman P, et al. In vivo oxidative stress in brain of Alzheimer disease transgenic mice: Requirement for methionine 35 in amyloid beta-peptide of APP. *Free Radical Bio Med*. 2010;48(1):136-44.
184. Ciccotosto GD, Tew D, Curtain CC, Smith D, Carrington D, Masters CL, et al. Enhanced toxicity and cellular binding of a modified amyloid beta peptide with a methionine to valine substitution. *J Biol Chem*. 2004;279(41):42528-34.
185. Nakamura M, Shishido N, Nunomura A, Smith MA, Perry G, Hayashi Y, et al. Three histidine residues of amyloid-beta peptide control the redox activity of copper and iron. *Biochemistry*. 2007;46(44):12737-43.
186. Kontush A, Berndt C, Weber W, Akopyan V, Arlt S, Schippling S, et al. Amyloid-beta is an antioxidant for lipoproteins in cerebrospinal fluid and plasma. *Free Radical Bio Med*. 2001;30(1):119-28.
187. Feaga HA, Maduka RC, Foster MN, Szalai VA. Affinity of Cu<sup>+</sup> for the Copper-Binding Domain of the Amyloid-beta Peptide of Alzheimer's Disease. *Inorg Chem*. 2011;50(5):1614-8.
188. Curtain CC, Ali F, Volitakis I, Cherny RA, Norton RS, Beyreuther K, et al. Alzheimer's disease amyloid-beta binds copper and zinc to generate an allosterically ordered membrane-penetrating structure containing superoxide dismutase-like subunits. *J Biol Chem*. 2001;276(23):20466-73.
189. Smith DG, Cappai R, Barnham KJ. The redox chemistry of the Alzheimer's disease amyloid beta peptide. *Biochimica Et Biophysica Acta-Biomembranes*. 2007;1768(8):1976-90.
190. Naylor R, Hill AF, Barnham KJ. Neurotoxicity in Alzheimer's disease: is covalently crosslinked A beta responsible? *European Biophysics Journal with Biophysics Letters*. 2008;37(3):265-8.

191. Miura T, Suzuki K, Kohata N, Takeuchi H. Metal binding modes of Alzheimer's amyloid beta-peptide in insoluble aggregates and soluble complexes. *Biochemistry*. 2000;39(23):7024-31.
192. Cherny RA, Atwood CS, Xilinas ME, Gray DN, Jones WD, McLean CA, et al. Treatment with a copper-zinc chelator markedly and rapidly inhibits beta-amyloid accumulation in Alzheimer's disease transgenic mice. *Neuron*. 2001;30(3):665-76.
193. Dai XL, Sun YX, Gao ZL, Jiang ZF. Copper Enhances Amyloid-beta Peptide Neurotoxicity and non beta-Aggregation: A Series of Experiments Conducted upon Copper-Bound and Copper-Free Amyloid-beta Peptide. *J Mol Neurosci*. 2010;41(1):66-73.
194. Hane F, Tran G, Attwood SJ, Leonenko Z. Cu(2+) Affects Amyloid-beta (1-42) Aggregation by Increasing Peptide-Peptide Binding Forces. *Plos One*. 2013;8(3):11.
195. Braak H, Braak E, Bohl J, Lang W. Alzheimers-Disease - Amyloid Plaques in the Cerebellum. *J Neurol Sci*. 1989;93(2-3):277-87.
196. German DC, Manaye KF, White CL, Woodward DJ, Mcintire DD, Smith WK, et al. Disease-Specific Patterns of Locus-Ceruleus Cell Loss. *Ann Neurol*. 1992;32(5):667-76.
197. Mold M, Ouro-Gnao L, Wieckowski BM, Exley C. Copper prevents amyloid-beta(1-42) from forming amyloid fibrils under near-physiological conditions in vitro. *Sci Rep-Uk*. 2013;3:1256.
198. Jiang DL, Zhang L, Grant GPG, Dudzik CG, Chen S, Patel S, et al. The Elevated Copper Binding Strength of Amyloid-beta Aggregates Allows the Sequestration of Copper from Albumin: A Pathway to Accumulation of Copper in Senile Plaques. *Biochemistry*. 2013;52(3):547-56.
199. Rogers JT, Bush AI, Cho HH, Smith DH, Thomson AM, Friedlich AL, et al. Iron and the translation of the amyloid precursor protein (APP) and ferritin mRNAs: riboregulation against neural oxidative damage in Alzheimer's disease. *Biochem Soc Trans*. 2008;36(Pt 6):1282-7.
200. Bodovitz S, Falduto MT, Frail DE, Klein WL. Iron levels modulate alpha-secretase cleavage of amyloid precursor protein. *J Neurochem*. 1995;64(1):307-15.
201. Duce JA, Tsatsanis A, Cater MA, James SA, Robb E, Wikke K, et al. Iron-export ferroxidase activity of  $\beta$ -amyloid precursor protein is inhibited by zinc in Alzheimer's disease. *Cell*. 2010;142(6):857-67.
202. Ha C, Ryu J, Park CB. Metal ions differentially influence the aggregation and deposition of Alzheimer's beta-amyloid on a solid template. *Biochemistry*. 2007;46(20):6118-25.
203. Exley C. Aluminium and iron, but neither copper nor zinc, are key to the precipitation of beta-sheets of A $\beta$ <sub>42</sub> in senile plaque cores in Alzheimer's disease. *J Alzheimers Dis*. 2006;10(2-3):173-7.
204. Tabner BJ, Turnbull S, El-Agnaf OM, Allsop D. Formation of hydrogen peroxide and hydroxyl radicals from A(beta) and alpha-synuclein as a possible mechanism of cell death in Alzheimer's disease and Parkinson's disease. *Free Radic Biol Med*. 2002;32(11):1076-83.
205. Hardy J, Selkoe DJ. Medicine - The amyloid hypothesis of Alzheimer's disease: Progress and problems on the road to therapeutics. *Science*. 2002;297(5580):353-6.
206. Walsh DM, Selkoe DJ. Deciphering the molecular basis of memory failure in Alzheimer's disease. *Neuron*. 2004;44(1):181-93.
207. Bozso Z, Penke B, Simon D, Laczko I, Juhasz G, Szegedi V, et al. Controlled in situ preparation of A beta(1-42) oligomers from the isopeptide "iso-A beta(1-42)", physicochemical and biological characterization. *Peptides*. 2010;31(2):248-56.
208. Sakono M, Zako T. Amyloid oligomers: formation and toxicity of A beta oligomers. *Febs Journal*. 2010;277(6):1348-58.
209. Crouch PJ, Harding SME, White AR, Camakaris J, Bush AI, Masters CL. Mechanisms of A beta mediated neurodegeneration in Alzheimer's disease. *International Journal of Biochemistry & Cell Biology*. 2008;40(2):181-98.

210. Lauren J, Gimbel DA, Nygaard HB, Gilbert JW, Strittmatter SM. Cellular prion protein mediates impairment of synaptic plasticity by amyloid-beta oligomers. *Nature*. 2009;457(7233):1128-U84.
211. Chafekar SM, Baas F, Scheper W. Oligomer-specific A beta toxicity in cell models is mediated by selective uptake. *Biochimica Et Biophysica Acta-Molecular Basis of Disease*. 2008;1782(9):523-31.
212. Rajendran L, Honscho M, Zahn TR, Keller P, Geiger KD, Verkade P, et al. Alzheimer's disease beta-amyloid peptides are released in association with exosomes. *Proceedings of the National Academy of Sciences of the United States of America*. 2006;103(30):11172-7.
213. Tseng BP, Green KN, Chan JL, Blurton-Jones M, LaFerla FM. A beta inhibits the proteasome and enhances amyloid and tau accumulation. *Neurobiology of Aging*. 2008;29(11):1607-18.
214. Parihar MS, Hemnani T. Alzheimer's disease pathogenesis and therapeutic interventions. *Journal of Clinical Neuroscience*. 2004;11(5):456-67.
215. Tabner BJ, Turnbull S, King JE, Benson FE, El-Agnaf OMA, Allsop D. A spectroscopic study of some of the peptidyl radicals formed following hydroxyl radical attack on beta-amyloid and alpha-synuclein. *Free Radical Research*. 2006;40(7):731-9.
216. Bucossi S, Ventriglia M, Panetta V, Salustri C, Pasqualetti P, Mariani S, et al. Copper in Alzheimer's Disease: A Meta-Analysis of Serum, Plasma, and Cerebrospinal Fluid Studies. *J Alzheimers Dis*. 2011;24(1):175-85.
217. Ventriglia M, Bucossi S, Panetta V, Squitti R. Copper in Alzheimer's Disease: A Meta-Analysis of Serum, Plasma, and Cerebrospinal Fluid Studies (vol 24, pg 175, 2011). *J Alzheimers Dis*. 2012;30(4):981-4.
218. Miller LM, Wang Q, Teliwalla TP, Smith RJ, Lanzirrotti A, Miklossy J. Synchrotron-based infrared and X-ray imaging shows focalized accumulation of Cu and Zn co-localized with beta-amyloid deposits in Alzheimer's disease. *J Struct Biol*. 2006;155(1):30-7.
219. Magaki S, Raghavan R, Mueller C, Oberg KC, Vinters HV, Kirsch WM. Iron, copper, and iron regulatory protein 2 in Alzheimer's disease and related dementias. *Neuroscience Letters*. 2007;418(1):72-6.
220. Brewer GJ. Copper excess, zinc deficiency, and cognition loss in Alzheimer's disease. *Biofactors*. 2012;38(2):107-13.
221. Peter Faller CH, and Olivia Berthoumieu. Role of Metal Ions in the Self-assembly of the Alzheimer's Amyloid $\beta$  Peptide. *Inorg Chem*. 2013;52(21):12193-12206.
222. Cherny RA, Barnham KJ, Lynch T, Volitakis I, Li QX, McLean CA, et al. Chelation and intercalation: Complementary properties in a compound for the treatment of Alzheimer's disease. *J Struct Biol*. 2000;130(2-3):209-16.
223. Ritchie CW, Bush AI, Mackinnon A, Macfarlane S, Mastwyk M, MacGregor L, et al. Metal-protein attenuation with iodochlorhydroxyquin (clioquinol) targeting A beta amyloid deposition and toxicity in Alzheimer disease - A pilot phase 2 clinical trial. *Archives of Neurology*. 2003;60(12):1685-91.
224. Squitti R, Rossini PM, Cassetta E, Moffa F, Pasqualetti P, Cortesi M, et al. D-penicillamine reduces serum oxidative stress in Alzheimer's disease patients. *Eur J Clin Invest*. 2002;32(1):51-9.
225. Chen TT, Wang XY, He YF, Zhang CL, Wu ZY, Liao K, et al. Effects of Cyclen and Cyclam on Zinc(II)- and Copper(II)-Induced Amyloid beta-Peptide Aggregation and Neurotoxicity. *Inorg Chem*. 2009;48(13):5801-9.
226. Chen SY, Chen Y, Li YP, Chen SH, Tan JH, Ou TM, et al. Design, synthesis, and biological evaluation of curcumin analogues as multifunctional agents for the treatment of Alzheimer's disease. *Bioorgan Med Chem*. 2011;19(18):5596-604.
227. Botelho MG, Wang X, Arndt-Jovin DJ, Becker D, Jovin TM. Induction of Terminal Differentiation in Melanoma Cells on Downregulation of beta-Amyloid Precursor Protein. *J Invest Dermatol*. 2010;130(5):1400-10.

228. Ko SY, Lin SC, Chang KW, Wong YK, Liu CJ, Chi CW, et al. Increased expression of amyloid precursor protein in oral squamous cell carcinoma. *Int J Cancer*. 2004;111(5):727-32.
229. Hansel DE, Rahman A, Wehner S, Herzog V, Yeo CJ, Maitra A. Increased expression and processing of the Alzheimer amyloid precursor protein in pancreatic cancer may influence cellular proliferation. *Cancer Res*. 2003;63(21):7032-7.
230. Meng JY, Kataoka H, Itoh H, Koono M. Amyloid beta protein precursor is involved in the growth of human colon carcinoma cell in vitro and in vivo. *Int J Cancer*. 2001;92(1):31-9.
231. Fukuchi K, Deeb SS, Kamino K, Ogburn CE, Snow AD, Sekiguchi RT, et al. Increased expression of beta-amyloid protein precursor and microtubule-associated protein tau during the differentiation of murine embryonal carcinoma cells. *J Neurochem*. 1992;58(5):1863-73.
232. LeBlanc AC, Kovacs DM, Chen HY, Villare F, Tykocinski M, Autilio-Gambetti L, et al. Role of amyloid precursor protein (APP): study with antisense transfection of human neuroblastoma cells. *J Neurosci Res*. 1992;31(4):635-45.
233. Takayama K, Tsutsumi S, Suzuki T, Horie-Inoue K, Ikeda K, Kaneshiro K, et al. Amyloid precursor protein is a primary androgen target gene that promotes prostate cancer growth. *Cancer Res*. 2009;69(1):137-42.
234. Yang ZL, Fan YB, Deng ZX, Wu B, Zheng Q. Amyloid precursor protein as a potential marker of malignancy and prognosis in papillary thyroid carcinoma. *Oncol Lett*. 2012;3(6):1227-30.
235. Cuesta A, Zambrano A, Royo M, Pascual A. The tumour suppressor p53 regulates the expression of amyloid precursor protein (APP). *Biochem J*. 2009;418:643-50.
236. Mattson MP. Cellular actions of beta-amyloid precursor protein and its soluble and fibrillogenic derivatives. *Physiol Rev*. 1997;77(4):1081-132.
237. Behr D, Hesse L, Masters CL, Multhaup G. Regulation of amyloid protein precursor (APP) binding to collagen and mapping of the binding sites on APP and collagen type I. *J Biol Chem*. 1996;271(3):1613-20.
238. Narindrasorasak S, Lowery DE, Altman RA, Gonzalez-DeWhitt PA, Greenberg BD, Kisilevsky R. Characterization of high affinity binding between laminin and Alzheimer's disease amyloid precursor proteins. *Lab Invest*. 1992;67(5):643-52.
239. Skerrow CJ. Intercellular adhesion and its role in epidermal differentiation. *Invest Cell Pathol*. 1978;1(1):23-37.
240. Jiang L, Yu GP, Meng W, Wang ZX, Meng FY, Ma WL. Overexpression of amyloid precursor protein in acute myeloid leukemia enhances extramedullary infiltration by MMP-2. *Tumor Biol*. 2013;34(2):629-36.
241. Hayashi Y, Kashiwagi K, Ohta J, Nakajima M, Kawashima T, Yoshikawa K. Alzheimer amyloid protein precursor enhances proliferation of neural stem cells from fetal rat brain. *Biochem Biophys Res Commun*. 1994;205(1):936-43.
242. Ohsawa I, Takamura C, Morimoto T, Ishiguro M, Kohsaka S. Amino-terminal region of secreted form of amyloid precursor protein stimulates proliferation of neural stem cells. *Eur J Neurosci*. 1999;11(6):1907-13.
243. Hansel DE, Rahman A, Wehner S, Herzog V, Yeo CJ, Maitra A. Increased expression and processing of the alzheimer amyloid precursor protein in pancreatic cancer may influence cellular proliferation. *Cancer Res*. 2003;63(21):7032-7.
244. Rossjohn J, Cappai R, Feil SC, Henry A, McKinstry WJ, Galatis D, et al. Crystal structure of the N-terminal, growth factor-like domain of Alzheimer amyloid precursor protein. *Nat Struct Biol*. 1999;6(4):327-31.
245. Lee SB, Schramme A, Doberstein K, Dummer R, Abdel-Bakky MS, Keller S, et al. ADAM10 is upregulated in melanoma metastasis compared with primary melanoma. *J Invest Dermatol*. 2010;130(3):763-73.
246. Siemes C, Quast T, Klein E, Bieber T, Hooper NM, Herzog V. Normalized proliferation of normal and psoriatic keratinocytes by suppression of sAPP alpha-release. *J Invest Dermatol*. 2004;123(3):556-63.

247. Krause K, Karger S, Sheu SY, Aigner T, Kursawe R, Gimm O, et al. Evidence for a role of the amyloid precursor protein in thyroid carcinogenesis. *J Endocrinol*. 2008;198(2):291-9.
248. Hoffmann J, Pietrzik CU, Kummer MP, Twiesselmann C, Bauer C, Herzog V. Binding and selective detection of the secretory N-terminal domain of the alzheimer amyloid precursor protein on cell surfaces. *J Histochem Cytochem*. 1999;47(3):373-82.
249. Wehner S, Siemes C, Kirfel G, Herzog V. Cytoprotective function of sAPP alpha in human keratinocytes. *European Journal of Cell Biology*. 2004;83(11):701-8.
250. Yang WL, Lau AYC, Luo SZ, Zhu Q, Lu L. Characterization of amyloid-beta precursor protein intracellular domain-associated transcriptional complexes in SH-SY5Y neurocytes. *Neurosci Bull*. 2012;28(3):259-70.
251. Ozaki T, Li Y, Kikuchi H, Tomita T, Iwatsubo T, Nakagawara A. The intracellular domain of the amyloid precursor protein (AICD) enhances the p53-mediated apoptosis. *Biochemical and Biophysical Research Communications*. 2006;351(1):57-63.
252. Bertrand E, Brouillet E, Caille I, Bouillot C, Cole GM, Prochiantz A, et al. A short cytoplasmic domain of the amyloid precursor protein induces apoptosis in vitro and in vivo. *Molecular and Cellular Neuroscience*. 2001;18(5):503-11.
253. Zhao H, Zhu J, Cui K, Xu X, O'Brien M, Wong KK, et al. Bioluminescence imaging reveals inhibition of tumor cell proliferation by Alzheimer's amyloid beta protein. *Cancer Cell Int*. 2009;9:15.
254. Porayette P, Gallego MJ, Kaltcheva MM, Bowen RL, Meethal SV, Atwood CS. Differential Processing of Amyloid-beta Precursor Protein Directs Human Embryonic Stem Cell Proliferation and Differentiation into Neuronal Precursor Cells. *J Biol Chem*. 2009;284(35):23806-17.
255. Casal C, Serratosa J, Tusell JM. Effects of beta-AP peptides on activation of the transcription factor NF-kappa B and in cell proliferation in glial cell cultures. *Neurosci Res*. 2004;48(3):315-23.
256. Luo Y, Sunderland T, Roth GS, Wolozin B. Physiological levels of beta-amyloid peptide promote PC12 cell proliferation. *Neuroscience Letters*. 1996;217(2-3):125-8.
257. Almeida OP, Waterreus A, Spry N, Flicker L, Martins RN. One year follow-up study of the association between chemical castration, sex hormones, beta-amyloid, memory and depression in men. *Psychoneuroendocrinology*. 2004;29(8):1071-81.
258. Rosario ER, Pike CJ. Androgen regulation of beta-amyloid protein and the risk of Alzheimer's disease. *Brain Res Rev*. 2008;57(2):444-53.
259. Kaiafa GD, Saouli Z, Diamantidis MD, Kontoninas Z, Voulgaridou V, Raptaki M, et al. Copper levels in patients with hematological malignancies. *Eur J Intern Med*. 2012;23(8):738-41.
260. Hrgovcic M, Tessmer CF, Minckler TM, Mosier B, Taylor GH. Serum Copper Levels in Lymphoma and Leukemia - Special Reference to Hodgkins Disease. *Cancer*. 1968;21(4):743-55.
261. Tessmer CF, Hrgovcic M, Thomas FB, Fuller LM, Castro JR. Serum Copper as an Index of Tumor Response to Radiotherapy. *Radiology*. 1973;106(3):635-9.
262. Gupte A, Mumper RJ. Elevated copper and oxidative stress in cancer cells as a target for cancer treatment. *Cancer Treatment Reviews*. 2009;35(1):32-46.
263. Jain S CJ, Ward MM, Kornhauser N, Chuang E, Cigler T, Moore A, Donovan D, Lam C, Cobham MV, Schneider S, Hurtado Rúa SM, Benkert S, Mathijssen Greenwood C, Zekowitz R, Warren JD, Lane ME, Mittal V, Rafii S, Vahdat LT. Tetrathiomolybdate-associated copper depletion decreases circulating endothelial progenitor cells in women with breast cancer at high risk of relapse. *Ann Oncol*. 2013.
264. Yoo JY, Pradarelli J, Haseley A, Wojton J, Kaka A, Bratasz A, et al. Copper Chelation Enhances Antitumor Efficacy and Systemic Delivery of Oncolytic HSV. *Clin Cancer Res*. 2012;18(18):4931-41.

265. Ishida S, McCormick F, Smith-McCune K, Hanahan D. Enhancing Tumor-Specific Uptake of the Anticancer Drug Cisplatin with a Copper Chelator. *Cancer Cell*. 2010;17(6):574-83.
266. Kubiak K MK, Langer E, Dziki Ł, Dziki A, Majsterek I. Effect of Cu(II) coordination compounds on the activity of antioxidant enzymes catalase and superoxide dismutase in patients with colorectal cancer. *Pol Przegl Chir*. 2011;83(3):155-60.
267. Parr-Sturgess CA, Tinker CL, Hart CA, Brown MD, Clarke NW, Parkin ET. Copper Modulates Zinc Metalloproteinase-Dependent Ectodomain Shedding of Key Signaling and Adhesion Proteins and Promotes the Invasion of Prostate Cancer Epithelial Cells. *Mol Cancer Res*. 2012;10(10):1282-93.
268. Mahabir S, Spitz MR, Barrera SL, Beaver SH, Etzel C, Forman MR. Dietary zinc, copper and selenium, and risk of lung cancer. *Int J Cancer*. 2007;120(5):1108-15.
269. Kamamoto Y, Makiura S, Sugihara S, Hiasa Y, Arai M, Ito N. Inhibitory Effect of Copper on DL-Ethionine Carcinogenesis in Rats. *Cancer Res*. 1973;33(5):1129-35.
270. Davis CD, Newman S. Inadequate dietary copper increases tumorigenesis in the Min mouse. *Cancer Lett*. 2000;159(1):57-62.
271. Disilvestro RA, Greenson JK, Liao ZM. Effects of Low Copper Intake on Dimethylhydrazine-Induced Colon Cancer in Rats. *P Soc Exp Biol Med*. 1992;201(1):94-7.
272. Greene FL, Lamb LS, Barwick M, Pappas NJ. Effect of Dietary Copper on Colonic Tumor Production and Aortic Integrity in the Rat. *J Surg Res*. 1987;42(5):503-12.
273. Senesse P, Meance S, Cottet V, Faivre J, Boutron-Ruault MC. High dietary iron and copper and risk of colorectal cancer: A case-control study in Burgundy, France. *Nutr Cancer*. 2004;49(1):66-71.
274. Nicodemus KK, Sweeney C, Folsom AR. Evaluation of dietary, medical and lifestyle risk factors for incident kidney cancer in postmenopausal women. *Int J Cancer*. 2004;108(1):115-21.
275. Biedler JL, Rofflertarlov S, Schachner M, Freedman LS. Multiple Neurotransmitter Synthesis by Human Neuroblastoma Cell Lines and Clones. *Cancer Res*. 1978;38(11):3751-7.
276. Biedler JL, Helson L, Spengler BA. Morphology and Growth, Tumorigenicity, and Cytogenetics of Human Neuroblastoma Cells in Continuous Culture. *Cancer Res*. 1973;33(11):2643-52.
277. [www.lgcstandards-atcc.org](http://www.lgcstandards-atcc.org).
278. Horoszewicz JS, Leong SS, Kawinski E, Karr JP, Rosenthal H, Chu TM, et al. Lncap Model of Human Prostatic-Carcinoma. *Cancer Res*. 1983;43(4):1809-18.
279. Stone KR, Mickey DD, Wunderli H, Mickey GH, Paulson DF. Isolation of a Human Prostate Carcinoma Cell Line (Du 145). *Int J Cancer*. 1978;21(3):274-81.
280. Kaighn ME, Narayan KS, Ohnuki Y, Lechner JF, Jones LW. Establishment and Characterization of a Human Prostatic-Carcinoma Cell-Line (Pc-3). *Invest Urol*. 1979;17(1):16-23.
281. Parkin ET, Watt NT, Hussain I, Eckman EA, Eckman CB, Manson JC, et al. Cellular prion protein regulates beta-secretase cleavage of the Alzheimer's amyloid precursor protein. *Proceedings of the National Academy of Sciences of the United States of America*. 2007;104(26):11062-7.
282. Hooper NM. *Alzheimer's Disease: Methods and protocols*. New Jersey: Humana Press Inc. 2000.
283. Kim M, Suh J, Romano D, Truong MH, Mullin K, Hooli B, et al. Potential late-onset Alzheimer's disease-associated mutations in the ADAM10 gene attenuate alpha-secretase activity. *Hum Mol Genet*. 2009;18(20):3987-96.
284. Jiang H, Hampel H, Prvulovic D, Wallin A, Blennow K, Li RN, et al. Elevated CSF levels of TACE activity and soluble TNF receptors in subjects with mild cognitive impairment and patients with Alzheimer's disease. *Mol Neurodegener*. 2011;6:69.

285. Arima T, Enokida H, Kubo H, Kagara I, Matsuda R, Toki K, et al. Nuclear translocation of ADAM-10 contributes to the pathogenesis and progression of human prostate cancer. *Cancer Sci.* 2007;98(11):1720-6.
286. Xiao LJ, Lin P, Lin F, Liu X, Qin W, Zou HF, et al. ADAM17 targets MMP-2 and MMP-9 via EGFR-MEK-ERK pathway activation to promote prostate cancer cell invasion. *Int J Oncol.* 2012;40(5):1714-24.
287. Harris B, Pereira I, Parkin E. Targeting ADAM10 to lipid rafts in neuroblastoma SH-SY5Y cells impairs amyloidogenic processing of the amyloid precursor protein. *Brain Res.* 2009;1296:203-15.
288. Parr-Sturgess CA, Rushton DJ, Parkin ET. Ectodomain shedding of the Notch ligand Jagged1 is mediated by ADAM17, but is not a lipid-raft-associated event. *Biochem J.* 2010;432:283-94.
289. Acevedo KM, Hung YH, Dalziel AH, Li QX, Laughton K, Wikke K, et al. Copper Promotes the Trafficking of the Amyloid Precursor Protein. *J Biol Chem.* 2011;286(10):8252-62.
290. Lutsenko S, Bhattacharjee A, Hubbard AL. Copper handling machinery of the brain. *Metallomics.* 2010;2(9):596-608.
291. Reinhold JG. Trace-Elements - Selective Survey. *Clin Chem.* 1975;21(4):476-500.
292. Hesse L, Behr D, Masters CL, Multhaup G. The Beta-A4 Amyloid Precursor Protein-Binding to Copper. *Febs Lett.* 1994;349(1):109-16.
293. Atwood CS, Scarpa RC, Huang XD, Moir RD, Jones WD, Fairlie DP, et al. Characterization of copper interactions with Alzheimer amyloid beta peptides: Identification of an attomolar-affinity copper binding site on amyloid beta 1-42. *J Neurochem.* 2000;75(3):1219-33.
294. Latasa MJ, Belandia B, Pascual A. Thyroid hormones regulate beta-amyloid gene splicing and protein secretion in neuroblastoma cells. *Endocrinology.* 1998;139(6):2692-8.
295. Kardos J, Kovacs I, Hajos F, Kalman M, Simonyi M. Nerve-Endings from Rat-Brain Tissue Release Copper Upon Depolarization - a Possible Role in Regulating Neuronal Excitability. *Neuroscience Letters.* 1989;103(2):139-44.
296. Gaier ED, Eipper BA, Mains RE. Copper signaling in the mammalian nervous system: Synaptic effects. *Journal of Neuroscience Research.* 2013;91(1):2-19.
297. von Rotz RC, Kohli BM, Bosset J, Meier M, Suzuki T, Nitsch RM, et al. The APP intracellular domain forms nuclear multiprotein complexes and regulates the transcription of its own precursor. *Journal of Cell Science.* 2004;117(19):4435-48.
298. Simons K, Ikonen E. Functional rafts in cell membranes. *Nature.* 1997;387(6633):569-72.
299. Nizzari M, Venezia V, Repetto E, Caorsi V, Magrassi R, Gagliani MC, et al. Amyloid precursor protein and presenilin1 interact with the adaptor GRB2 and modulate ERK1,2 signaling. *J Biol Chem.* 2007;282(18):13833-44.
300. Wang R, Meschia JF, Cotter RJ, Sisodia SS. Secretion of the Beta-A4 Amyloid Precursor Protein Identification of a Cleavage Site in Cultured-Mammalian-Cells. *J Biol Chem.* 1991;266(25):16960-4.
301. Marcu M, Radu E, Sajin M. Neuroendocrine transdifferentiation of prostate carcinoma cells and its prognostic significance. *Romanian Journal of Morphology and Embryology.* 2010;51(1):7-12.
302. Disantagnese PA, Jensen KLD. Neuroendocrine Differentiation in Prostatic-Carcinoma. *Human Pathology.* 1987;18(8):849-56.
303. Abrahamsson PA, Falkmer S, Falt K, Grimelius L. The Course of Neuro-Endocrine Differentiation in Prostatic Carcinomas - an Immunohistochemical Study Testing Chromogranin-a as an Endocrine Marker. *Pathol Res Pract.* 1989;185(3):373-80.
304. Bang YJ, Pirnia F, Fang WG, Kang WK, Sartor O, Whitesell L, et al. Terminal Neuroendocrine Differentiation of Human Prostate Carcinoma-Cells in Response to Increased

- Intracellular Cyclic-Amp. Proceedings of the National Academy of Sciences of the United States of America. 1994;91(12):5330-4.
305. Acloque H, Adams MS, Fishwick K, Bronner-Fraser M, Nieto MA. Epithelial-mesenchymal transitions: the importance of changing cell state in development and disease. *Journal of Clinical Investigation*. 2009;119(6):1438-49.
306. Fuchs IB, Lichtenegger W, Buehler H, Henrich W, Stein H, Kleine-Tebbe A, et al. The prognostic significance of epithelial-mesenchymal transition in breast cancer. *Anticancer Res*. 2002;22(6A):3415-9.
307. Chaw SY, Majeed AA, Dalley AJ, Chan A, Stein S, Farah CS. Epithelial to mesenchymal transition (EMT) biomarkers - E-cadherin, beta-catenin, APC and Vimentin - in oral squamous cell carcinogenesis and transformation. *Oral Oncol*. 2012;48(10):997-1006.
308. Levi-Schaffer F, Slovik D, Armetti L, Pickholtz D, Touitou E. Activation and inhibition of mast cells degranulation affect their morphometric parameters. *Life Sci*. 2000;66(21):PI283-PI90.
309. Mandell JW, Heffron DS. Opposing roles of ERK and P38 map kinases in FGF2-induced astroglial process extension. *J Neuropath Exp Neur*. 2004;63(5):511.
310. Barbagallo APM, Wang ZL, Zheng H, D'Adamio L. A Single Tyrosine Residue in the Amyloid Precursor Protein Intracellular Domain Is Essential for Developmental Function. *J Biol Chem*. 2011;286(11):8717-21.
311. Barbagallo APM, Weldon R, Tamayev R, Zhou DW, Giliberto L, Foreman O, et al. Tyr(682) in the Intracellular Domain of APP Regulates Amyloidogenic APP Processing In Vivo. *Plos One*. 2010;5(11).
312. Russo C, Salis S, Dolcini V, Venezia V, Song XH, Teller JK, et al. Identification of amino-terminally and phosphotyrosine-modified carboxy-terminal fragments of the amyloid precursor protein in Alzheimer's disease and Down's syndrome brain. *Neurobiology of Disease*. 2001;8(3):540.
313. Matrone C, Barbagallo APM, La Rosa LR, Florenzano F, Ciotti MT, Mercanti D, et al. APP is Phosphorylated by TrkA and Regulates NGF/TrkA Signaling. *Journal of Neuroscience*. 2011;31(33):11756-61.
314. Takahashi K, Niidome T, Akaike A, Kihara T, Sugimoto H. Phosphorylation of amyloid precursor protein (APP) at Tyr687 regulates APP processing by alpha- and gamma-secretase. *Biochemical and Biophysical Research Communications*. 2008;377(2):544-9.
315. Rebelo S, Vieira SI, Esselmann H, Wiltfang J, Silva EFDE, Silva OABDE. Tyrosine 687 phosphorylated Alzheimer's amyloid precursor protein is retained intracellularly and exhibits decreased turnover rate. *Neurodegener Dis*. 2007;4(2-3):78-87.
316. Tarr PE, Roncarati R, Pelicci G, Pelicci PG, D'Adamio L. Tyrosine phosphorylation of the beta-amyloid precursor protein cytoplasmic tail promotes interaction with Shc. *J Biol Chem*. 2002;277(19):16798-804.
317. Mario Nizzari ST, Alessandro Corsaro, Valentina Villa,, Aldo Pagano CP, Claudio Russo, and Tullio Florio. Neurodegeneration in Alzheimer Disease: Role of Amyloid Precursor Protein and Presenilin1 Intracellular Signaling. *Journal of Toxicology*. 2011;2012:13.
318. Knusel B, Winslow JW, Rosenthal A, Burton LE, Seid DP, Nikolics K, et al. Promotion of Central Cholinergic and Dopaminergic Neuron Differentiation by Brain-Derived Neurotrophic Factor but Not Neurotrophin 3. *Proceedings of the National Academy of Sciences of the United States of America*. 1991;88(3):961-5.
319. Mobley WC, Neve RL, Prusiner SB, Mckinley MP. Nerve Growth-Factor Increases Messenger-Rna Levels for the Prion Protein and the Beta-Amyloid Protein-Precursor in Developing Hamster Brain. *Proceedings of the National Academy of Sciences of the United States of America*. 1988;85(24):9811-5.
320. Cosgaya JM, Latasa MJ, Pascual A. Nerve growth factor and ras regulate beta-amyloid precursor protein gene expression in PC12 cells. *J Neurochem*. 1996;67(1):98-104.

321. Hurle RA, Davies G, Parr C, Mason MD, Jenkins SA, Kynaston HG, et al. Hepatocyte growth factor/scatter factor and prostate cancer: a review. *Histol Histopathol*. 2005;20(4):1339-49.
322. Abounader R, Lateral J. Scatter factor/hepatocyte growth factor in brain tumor growth and angiogenesis. *Neuro-Oncology*. 2005;7(4):436-51.
323. Liu F, Su YA, Li BL, Ni BH. Regulation of amyloid precursor protein expression and secretion via activation of ERK1/2 by hepatocyte growth factor in HEK293 cells transfected with APP(751). *Experimental Cell Research*. 2003;287(2):387-96.
324. Kang J, Mullerhill B. Differential Splicing of Alzheimers-Disease Amyloid A4 Precursor Rna in Rat-Tissues - Prea4695 Messenger-Rna Is Predominantly Produced in Rat and Human Brain. *Biochemical and Biophysical Research Communications*. 1990;166(3):1192-200.
325. Parkin ET, Watt NT, Turner AJ, Hooper NM. Dual mechanisms for shedding of the cellular prion protein. *J Biol Chem*. 2004;279(12):11170-8.
326. Brazier MW, Davies P, Player E, Marken F, Viles JH, Brown DR. Manganese binding to the prion protein. *J Biol Chem*. 2008;283(19):12831-9.
327. Milacic V, Chen D, Giovagnini L, Diez A, Fregona D, Dou QP. Pyrrolidine dithiocarbamate-zinc(II) and -copper(II) complexes induce apoptosis in tumor cells by inhibiting the proteasomal activity. *Toxicology and Applied Pharmacology*. 2008;231(1):24-33.
328. Linder MC. The relationship of copper to DNA damage and damage prevention in humans. *Mutat Res-Fund Mol M*. 2012;733(1-2):83-91.
329. Sandbrink R, Masters CL, Beyreuther K. Beta-A4-Amyloid Protein-Precursor Messenger-Rna Isoforms without Exon-15 Are Ubiquitously Expressed in Rat-Tissues Including Brain, but Not in Neurons. *J Biol Chem*. 1994;269(2):1510-7.
330. Hsiao K, Chapman P, Nilsen S, Eckman C, Harigaya Y, Younkin S, et al. Correlative memory deficits, A beta elevation, and amyloid plaques in transgenic mice. *Science*. 1996;274(5284):99-102.
331. Bellingham SA, Ciccotosto GD, Needham BE, Fodero LR, White AR, Masters CL, et al. Gene knockout of amyloid precursor protein and amyloid precursor-like protein-2 increases cellular copper levels in primary mouse cortical neurons and embryonic fibroblasts. *J Neurochem*. 2004;91(2):423-8.
332. White AR, Reyes R, Mercer JFB, Camakaris J, Zheng H, Bush AI, et al. Copper levels are increased in the cerebral cortex and liver of APP and APLP2 knockout mice. *Brain Res*. 1999;842(2):439-44.
333. Lichtenthaler SF. Alpha-secretase in Alzheimer's disease: molecular identity, regulation and therapeutic potential. *J Neurochem*. 2011;116(1):10-21.
334. Roskoski R. ERK1/2 MAP kinases: Structure, function, and regulation. *Pharmacol Res*. 2012;66(2):105-43.
335. Valensin D, Mancini FM, Luczkowski M, Janicka A, Wisniewska K, Gaggelli E, et al. Identification of a novel high affinity copper binding site in the APP(145-155) fragment of amyloid precursor protein. *Dalton T*. 2004(1):16-22.
336. Kong GKW, Adams JJ, Harris HH, Boas JF, Curtain CC, Galatis D, et al. Structural studies of the Alzheimer's amyloid precursor protein copper-binding domain reveal how it binds copper ions. *J Mol Biol*. 2007;367(1):148-61.
337. Palmert MR, Usiak M, Mayeux R, Raskind M, Tourtellotte WW, Younkin SG. Soluble derivatives of the beta-amyloid protein-precursor in cerebrospinal-fluid - alterations in normal aging and in Alzheimers-disease. *Neurology*. 1990;40(7):1028-34.
338. Gandy SE, Bhasin R, Ramabhadran TV, Koo EH, Price DL, Goldgaber D, et al. Alzheimer beta/A4-amyloid precursor protein - evidence for putative amyloidogenic fragment. *J Neurochem*. 1992;58(1):383-6.

339. Humez S, Monet M, Legrand G, Lepage G, Delcourt P, Prevarskaya N. Epidermal growth factor-induced neuroendocrine differentiation and apoptotic resistance of androgen-independent human prostate cancer cells. *Endocrine-Related Cancer*. 2006;13(1):181-95.
340. Cussenot O, Villette JM, Cochand-Priollet B, Berthon P. Evaluation and clinical value of neuroendocrine differentiation in human prostatic tumors. *Prostate Suppl*. 1998;8:43-51.
341. Slattery C, Campbell E, McMorrow T, Ryan MP. Cyclosporine A-induced renal fibrosis - A role for epithelial-mesenchymal transition. *American Journal of Pathology*. 2005;167(2):395-407.
342. De Craene B, Berx G. Regulatory networks defining EMT during cancer initiation and progression. *Nature Reviews Cancer*. 2013;13(2):97-110.
343. Gunderson WA, Hernandez-Guzman J, Karr JW, Sun L, Szalai VA, Warncke K. Local Structure and Global Patterning of Cu<sup>2+</sup> Binding in Fibrillar Amyloid-beta [A beta(1-40)] Protein. *J Am Chem Soc*. 2012;134(44):18330-7.
344. Furlan S, Hureau C, Faller P, La Penna G. Modeling Copper Binding to the Amyloid-beta Peptide at Different pH: Toward a Molecular Mechanism for Cu Reduction. *J Phys Chem B*. 2012;116(39):11899-910.
345. Kienlen-Campard P, Tasiaux B, Van Hees J, Li ML, Huysseune S, Sato T, et al. Amyloidogenic processing but not amyloid precursor protein (APP) intracellular C-terminal domain production requires a precisely oriented APP dimer assembled by transmembrane GXXXG motifs. *J Biol Chem*. 2008;283(18):12680.
346. Syme CD, Nadal RC, Rigby SEJ, Viles JH. Copper binding to the amyloid-beta (A beta) peptide associated with Alzheimer's disease - Folding, coordination geometry, pH dependence, stoichiometry, and affinity of A beta-(1-28): Insights from a range of complementary spectroscopic techniques. *J Biol Chem*. 2004;279(18):18169-77.